Neonatal brain connectivity and association with outcome in infants born preterm

Toulmin, Hilary

Awarding institution:
King's College London

Neonatal brain connectivity and association with outcome in infants born preterm

Dr Hilary Toulmin MA MBBS

Thesis submitted for the degree of

Doctor of Philosophy

Centre for the Developing Brain

Faculty of Life Science and Medicine

King’s College, London, UK

Abstract

In adults, thalamus and corpus striatum contain topographic cortical representations. It is not known whether newborn infants demonstrate adult-like thalamic or striatal topography, and it is not known how development or disruption of this architecture affects the acquisition of neurocognitive capabilities. This thesis explores the hypothesis that both thalamus and corpus striatum have topographic and integrative cortical representations at the time of normal birth; that these are modulated by early-life adversity; and that the strength of perinatal thalamocortical and corticostriatal functional connectivity would predict later functionality.

Using resting state functional magnetic resonance imaging (rfMRI) at the time of normal birth to define cortical regions of interest, and estimating functional connectivity using seed-based correlations, connectivity between bilateral cortical regions and thalamus and striatum in a cohort of 47 preterm infants born between 24- and 32-weeks gestational age, and 19 term-born infants was modelled and precise topographic representations found. This topography is similar to that found in adults with regards to thalamocortical connections, but dissimilar to the pattern found in adult studies with regards to striatocortical connections. Linear regression with gestational age at birth shows that preterm infants have altered connectivity between both thalamus and striatum and a network consisting of fronto-parietal insular cortex. Thalamocortical connectivity with anterior cingulate and dorsolateral prefrontal cortex and striatocortical connectivity with sensory-motor association area is also correlated with degree of preterm birth.

To investigate connectivity at birth and neurodevelopmental outcome around 20 months, a cohort of 102 preterm infants, born between 24- and 32-weeks gestational age, was imaged at birth and subsequently followed up at 20 months old with neurodevelopmental testing using Bayley Scales of Infant and Toddler Development. Only subcortical connections with motor and pre-motor cortex are associated with developmental scores. Striatal-pre-motor connectivity is associated with cognitive and language abilities, and thalamo-pre-motor with motor function. Primary sensory-

motor cortex connectivity to striatum is correlated with motor scores and to thalamus with cognitive scores.

Thalamus and corpus striatum thus show precise cortical topographic connections at the time of normal birth which are required for normal development and vulnerable to adverse perinatal events.

Declaration of Originality

This thesis and the work presented herein are my own and were conducted at King's College, London, Between January 2012 and July 2017. I have appropriately referenced all sources. This work has not been submitted to obtain any other degree at this university or any other institution.

Hilary Toulmin

Acknowledgements

I would like to thank my supervisors Professor David Edwards and Professor Christian Beckmann and Wellcome Trust for their support and the opportunity to investigate preterm brain connectivity using magnetic resonance imaging.

Many people worked to collect such a rich dataset and I would like to thank them and the parents and children who took part.

In professional work and in life: “it takes a village to bring up a child.”

Statement of publications

Journal papers

Hilary Toulmin, Christian F. Beckmann, Jonathan O'Muircheartaigh, Gareth Ball, Pumza Nongena, Antonios Makropoulos, Ashraf Ederies, Serena J. Counsell, Nigel Kennea, Tomoki Arichi, Nora Tusor, Mary A. Rutherford, Denis Azzopardi, Nuria Gonzales-Cinca, Joseph V. Hajnal and A. David Edwards. Specialisation and integration of functional thalamocortical connectivity in the human infant. Proceedings of the National Academies of Science, 112 (20) 6485-6490 (2015).

Hilary Toulmin, Jonathan O'Muircheartaigh, Serena Counsell, Shona Falconer, Andrew Chew, Christian Beckmann, A. David Edwards. Cortical-subcortical connectivity at term predicts outcome at 2 years after preterm birth using fMRI.
Under revision June 2018

Conference abstracts

Hilary Toulmin, Christian F. Beckmann, Jonathan O'Muircheartaigh, Gareth Ball, Pumza Nongena, Antonios Makropoulos, Ashraf Ederies, Serena J. Counsell, Nigel Kennea, Tomoki Arichi, Nora Tusor, Mary A. Rutherford, Denis Azzopardi, Nuria Gonzales-Cinca, Joseph V. Hajnal and A. David Edwards. Functional connectivity of the basal ganglia in the preterm brain is established by term age. Vienna Biennial Resting State Conference 2016

Hilary Toulmin, Christian Beckmann, Phumza Nongena, Serena Counsell, Ashraf Ederies, Tomoki Arichi, Nora Tusor, A. David Edwards. Preterm birth disrupts thalamocortical connectivity. Organisation for Human Brain Mapping 2014

Hilary Toulmin, Christian Beckman, A.David Edwards. Investigation the establishment of thalamocortical connectivity in neonates using resting state fMRI. Human Brain Mapping 2012

Hilary Toulmin, Valentina Doria, Tomoki Arichi, Ioannis S. Gousias, Serena J Counsell, Christian F Beckmann, A. David Edwards. Functional thalamocortical connectivity shown with resting state functional magnetic resonance imaging. Pediatric Academic Society USA (PAS) 2011.

Table of Contents

Part One - Literature

Chapter One. Thalamocortical organisation

Part Two - Materials and Methods

Chapter Five. Study-specific materials and methods

Part Three - Results and Discussion

List of tables, equations and figures

Tables

Equations

Figures

Thalamocortical organisation

Striatocortical organisation

Materials and methods

Appendix Figure 1 Different contrast of a T2-weighted image according to age of subject: neonatal brain (left) compared with adult (right)

Appendix Figure 2 Comparison of traditional rigid registration with 6 degrees of freedom and correlation cost function (top row), with the additional boundary-based registration (bottom row)

Abbreviations

AChE	acetyl cholinesterase
AD	axial diffusivity
ADC	apparent diffusion coefficient
ADP	adenosine diphosphate
AROMA	automatic removal of motion artefact
ATP	adenosine triphosphate
BOLD	blood oxygen level dependent
Cho	choline
CI	confidence intervals
CM	centromedian nucleus of the thalamus
CSF	cerebrospinal fluid
CT	computed tomography
DEHSI	diffuse excessive high signal intensity
dHCP	Developing Human Connectome Project
DLPFC	dorsolateral prefrontal cortex
DMN	default mode network
DQ	developmental quotient
EEG	electroencephalograph
EPI	echo planar imaging
EPSP	excitatory postsynaptic potential
FA	fractional anisotropy
fMRI	functional magnetic resonance imaging
FWHM	full width at half maximum
FT	infants born at full term
GA	gestational age
GABA	gamma-aminobutyric acid
GAP	growth-associated protein
GMFCS	gross motor function classification system
GMH	germinal matrix haemorrhage
GPe	globus pallidus external segment
GPi	globus pallidus internal segment
ICA	independent component analysis

IPSP	inhibitory postsynaptic potential
IVH	intraventricular haemorrhage
MD	medial dorsal nucleus of thalamus
MI	myo-inositol
MNI	Montreal Neurological Institute
MRI	magnetic resonance imaging
ms	milliseconds
NAA	N-acetylaspartate
NMV	net magnetisation vector
OHBM	Organisation for Human Brain Mapping
PMA	post-menstrual age
PVL	periventricular leukomalacia
PWML	posterior white matter lesions
RD	radial diffusivity
RF	radio frequency
rfMRI	resting state functional MRI
ROI	region of interest
SMA	supplementary motor area
SNpc	substantia nigra pars compacta
SNR	signal to noise ratio
SNr	substantia nigra pars reticulata
STN	subthalamic nucleus
TBSS	tract-based spatial statistics
TE	echo time
TEA	term-equivalent age
TFCE	threshold-free cluster enhancement
TR	repetition time
TRN	reticular nucleus of the thalamus
VA	ventral anterior nucleus of thalamus
VLa	ventral lateral nucleus of thalamus anterior portion
VLp	ventral lateral nucleus of thalamus posterior portion
VM	ventral median nucleus of the thalamus
VPL	ventral posterolateral nucleus of the thalamus
VPM	ventral posteromedian nucleus of the thalamus

VP	ventral posterior nucleus of the thalamus

Contributions

Implementation of resting state functional connectivity analysis for the investigation of connectivity in the preterm brain including pre-processing steps, image registration methodology, analysis and interpretation in this thesis is my own work.

FIX: The motion correction step used in the second cohort in this thesis was implemented by Gareth Ball as referenced in the text and performed on the data by Jonathan O'Muircheartaigh.

I was very lucky to be able to use the magnetic resonance imaging and Bayley III follow up data collected as part of the EPRIME imaging study carried out at Queen Charlotte and Chelsea Hospital.

Prologue

Neuroplasticity

Underlying the analysis of brain connectivity using magnetic resonance imaging and the statistical analysis upon which it is founded, are cells, synapses and neurotransmitters which respond to their environment. The principle of neuroplasticity was first coined by psychologist William James in "The Principles of Psychology" which was published in 1890. Plasticity is described as acting upon

> "a structure weak enough to yield an influence, but strong enough not to yield all at once. The current, once in, must find a way out. In getting out, they leave their traces in the paths they take. The only thing they can do, in short, is to deepen old paths or make new ones." (William James 1890 (James, 1950).

In 1894, Santiago Ramón y Cajal suggested that plasticity occurs at the junctions between nerve cells (later termed synapses) and that mental exercise leads to growth of new nerve fibre branches (subsequently called arborisation). He said at a lecture at the Royal Society in London in 1894 "we could say that the cerebral cortex is like a garden planted with innumerable trees - the pyramidal cells - which, thanks to intelligent cultivation, can multiply their branches and sink their roots deep, producing fruits and flowers of ever greater variety and quality".

When standing by a poster at a conference, I was once told that it was unfair to compare preterm infants with term infants at the time of normal birth as the preterm infants had a large advantage being, in some cases, 4 months older. There are, however, no known advantages to being born preterm and as a group, these infants are at increased risk of motor, cognitive and psychological difficulties when compared with their term-born peers. The origins of the difference are to be found in the

difference in experience of the third trimester and can be conceptualised as premature removal from the intrauterine environment and premature exposure to the extrauterine environment: in both cases engaging in adaptive processes during a sensitive developmental period (Johnson, 2017).

Premature removal from the intrauterine environment

The loss of placental and cord function provides challenges for all physiological systems. The placenta performs many functions which cannot be replicated in the neonatal intensive care unit: multiple homeostatic endocrine placental functions (including thyroid and insulin regulation) and last trimester immune cell transfusion for example. Many factors, such as the difference in oxygen tension from the physiological in utero level of 80-90% (depending where in the fetal circulation it is measured) and mediated by fetal haemoglobin to the ex utero level of 99% mediated by haemoglobin A and A2, have, as yet, unknown effects on cell differentiation and gene expression. Late-born neurons such as Von Economo Neurons appear 'mainly after birth' (in term-born infants examined post-mortem) but it is not known what initiates their appearance at this time (John M Allman, personal correspondence). Although the quality of placental function may have been variable prior to birth, these challenges are shared by all preterm infants: the effect on the brain and outcome, therefore might be expected to be determined by the degree of prematurity.

Premature exposure to the extrauterine environment

Premature exposure to the extrauterine environment involves the different sensory stimuli of the neonatal unit where the immature infant is exposed to greater visual stimulus, different and greater auditory input, greater direct sensory stimulation of the skin, and pain (Grunau *et al.*, 2009; Vinall *et al.*, 2013). Preterm exposure forces immature and rapidly developing physiological systems to perform mature functions such as gas exchange in the lungs and digestion in the gut. The course on the intensive care unit will vary between infants with some infants having a less eventful journey than others and this will depend on a combination of their intrauterine experience, genetic susceptibility and congenital and acquired illnesses.

Introduction

This thesis investigates the connectivity of cortex and subcortical structures at the time of normal birth and whether this connectivity is different in preterm infants compared with those born at the normal time. This connectivity is then compared with the outcome of each infant at the age of two years to determine whether it predicts outcome in any or all of three domains: motor, cognitive or language.

The impact of preterm birth

This is an important area of investigation as preterm birth affects an estimated 14.9 million babies globally, with 517,400 babies born before 37 weeks' gestation in the United States of America in a single year (Blencowe *et al.*, 2012). Preterm birth is the leading cause of child deaths in high-income countries (Liu *et al.*, 2012) and has lifelong neurodevelopmental effects and increased risk of chronic disease stretching into adulthood (Wood *et al.*, 2005; Dyet *et al.*, 2006; Aarnoudse-Moens *et al.*, 2009; Boardman *et al.*, 2010; Nagy *et al.*, 2011; Mwaniki *et al.*, 2012; Nosarti *et al.*, 2014; Papini *et al.*, 2016; Linsell *et al.*, 2018) with more than 50% of children born with a birth weight under 1500g (63,000 children in USA in 2006) experiencing disability (Martin *et al.*, 2008). This percentage increases to a level of 74% moderate or severe neurodevelopment impairment by the age of two years in surviving infants with a birth weight of less than 400g (Brumbaugh *et al.*, 2019). The earlier the birth, the greater the effect on the developing brain and this is often referred to as the 'dose-dependent effect' of preterm birth (Bhutta *et al.*, 2002). Even in the absence of significant post-natal sequelae, the effects on measures of cortical thickness, brain volume and surface area endure into childhood (Lax *et al.*, 2013) and adulthood (Kalpakidou *et al.*, 2014). The follow-up to the EPICURE study shows increasing rates of survival, increasing percentage of those surviving without disability, but an overall increase in numbers with severe disability as a result of the increased rate of survival (Costeloe *et al.*, 2012). The impact of preterm birth will therefore increase (see Appendix C for definitions of preterm birth).

Infants born extremely preterm (22-27 weeks) represent the severe end of a spectrum of health and developmental adversity with 57-72% of survivors experiencing motor, cognitive and language impairments by secondary school or adolescences (Marlow, 2004; Saigal and Doyle, 2008; Moore *et al.*, 2012; Hutchinson *et al.*, 2013; Johnson and Marlow, 2017). Those born very preterm (28-<32 completed weeks of gestation) as well as moderate to late preterm-born infants are also at increased risk of neurodevelopmental difficulties. Those born between 32 and 37 weeks comprise the majority of preterm births (70% of all preterm births in Australia for example) and therefore contribute significantly to the health burden associated with preterm birth (Cheong and Doyle, 2012). These children experience problems in the cognitive domain (Johnson *et al.*, 2015) being less likely to complete basic schooling (Mathiasen *et al.*, 2010) and may have difficulty with emotional regulation (van Baar *et al.*, 2009), language (Cheong *et al.*, 2017), visuospatial reasoning, attention control, inhibition and executive functioning but show no difference in visuomotor and motor skills when compared with their term-born peers (Cserjesi *et al.*, 2012): these problems are less tractable to neurodevelopmental testing at 2 years old.

Why study thalamic and striatal topography in the newborn?

The adult thalamus shows well developed, topographically-organised thalamocortical connectivity with overlapping cortical representations that support integration of diverse cortical inputs (Behrens *et al.*, 2003; Jones, 2007; Draganski *et al.*, 2008; Zhang *et al.*, 2008; Sherman and Guillery, 2013). The mature corpus striatum also contains topographic and integrating cortical connections, with non-adjacent cortical regions that serve similar functions connecting with distinct functional striatal territories (Haber *et al.*, 2006; Averbeck *et al.*, 2014). It is not yet known, however, if this striatocortical and thalamocortical architecture is present in the perinatal period.

Why study cortical-subcortical connectivity in preterm infants ?

In adults, both thalamocortical and striatocortical systems are essential for processes such as reinforcement or reward-driven learning that are highly relevant to early neurodevelopment (Haber, 2014; Oldehinkel *et al.*, 2016; Gerraty *et al.*, 2018; Wang *et al.*, 2018) although it is unclear whether this thalamic and striatal functionality is

important as early as the perinatal period, or if disruption might impact on the acquisition of later capabilities. Thalamocortical and striatocortical connections in the mature brain are discussed in the following two chapters, thalamocortical organisation and striatocortical organisation. Important developmental events concerning the establishment of these systems during the third trimester are introduced here.

Important vulnerabilities in the third trimester

Thalamocortical organisation

Cortical projection neurons are generated in the ventricular zone (VZ) and subsequently in the sub ventricular zone (SVZ) (Bystron *et al.*, 2008) and follow a stereotyped radial pattern of migration leading to the inside out patterning of the neocortex (Sauer, 1935; Angevine and Sidman, 1961). The process of correct topographic patterning is facilitated by the sub-plate, a structure which hosts thalamocortical projections before they penetrate the cortical plate (Allendoerfer and Shatz, 1994; Bystron *et al.*, 2008; Kostović *et al.*, 2010). In humans, the subplate reaches maximum thickness between 17-24 weeks post-menstrual age, depending on the cortical area investigated, and remains at this thickness until 37 weeks due to the in-growth of fibres from many different systems including basal forebrain fibres, thalamic afferents and axons originating in ipsilateral cortex: there is an opportunity for interaction during the establishment of the six-layered cortical plate (Kostovic and Rakic, 1990). The process of establishing thalamocortical connections appears necessary for subsequent normal morphogenesis to take place (Kanold *et al.*, 2003; Constantinople and Bruno, 2013; Li *et al.*, 2013) and is disrupted by preterm birth (Malik *et al.*, 2013).

Prior to sensory information processing, spontaneous thalamic calcium waves from sensory thalamic nuclei appear to regulate the size of their cortical area in mouse (Moreno-Juan *et al.*, 2017). The onset of central responses to external sensory input has been widely debated in the context of consciousness; even prior to the establishment of definitive circuits, neurons in the subplate are formed as early as the second trimester (Kostovic and Judaš, 2006; Vanhatalo and Kaila, 2006) with neurons in the subplate of ferrets responding to auditory stimuli, as recorded using electrophysiological methods (Wess *et al.*, 2017). The exact timings in response to

different sensory modalities are not known, but auropalpebral ('blink-startle') reflexes to sound can be seen on ultrasound scans between 24-25 weeks gestational age (Birnholz and Benacerraf, 1983). Circuits involving primary cortex (further discussed in Chapter 1: Thalamocortical organisation) are known to be refined via sensory experience in the time period after the thalamic axons grow into cortical layer IV (Friauf and Shatz, 1991; Allendoerfer and Shatz, 1994; Kanold and Shatz, 2006), that is during the third trimester, giving rise to the suggestion that the abnormal sensory experience of the preterm infant might have an effect on the balance of these circuits (Slater *et al.*, 2012; Duerden *et al.*, 2018). With global connections and involvement in multiple cognitive functions (Hwang *et al.*, 2017), the thalamus has been shown to be a critical hub for information processing and integration, with an intact system of thalamocortical connectivity in adults proving essential for maintaining cognitive performance (Ystad *et al.*, 2011; Hughes *et al.*, 2012; Hwang *et al.*, 2017). Altered development of networks involving the thalamus is reported in the preterm population (Ball *et al.*, 2013).

Striatocortical organisation

In addition to the ventricular (VZ) and fetal neocortical subventricular zone (SVZ) mentioned above, three additional divisions of the SVZ can be found in the human forebrain: medial, lateral and caudal ganglionic eminences (Brazel *et al.*, 2003). These provide tangentially-migrating GABAergic interneurons (Wonders and Anderson, 2006) which are destined for thalamic association nuclei such as the pulvinar, anterior nuclear complex and medial dorsal nuclei (Letinić and Kostović, 1997), pallidum, neocortex and striatum (Wonders and Anderson, 2006). In the case of the pulvinar, these interneurons are not received until the 5-8th gestational month (Rakić and Sidman, 1969) leaving them potentially vulnerable to events during the third trimester. The GABAergic system develops in the second half of gestation with 20% of interneurons migrating during late gestation, while the rest (the majority) are resident in the subplate and play a role in corticothalamic circuit formation (Kostovic and Rakic, 1980; Kostović *et al.*, 2011).

The maturation of medium spiny neurons, the principal neuron of the striatum, is a postnatal event continuing for weeks or months after birth in monkey, cat and rat (Difiglia *et al.*, 1980; Levine *et al.*, 1986; Tepper *et al.*, 1998). The maturity of the

electrophysiological and morphological properties of the rat striatum are dependent on the arrival of excitatory efferents from cortex and thalamus (Tepper *et al.*, 1998). There is a paucity of evidence of the early development of these circuits (Peixoto *et al.*, 2016) but it is known that markers of gamma-aminobutyric acid circuitry (GABA), such as glutamic acid decarboxylases are still not detected in the ventral anterior and centromedian nuclei by 23 gestational weeks (Kultas-Ilinsky *et al.*, 2004) with the conclusion that connectivity of thalamostriatal circuits is not yet established. With regard to circuit formation, it is important to note that immature GABAergic neurons behave differently to those in the adult brain as a result of the increased expression of the chloride exporter potassium-chloride co-transporter 3 (KCC2) which maintains a higher intracellular chloride concentration compared with extracellular concentration (Yamada *et al.*, 2004). Activation of the A-type GABAergic receptor, which in adults mediates the major fast inhibitory action of GABA, instead leads to an efflux of chloride ions resulting in depolarisation. Immature interneurons are therefore excitatory during late gestation, whereas in adulthood they are inhibitory (Xu *et al.*, 2011). The switch to mature function comes in two phases, initially a reversible effect during birth, mediated by oxytocin's action on the KCC2 chloride co-transporter (Leonzino *et al.*, 2016) and may increase the resistance of fetal neurons to hypoxic insults during delivery (Tyzio *et al.*, 2006) and the second, permanent change to inhibitory status, which is completed by the end of the first postnatal week in rodents (Valeeva *et al.*, 2013). Consequently, in the third trimester in utero, both glutamatergic and GABAergic neurons synergistically promote proliferation, migration, maturation and differentiation (Manent and Represa, 2007) by inducing depolarisation and calcium influx through voltage-operated calcium channels (Leonzino *et al.*, 2016). There is potential for the balance of the emerging circuits to be altered (Kozorovitskiy *et al.*, 2012) by the experience of preterm birth.

The ganglionic eminences (of which a small part forms the germinal matrix in the fetus) are vulnerable to haemorrhage in the preterm population, as classified using computed tomography (CT) (Papile *et al.*, 1978) until around 32 weeks post menstrual age when the structure of the blood vessels in this area matures (Ballabh *et al.*, 2004; Ballabh, 2010). The anterior portion of the caudate head and anterior limb of the internal capsule (as well as nucleus accumbens, medial portion of orbitofrontal cortex, olfactory regions and anterior hypothalamus) share arterial supply with the germinal

matrix in the form of the recurrent artery of Heubner (Mavridis and Anagnostopoulou, 2010) and the vulnerability to injury following a bleed may be increased by the lack of anastomoses in the microvascular supply to the striatum (Feekes and Cassell, 2006). The incidence of intraventricular haemorrhage (IVH) in extremely premature infants weighing 500-750g is 45% (Wilson-Costello *et al.*, 2005) and is associated with decreased cell proliferation thereby providing one possible contribution to the reduced cortical thickness seen in preterm infants (Del Bigio *et al.*, 2011). In addition to the derivation of oligodendrocytes from radial glia (Rowitch and Kriegstein, 2010) the ganglionic eminences are also the principal source of oligodendroglial precursor cells, which are responsible for myelination (Volpe, 2018).

Disruption of neural circuits involving the striatum have long been recognised to result in cognitive and psychiatric deficits in addition to problems of motor execution, planning and control (Middleton and Strick, 2002). Early case reports of Huntington and Parkinson's Diseases include descriptions of psychiatric problems and cognitive impairments, and lesion studies in the first part of the twentieth century showed that the putamen and globus pallidus were associated with parkinsonian signs, dystonia and hemiballismus (Wilson, 1925). More specifically, volumes of caudate and putamen in preterm infants at term-equivalent age are positively related to motor scores, Wechsler abbreviated scale of intelligence and academic outcomes at 7 years. This association remains if infants with brain lesions such as periventricular leukomalacia (PVL) or grades III or IV intracranial haemorrhage, known to cause neuronal loss in the basal ganglia and thalamus of preterm infants with PVL (Pierson *et al.*, 2007) are excluded from analysis: the relationship between volume and motor function is the most robust (Loh *et al.*, 2017). There is also evidence that the specific vulnerability of caudate projection neurons to hypoxia-ischaemia in the preterm period leads to altered morphology with fewer dendritic branches but without acute or delayed cell death (Dean *et al.*, 2013; McClendon *et al.*, 2014).

Evidence from MRI at birth

There is a large body of evidence from structural and functional studies which suggests that Magnetic Resonance Imaging is a suitable technique to explore the effects of preterm birth on cortical-subcortical connections. Measurements of volumes of both thalamus and striatum show reduction in size in children born preterm (Loh *et al.*, 2017) with reduced thalamic volume predicting reduced volume in frontal and temporal lobes (Ball *et al.*, 2011) and associations between caudate and putamen growth and neurodevelopmental outcomes at 4 years (Young *et al.*, 2015). MRI measurements of the striatum show a reduction in the size of the caudate nucleus in particular (Abernethy *et al.*, 2004) and striatal volumes in general (Peterson *et al.*, 2000; Inder *et al.*, 2005; Ball *et al.*, 2011; Karolis *et al.*, 2017). Reduction in the volume of putamen and insular cortex has been linked with specific mathematical difficulties for those born at less than 30 weeks gestational age (Ullman *et al.*, 2015). An intact corticostriatal system appears crucial for many cognitive and motor functions including action selection, motor control, sequence learning and habit formation (Pennartz *et al.*, 2009) and executive function (Postuma and Dagher, 2006) as assessed using MRI. Areas of the striatum receiving inputs from all of the prefrontal regions have been identified as training the prefrontal cortex with which they are connected (Pasupathy and Miller, 2005) thereby forming information-processing hubs (Averbeck *et al.*, 2014) where motor, cognitive and reward functions can both interact and be disrupted.

Conventional neuroimaging at the time of birth has produced a wide-ranging account of the neuroanatomical locations and associated difficulties of preterm birth but is only just beginning to be able to predict some neurocognitive outcomes. While some studies demonstrate regional variability in the susceptibility of the effects of perinatal factors (Rogers *et al.*, 2016), others identify single regions affected by preterm birth (Aeby *et al.*, 2013) and others more global effects (Ball *et al.*, 2017). The mixed picture is evident with all imaging modalities currently employed. There is a difference in white matter maturation in tracts associated with motor and cognitive scores (Nieuwenhuys, 2012; van Kooij *et al.*, 2012; Duerden *et al.*, 2015), language (Aeby *et al.*, 2013; Salvan *et al.*, 2017) and evidence that multiple perinatal adversities effect white matter and outcome in motor, cognitive and language domains (Barnett *et al.*, 2018). Measures of subcortical growth have been associated with reduced

language scores (Young *et al.*, 2015) and both cognitive and language scores (Cheong *et al.*, 2016). White matter and reduced subcortical grey matter have also been associated with reduced cognitive scores at 2 years (Boardman *et al.*, 2010; Ball *et al.*, 2015). Resting state functional connectivity measures are a promising adjunct for providing prognostic information at the time of normal birth to complement investigations using diffusion weighted imaging which investigate the white matter microstructure. Circuits involving thalamus, cortex and striatum have particular vulnerabilities in the preterm brain and resting state methodology may be able to provide clarity as to specific circuits affected by prematurity and therefore predict the future function that may be affected.

Predicting outcome

Gestational age and other perinatal clinical details are often used when counselling parents about the outcome of being born prematurely but are imperfect predictors of outcome across the gestational range. Moreover, the predictors developed through research, may not reflect the values of parents, for whom behavioural problems and ability to live independently may be more important than categorisations of gross motor function (Janvier *et al.*, 2016; Lemmon *et al.*, 2019).

With regards to severe motor impairments such as cerebral palsy, abnormal pathologies detected with cranial ultrasound or MRI at term equivalent age, such as cystic periventricular leukomalacia and large intraventricular haemorrhages, are predictive of cerebral palsy with or without cognitive impairment depending on the extent and location of the lesion. Serial ultrasound during the first few post-natal weeks and then again at term equivalent age is able to identify lesions in 83% of those who go on to develop cerebral palsy (De Vries *et al.*, 2004) with MRI at term identifying myelination of the posterior limb of the internal capsule enabling prediction of non-ambulatory cerebral palsy (de Vries *et al.*, 2011). Structural imaging using MRI to identify white matter abnormalities using signal abnormality, periventricular white matter loss, cystic abnormalities, ventricular dilation and thinning of the corpus callosum increases the odds of a motor impairment at the age of five even after excluding children with cerebral palsy at 2 years from the analysis (Spittle *et al.*, 2011). Such criteria still leave infants without such structural

abnormalities at high risk of motor, cognitive, language and social and emotional problems (Edwards *et al.*, 2018). Meta-analysis of motor impairment in preterm children who do not go on to develop cerebral palsy found a pooled estimate for mild-moderate impairment of motor skills in such children at 40.5/100 (Williams *et al.*, 2010). There has been modest progress recently in selected cohorts without such structural abnormalities at the time of normal birth, such as studies of punctate white matter lesions (Tusor *et al.*, 2017) and mild germinal matrix-intraventricular haemorrhage (Tortora *et al.*, 2018). The ability of MRI to predict and demonstrate associations with outcome will be discussed in Chapter Three.

Outline of the thesis

In Chapter One, the established literature concerning the anatomical connections of thalamus and parcellations of the thalamus in the mature brain are presented first, followed by studies using magnetic resonance imaging, firstly with structural imaging, then diffusion-weighted imaging and finally using blood-oxygen level dependent imaging (BOLD) as is used in resting-state functional connectivity analysis in this thesis. The literature concerning thalamocortical connectivity in infants and children using magnetic resonance imaging is then presented in detail. Literature concerning the striatum and its parcellation is then presented in the same order in Chapter Two. Chapter Three presents all studies where imaging data were acquired at the time of normal birth and correlated with neurodevelopmental outcome measures collected around two years of age in preterm infants. A complete table of these studies' subjects, methods and results is then provided. When reviewing the literature, in order to analyse studies reflecting the characteristics of our cohort, only studies carried out after the widespread introduction of surfactant are included. This is because some studies show that the developmental trajectory of preterm infants before the introduction of surfactant, first shown to be effective in rodent in 1980 (Morley *et al.*, 1980; Wigglesworth, 1980; Halliday, 2005) and established as a safe treatment by the early 1990s (Engle and American Academy of Pediatrics Committee on Fetus and Newborn, 2008) is different from those born after (Doyle *et al.*, 2011).

After statement of Aims and Objectives, the materials and methods then follow with general methods in Chapter Four and study-specific methods in Chapter Five. This includes description of the EPRIME cohort and the criteria for subject selection

followed by imaging methods and the adaptations and optimisations I made for neonatal imaging: the study-specific parameters used in this thesis are then stated. Chapters Six, Seven and Eight then present results and discussions with Chapter Six presenting results of thalamocortical connectivity at the time of birth and the effect of prematurity, Chapter Seven, striatocortical connectivity at the time of birth and the effect of prematurity and Chapter eight, cortico-subcortical connectivity at birth and the correlation with outcome at two years. The thesis concludes with Chapter Nine in which methodological limitations are considered. In the Appendix A, a description of the implementation of boundary-based registration for neonatal imaging can be found and studies exploring the possibility of providing prognosis using imaging prior to term equivalent age are followed by the bibliography and publications.

Statement of research questions

1. What is the pattern of functional connectivity between cortex and thalamus or striatum at the time of normal birth and is this pattern altered in infants born preterm.
2. Is it possible to predict neurodevelopmental outcome at the age of two years from these measures of cortical-subcortical connectivity at the time of normal birth.

Part One

Literature

Chapter One

Thalamocortical organisation

Overview

This chapter discusses the literature regarding thalamocortical organisation from different perspectives arranged in the order in which the techniques were used. Firstly, an orientation of the established connectivity of the dorsal thalamus (referred to as thalamus, see Figure 1.1) based on post-mortem studies in humans and non-human primates using tract-tracing and immunoreactivity is presented, followed by parcellation of the thalamus according to the nature of subcortical input. As techniques have allowed investigation at a higher resolution, layer-specific cortical connections have been used to categorise and understand connectivity. The results from all of these methods have been synthesised to provide atlases defining connectivity not just between specific parings but in the whole brain of a species, motivated by the need for precision in stereotactic neurosurgery. Finally, the advent of magnetic resonance imaging has allowed the investigation of connectivity in humans in vivo.

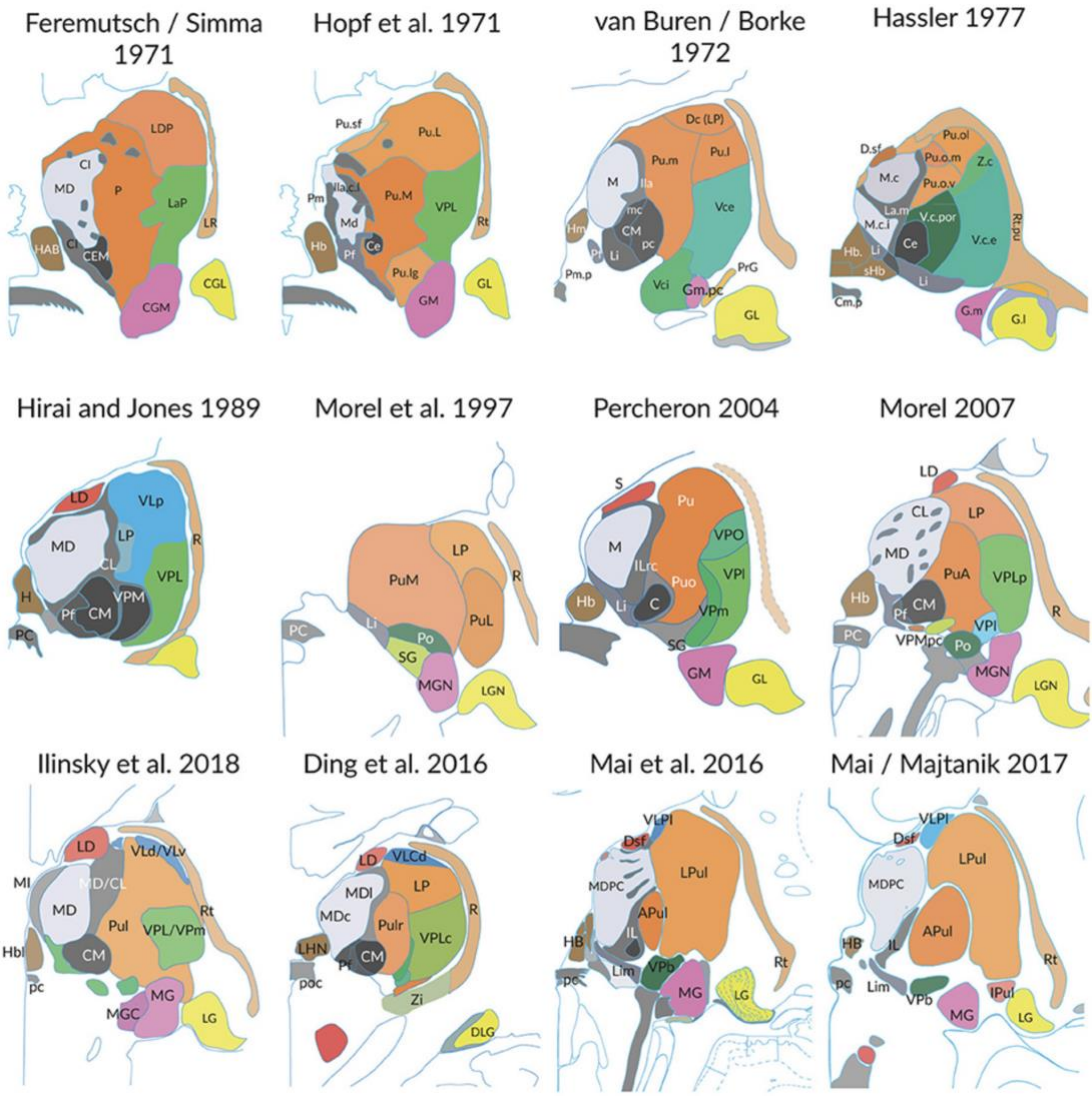

Figure 1.1 Competing parcellations between different atlases of the human thalamus (from Mai and Majtanik, 2019). Abbreviations to be found in supplementary table 5. Blue: cerebellar territory, green: somatosensory complex, orange: pulvinar, light grey: mediodorsal nucleus, dark grey and black: intralaminar nuclei).

Introduction

Parcellations of the thalamus and cortex have been attempted for over a century and in some cases, have led to the construction of 3-D maps, or atlases, of different structures. Different techniques and a multitude of careful studies in non-human primates and post-mortem human subjects over more than a century have contributed rich information, sometimes competing and sometimes complementary, about the complex arrangement between thalamus and cortex. Golgi staining was used by Santiago Ramón y Cajal and was one of the first methods to uncover the morphology and organisation of not only cortex but also of thalamic nuclei (Jones, 2002). The thalamus itself was the focus for Cécile Vogt at the beginning of the 20th century and she was joined in her laboratory by Korbinian Brodmann ((Vogt, 1909), www.wineurope.eu): the focus on cyto- and myeloarchitectural investigations has continued, perhaps most notably in the laboratories of Karin Amunts and Karl Zilles (Amunts and Zilles, 2015) and Edward Jones (Jones, 2007). Other ways of categorising the thalamus such as into relay and association nuclei by presence or lack of subcortical input (disputed by Jones 2007) aim to discover more about the function of individual nuclei of the thalamus rather than their structure (Sherman and Guillery, 2013). These investigations are complemented by studies which aim to understand larger units, such as thalamus in macaque (Olszewski, 1952) frontal cortex in monkey (Kievit and Kuypers, 1977) , thalamocortical connections in cat (Scannell, 1999) and the complete mature human thalamus in common stereotactic space for use in neurosurgery (Morel *et al.*, 1997; Niemann *et al.*, 2000; Krauth *et al.*, 2010). There is no neonatal thalamic or striatal atlas to facilitate identification and perform group analysis.

Prior to the advances in magnetic resonance imaging in the last decade of the twentieth century, there were no methods to track connections non-invasively and this resulted in incomplete understanding of the organisation of brain systems particularly with regards to those supporting cognition in humans (Crick and Jones, 1993). Using magnetic resonance imaging, the thalamus has been parcellated according to its cortical connections using both diffusion weighted imaging (Behrens *et al.*, 2003; Johansen-Berg *et al.*, 2005; O'Muircheartaigh *et al.*, 2011) and resting state functional connectivity (Zhang *et al.*, 2008; Fair *et al.*, 2010; Woodward *et al.*, 2012; Toulmin *et*

al., 2015). Increasingly, higher field strengths are being used to image the brain at a scale closer to that of the cyto- and myeloarchitectural investigations (Nunes *et al.*, 2019). These advances, at the scale of the cortical layer, are bringing new insights in connections between thalamus and cortex and will potentially establish a different hierarchy of thalamocortical connectivity than that defined in the literature so far.

Connectivity of thalamic nuclei by region

In the mammalian embryo (rabbit, rat and primate), the thalamus originates from the diencephalon as five undifferentiated pronuclei from which further subdivisions are made until the mature arrangement of greater than 30 nuclei is established (Rose, 1942; Swanson LW, 1992; Jones, 2007) each with their own cortical targets, anatomical position, markers, membrane properties and morphology. These differentiations are controlled by signalling proteins such as sonic hedgehog which controls the thalamic expression of Gbx3 transcription factor described in chick embryos (Hashimoto-Torii *et al.*, 2003) in both ventral thalamus (Kiecker and Lumsden, 2004; Vieira *et al.*, 2005) and dorsal thalamus (Szabo *et al.*, 2009). It should be noted that available evidence as to the structure of the thalamus has been obtained from a wide range of mammals and non-human primates (e.g. mouse, rat, rabbit, cat, New World Owl monkeys, squirrel monkeys, marmoset, rhesus monkey, new world titi monkey, macaque) and underlying architecture differs depending according to the species studied. The following account concentrates on studies in human and non-human primates with clarification where necessary.

Superior region

Nuclei belonging to this region include the anterior group of nuclei (such as anterior nucleus) and the superficial dorsal nucleus (or dorsalis superficialis) which shares architectonic characteristics as well as pathways (Nissl, 1889; Jones, 2007; Krauth *et al.*, 2010; Nieuwenhuys, 2013). Development of this region of nuclei starts late relative to other thalamic regions and final differentiation, according to

immunoreactivity for the marker CD15 is seen after the 16th week of gestation (18 weeks post menstrual age)

(Mai and Paxinos, 2012). Significant CD15 expression is associated with periods of circuit formation with low levels expressed during subsequent circuit maintenance (Andressen C, Thesis 2001, cited by (Forutan *et al.*, 2001)) and up- and down-regulation has been demonstrated during developmental events in the human central nervous system, including thalamic development, such as of the lateral geniculate body (Mai and Schönlau, 1992) and the basal ganglia (Mai *et al.*, 1999). Interneurons make up 50% of the neurons, second only to the medial dorsal nucleus (Dixon and Harper, 2001). The posterior border of the superior region consists of the superficial dorsal nucleus which merges with the pulvinar (Sachs, 1909). This region receives input from the hippocampus (caudal hippocampal formation (Aggleton *et al.*, 2010)) via the mammillary bodies and the mamillothalamic tract (Aggleton *et al.*, 1986). Subcortical afferents have also been established as coming from lateral hypothalamus, amygdala, pretectum (Irle and Markowitsch, 1982; Robertson, 1983)), pallidum (Parent *et al.*, 2001) with a diverse array of neurotransmitter systems (Mai and Paxinos, 2012). With regards to cortical relationships, these are with the anterior cingulum (Baleydier and Mauguiere, 1980; Shibata and Naito, 2005) and posterior cingulate cortex (Vogt *et al.*, 1979; Mikol *et al.*, 1984).

Medial region

The medial dorsal (MD) nucleus is located with the medial side bordering the third ventricle and other borders with the internal medullary lamina (Mai and Paxinos, 2012). It can be divided into three subdivisions based on features of myelo- cyto- or chemoarchitectonic architecture and distinct relations with the frontal cortex, namely, in studies in monkey, to orbital cortex, dorsolateral cortex and frontal eye fields (Walker, 1940; Kievit and Kuypers, 1977; Creutzfeldt *et al.*, 1979; Siwek and Pandya, 1991; Ray and Price, 1992; Ongür and Price, 2000). This thalamocortical circuitry is thought to be reciprocal (Mai and Paxinos, 2012) and probably linked to distinct functional and cognitive roles through the circuits involving cingulate cortex (Vogt *et al.*, 1979), insular cortex (Mufson and Mesulam, 1984; Ray and Price, 1992) and frontal lobe (Ray and Price, 1992; Floresco and Grace, 2003). Additional connections

have been defined in monkey which are thought likely to also be present in human such as with the supplementary area of the premotor cortex (Schell and Strick, 1984) and parietal cortex (Kasdon and Jacobson, 1978). Unidirectional input comes from the temporal lobe (Gloor, 1997). Subcortical afferents are GABAergic from the ventral palladium and substantia nigra (Ilinsky *et al.*, 1985; Percheron *et al.*, 1993), brainstem, amygdala and basal forebrain nuclei (Russchen *et al.*, 1987). The MD nucleus has the highest metabolic demands of the thalamus probably due to its high density of interneurons and these high demands are also seen in structures it connects with namely orbitofrontal cortex, amygdala and hippocampus (Baxter, 1992).

Intralaminal formation

Nuclei of the intralaminal formation share a common developmental history (Szabo *et al.*, 2009), cell type (Scheibel and Scheibel, 1967) and projections to the striatum (Van der Werf *et al.*, 2002). Cells can be categorised according to their pattern of Acetyl Cholinesterase activity which in the anterior division has a medial to lateral gradient (Jones, 2007). The centromedian nucleus (CM) and other anterior intralaminal group nuclei have reciprocal connections with all basal ganglia structures (Sadikot *et al.*, 1992; Parent and Parent, 2005). Centromedian nucleus projects to the motor and premotor cortices (Catsman-Berrevoets and Kuypers, 1978) where, in squirrel monkey, the efferents terminate in cortical layers V and VI (Parent and Parent, 2005) with reciprocal corticothalamic connections (Kultas-Ilinsky *et al.*, 2003). There are also efferent fibres from the CM to the limbic cortex (entorhinal and cingulate) (Insausti *et al.*, 1987; Vogt *et al.*, 1987; Sadikot *et al.*, 1992). Inputs to the anterior group of the intralaminar formation come from cerebellar, brainstem and spinal sources while inputs to the posterior group come from the globus pallidus. The posterior intralaminar group of nuclei also send efferents to the striatum and outer palladium (Parent *et al.*, 1983). Because of connections with virtually all structures of the basal ganglia, the CM nucleus is a candidate structure for modulation of basal ganglia function and as such is targeted in deep brain stimulation. It is considered by some to be an integral part of the basal ganglia system (Parent and Parent, 2005). Interestingly, the immunoreactivity of the medial dorsal nucleus to CD15 displays a matrix and striosome pattern reminiscent of the arrangement in the striatum with which it is connected (Forutan *et al.*, 2001). The parafascicular thalamic nucleus (Pf)

is also part of this region and along with the CM is important for attention, action selection behavioural flexibility (Brown *et al.*, 2010).

Lateral region

This refers to the motor thalamus (ventral anterior nucleus (VA) and ventral lateral nucleus (VL) and somatosensory thalamus (ventral posterior nucleus (VP).

i) Motor Thalamus

Subdivisions of the motor thalamus were defined in 1909 by their subcortical inputs which come from basal ganglia and cerebellum (Vogt, 1909) and updated with knowledge of contribution from the substantia nigra (SN) and identification of the internal segment of the globus pallidus (GPi) (Percheron *et al.*, 1996). Due to their definitions in different species, there is competing terminology and resulting confusion in the literature as to the delineation between the ventral anterior and ventral lateral nuclei; for example the ventral lateral anterior, as defined by Jones et al, is named as the ventral anterior (densocellular) nucleus by Ilinsky (Ilinsky and Kultas-Ilinsky, 1987) adopted by Mai (Mai and Paxinos, 2012) and named lateral oralis by Percheron (Percheron *et al.*, 1996). It is simplest here to describe the inputs to separate thalamic territory (deep cerebellar nuclei, globus pallidus internal segment and substantia nigra) and outputs of each region and refer to the 'motor thalamus'. One view of the 'extreme confusion' resulting from different nomenclature and parcellation in different species using different methodologies can be found in (Percheron *et al.*, 1996).

The inputs to motor thalamus (ventral anterior and ventral lateral nuclei), from GPi and SN, follow different developmental timelines (Kultas-Ilinsky *et al.*, 2003) and have segregated, non-overlapping forward connections with the cortex (Kuo and Carpenter, 1973) which are reviewed by Percheron (Mai and Paxinos, 2012). This area of the motor thalamus also receives input from the superior colliculus and from the amygdala, whose efferents subsequently project to the prefrontal cortex as part of the nigral-thalamic-cortical pathway (Mai and Paxinos, 2012). Direct efferents also go to the premotor cortex including the supplementary motor cortex (Strick, 1976; Morel *et*

al., 2005) and the primary motor cortex (Kultas-Ilinsky *et al.*, 2003), which projects directly to the spinal cord. The posterior part of the motor thalamus receives subcortical input (probably somatotopically organised) from the cerebellum and subsequently projects onwards to Brodmann area 4, the primary motor cortex (Jones *et al.*, 1978) where it reaches cortical layers 3-5. This is different from the onward projections from basal ganglia to thalamus which mostly project onwards to cortical layer 1 (Arbuthnott *et al.*, 1990; Kuramoto *et al.*, 2009; Shigematsu *et al.*, 2016). Functionally, the motor thalamus is part of the cortico-subcortical circuits described by Alexander et al (Alexander *et al.*, 1986) which help to prompt, enact and guide different aspects of voluntary movements (Middleton and Strick, 2002) (Middleton and Strick 2000) and are essential for motor learning (Tanaka *et al.*, 2018).

In addition to these direct circuits, there is an additional way in which the motor thalamus influences motor outputs. Inputs to the motor thalamus, come from branching axons where other branches also innervate other motor centres, thereby providing a duplicate message sent on to a different cortical area about upcoming motor actions (Sherman and Guillery, 2013). In this way an instruction about an upcoming eye movement, for example, can be duplicated to warn that the eye will be moving rather than make the mistake of interpreting the visual field movement as real motion in the world. When actions therefore happen, they are expected: these messages have been called 'efference copies' or 'corollary discharges' (Sherman and Guillery, 2013). The efference copies will reach cortical areas before the motor instruction will be enacted by muscle (via the spinal cord), thereby allowing a model or 'forward model' of how our body will relate to the environment (Wolpert and Miall, 1996; Wolpert and Ghahramani, 2000). These efference copies also help distinguish our own actions from those of others, usefully explained as 'we cannot tickle ourselves' (Blakemore *et al.*, 1998).

ii) Somatosensory Thalamus

The sensory thalamus is composed of distinct nuclei each with a different set of afferents and efferents to cortical areas. Together they are the relay between sensory input from the contralateral side of the body and cortex (le Gros Clark, 1936).

The ventral posterior nucleus is composed of two histologically-distinct subunits: ventral posterolateral nucleus (VPL) and ventral postermedial nucleus (VPM) with the VPL predominating in primates due to the larger representation of hands and feet (Rose and Mountcastle, 1952). VPL receives fibres of the spino-thalamic tract conveying information about noxious stimuli, temperature and sensation from the trunk and extremities, as well as lemniscal fibres carrying information about discrimination and proprioception (Mai and Paxinos, 2012). The lateral spinothalamic tract synapses in the VPL after which onward projections run to the mid/posterior insula and then onwards to the anterior insula providing information about the physiological status of the body (Craig, 2002). The VPM receives trigeminal fibres from the face and mouth (Mai 2012). Although the VPL and VPM are histologically distinct, they function as a single unit sometimes described as the ventralposterior (VP) nucleus (Kaas, 2007). All portions of the VP nucleus project somatotopically to the post-central somatosensory areas described as Brodmann areas 1,2,3 with continued segregation of modality (Padberg and Krubitzer, 2006). A discrete part of the VP nucleus (the parvicellular part) has efferents to the gustatory portion of the insula (Mufson and Mesulam, 1984) lateral and central amygdala and auditory cortex (De La Mothe *et al.*, 2006).

Posterior Group

In adult humans, the pulvinar makes up about 30% of the volume of the thalamus and has a comparatively late and protracted embryological and fetal course of development (Sidman and Rakic, 1973). The pulvinar is not amenable to classic architectonic mapping as there are gradual transitions between different cell types and groups, but although architecture, immunohistochemistry and known functional connectivity provide mismatching information about structure and function of the pulvinar (and therefore nomenclature), there are widely segregated connections with the cortex and different functional activities in different areas (Mai and Paxinos, 2012).

The medial pulvinar (MPul) has widespread projections to the prefrontal cortex as well as to multi-sensory areas (Barbas *et al.*,1991;Romanski *et al.*,1997). It is, itself, divided into a medial section and a lateral section with the medial section having

reciprocal connections with prefrontal cortex as well as superior temporal gyrus, cingulate cortex and amygdala whereas the lateral medial pulvinar also projects to a wide range of limbic cortices including insula, but unlike the medial portion, does not project to the amygdala (Yeterian and Pandya, 1991). The lateral pulvinar (LPul) is adjacent to the medial geniculate nucleus (MGN) and is connected with visual areas V1, V2 and ventral stream and a separate part has connections with inferior parietal and prefrontal cortex and is not involved with visual or sensory processing (Benevento and Miller, 1981; Kaas and Lyon, 2007). The inferior pulvinar is connected with the ventral stream of visual processing and contains a complete retinotopic representation of the contralateral visual hemifield (Petersen *et al.*, 1987).

Lateral geniculate Nucleus

This nucleus is shaped as an inverted U in monkeys, apes and humans and is named geniculate for its 'bent knee' shape (Jones, 2007; Mai and Paxinos, 2012). It is a laminar structure, composed of 6 magnocellular and parvocellular layers which are alternatively innervated by the contralateral and ipsilateral eye, forming retinotopic representations (Mai and Paxinos, 2012). It is intimately connected with the visual system, the optic tract entering at its hilus and the optic radiations leaving from the dorsal convex surface to relay to primary visual cortex (Jones, 2007; Mai and Paxinos, 2012).

Medial geniculate complex

The medial geniculate complex provides the relay station for auditory information and is organised into areas which are tonotopically patterned or layered in iso-frequency planes (Nieuwenhuys *et al.*, 2008). It is composed of three nuclei whose positions are ventral, dorsal and medial. The ventral nucleus is the most clearly defined nucleus of the medial geniculate complex (Hirai and Jones, 1989), receiving ascending auditory pathways via the ipsilateral and contralateral inferior colliculi and like the colliculi, displays lamellar, tonotopic representation (Merzenich and Reid, 1974). It subsequently projects to primary auditory cortex (Jones, 2007). The other two nuclei are not so clearly defined in terms of inputs and outputs. The dorsal nucleus has some

brainstem inputs and then projects to areas around the primary auditory cortex. The medial nucleus has a more diffuse projection including to the amygdala (Jones, 2007).

Reticular Formation

Connections between cortex and thalamus are arranged topographically within the thalamic reticular nucleus (TRN), with all thalamic relay cells from the thalamus having contact with nuclei of the reticular nucleus while passing through it on their way to layer 4 of the cortex, while afferents from layer 6 of the cortex pass through the reticular nucleus to reach the thalamus. As a result of the visual, auditory, somatosensory and motor sections, the TRN can act upon a subset or all thalamocortical pathways to modulate the firing patterns of thalamocortical connections (Guillery *et al.*, 1998). Its' well-known role in sleep and epilepsy are outside the scope of this thesis and structurally, it cannot currently be resolved on an MRI scan at the time of normal birth. The importance of a structure with influence over all thalamocortical efferents and afferents, however, is likely to be substantial.

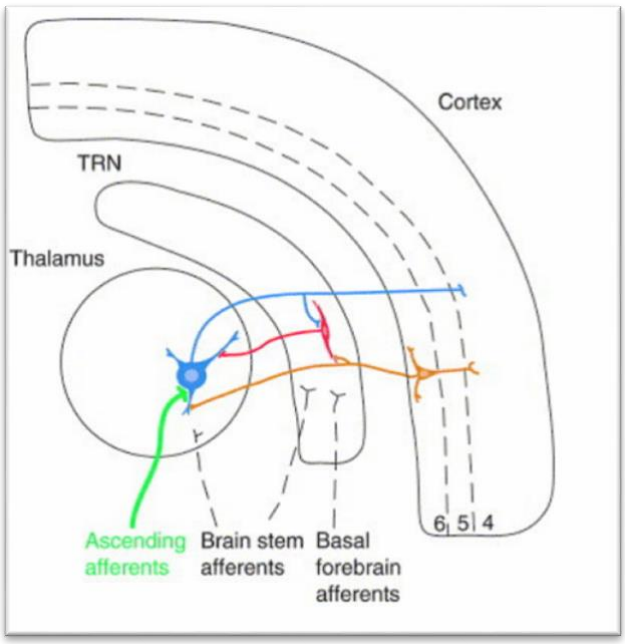

Figure 1.2. The major connections between thalamic relay cells (blue) cells of the thalamic reticular nucleus (TRN; red) and the cerebral cortex (orange). This shows connections from cortical layer 6 to thalamus and from thalamus to cortical layer 4 as it the case for most relay/first order thalamic nuclei (Guillery *et al.*, 1998).

Parcellation according to presence or absence of subcortical input

Information about nuclei of the thalamus has been explored in greatest depth for those nuclei concerned with major sensory pathways as it is possible to trace the input, via the thalamus to a known cortical destination which is malleable to experimentation such as visual input from the retina to the lateral geniculate nucleus of the thalamus and onwards to visual cortex (Hubel and Wiesel, 1962, 1966). These thalamic nuclei have been termed 'relay' nuclei, or 'first order' as the information comes from a subcortical source and appears to be 'relayed' to a well-characterised area of cortex unchanged (Sherman and Guillery, 2013). The areas of cortex which these first order nuclei connect with in a reciprocal fashion are termed 'primary' cortex and the organisation of this type of cortex is characterised by topographic maps whereby neighbouring points in the periphery are represented by adjacent locations in the cortex. Higher order nuclei (sometimes called association nuclei) receive messages from cortex to relay to distant cortex and some of these messages are modulated by the thalamus and some are propagated unchanged (Sherman and Guillery, 2013). It is experimentally difficult to determine whether a synapse is passing on a changed or unchanged message and this remains incomplete as a way of characterising thalamic function, but serves to place the thalamus at the centre of the understanding of brain function and connectivity and moves away from regarding the cortex as the basic unit of understanding (Sherman and Guillery, 2013). Categorisation using subcortical input has been challenged by Edward Jones as all nuclei have been shown to have subcortical input (Jones, 2007). As the greater complexity of thalamocortical connectivity is uncovered, it may still be useful to retain the simple distinction in terms of dominant functions of these nuclei.

Parcellation according to layer specific cortical connections

A further way of understanding thalamocortical connectivity is possible due to the increased magnification and characterisation of the inputs and outputs of different cortical layers. Recently, cortical layer-specific imaging has become possible at 9.4T in rat and shows the connections of the ventral posterolateral nucleus with layers 4 and

5 of somatosensory cortex (Nunes *et al.*, 2019). Given the different timings of the onset of functional connectivity of neural circuits, this will become important to the understanding of preterm brain injury as more is understood about these timings and of vulnerabilities: it will therefore be mentioned here briefly. In the schema of Sherman and Guillery mentioned above, thalamic function is divided into those areas which modulate messages (modulators) and those which pass on a message unchanged (drivers). Corticothalamic axons can be categorised by their morphology and function as modulators, which arrive from cortical layer VI and have reciprocal thalamocortical axons (Guillery, 1967; Llano and Sherman, 2008) and drivers (according to available evidence) which arrive from layer V of cortex and only go to higher order thalamic nuclei (Sherman and Guillery, 2013). Projections from layer V go to a different thalamic region to that providing the input into cortical layer V and these layer V connections may be the location of the functional overlap of cortical areas. Retrogradely transported tracers injected into any thalamic nucleus will label layer VI, but only tracer injected into higher order nuclei will label layer V (Gilbert and Kelly, 1975). To give an example from the visual system, layer VI of primary visual cortex receives input from the lateral geniculate and sends reciprocal output back to the lateral geniculate. The layer V outputs from the primary visual cortex, however, go to pulvinar or posterior medial nucleus (Van Horn and Sherman, 2004; Llano and Sherman, 2008). These connections are not established simultaneously, with those involving primary cortical areas being significantly more mature at the time of normal birth than those with 'higher' cortical areas such as pulvinar (Feig, 2005). Sherman and Guillery conclude that as the 'higher' areas are set up to monitor the motor output of the lower cortical areas, it makes sense for the circuits of primary cortex to be established first (Sherman and Guillery, 2013). Thalamic areas involved in reciprocal layer VI connectivity (compared with those receiving layer V output) are also areas which send initial thalamocortical efferents to subplate and onwards to layer IV of cortex rather than to cortical layer III (Guillery, 2005). These two characteristics of cortical connections with thalamus appear to be fundamental organising features of network formation: areas of cortex lacking layer IV (defined as having agranular cytology) correspond to areas which form the default mode network as well as association areas such as the insula and parietal lobes known to act as hubs for information integration (Wylie *et al.*, 2015).

Different layers of cortex are differently influenced by excitatory or inhibitory synapses: the detail is beyond the scope of this thesis. But briefly, in addition to the glutamatergic, corticothalamic axons from cortical layers VI and V (described above), the subcortical input to relay nuclei is also glutamatergic. Other inputs to the thalamus come from serotonergic cells in the raphe nuclei of the brainstem, histaminergic cells in the hypothalamus, dopaminergic input from the ventral tegmental area and noradrenergic cells in the parabrachial region (for review see Jones 2007). GABAergic input comes from local interneurons, striatum (globus pallidus) and zona incerta amongst others. These inputs and the reticular nucleus mentioned above, appear to play a role in modulating the way in which other incoming messages are relayed to the cortex (Sherman and Guillery, 2013).

Atlases

The need for an accurate thalamic atlas based on human data in order to improve the stereotactic precision with which neurosurgical treatments could target the thalamus, was the motivation for the seminal work by Morel et al (Morel *et al.*, 1997). Their atlas was based on neurochemical markers to identify architectonic parcellations and provide coordinates available to surgeons and was subsequently refined to relate it to neuroimaging (Niemann *et al.*, 2000; Krauth *et al.*, 2010). The thalamus is presented in lateral, medial, posterior and anterior groups and the connections of lateral somatosensory and motor nuclei, posterior complex and intralaminar nuclei are emphasised due to their neurosurgical relevance to neurogenic pain and movement disorders. The description of the structures of the nuclei is based on the work of others in human and non-human primates, such as the connections outlined above as well as the results of staining for the calcium-binding proteins parvalbumin, calbindin and calretinin which further delineate nuclei and subdivisions of nuclei for neurosurgical planning. The results show that nuclei expressing parvalbumin are largely separate from those expressing the other two proteins and include primary sensory relays (ventroposterior complex, lateral geniculate nucleus and medial geniculate nucleus) and centromedian nucleus. Calbindin appears where parvalbumin is not dominant while calretinin is concentrated in medial and anterior thalamic nuclei correlating with

their strong connections with limbic areas in cortex and basal ganglia and in the reticular nucleus which is the only area to contain both dense parvalbumin and calretinin. These results delineate a functional parcellation of the thalamus based on these calcium binding proteins. An important caveat here when consulting the Morel atlas for analysis of neonatal studies is the observation that the distribution pattern of parvalbumin and calbindin used by Morel et al to delineate the adult thalamus, is not yet established in the fetal thalamus (Forutan *et al.*, 2001).

An attempt to characterise the whole corticothalamic network in a single species (cat) using data mainly from connection tracing, but also cyto- and chemo- architectonics and data from electrophysiological mapping, was published in 1999 (Scannell *et al.*, 1999) and followed similar studies characterising the cortex alone (Scannell *et al.*, 1995; Scannell, 1997). The thalamocortical study by Scannell et al makes many explicit a priori assumptions about the data in order to construct a connectome from available studies. One such assumption, that thalamocortical connections 'show complete reciprocity', has not held true, but perhaps came about as a result of another problem identified by the authors: that of missing data mainly from areas of agranular cortex which do not show reciprocity (those areas with initial thalamocortical connections to cortical layer III). In spite of these challenges, Scannell et al identify four major thalamocortical systems which inform the cortical parcellations in imaging studies which followed: visual, auditory, combined somatosensory and motor system and a fronto-limbic system (prefrontal, cingulate, insular parahippocampal cortex, associated thalamic nuclei). They also identify that the association between fronto-limbic and somato-motor systems is particularly close.

Defining thalamocortical connectivity using magnetic resonance imaging in adults

Diffusion imaging

In the same year that Scannell et al published a corticothalamic parcellation in cat, magnetic resonance imaging, using properties of water diffusion along fibres bundles, was first used to demonstrate thalamocortical connectivity in vivo. Conturo et al performed non-invasive neuronal fibre tracking using the magnetic resonance properties of water diffusion to map the geniculo-calcarine pathway from a location (seed) in the lateral geniculate nucleus defined both from a T1 anatomical scan and from a task-based visual stimulation paradigm, via the optic radiations, to the primary visual cortex (Conturo *et al.,* 1999). The results are consistent with gross dissections, animal tracer studies and lesion analysis. These tracts were chosen for initial investigation due to their high anisotropy: the authors note the difficulty of tracking fibres using this methodology in cortical grey matter due to the low anisotropy in this tissue (Conturo *et al.,* 1999). Further details about diffusion imaging can be found in Materials and Methods.

Refinements in the analysis of diffusion data such as using k-means clustering to find voxels within the thalamus which are close both in position and diffusion as well as using information from the entire diffusion tensor to define the diffusion tensor distance term (rather that the principal eigenvector as in Conturo et al above) Wiegell et al resolve thalamic nuclei in the human thalamus which they compare with the Niemann/Morel (Niemann *et al.,* 2000) MR atlas of the thalamus (Wiegell *et al.,* 2003). They describe the clusters of common fibre orientation within each nucleus to be consistent with those defined by Morel and show a histological comparison which they say shows correspondence between clusters with similar diffusion orientation and the borders of the nuclei when defined histologically: in the two slices provided, however, plenty of contradictions exist with few obvious correspondences.

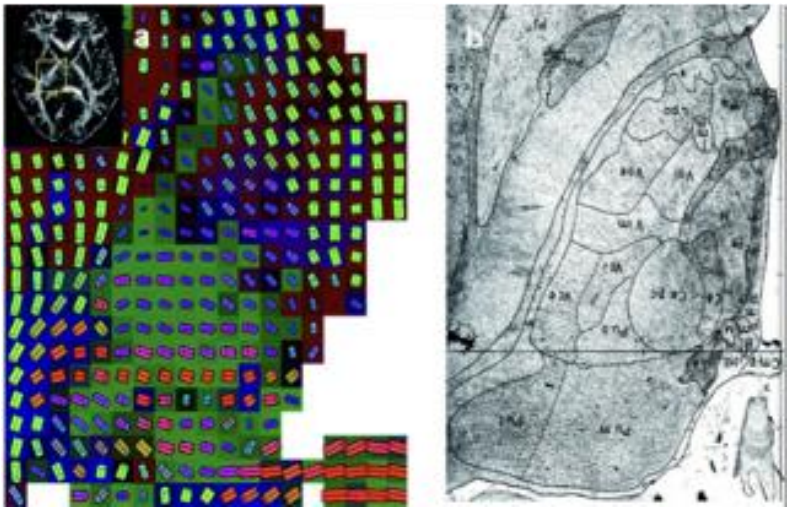

Figure 1.3. Wiegell et al 2003 showing a) diffusion tensor image compared with b) histological slice at a similar anatomical level from Van Buren and Borke 1972.

Using probabilistic tractography, that is taking the probability distributions of fibre directions at single voxels originating in the thalamus and identifying the cortical voxel which each thalamic voxel was most likely to terminate in, Behrens et al produced the first parcellation of the thalamus according to connections with the cortex both in an individual subject and in a small group (Behrens *et al.*, 2003). Importantly, they make no claim about the polarity of the connection as this methodology (in common with functional connectivity defined using resting state imaging) cannot define thalamocortical connectivity compared with corticothalamic connectivity. Of note, they did not include the insula in their possible cortical targets.

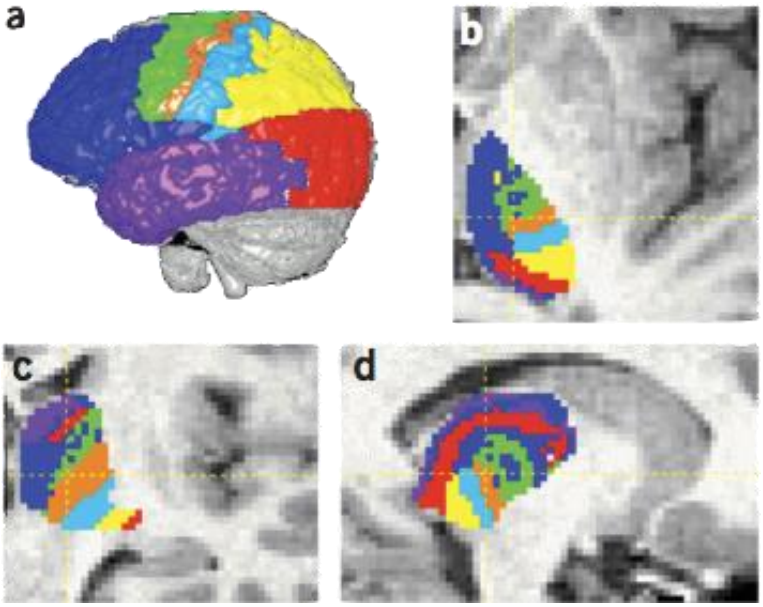

Figure 1.4. Shows the cortical masks, based on anatomical divisions and their corresponding most likely locations in the thalamus (Behrens *et al.*, 2003).

Following on from this study, the authors tested their results against a cytoarchitectonically-defined thalamic parcellation (Morel *et al.*, 1997) and against task-based functional activations in order to examine the link between structure and function (Johansen-Berg *et al.*, 2005). The 7 cortical regions of interest are similar to those in Behrens et al and this small number are used to simplify the analysis in order to overcome the problem of multiple thalamic targets from single cortical regions and multiple cortical targets from single thalamic regions. This oversimplification is, however, acknowledged and analysis in included which shows the existence of multiple cortical connections from each thalamic parcel. Prefrontal cortex, for example, could be defined as connecting with mediodorsal nucleus and also with ventrolateral nucleus but both connections were not present in all subjects. Areas of the thalamus activated during motor tasks were found to be regions of high probability of connection with sensorimotor and premotor areas, while those active in a memory or task assessing executive function co-localised with thalamic regions connected with the prefrontal cortex. This thalamic parcellation was likened by the authors to thalamic nuclei identified from histology, but while there may be similarities, it can be seen that diffusion imaging produces parcellations in strips perpendicular to the internal capsule rather than the shapes of thalamic nuclei defined by histology. There is, however, some evidence of this pattern from the labelling of thalamic nerve terminals in monkey frontal cortex which finds that thalamic regions sharing cortical connections are

arranged in bands which are arranged medial to lateral and which map onto cortical areas arranged in a transverse fashion (Kievit and Kuypers, 1977; Pandya and Yeterian, 1985; Parvizi *et al.*, 2006).

Motivated by the requirements of accurate electrode placement in deep brain stimulation and to explore the role of the thalamus in health and disease, Traynor et al built on the work by Behrens et al and Johansen-Berg et al to investigate the reproducibility of thalamic segmentation using probabilistic tractography (Traynor *et al.*, 2010). Cortical targets were defined anatomically, but in much greater detail than in previous studies, with the 83 cortical and sub-cortical labels (Heckemann *et al.*, 2006) propagated onto each subject. Two different sets of regions were investigated, 12 regions (6 per hemisphere) and 62 regions (31 per hemisphere). The regions were then segmented to produce masks of grey matter only. 5000 streamlines were then followed from each voxel in the thalamus mask, the grey matter cortical region of interest then being the termination mask. Each voxel in the thalamus was defined according to the cortical target to which the greatest number of streamlines from that voxel propagated. Using the six bilateral cortical targets, the following segmentation was produced:

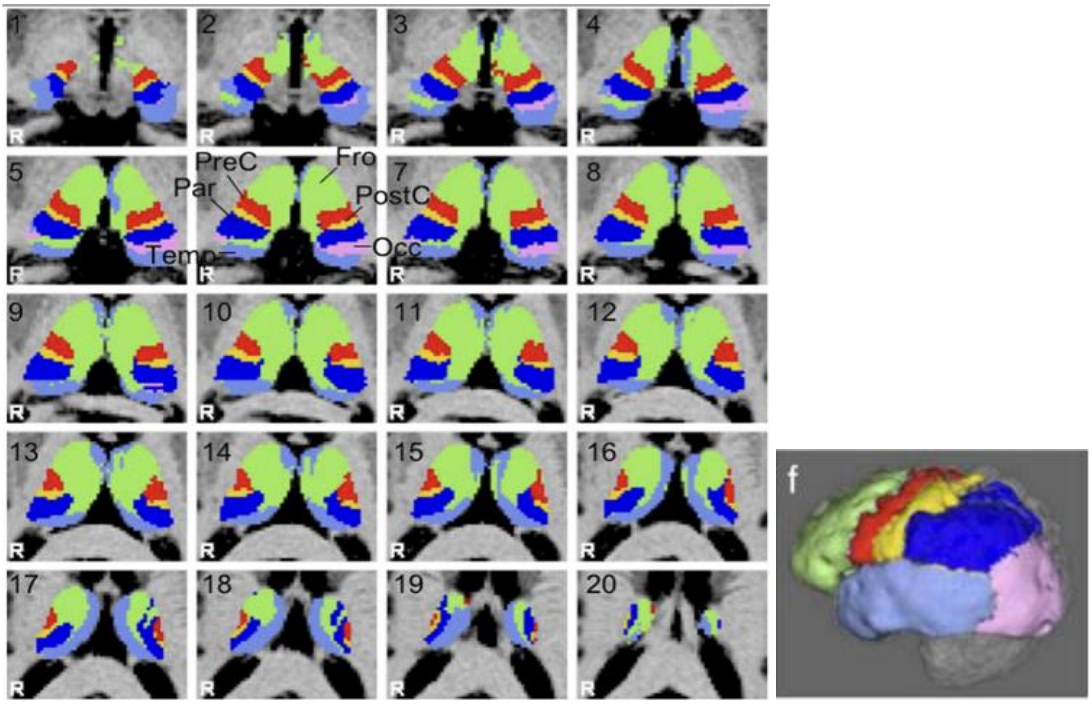

Figure 1.5. Thalamic parcellation based on 6 cortical regions using probabilistic tractography. Colour code as per cortical segmentation above (Traynor *et al.*, 2010).

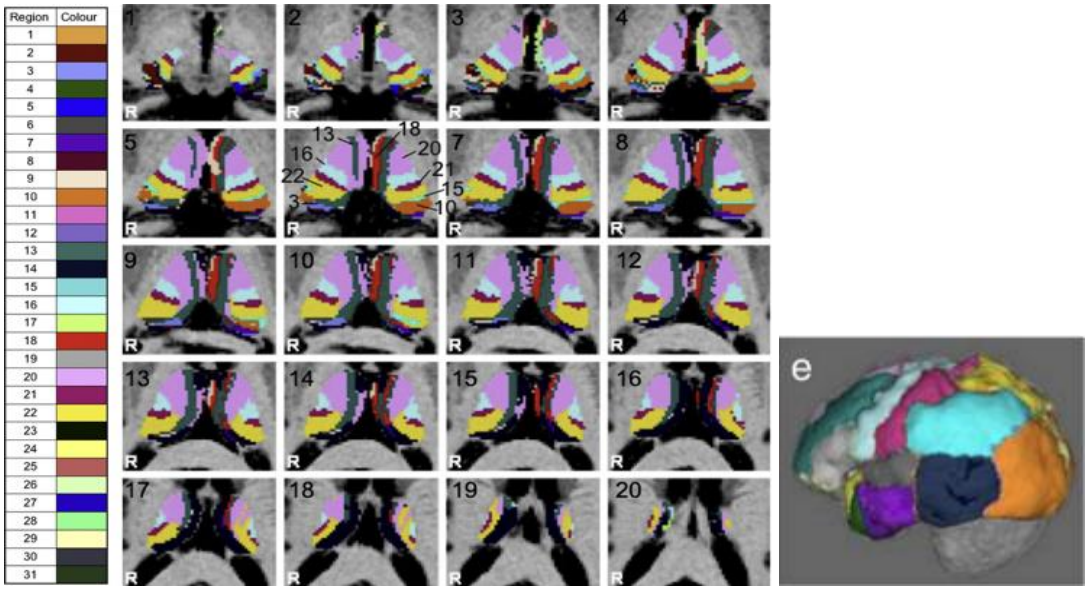

Figure 1.6. Thalamic parcellation based on 31 cortical regions using probabilistic tractography. Colour code as per cortical segmentation above (Traynor *et al.*, 2010).

To assess reproducibility, multiple datasets from the same subject were analysed in the same way. 55.5% of voxels in the right thalamus and 44.2% of voxels in the left thalamus received the same cortical label in all 16 sets of results. Using the 31 cortical segmentation, the results were 30.7% of voxels in the right thalamus and 25.4% of the left were labelled in the same way in all 16 sets of results. The consistent labelling was focused along the lateral edges of right and left thalami with more variation in the medial and posterior regions, as might be consistent with the role of medial and posterior nuclei in multiple different networks and with the technical difficulty of modelling crossing fibres in probabilistic tractography; variability also occurred at the boundaries between different thalamic parcels as would be expected. Reliability across subjects was decreased for the smallest cortical regions (post-central and occipital) and was also lower for a single subject suggesting there might be different thalamic anatomy (or connectivity) between subjects and therefore the potential to investigate between subject differences in disease using these methods (Traynor *et al.*, 2010).

Acknowledging the a priori assumptions about numbers of regions of interest as well as the other structures, such as basal ganglia and cerebellum which form integral parts of thalamic function, O'Muircheartaigh et al used independent component analysis as applied to diffusion tensor data (O'Muircheartaigh *et al.*, 2015). In this way, the large cortical areas could be interrogated for different source signals.

In addition, spatial overlap between regions from a single thalamic voxel (2mm isotropic) could be explored. The resulting thalamic partitions were used for functional connectivity analysis resulting in 7 spatial patterns of thalamic activity which are described by 7 rostral to caudal cortical and subcortical networks, connected with 7 medial to lateral thalamic regions, which the authors describe as strongly reminiscent of the pattern of connectivity described by Scannell in Cat and Kievit in monkey (Kievit and Kuypers, 1977; Scannell *et al.*, 1999).

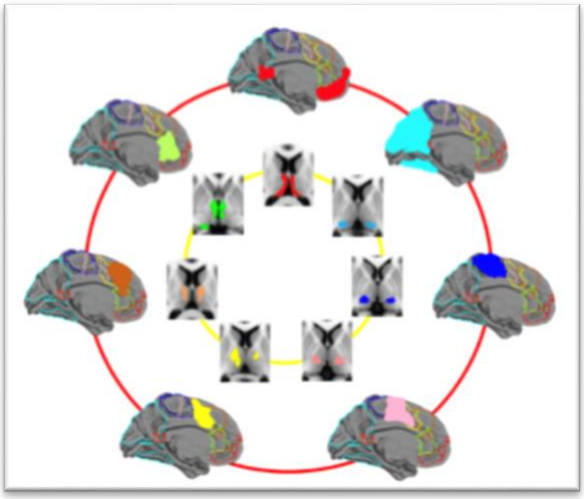

Figure 1.7. Summary of the rostral-caudal pattern of cortical connectivity and the medial to lateral connectivity in the thalamus (O'Muircheartaigh *et al.*, 2015).

Using spatial orientation of fibres to parcellate the thalamus, Vinod Kumar and colleagues define five clusters, common to 90% of all subjects which are located in the anterior, medial, lateral and posterior thalamus and therefore related to anterior nuclear group, medial dorsal nucleus (MD), medial pulvinar and the lateral group of nuclei. These structures had cortical connectivity with limbic structures, prefrontal cortex and medial temporal lobe, visual areas and medio frontal areas and motor and pre-motor and central sulcal areas of the cortex in line with anatomical studies in animals (Kumar *et al.*, 2014). Further work on thalamic parcellation was done by this group using resting state functional connectivity measures which will be discussed in the next section.

Resting state functional connectivity

The study by Zhang et al which used functional connectivity with the cortex to parcellate the thalamus was the starting point with regards to techniques to adapt for use in the neonatal population in this thesis (Zhang *et al.*, 2008). Dividing up the cortex into 7 areas on anatomical grounds, and then combining parietal with occipital and motor with premotor (again not including the insula) Zhang et al calculated the mean time series of each cortical region of interest (seed) and correlated it with voxels of the thalamus in a healthy adult cohort. In functional connectivity MRI (fcFMRI), as for diffusion imaging, information about the polarity of these connections cannot be inferred.

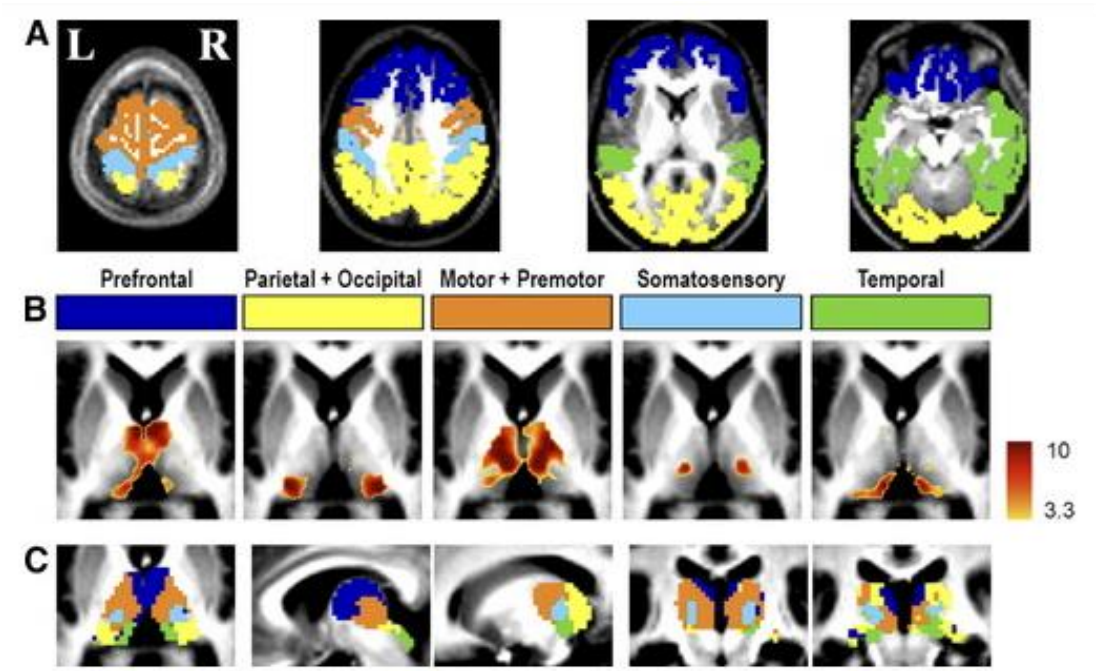

Figure 1.8. Cortical parcellations (A) and partial correlation maps for each cortical regions of interest (B). Winner takes all maps are shown in (C) showing the thalamic voxel according to the cortical ROI with highest partial correlation value (only including those where the winning Z-scare significance exceeded $P < 0.05$). In this study, the authors report that most thalamic voxels exhibited strong partial correlations with only one cortical ROI, with the exception of the medial pulvinar which had correlations with both prefrontal and temporal areas. The results for this study were repeated in a single hemisphere and the results were found to be similar to those obtained using bilateral cortical targets and thalamic seeds with the exception of the motor and premotor areas (orange) and the somatosensory cortex (light blue) (Zhang *et al.*, 2008).

Using similar methods to those in Zhang but cortical regions of interest reminiscent of those in Behrens et al 2003), Woodward et al parcellated the thalamus in 77 healthy subjects and 66 patients with schizophrenia (Woodward *et al.*, 2012) with results in healthy adults replicating those both those found in Zhang 2008 and in the adults included in the study by Fair et al (see imaging in infants and children). In subjects with schizophrenia, reduced connectivity was found with prefrontal areas and increased connectivity with motor and somatosensory networks showing this technique amenable to the investigation of between group differences.

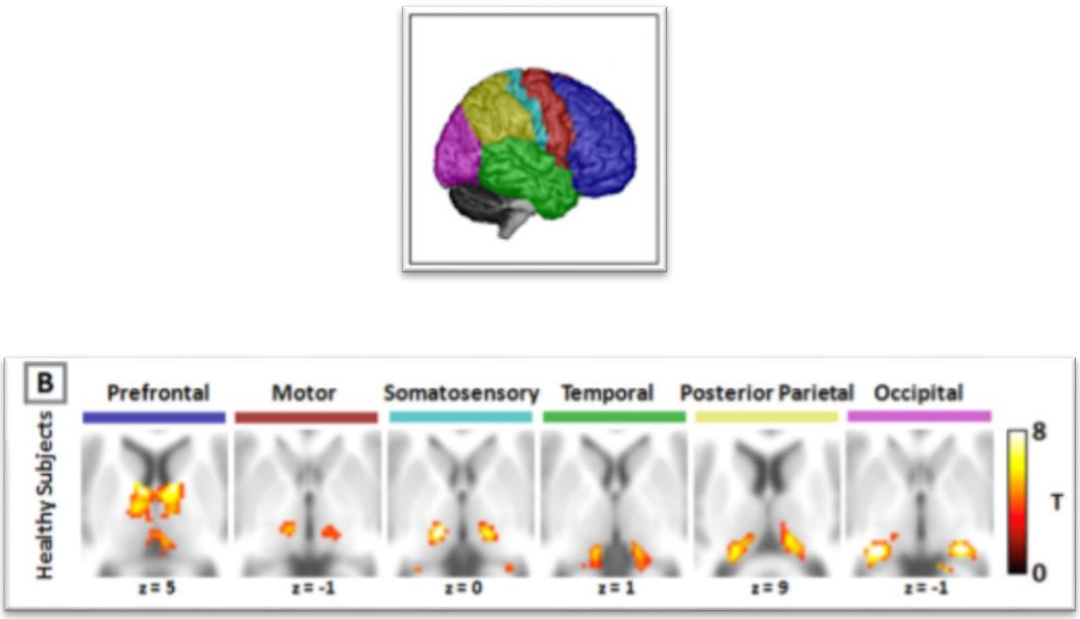

Figure 1.9. Thalamocortical connectivity in healthy adults using seed-based functional connectivity MRI based on anatomical regions of interest (Woodward *et al.*, 2012).

In a move away from anatomically-defined cortical areas to a data-driven approach, Kim et al use independent component analysis (further information in Materials and Methods) with a dimensionality of 50 from which 31 cortical components were selected (Kim *et al.*, 2013). Three of these represented the basal ganglia and thalamus and were used to define a second level of independent component analysis within these structures. Time series were extracted from each of the subcortical components and these time series were correlated with those from the original cortical components. A credible parcellation, with a symmetry in subcortical nuclei which had been split into lateralised components is shown; these subcortical seeds do not generally correlate

(using simple correlations) with bilateral cortical targets, however. There are a few aspects of the acquisition, such as a voxel size of 2.75 x 2.75 x 4.5mm in conjunction with a spatial smoothing (8mm FWHM) and lack of motion correction which make conclusions about the small structures investigated, insecure.

Comparing the two different methods of defining thalamocortical connectivity using resting state functional connectivity, that of seed-based functional connectivity and independent component analysis-defined corticothalamic networks, Hale et al use the methods from Zhang et al 2008, including anatomical definitions of 5 cortical regions of interest, to define a single mean time course with which to correlate time courses from each thalamic voxel using partial correlations (Hale *et al.*, 2015). Connectivity is then defined using a winner takes all approach at the subject level and the results are then averaged across subjects. The ICA approach employed, involves using the thalamus mask to interrogate the resting state data using independent component analysis on the data within the mask only (as is also carried out by Kim et al 2013). This was carried out at a lower dimensionality than that used by Kim et al, with Hale et al presenting results with a dimensionality of both 10 and 20: most components at a dimensionality of 10, with one exception, were found to have bilateral thalamic representation. The seed-based results did not show strong overlap with those from the histology-based thalamic atlas (Krauth/Morel) with the most overlap seen with that of the ventral lateral posterior nuclei with 'motor and premotor cortex' (dice coefficient of 0.14) and mediodorsal and ventral anterior nuclei to the prefrontal region of interest (dice coefficient of 0.15). The overlap between histological atlas and thalamic parcellations from ICA were greater with the mediodorsal nuclei having a dice coefficient of 0.38, while other components showed less overlap. Interesting structure was uncovered using the seed-based connectivity methods: the only connectivity map to overlap with a single thalamic nucleus was the 'Temporal' FC map which connected with the median geniculate nucleus (with which it has been found to have unidirectional anatomical connectivity according to Gloor et al 2007 above). Other structure uncovered includes the overlap between the ventral lateral nuclei and both 'Motor and Premotor' and 'Somatosensory' regions of interest, which is found anatomically, and this pairing is commonly found as a single cortical network in resting state cortical independent component analysis.

Acknowledging the more detailed connectivity existing between a single lobe of the cortex and the thalamus, Yuan et al employed an approach more like that developed for this thesis in order to provide a more detailed parcellation. Instead of using mean time series derived from 5 anatomical parcellations of the cortex, they use a more data-driven approach deriving whole brain functional connectivity maps for each voxel of the thalamus followed by independent component analysis in order to generate connectivity maps identifying spatially independent connections between thalamus and cortex (Yuan *et al.*, 2016). Using this methodology, they derive 20 independent components, of which 10 were 'visually identified as being quite similar to the standard networks that have generally been observed in resting-state fMRI studies.' No formal comparisons with published networks (such as Smith 2012) are made.

Also comparing the results of ICA-based parcellation with seed-based connectivity parcellations, Sheng Zhang and Chiang R. Li used a similar technique to that in Yuan et al for the ICA parcellation while the seed-based methodology developed that used by Zhang et al 2008 (Zhang and Li, 2017). To compute the seed-based correlations, the time course from thalamic subdivisions generated from the ICA were averaged for all voxels in each thalamic parcel. The correlation coefficient was then computed between this averaged time course and that of all the other voxels in the brain. Using the ICA methodology, they identify 10 thalamic components each with spatially distinct distribution and the same pattern of haemodynamic change over time; importantly; one of their metrics of comparison between the two methods is the degree of overlap between the parcels. The mean overlap rate using the ICA approach was 13% plus or minus 16, whereas there was greater overlap using seed-based connectivity methods (84% + or - 6%). Of interest methodologically, this study uses temporal band pass filter (0.009 Hz and 0.08Hz) and global signal regression as well as scrubbing individual data points with a range of 1 - 9% of data being removed per individual (96 in the study). They also retain the positive and negative correlations in seed-based correlation analysis which are of unknown significance and most studies (including this thesis) use absolute correlations rather than averaging positive and negative ones. The conclusion that less overlap using the seed-based methodology reveals a more detailed functional connectivity map may be true, but it may also be true that territories of the thalamus are shared between different cortical areas. It

highlights the problem of using overlapping seeds: when analysed, 82% of the voxels in one component (IC8) went into computing the time course for IC6 and therefore the time courses are very similar. When only non-overlapping voxels were used to compute time courses, it was found that the negative contribution and positive contributions of the correlations cancelled each other out. It may be that with a voxel size of 4mm isotropic and a smoothing with a Gaussian kernel of 8mm at full width half maximum, that spatial precision to analyse the connectivity of thalamic nuclei at the sub-nuclear level has been lost: spatial smoothing is not performed on data used for seed-based correlation analysis in other studies using this technique (Zhang *et al.*, 2008; Fair *et al.*, 2010; Woodward *et al.*, 2012; Yuan *et al.*, 2016) or in the analysis of seed-based connectivity in this thesis.

Continuing interest in thalamic parcellations, previously using diffusion weighted imaging (Kumar *et al.*, 2014) Kumar et al derived parcellations of the thalamus using resting state fMRI and methods with similarity to those used in this thesis, such as the use of FIX for data denoising and functionally-derived cortical parcels using ICA. Right and left thalamus were interrogated separately. An additional step was employed prior to the ICA which resulted in a parcellation of the thalamus into sub-regions according to temporal characteristics by performing an initial spatial regression on the resting state data using data from within the anatomical thalamic mask to obtain average time courses per subject and subsequently correlating these with the time series of every voxel. Group ICA was then performed on all these individual results (Kumar *et al.*, 2017). As estimated using split half reproducibility, there were 14-15 reliable parcels on the right and 15-17 on the left. The number of 15 parcels was chosen for each thalamus. The authors compare results with anatomical atlases and visually show similarities when this number was confined to 9 major nuclei on each side: they accurately assert that direct anatomical comparisons are made very difficult because of the difference in definition, naming and number of human thalamic nuclei in the literature.

Defining thalamocortical connectivity using magnetic resonance imaging in infants and children

The literature defining connectivity at birth and alterations with preterm birth is sparse. Studies using diffusion imaging are presented first, followed by those using resting state functional connectivity measures.

Diffusion Imaging

Similar methods to those used by Behrens el at in adults are used by Counsell et al in a group of 12 infants, using 4 cortical masks corresponding to frontal-temporal cortex, occipital-parietal cortex, motor region and somatosensory cortex (Counsell *et al.*, 2007). They find connections to be strongest between frontal-temporal cortex and a thalamic area including the mediodorsal nucleus, parietal-occipital cortex and pulvinar, motor area and ventrolateral nuclei and somatosensory area and ventral posterior nuclei in line with those found in adults using diffusion imaging and in congruence with anatomical studies. In a proof-of-concept study, they show that these connections were altered in an infant with a large porencephalic cyst. Using a hand-drawn thalamic template, Ball et al use the measure of deformation required to transform images of 71 preterm thalami to a reference template using non-linear registration (Ball *et al.*, 2011). In addition to deformation-based morphometry, Tract-based spatial statistics (TBSS) were used to analyse white matter tracts. At term-equivalent age, they find that increasing prematurity is associated with a reduction in size of the thalamus and this covaries with a reduction in cortical volume in white and grey matter proximal to the thalamus as well as the orbitofrontal lobes, posterior cingulate, hippocampus and centrum semiovale suggesting a widespread effect of prematurity associated with disruption to thalamocortical connections.

In a subsequent study, Ball et al used diffusion imaging between thalamus and cortex and avoided the need for accurate delineation of corresponding cortical regions across subjects by choosing iterative mapping of 25 random parcellations of the cortex for each of the infants studied (Ball *et al.*, 2013). Connectivity with the ipsilateral hemisphere only was investigated and different connectivity between thalamus and cortex in a term-born group of 18 infants and the preterm group of 47 preterm infants (range 23+4 - 34 +6) was studied. Thalamocortical connectivity was significantly

affected by immaturity at birth in multiple cortical regions but no specific pairings between thalamic regions and cortical regions were identified using this method. Duerden et al (2018) aimed to identify more specific pairings of thalamocortical disruptions in infants with white matter injury demonstrated on structural T1-weighted scans (Duerden *et al.*, 2019). Their findings, based on diffusion imaging, were that connectivity strength between thalamus and parietal networks and thalamus and sensorimotor networks is associated with lateralised differences in the volumes of various white matter tracts. This provides some specificity concerning the impact of white matter injury on thalamocortical connectivity.

Resting state functional connectivity imaging

Using resting state functional connectivity imaging, Doria et al placed a manually defined seed in the left ventral lateral nucleus of the thalamus in preterm infants with a medial gestation age at birth of 30.2 weeks (range of 25.4 - 35.4 weeks) and at term equivalent age and found correlations with the ipsilateral sensory-motor cortex, both with the lateral and medial portions and limited connectivity in homotopic cortex contralaterally (Doria *et al.*, 2010). This study excluded infants with overt brain lesions on conventional MRI but had a high proportion (35 out of 62 infants) with defuse excessive high signal intensity (DEHSI) in the white matter. Another study also excluding 'prominent neuropathology' investigated both resting state networks and connections involving the thalamus in preterm infants (Smyser *et al.*, 2010). Smyser et al collected images of preterm infants within the first 2 weeks of life, with the first scans being performed at 26 weeks post-menstrual age PMA and again every 4-5 weeks until the time of normal birth. This study resulted in data at two time points for 28 infants and 3 time points for 5 subjects. It was designed to look at the development of thalamocortical connectivity over time rather than the effects of prematurity but results comparing preterm infants imaged at term show a more robust localised and inter hemispheric connections as shown by increased voxels in each hemisphere in the term control infants when compared with the preterm infants. In addition, connections

between thalamus and sensorimotor cortex are stronger in the control term group compared with the preterm infants (Smyser *et al.*, 2010).

In a study designed to look at the development of thalamocortical connectivity in the first two years after birth, 143 subjects who had been born between 35- and 42-weeks gestational age and who had been scanned at two separate time-points were identified from a cohort of healthy and high-risk children with no significant abnormalities on MRI scan (Alcauter *et al.*, 2014). Nine networks identified in adults in Smith et al 2009 were used to define non-overlapping cortical targets from which average time series were obtained per-subject and partial correlation were computed with each thalamic voxel using all other cortical time series. With regards to the resting state networks adopted from Smith et al 2009, Alcauter find networks involving primary cortex such as sensorimotor, auditory, medial visual and occipital to have adult-like anatomical distributions. The salience network in infants is found to encompass the key structures attributed to this network in adults (Seeley *et al.*, 2007) namely bilateral anterior insula, anterior cingulate and bilateral prefrontal cortex and is found to undergo local specialisation during the postnatal period. The other higher order networks are described as undergoing dramatic improvements in network topography, from single homotopic anatomical regions to distributed networks by the first year. With regards to thalamocortical connectivity in the neonatal group, bilateral symmetrical clusters were observed with a large sensorimotor cluster covering the central portion of the thalamus (ventral nuclear group extending into anterior, medial dorsal and pulvinar), while the salience network was limited to the most anterior portion of the thalamus (anterior nuclei territory). By one year of age, sensorimotor connectivity occupies a neater area of the ventral and lateral regions, while the salience network had extended to include a larger anterior and dorsal portion of the thalamus. Results at the time of normal birth differ from those found in this thesis and this is discussed in Chapter Six.

The same cortical areas as those used by Zhang et al (2008) were adopted by Fair et al to look at functional connectivity over development using groups of 17 7-9-year

olds, 21 aged 11-16 and 14 aged 19-32 (Fair *et al.*, 2010). The results in adults are in agreement with those in Zhang et al 2008 and correspond to expected connectivity between thalamus and cortex as described by tracers (as detailed earlier in this chapter). Over the course of development, Fair et al describe substantial differences in connectivity patterns between thalamus and frontal lobe and thalamus and temporal lobe, with the frontal connections appearing weak in childhood compared with adults and temporal connections stronger in childhood and decreasing by adulthood (Fair *et al.*, 2010).

Chapter Two

Striatocortical organisation

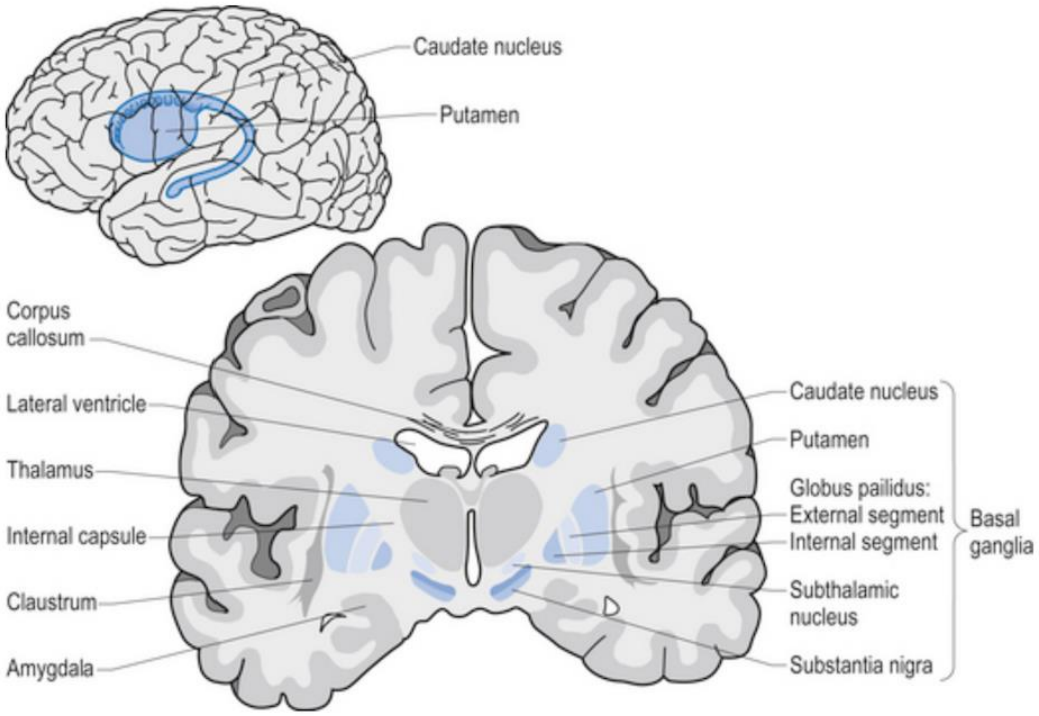

Figure 2.1 Basal ganglia and related structures (from clinicalgate.com/the-basal-ganglia)

Introduction

Various different models have been proposed to describe the architecture of the mature basal ganglia. Different categorisations have been proposed such as by cortical regions to which circuits through the basal ganglia return (Alexander *et al.*, 1986), three distinct zones of the basal ganglia, namely associative, sensorimotor and limbic using cyto- and myeloarchitecture, tracing studies and tract degeneration studies (Parent, 1990), basal ganglia regions defined by connectivity with thalamus (McFarland and

Haber, 2000, 2002) and integration of frontal networks involving basal ganglia in a rostral-caudal organisation of corticostriatal fibres (Haber, 2003). More recently, studies in adult human using functional MRI have suggested 5 main parcels according to functional connections: sensorimotor, premotor, limbic and two association networks (Choi *et al.*, 2012) while task-based studies have suggested a parcellation into sensorimotor, social and language, stimulus value, action value and executive function (Pauli *et al.*, 2016). This chapter presents evidence of connectivity between striatum and other structures, concentrating on those with thalamus and cortex, firstly using methods which explore anatomical connectivity and then proceeding to present literature concerning striatocortical connectivity using magnetic resonance imaging, both diffusion imaging and resting state functional connectivity. A detailed review of connectivity using anatomical methodologies can be found in Parent and Hazrati (Parent and Hazrati, 1995).

Definition

The Corpus Striatum refers to the paired structures of caudate nucleus and putamen which are characterised by a central striped (striated) portion due to the throughput of cortical axons. With the discovery that the nucleus accumbens, medial and ventral portions of caudate and putamen and parts of olfactory tubercle shared connections, cell morphology and architecture (Heimer and Kalil, 1978), these additional areas have been referred to as ventral striatum and the former dorsal striatum by Suzanne Haber (Mai and Paxinos, 2012). The dorsal striatum, however, is commonly referred to as 'striatum' and will be in this thesis. The pallidal complex, is comprised of the globus pallidus internal and external segments and, together with the putamen, these are known as the lentiform nuclei due to the lens-like shape. The sub thalamic nucleus and the substantia nigra are also considered components of the basal ganglia but are not included in the analysis in this thesis, or in the imaging studies reviewed in this chapter. Nomenclature regarding basal ganglia and striatum is often imprecisely used. Although striato-pallidal complex would be more accurate, this thesis has, like many other investigations into the structure, adopted 'striatum' to refer to the adjoining parts of the basal ganglia.

Structure

In contrast with the nucleated structure of the thalamus, cytoarchitectural studies of the striatum show a rather homogenous form. Immunohistochemical evidence using acetylcholinesterase (AChE) staining reveals areas which have weak AChE activity, named 'striosomes' or 'patches', and those which stain more intensely for AChE named 'matrix' (Graybiel and Ragsdale, 1978). The patches are visible in the putamen by the 16-18th week of gestation, but lag behind in the caudate, with clumping of cholinesterase first seen from the time of normal birth and the adult pattern displayed by the fourth postnatal month (Graybiel and Ragsdale, 1980). Motor and sensory areas of cerebral cortex along with thalamostriatal projections, mainly innervate the matrix, whereas cortical limbic areas target striosomes with these inputs arriving from different cortical layers (Künzle, 1975; DeLong *et al.*, 1985; Eblen and Graybiel, 1995; Reiner *et al.*, 2003; Crittenden and Graybiel, 2011). Medium spiny neurons, the predominant neuron of the striatum, also receive input from ventral, midline and intralaminar nuclei of the thalamus (Purves *et al.*, 2011). A single cortical axon contacts multiple medium spiny neurons in the striatum providing a mechanism to integrate cortical information. Interactions between these functional territories have been investigated and found to be extensive and occurring in regions where the terminal fields from different functional cortical regions converge: such as those known to be involved in reward and cognition (Haber *et al.*, 2006). It is the striatum which is identified as the trainer of the prefrontal cortex during acquisition of associative motor learning such as 'stop at red' (Pasupathy and Miller, 2005). Areas of the striatum which receive inputs from multiple cortical regions are therefore 'candidates as information-processing hubs' (Averbeck *et al.*, 2014) providing a location for the interaction of cognition, motor function and reward.

Connections of the striatum

Overview

The circuitry of the striatum is also very different from that of the thalamus: the striato-pallidal complex has input, internal and output segments and two separate circuits known as 'direct' and 'indirect' are classically described (Mai and Paxinos, 2012). Wherever the cortical input to the striatum has originated, the 'direct' pathway is

GABAergic via striatal neurons containing substance P and projects to globus pallidus internal segment or Substantia Nigra pars reticulata (SNr) while the 'indirect' pathways, which is also GABAergic, but from striatal neurons containing enkephalin, projects via a sequence of connections involving globus pallidus external segment and subthalamic nucleus to the globus pallidus internal segment (GPi) or SNr (Alexander *et al.*, 1990). With increased research into the subthalamic nucleus, this has been amended with a third, 'hyper direct', pathway which bypasses the striatum altogether providing cortical input to the subthalamic nucleus and onwards to the globus pallidus (Nambu *et al.*, 2002). The subthalamic nucleus (STN) receives direct cortical projections from frontal lobe, such as the somatotopically-organised projections from primary motor cortex, supplementary motor area and parts of premotor cortex (Nambu *et al.*, 1996). This hyper direct pathway has been integrated into basal ganglia motor theory as providing a corollary signal generated by cortex at the same time as a voluntary movement. This activates the GPi which serves to inhibit areas of the thalamus and cortex which are concerned with all motor programmes: the direct and then indirect pathways deliver sequential corollaries which function to allow only the selected motor programme to be initiated, executed and then terminated (Nambu *et al.*, 1996). The white matter tract underlying the hyper direct pathway has been demonstrated using diffusion-weighted MRI and task-based functional magnetic resonance imaging (Aron *et al.*, 2007). The different influences on these three different pathways can be briefly mentioned: cortical-STN neurons originate from collaterals of pyramidal tract neurons and so are directly related to movements, whereas cortical-striatal neurons have been shown to be context (Kimura, 1990) and reward-dependent (Kawagoe *et al.*, 1998; Samejima *et al.*, 2005). This is the result of different influences on each of these inputs. The putamen, for example, receives inputs from multiple sensory cortices in addition to cortical motor areas and the area of the putamen adjacent to the caudate tail which receives visual input from the contralateral hemifield, controls aspects of saccades and attention (Kunimatsu *et al.*, 2018).

With regards to the detailed connections between frontal cortex and striatum, multiple closed cortico-striato-thalamo-cortical circuits connecting back to the cortex have been described (Alexander *et al.*, 1986, 1990) and this model has been expanded to show both segregated loops and the extensive overlap of the terminal cortical domains

(Selemon and Goldman-Rakic, 1985). Many of these studies and more recent imaging studies have concentrated on the connections between frontal cortex and striatum, often in the investigation of reward (Haber and Knutson 2010), although inputs to striatum have been demonstrated from almost the entire cerebral cortex (Selemon and Goldman-Rakic, 1985) with the primary auditory cortex and primary visual cortices the only cortical areas which have not been found to innervate the striatum (Purves *et al.*, 2011). Tractography studies in humans, however, have not identified projections from temporal or parietal cortices (Draganski *et al.*, 2008; Verstynen *et al.*, 2012). Understanding the role of the thalamus in these circuits, itself receiving direct input from the cortex, has allowed the expansion of the idea of closed loops, allowing modulation of the circuits at the level of the thalamus (McFarland and Haber, 2002; Sherman and Guillery, 2002).

Cortical input

Cortical projections to the basal ganglia are to the caudate and putamen and are thought to come from the pyramidal neurons of cortical layer V although there are some areas where layer III also contributes (Jones *et al.*, 1977; McFarland and Haber, 2000). The cortex projects to the input areas of the striatum topographically (Selemon and Goldman-Rakic, 1985), and, by association with cortical regions, the striatum is associated with the different specialisations of cortical regions: caudate nucleus with cognition, putamen with sensorimotor control and ventral striatum with emotion and reward. Cortical input is further organised, such as the somatotopic representation of the projections of the sensorimotor cortex in the putamen demonstrated in monkey (Künzle, 1975; DeLong *et al.*, 1985).

With regards to motor connections, tracer injections to the hand region of the primary motor cortex and SMA (ipsilateral cortex) in monkeys show that the SMA projects more medially and the motor cortex more laterally in the monkey putamen (Takada *et al.*, 1998). An inverted topography is contained within the representation of the primary motor cortex, with the foot found in the superior putamen and the tongue inferiorly using tracer studies (Künzle, 1975; Flaherty and Graybiel, 1993). This detail has been replicated in studies of the basal ganglia in human adults (Verstynen *et al.*,

2012) and adolescents (Greene *et al.*, 2014) using MRI fibre tractography. These studies using in-vivo white matter tracking methods have not found the connectivity with the parietal and temporal lobes shown in tracer studies, possibly due to the areas of complex fibre crossing required to reach the striatum from these two lobes (Verstynen *et al.*, 2012). The contribution of the insular cortex has been demonstrated using anatomical methods, but it was not included in models of cortico-striato-thalamic loops as proposed by Alexander et al and others and has not been included in most analyses of connectivity using diffusion imaging methods or resting state functional connectivity imaging. The contribution of insular cortex to these loops may be suggested by the different cytoarchitectonic location of insular inputs to the striatum: Chikama et al, found that the ventral striatum (often labelled 'limbic') receives inputs from agranular insular regions, while the granular insular projects to the dorsolateral ('sensorimotor') striatum (Chikama *et al.*, 1997). As seen in chapter one, the thalamus has also been categorised according to whether inputs come from cortical areas with layer IV (described as granular) or absent layer IV (agranular).

Intrinsic connections

The basal ganglia can be divided into components which receive input (caudate, putamen), and the site of output (globus pallidus internal segment (GPe) and substantia nigra pars reticulata (SNr) and those parts which connect internally and are thought of as 'intrinsic nuclei' (globus pallidus external segment (GPe) and substantia nigra pars compacta (SNpc)). Fibres from the Putamen terminate in the ventral two-thirds of the globus pallidus, with only a few fibres running to the substantia nigra: the opposite is true for fibres from the caudate, which run sparsely to the dorsal third of the globus pallidus but show 'profuse arborisation' in the rostral two-thirds of the substantia nigra (Smith and Parent, 1986). This is simplistic as there is a complex organisation within the basal ganglia circuitry itself, for example, the GPe and GPi are reciprocally connected classifying the GPi also as intrinsic nuclei, able to act as an integrative area for information processing within the basal ganglia (Parent and Hazrati, 1995).

The subthalamic nuclei have been regarded as a control structure, somewhat outside the circuits described, receiving inputs from many structures involved in basal ganglia

circuits, although not from striatum, or GPi/SNr (substantia nigra pars reticulata): outputs are to GPe (with which it has reciprocal connections), GPi/SNr and thalamus (Parent and Hazrati, 1995). Thalamo-subthalamic projections are topographically organised and bilateral allowing modulation of multiple basal ganglia pathways (Nauta and Cole, 1978). The sub thalamic nucleus is too small to be modelled in our experiments and so was not included in this study.

Output from the basal ganglia to thalamus and onwards

The output of the basal ganglia is from the globus pallidus internal segment and the substantia nigra, to the thalamus, namely to ventral anterior (VA), ventral lateral (VL) and intralaminar nuclei via GABAergic (gamma-aminobutyric acid) inhibitory pathways and on to the frontal lobe of the cerebral cortex (Alexander *et al.*, 1990; Parent and Hazrati, 1995). The medial dorsal, centromedian and centrolateral nuclei are also innervated by fibres from basal ganglia (Ilinsky *et al.*, 1985; Ilinsky and Kultas-Ilinsky, 1987). As mentioned in chapter one, there is segregated flow of the nigro-thalamocortical systems via the lateral group of thalamic nuclei (extrapolation to human is complicated by different nomenclature for thalamic nuclei in different species); through these segregated pathways the globus pallidus targets the premotor cortex (Schell and Strick, 1984) and the substantia nigra projects via thalamus to prefrontal cortex (Ilinsky *et al.*, 1985) and cerebellum via lateral thalamic nuclei targets the motor cortex (Asanuma *et al.*, 1983a, b).

In addition to receiving corticostriatal output, the ventral thalamic nuclei project back to the striatum (McFarland and Haber, 2000). These have a generally topography so that those areas of the frontal motor cortex which project to the ventral anterior and ventral lateral nuclei of the thalamus (VA/VL) also project to the same area of striatum, but VA/VL projections to the striatum overlap extensively (McFarland and Haber, 2001). This is another level of the cortico-striato-thalamo-cortical circuit where there is potential for integration and modulation. This is also true for the parts of the striatum which receive projections from the intralaminar nuclei of the thalamus: the striatal projections of the centromedian thalamic nucleus are to the putamen and part of the head of the caudate which gets corticostriatal input from the sensory-motor areas

(Künzle, 1975). The parafascicular nucleus of the thalamus projects to the head of the caudate and anterior putamen, which gets its cortical inputs from the prefrontal and parietotemporal cortex (Selemon and Goldman-Rakic, 1985). The anterior group of the intralaminar nuclei share territory of the putamen with parietotemporal and cingulate cortical projections.

Nucleus Accumbens

For the nucleus accumbens, input is via glutamatergic projections from the subiculum (which lies between the hippocampus and the entorhinal cortex) and amygdala, hippocampus, prelimbic and prefrontal cortex. The main output is via medium spiny neurons that project to globus pallidus, thalamus, substantia nigra and cingulate cortex. A review can be found in Salgado et al (Salgado and Kaplitt, 2015). Circuitry with the midline thalamic nuclei provides input to the same part of the nucleus accumbens as the cortical areas that they project to (Wright and Groenewegen, 1996). Studies have suggested that the Nucleus Accumbens plays a central role in locomotion, learning, impulsivity, risk-taking behaviour, incentive and reward and is considered part of the basal ganglia (Heimer and Kalil, 1978). It is not directly modelled in the experiments in the thesis or in the magnetic resonance imaging studies reviewed here.

The contribution of Alexander GE, DeLong MR and Strick PL

The conceptualisation of the basal ganglia as component parts of orthogonal corticothalamic loops, rather than of part of a single, sequential input, throughput and output sequence, was proposed by Alexander, DeLong and Strick (1986) and reviewed as part of a highly cited review of basal ganglia function (Alexander *et al.*, 1990). The authors synthesise the findings of striatal involvement in sensorimotor circuits in which different inputs act on restricted portion of the frontal cortex (Schell and Strick, 1984), with the research in the motor function of the basal ganglia which also return to a restricted but different portion of frontal cortex (Künzle, 1975) and, using available data from other known basal ganglia-frontal lobe pathways, suggest a total of ‘at least’ five circuits in parallel with the motor circuit described by Heinz Künzle.

The general arrangement of these circuits is of multiple inputs from cortex to striatum which are then channelled during their progress through the sequential parts of the basal ganglia until they project to a restricted part of the thalamus and then back to a single area of (frontal) cortex. They conceptualise the role of these loops not as 'self-enclosed pathways' but ones with diverse influences but a termination in a single cortical area. A caveat which is emphasised, is that the synthesis of knowledge of these loops relies on studies in many different animals, all of which have different anatomical organisation of the nuclei (and nomenclature for these nuclei, as is seen in the efforts to define the 'motor' nuclei of the thalamus in chapter one), and all results are being extrapolated to humans (Alexander *et al.*, 1986).

The first loop defined by Alexander et al was the 'motor' loop first detailed by Kunzle as involving the putamen, receiving inputs from motor (Künzle, 1975) and somatosensory cortices (Künzle, 1977) and displaying somatotopic organisation. In addition, topographic projections are received from superior parietal lobule of the post central gyrus (Brodmann area 5), premotor cortex (Brodmann lateral area 6) and from the supplementary motor area (Jones *et al.*, 1977; Künzle, 1978; Selemon and Goldman-Rakic, 1985). There are slight extensions into the neighbouring caudate, but the terminal arborisations are primarily to the putamen. The projection to the globus pallidus subsequently projects to a portion of the VL nucleus of the thalamus (Nauta and Mehler, 1966) which projects to the supplementary motor area (Schell and Strick, 1984).

The second proposed circuit involves oculomotor control and originates in the frontal eye fields (Brodmann area 8) as well as dorsolateral prefrontal cortex and posterior parietal cortex (Yeterian and Van Hoesen, 1978; Selemon and Goldman-Rakic, 1985) from which the central body of the caudate is targeted (Künzle and Akert, 1977). This in turn projects to GPi and onwards to parts of the ventral anterior nucleus and medial dorsal nuclei but to different parts of these nuclei than those involved in the dorsolateral prefrontal circuit (Ilinsky *et al.*, 1985). It then 'returns' to the cortex to the frontal eye fields (Kievit and Kuypers, 1977) providing a second 'closed loop'.

Two prefrontal circuits are described: the dorsolateral prefrontal circuit and lateral orbitofrontal circuit. The dorsolateral prefrontal comes from cortex in dorsolateral prefrontal area, but also targeting the same area of caudate, are corticostriatal projections from posterior parietal cortex and arcuate premotor area (Künzle, 1978; Selemon and Goldman-Rakic, 1985). The striatal area defined by these inputs is the dorsolateral head of caudate nucleus and onwards to the tail of the caudate (Goldman and Nauta, 1977; Yeterian and Van Hoesen, 1978; Selemon and Goldman-Rakic, 1985). Projections are then to globus pallidus and substantia nigra (Parent *et al.*, 1984) and onwards to portions of ventral anterior nucleus and medial dorsal nucleus and then to frontal lobe including caudal prefrontal areas (Kievit and Kuypers, 1977) and the MD projections to dorsolateral prefrontal cortex (Pribram *et al.*, 1953).

Finally, an anterior cingulate loop which was originally conceptualised by Heimer and Wilson (Heimer and Wilson, 1975) projects to the ventral striatum and substantia nigra (Nauta and Cole, 1978) from anterior cingulate and temporal lobe, hippocampus, amygdala and entorhinal and perirhinal cortices, and returns to the anterior cingulate. Reciprocal connections exist between medial dorsal nucleus of the thalamus and anterior cingulate cortex (Vogt *et al.*, 1979; Baleydier and Mauguiere, 1980; Jürgens, 1983).

Defining striatocortical connectivity using magnetic resonance imaging in adults

The reviews by Alexander et al (1986 and 1990) are relied on heavily in the human MRI literature, but the caveats presented by Alexander et al should be kept in mind. When applying the literature to preterm images, the difficulties of extrapolating these theories, based on synthesis of data, across many animal species, via the adult brain to the developing human brain, are not insignificant. The resolution possible in MRI studies, as well as the lack of ability to separate the influence of different directions of axonal connections as is possible with techniques such as anterograde and retrograde

tracers, mean that the precise detail achieved in the animal studies detailed above is not currently possible using magnetic resonance imaging.

Diffusion Imaging

The striatum has been investigated in adults using imaging modalities such as diffusion tractography (Lehéricy *et al.*, 2004; Draganski *et al.*, 2008) and functional connectivity magnetic resonance imaging (Di Martino *et al.*, 2008; Choi *et al.*, 2012; Pauli *et al.*, 2016; Sanefuji *et al.*, 2017) and has been combined with task-based functional imaging to demonstrate the basal ganglia's role in motor execution, motor planning and sensory-motor integration as well as the processes which precede movement such as motivation, emotion and cognition (Pauli *et al.*, 2016).

An early study using diffusion tensor imaging in 9 healthy adults was published in 2004 by Lehericy et al, using four regions of interest in a single hemisphere consisting of a posterior putamen, anterior putamen, caudate nucleus and ventral striatum. The authors found evidence of discrete circuits similar to those proposed by Alexander et al 1986 based on the work on the motor system in monkey (Macaca fascicularis) notably by Kunzle (Künzle, 1975). The posterior part of the putamen was connected with the primary sensory and motor areas as well as to the posterior SMA. The anterior striatum was connected with the prefrontal cortex, frontal pole and pre-SMA, cortical input areas in Alexander et al's 'motor' loop. The ventral striatum is connected with the amygdala (Lehéricy *et al.*, 2004). Using data from 30 subjects and an additional method to allow voxel-based connectivity profiles which allow representation of a single source to multiple target regions, Draganski et al also found similar results to those found in tracer studies (Draganski *et al.*, 2008). They found nearly symmetrical clusters of voxels which were connected with cortical targets, or with basal ganglia areas. The role of the thalamus in segregated and integrated loops was also considered in this study with well-recognised thalamocortical coupling of medial dorsal nucleus to prefrontal cortex and occipitofrontal cortex, ventral anterior (VA) nucleus to dorsolateral prefrontal cortex, ventral lateral nucleus (VL) to motor and premotor areas and ventral posterior (VP) nucleus to somatosensory cortical regions. They were able to track connections between different nuclei of the basal ganglia showing that most

caudate projections were to the dorsomedial pallidum, while putamen projected to ventrolateral palladium and thalamus connected with ventromedial palladium. With regards to the thalamus, medial thalamic nuclei projected to ventral striatal areas while lateral thalamic nuclear projections were to dorsal striatal areas, reflecting the 'limbic' and 'motor' functions.

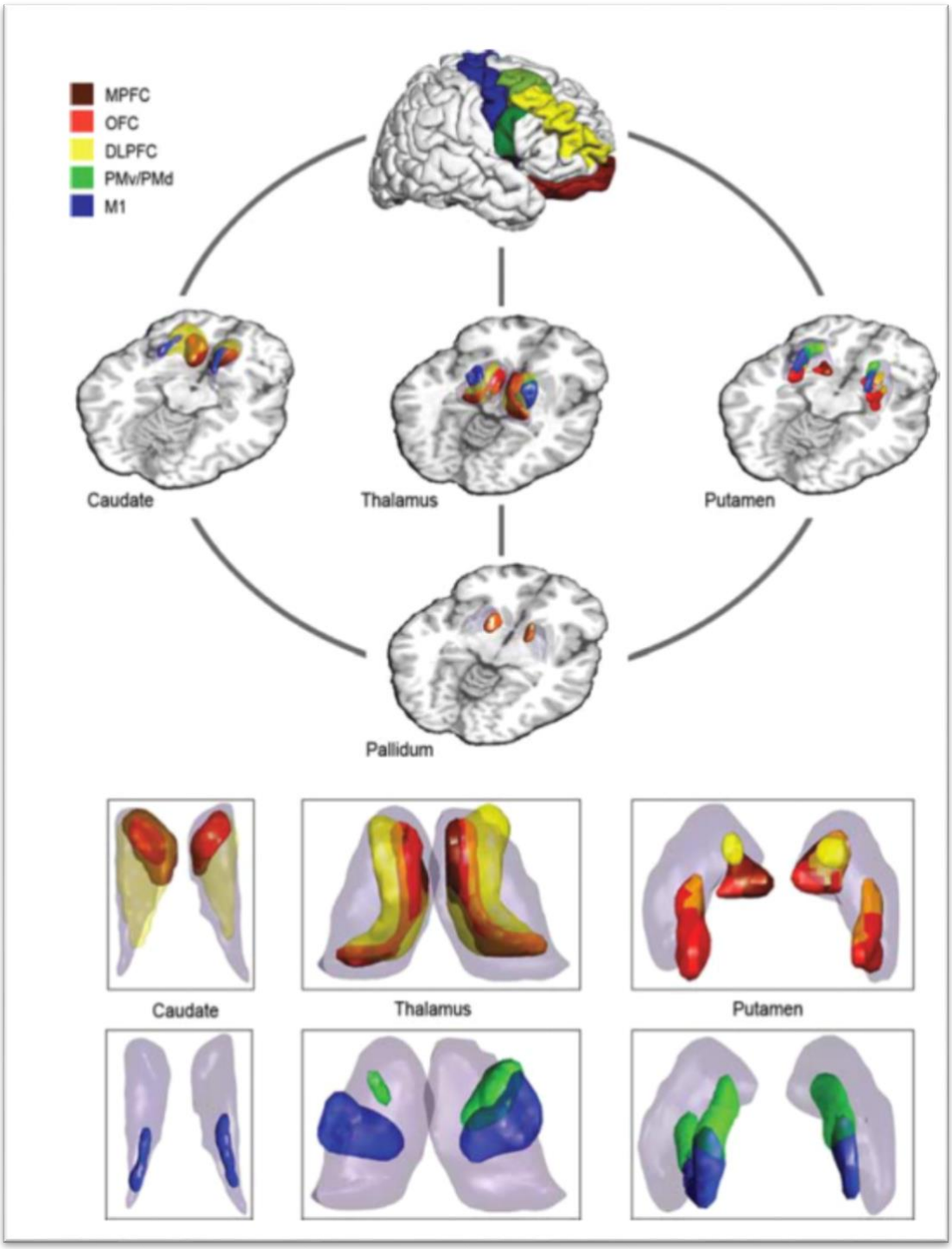

Figure 2.2. Connections between thalamus, cortex and basal ganglia, with orange showing areas connected with red and yellow cortical areas (Draganski *et al.*, 2008)

In a study to examine dopamine release in the striatum, results were also in agreement with these previous diffusion studies and tracer studies in non-human primates (Tziortzi *et al.*, 2014).

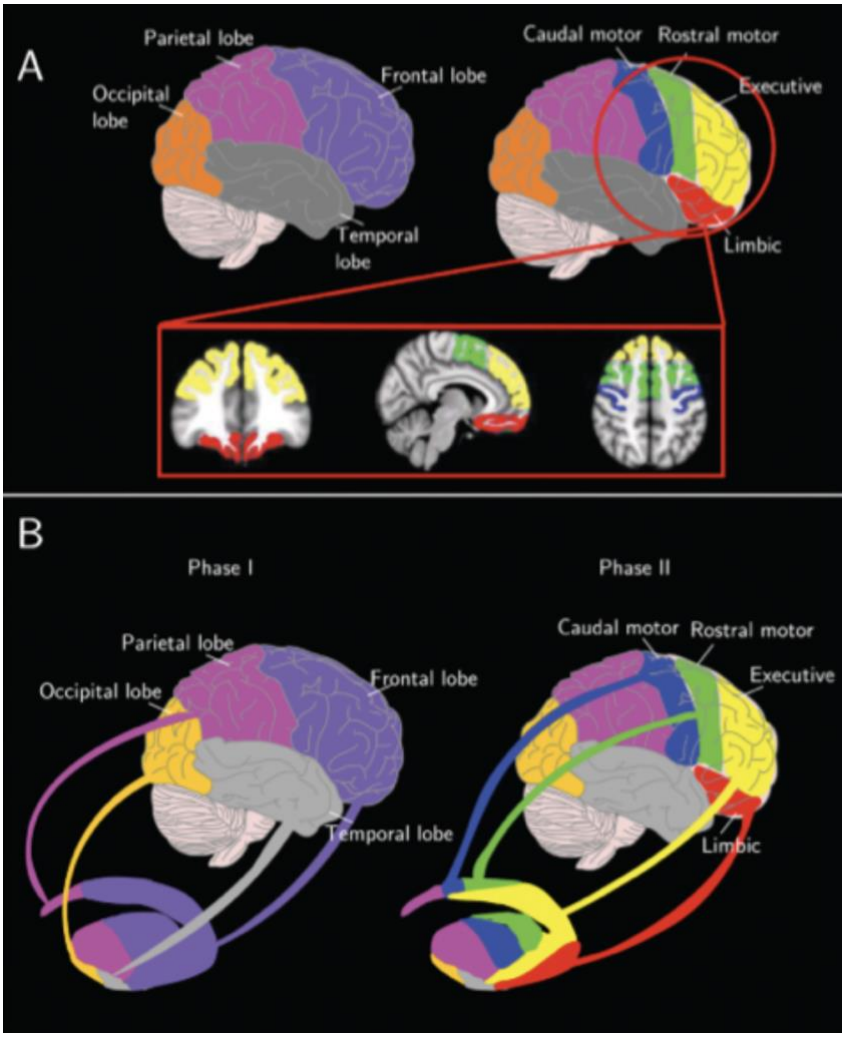

Figure 2.3. Parcellation of striatum using anatomical cortical regions of interest (Tziortzi *et al.*, 2014).

In contrast with Alexander, but in concordance with the studies using tractography by Lehericy (2004) and Draganski (2008), Verstynen et al found that these tracts were segregated according to cortical origin rather than cortical destination (Verstynen *et al.*, 2012) which is perhaps unsurprising given the techniques used. In addition, using high-angular-resolution techniques for imaging white mater microstructure (Verstynen *et al.*, 2011) a rostral-caudal topography was seen in addition to the somatotopic organisation of fibres from the motor cortex. This is in agreement with the findings in non-human primates presented by Suzanne Haber (Haber, 2003). The

cortical and striatal regions used were defined anatomically using *Freesurfer* on the T1 image (Fischl *et al.*, 2004) and tracking of fibres was terminated when the fractional anisotropy fell below a defined threshold, or when the turning angle exceeded 60 degrees, with these parameters being determined by the signal to noise ratio of each scan. The geometric distortions and partial voluming of the diffusion data were accounted for by expanding both cortical and subcortical regions of interest, but only retaining tracks that terminated within the striatum. The procedure was carried out separately for both the right and the left hemisphere. Using these methods to model cortical inputs, limbic fibres projected to head of caudate and rostral putamen, frontal projections were found caudally to these representations in the central and lateral caudate body, while motor projection was found on the lateral edges of the caudate and central putamen. Somatosensory fibres were found on the most caudal portion of the putamen. The limbic and frontal areas provided the most projections to the striatum, with lateral frontal cortex much more represented than motor or somatosensory fibres probably as a result of the number of voxels included in the cortical masks for these areas. Within the dorsolateral prefrontal cortex, fibres leaving the gyrus were shown to keep to the same relationship but perform a shift in position increasing to 90-degree shift in the most posterior fibres of the gyrus with regards to their position in the striatum. They also form a non-contiguous representation of the dorsolateral prefrontal cortex which is said to represent the patched striosome/matrix organisation of the striatum but could also represent striatal areas targeted by other cortical or other inputs. The rostral-caudal organisation was found in the middle frontal gyrus also. The authors were also able to find a somatotopic organisation of the projections from motor cortex to striatum as found in the non-human primate (Miyachi *et al.*, 2006).

These striatal representations are understood in the context of known cortical inputs to the striatum. They are demonstrated in anatomical regions of interest with an anatomical gradient of cortex represented in striatum also. We know that the inputs from cortex to striatal areas contain contributions from many cortical regions and this is not reflected by the methodology in Verstynen et al. The level of precision of corticostriatal tracking, however, is far beyond the resolution achievable with resting state functional connectivity and was achieved using data from ten adults who were

experienced in staying still in the magnet and a diffusion sequence duration of 45 minutes. No motion correction was performed, but participants with a low signal to noise due to motion underwent a repeat scan. While a beautifully detailed description is obtained, there are clear limits on these scanning parameters with regards to clinical populations and babies and children in particular.

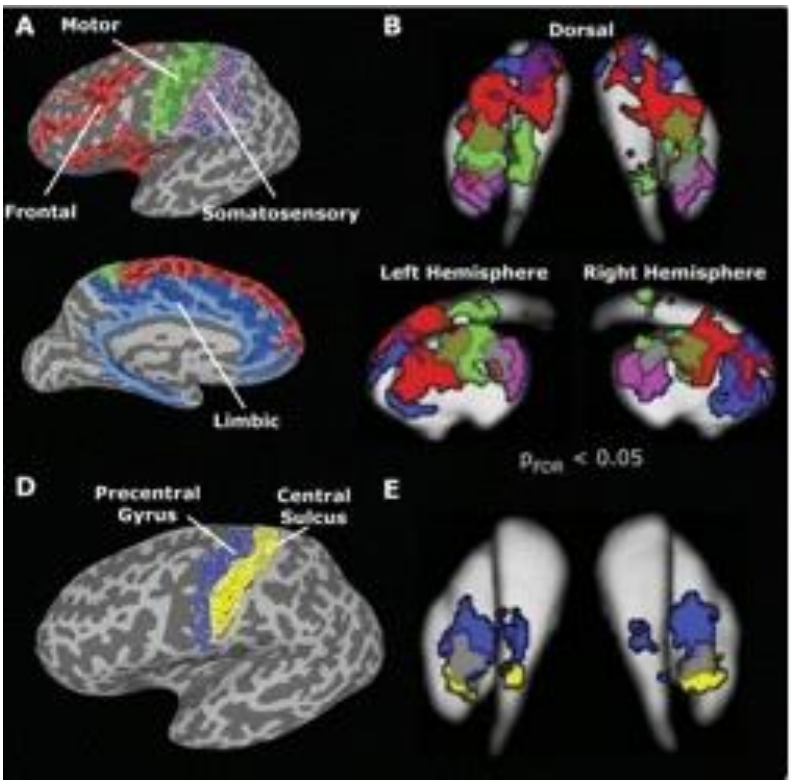

Figure 2.4. Striatal parcellation (Verstynen *et al.*, 2012).

The ability of MRI to resolve the relationship between striatum and thalamus is shown by O'Muircheartaigh et al. Using tractography to parcellate thalamic segments and then functional connectivity to map onto subcortical regions, O'Muircheartaigh et al identify associations between putamen/palladium and different thalamic parcellations including thalamic nuclei known to be associated with frontal brain regions (medial/anterior, ventral anterior/ventral lateral nuclei and ventral lateral/ventral posterior group), while caudate maps onto the medial/anterior thalamic nuclear group (O'Muircheartaigh *et al.*, 2015). This is commensurate with the cortico-striato-thalamo-cortical loops proposed by Alexander et al 1986 and with studies in non-

human primates (Künzle, 1975; Selemon and Goldman-Rakic, 1985; McFarland and Haber, 2001).

Resting State functional connectivity

In a study of 35 adults, Di Martino et al aimed to map distinct striatal circuits using functional magnetic resonance imaging acquired at rest with seed regions defined anatomically in the striatum (Di Martino *et al.*, 2008). Dorsal caudate predicted activity in the dorsolateral prefrontal cortex (DLPFC), ventral lateral prefrontal cortex and parietal association areas, confirming the involvement of dorsal caudate in cognitive control as in Alexander et al 1986 and Parent and Hazrati 1995. The dorsal caudate seed also predicted activity in the frontal eye field as outlined by Alexander et al 1986 in the oculomotor loop. The putamen seed predicted activity in primary and secondary motor cortices while other putamen seeds were linked to the DLPFC and anterior cingulate, areas linked to executive control. A separate putamen seed predicted activation of insular cortex, as did the ventral rostral putamen. Di Martino et al comment on symmetry of their results with differences only with the cerebellum. Results from this study are described as being consistent with a meta-analysis of 126 task-based functional studies described by Postuma and Dagher (Postuma and Dagher, 2006).

Using 1000 adult subjects split into two independent groups of 500 subjects, Choi et al used resting state functional connectivity data to estimate the topography of the striatum (Choi *et al.*, 2012). Instead of using the mean time series of a cortical ROI as is common in many studies, or the eigen timeseries as used in this thesis, Choi et al adopted a different model in order to capture the greater spatial diversity of connections. For each striatal voxel, the top 25 most correlated voxels were chosen and the cortical area with the most voxels belonging to it was assigned that striatal voxel. Five of the seven networks chosen were strongly represented in the striatum bilaterally (motor, ventral attention, frontoparietal, default, limbic) while the dorsal attention network was represented in the right posterior ventral putamen only and visual network was almost absent. Using these methods, Choi et al parcellated the adult striatum showing high degrees of symmetry especially when based on 7 major networks, but also with 17 networks. Some features of the parcellation remain of

uncertain significance, namely the large territory of the putamen most strongly associated with a cortical area including some of the anterior cingulate and medial surface of the frontal lobe which they attribute to an area prone to signal bleeding. When the signal from this cortical area was regressed out of the data, the putamen was assigned to the motor network (posterior putamen) and frontoparietal control network (central and ventral anterior putamen) which then agreed with tract tracing experiments in non-human primates. The authors conclude that the majority of striatal territory is concerned with association cortex (Choi *et al.*, 2012).

Using independent component analysis rather than tractography to define regions of interest, Kim et al parcellated both thalamus and basal ganglia into 31 components and investigated their correlations with cortical regions (Kim *et al.*, 2013). Unlike the thalamus where there is a possibility of histological comparison via an atlas, comparisons of 'likeness' between results found in imaging studies of the basal ganglia depend on a visual inspection and Kim et al report their results to be 'grossly' corresponding to the cortico-striato-thalamo-cortical circuits in the brain. On visual inspection, the parcellation of the thalamus displays more obvious symmetry than the basal ganglia and this may be the case, but in a group of 21 subjects with 160 volumes per subject, a spatial smoothing of 8mm (Gaussian kernel of 8 mm full width at half maximum (FWHM)), and a parcellation using 48 components, the data has been over-interrogated.

Meta-analysis

In a meta-analysis of the basal ganglia, searching task-based Positron Emission Tomography and functional magnetic resonance imaging publications, Postuma and Dagher find patterns of connectivity described as consistent with the parallel loop model (Alexander *et al.*, 1986) and tracer studies in non-human primates (Postuma and Dagher, 2006). As has been mentioned, insula is often not included in analysis possibly because it was not included in the original parallel loop models. The insula was included in the meta-analysis by Postuma and Dagher and was found to be strongly coactivated with both the putamen and caudate and it is noted that some of the diverse functions of the insular cortex are also shared by the striatum especially

between putamen and dorsal posterior insula and between caudate and ventral insula. With regards to coactivity with the thalamus, this was found to be between the ventrolateral nucleus of the thalamus and left putamen and between dorsomedial and anterior nuclei of the thalamus and caudate and right putamen.

In a different approach, analysing coactivation data from 5,809 human task-based imaging studies, Pauli et al identified different psychological processes associated with each of the five distinct striatal zones which exhibited discrete patterns of coactivation with cortical brain regions (Pauli *et al.*, 2016). This allowed the association of each functional zone of the striatum with distinct psychological processes, rather than infer striatal function by association with cortical areas. They found five distinct zones of the striatum according to the different psychological processes attributed to each zone: the parcellation from their study is shown below.

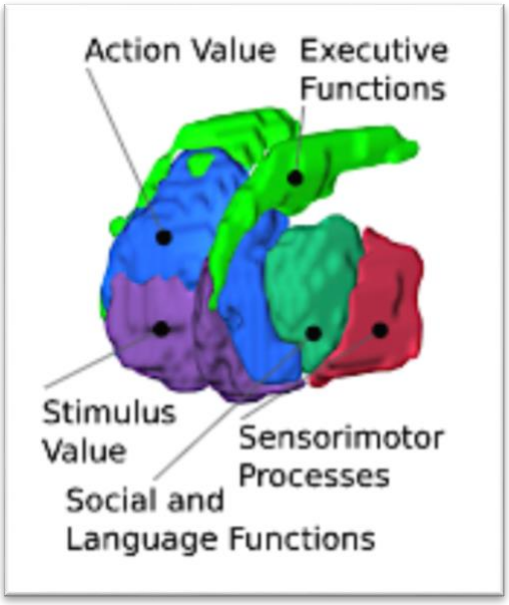

Figure 2.5. Psychological parcellation of the striatum. Summary of the main psychological functions of each functional zone (figure 3B as per Pauli et al 2016).

Defining striatocortical connectivity using magnetic resonance imaging in infants and children

Current knowledge about corticostriatal connectivity in infants

There are currently no published studies investigating corticostriatal connectivity at the time of normal birth or the effect of prematurity on the establishment of these connections using resting state functional connectivity methods or diffusion imaging.

Corticostriatal connectivity in preterm children

Modelling global connectivity using diffusion-weighted imaging in preterm children at the age of 7 and correlating with measures of outcome, Fischi-Gomez et al identify that earlier maturing fibre tracts have decreased fractional anisotropy at school age in both groups of early preterm and intrauterine growth restricted children compared with later maturing tracts such as cortico-cortical tracts in association with scores for socio-cognitive functioning as assessed with the Kaufman Assessment Battery for Children and Strengths and Difficulties questionnaire (Fischi-Gómez *et al.*, 2015). The authors suggest that weaker connections within the cortico-striato-thalamo-cortical circuit might represent less efficient simultaneous processing (or task switching) within the parallel loops of this circuit. In addition, the alterations in connectivity found were most marked between components involved in prefrontal-subcortical portions and limbic circuits which in adults are associated with executive function, social behaviour and motivation (Parent and Hazrati, 1995).

Corticostriatal Changes in Development

In a cohort of 120 young adults and 60 children (7-12 years old), basal ganglia parcellations were defined using partial correlation analysis using the same methodology as described in Zhang et al 2008 (see Chapter 1). In this study by Greene et al, 11 cortical areas were selected as regions of interest based on the work by Power et al, including auditory and visual systems which are not known to have direct anatomical corticostriatal connections (Power *et al.*, 2011; Greene *et al.*, 2014). Results were consistent with tracer studies, with somatomotor hand system correlating with dorsal posterior putamen and somatomotor face with the ventral posterior putamen. The partial correlation results in adults and children were similar, with the exception of a larger magnitude of correlations with the somatomotor face in children

compared with adults with an effect size of - 0.31 (calculated r^2 of 0.09). Signal regression of voxels adjacent to the basal ganglia was carried out as the cingulo-opercular network had high correlations with the putamen, but this did not affect the differences between children and adults: winner-takes-all analysis shown in this work does not analyse connectivity with the insular cortex or anterior cingulate. In the methods, the authors manage motion in their data by using scrubbing (removal of individual, isolated volumes outside the study's defined parameters) and mitigate the spurious autocorrelation introduced as a result of the scrubbing of motion-corrupted volumes by calculating partial correlations. The longer lasting effect of an episode of motion on connectivity was noted in the preliminary investigations for this thesis and are also detailed in Power et al 2014 (Power *et al.*, 2014). While partial correlations might account for this whole brain effect on connectivity, scrubbing still results in a varying contribution of each subject to the analysis (heteroscedasticity) which although is stated to be statistically insignificant, resulted in a range of 150-719 volumes per adult subject and 132-622 per child subject.

Analysing data in children aged between 7.6 and 13.5 in order to examine striatal functional connectivity in children with Autism, Di Martino et al characterise functional connectivity between six striatal areas of interest as defined in Di Martino et al 2008 above, which are described as grossly similar to those found in typical adults (Di Martino *et al.*, 2011). The results are useful for comparison with results in this thesis as they provide the youngest cohort with published results and include analysis of the insula. In the ventral striatum there is significant positive functional connectivity with paralimbic and association areas including the anterior insula and superior temporal gyrus bilaterally. With regards to the dorsal caudate, connections with dorsal anterior cingulate and lateral frontal cortex are found, mirroring those found in adults, but in addition, children have positive functional connectivity with the anterior and posterior insula and superior and middle temporal gyri bilaterally. Children with autism, displayed hyper connectivity with regard to striatal connections to heteromodal associative and limbic cortex such as superior temporal gyrus and insular cortex compared with typically developing children. These values were obtained using the scrubbing methods described in Greene et al, but without implementing partial correlation analysis to account for spurious autocorrelations (whole brain voxel-wise

correlations were used) and with regards to heteroscedasticity, details are not provided as to volumes remaining per subject.

Chapter Three

Neuroimaging at birth and outcome around two years old

Introduction

This chapter reviews studies which include imaging at birth (structural, diffusion and spectroscopy) and neurodevelopmental follow up at two years in order to set out the current state of the art and to provide context for the results contained in this thesis. Further information is provided in Table 3.1. Results from studies including analysis of infants without structural abnormalities on MRI at term equivalent age are explored in depth as these are currently the children who are most difficult to provide prognostic information for from MRI at term and reflect the cohort studied in this thesis. The large parallel-group randomised trial (from which the subjects in this thesis were drawn) which was designed to compare the efficacy of MRI and ultrasound scan with regards to maternal anxiety, provides an invaluable baseline as to the use of structural MRI in an unselected preterm cohort to predict outcome (Edwards et al 2018). 72 out of the 484 infants (14.9%) who underwent MRI, had scan results predicting adverse prognosis as per the criteria set out in Woodward et al (Woodward *et al.*, 2006) providing a positive predictive value of 38.9% (95% CI 27.6 - 51.1%) of a Bayley III motor domain score of less than 85. The positive predictive value from MRI of low cognitive and language scores (<85) at 2 years was higher at 43.1% (95% CI of 31.4 - 55.3) and 48.6% (95% CI of 36.7 - 60.7). Sensitivity, however, for lower language and cognitive scores was lower than that for motor scores (19.9%, 27.9%, 38.9% respectively). MRI at birth has a better sensitivity for a GMFCS score (Palisano *et al.*, 1997) of grade 2-5 at two years (60.6%) than it does for a Bayley III motor score of less than 85, but a poorer positive predictive value than all the other measures from the Bayley III (27.8% with 95% CI of 17.9 - 39.6). The 72 infants whose structural MRI scan results predicted adverse prognosis with a high specificity (specificity for motor, cognitive and language scores <85 at two years were 89.2%, 88.9% and

87.8%), were excluded from analysis in this thesis as the aim was to look at abnormal connectivity in those with normal scans at the time of normal birth.

Studies using measures of conventional MRI only

Kidokoro scoring system

Kidokoro et al investigate the use of a scoring system using structural MRI T1 and T2 images acquired at term equivalent age (Kidokoro *et al.*, 2013), to predict outcome at two years. 10% of the cohort of infants born at less than 30 weeks had severe brain injury apparent on MRI but in those without severe brain injury, two different patterns of impaired brain growth, characterised by reduced biparietal width and increased inter hemispheric distance, were noted (Kidokoro *et al.*, 2014). Both of these patterns were associated with poorer neurodevelopmental outcome at the age of two years, especially in the cognitive domain. Significance is included, but no further statistical measures of the relative contribution of these two measurements to poorer outcomes is given.

The same scoring system (Kidokoro *et al.*, 2013) was applied by Brouwer et al to a different cohort of slightly more immature infants born between 24- and 28-weeks gestational age (Brouwer *et al.*, 2017). Patterns of injury in this Dutch cohort of 239 infants were then compared with the original cohort recruited from Christchurch, Melbourne and St Louis (Kidokoro *et al.*, 2014). This second cohort were found to have a different pattern of brain abnormalities than in the original Kidokoro cohort with the two different patterns of impaired brain growth not seen. Global brain abnormality scores are inversely associated with cognitive scores, fine motor and gross motor scores. Specific domains are associated with a score from a single category: cognition at 2 years is exclusively related to cerebellar scores on MRI at term ($p = 0.002$, r^2 0.223) while fine motor scores are only associated with white matter scores ($p = 0.004$, r^2 0.134). Gross motor scores are related to deep grey matter ($p = < 0.001$) explaining 21% of this model. The authors also investigated a subgroup of infants

without brain pathology on cranial ultrasound or term MRI scan and found that the only association remaining was between width of the atrium of the lateral ventricle and cognitive scores. Corrections had been made in the case of cognitive score, for maternal education, non-Western ethnicity, female sex and test age, particularly important in this cohort was composed of two separate cohorts, one tested at 24 months and the other at 30 months. Brouwer et al conclude that, unlike the original Kidokoro cohort, the prognostic value of the term MRI scan in their well-performing cohort was limited, but that mechanical ventilation and days of parenteral nutrition were independent perinatal risk factors. In contrast to the study by Tusor et al (Tusor *et al.*, 2017) the presence of punctate lesions was not associated with neurodevelopmental outcome in this cohort (Brouwer *et al.*, 2017).

Other structural studies focused on infants without brain injury

In a longitudinal study designed to look at the change in tissue volumes between birth and term equivalent age using MRI, rather than a single term scan in order to predict neurodevelopmental outcome, a linear discriminant classifier based on tissue volumes contributed to the prediction of outcome at 2 years with regards to motor outcomes but did not add predictive value for cognitive outcomes at 2 years and 5 years over and above that provided by gestational age at birth and socio-economic status (Gui *et al.*, 2018). Motor outcome, however, was better predicted when the volumetric measurements from MRI at preterm and term were added to socioeconomic status and gestational age at birth (r^2 adjusted of 0.2576). The presence of major lesions on term scan was an exclusion criterion from this cohort, so the predictive value of tissue volumes to motor outcome is not simply that which could be predicted from the presence of gross abnormalities on term scans. In an approach which combined Kidokoro scoring system with regards to cerebellar injury, white matter scoring according to Woodward et al 2006, and brain injury identified by experienced neonatologists, and after controlling for severe brain injury, Keunen et al found ventricular volumes to be negatively related to cognitive composite and fine motor scores (Keunen *et al.*, 2016). They also found that unmyelinated white matter measures were related to gross motor performance at 2 years with both. After

controlling for those with severe impairment, Lind et al found a relationship between cerebellar volumes and neurodevelopmental outcome (Lind *et al.*, 2011).

Structural studies with discrete findings

Using birthweight as criteria, in this case infants below 1500g and less than 32 weeks gestational age, Rose et al found that cerebellar macrostructure correlated with lower cognitive composite scores (Rose *et al.*, 2015). A smaller hippocampal volume was found in newborn imaging in children who perseverated on a working memory task but the difference in sizes measured were in the order of 0.06 ml of hippocampal volume (Beauchamp *et al.*, 2008). A large study of 187 infants of less than 30 weeks gestational age which grouped subjects according to the presence or absence of white matter abnormality (assessed qualitatively) and employed a multivariate regression model which included gender and brain metrics, found that biparietal diameter was predictive of cognitive and motor abilities at two years. In addition to the study by Lind et al mentioned above, the association with cerebellum and outcome was also found in other studies (Lind *et al.*, 2011; Rose *et al.*, 2015; George *et al.*, 2017). An unselected sample of 76 infants using volumetric criteria, found that memory task performance was related to the proportion of cerebral tissues within the dorsolateral prefrontal cortex, premotor and supplementary motor cortices but the effect size is small with r^2 between 0.01 and 0.09 (Woodward *et al.*, 2005).

Extreme prematurity

A cohort of 38 infants with a mean gestational age of 25.5 weeks were scanned between late gestation and term (34.1 - 43.9 weeks) and were then followed up at two years of age with a Bayley III assessment (He and Parikh, 2013). An atlas segmentation using a probabilistic atlas for very preterm infants was constructed from 19 randomly selected subjects within the cohort and white matter signal abnormality volume was quantified on the T2 weighted images of 38 infants. Signal abnormality within the centrum semiovale was the best predictor of outcome with a r^2 of 0.3912 and a p value of < 0.0001. Park et al also studied extremely low birthweight infants (<1000g) and those of <1500g if they had an indication for MRI such as seizures,

hypoxic events or suspected PVL after ultrasound scan (Park *et al.*, 2014). This cohort had a 53% incidence of retinopathy of prematurity and 24% incidence of bronchopulmonary dysplasia which makes it unrepresentative of most preterm cohorts. With a comparatively wide range of ages at Bayley III assessment (16.1 months +- 6.4 months SD), they found that a short trans cerebellar diameter was associated with poor motor and cognitive function. In a large study of 187 infants with a gestational age of less than 30 weeks, biparietal diameter, bifrontal and transverse cerebellar diameters were measured at term equivalent age and infants with and without white matter abnormalities were investigated for difference in outcome scores (Tich *et al.*, 2011). Biparietal diameter was found to be most predictive of cognitive and motor abilities but the mean difference in outcome scores of motor and cognitive scales are small.

In contrast with studies (both structural and diffusion) which quantified white matter damage with measurement of diffuse high signal intensities (DEHSI) and found no correlation with outcome at 1 year (Leitner *et al.*, 2014) or 2 years old in infants with otherwise normal MRI scans (Hart *et al.*, 2011; Skiöld *et al.*, 2012), Tusor et al investigated the location of punctate lesions in the white matter, hitherto of unknown predictive value (Tusor *et al.*, 2017). This large study of 511 infants (the EPRIME cohort, as used in this thesis) evaluated 281 infants without cerebral lesions of whom 114 had punctate white matter lesions. They are predominantly found in the centrum semiovale and corona radiata (white matter axons which continues ventrally as the internal capsule and carry the majority of communications from and to the cerebral cortex) and are associated with a reduced thalamic volume. Lesions are associated with adverse motor outcomes at 2 years and a higher lesion load predicts functional motor outcome more precisely using Gross Motor Function Classification System (GMFCS) but does not correlate with language or cognitive scores. In a study investigating the effect of perinatal factors on white matter injury, Fractional anisotropy (FA) values in many white matter tracts such as the corpus callosum and the posterior limb of the internal capsule are found bilaterally and some right sided structures are positively correlated with motor composite score while radial diffusivity is negatively correlated with motor scores in other bilateral white matter tracts (Barnett

et al., 2018). FA globally is positively correlated with cognitive scores while language scores are correlated with FA in small parts of the body of the corpus callosum, left fornix and inferior longitudinal fasciculus and inferior fronto-occipital fasciculus but with no metrics given as to the size of these correlations.

Studies using measures of diffusion imaging

More information about diffusion weighted imaging can be found in Materials and Methods

Diffusion studies focused on those without overt brain injury

Measures of diffusion imaging were used to specifically investigate connectivity at term equivalent age in a cohort of 57 infants born at less than 35 weeks gestational age, who then underwent cognitive assessment at 2 years old (Ball *et al.*, 2015). These infants did not have evidence of focal abnormality on structural MRI. Measures, reflecting white matter microstructure, based on diffusional anisotropy and fibre orientation at each voxel, were used to calculate connectivity estimates between the thalamus and cortical target regions. Differences in connectivity explained 11% of the variance in cognitive scores, while the addition of gestational age at birth and socioeconomic group to the model explained 30% of the variance (Ball *et al.*, 2015). As with the study by Tusor et al, widespread areas of the brain were associated with poorer neurocognitive or motor outcome.

Studies by Boardman et al, Counsell et al and Krishnan et al, exclude infants with congenital malformations, congenital central nervous system infections, cystic periventricular leukomalacia, haemorrhagic parenchymal infarction or post-haemorrhagic ventricular dilatation. A characteristic neonatal imaging phenotype is described by Boardman et al which includes abnormally high ADC values in at least one white matter region at the level of the centrum semiovale, discrete tissue loss within the dorsomedial area of the thalami, globus pallidus and within the posterior periventricular white matter, corona radiata and centrum semiovale (Boardman *et al.*,

2010). There was a difference in the median developmental quotient (DQ) between those preterm infants with this phenotype and term controls ($p < 0.01$) whereas the difference between preterm group without the phenotype and controls nearly reached significance ($p = 0.054$, group was only 14 infants) but was not significant between the two preterm groups ($p = 0.354$) (Boardman *et al.*, 2010). This study also finds that 24.6% of the variance in DQ is explained by gestational age at birth. Counsell et al found DQ to be linearly related to FA values in parts of the corpus callosum; more specifically, eye-hand co-ordination was related to FA in the cingulum, fornix, anterior commissure, corpus callosum and right uncinate fasciculus with a modest slope value of 0.003 to 0.006 (Counsell *et al.*, 2007). Krishnan et al and Kaukola et al (in a cohort where major destructive lesions were excluded) found higher ADC in white matter at TEA (term-equivalent age) to be associated with a lower DQ at 2 years (Krishnan *et al.*, 2007; Kaukola *et al.*, 2010).

Germinal matrix haemorrhage and grade 1 and 2 intraventricular haemorrhage (GMH/IVH) are often seen on serial ultrasound scan during the preterm period. They are often said to have resolved on ultrasound scan at term equivalent age, but the effect on migrating neurons of the neurotoxic effects of haemosiderin (Del Bigio *et al.*, 2011) adjacent to the caudothalamic notch is unlikely to be benign. In a relatively small study of 24 preterm infants with GMH/IVH and 24 term controls using tract-based spatial statistics, those born before 29 weeks GA had lower fractional anisotropy of the corpus callosum as well as limbic pathways and cerebellar tracts (Tortora *et al.*, 2018). In addition, those with GMH/IVH were more likely to have poor neurodevelopmental outcomes compared with those preterm infants without ($p<0.048$). Correlation of diffusion measures and developmental outcomes for different brain regions are provided but no calculation of effect size is included. A germinal matrix haemorrhage might be expected to affect connections with the caudate, especially the head of the caudate and so the adverse effect on visuomotor and locomotor skills found at two years might be explained in this context and does not contradict the findings of a much larger study using ultrasound which found that rates of cerebral palsy are not increased in children with a GMH/IVH type 1 or 2 (Ancel *et al.*, 2006).

Unselected cohorts

The following studies are in unselected cohorts of infants, in whom the outcomes would be expected to be poorer than in the cohort studied in this thesis. In these cohorts, the main finding between measures of diffusion imaging at term equivalent age, and outcome at two years concern differences found in the corpus callosum, internal capsule and in measures of diffuse white matter injury.

Corpus Callosum

Increased mean diffusivity and fractional anisotropy (FA) in the genu of the corpus callosum is associated with slower gait velocity with a derived r^2 of 0.09 (Rose *et al.*, 2015), while Thompson et al find no structural measures of corpus callosum size predict outcome at 2 years. Instead, they find that reduced posterior skew is associated with impaired cognitive development (Thompson *et al.*, 2012): the more the size of an infant's corpus callosum was skewed towards the body and tail, the higher the MDI (cognitive and language score) with a beta of 71.4 but with wide confidence intervals of between 25 and 118 (Thompson *et al.*, 2012). De Bruine et al were able to predict psychomotor delay using apparent diffusion coefficient (ADC) values of the splenium of the corpus callosum with 100% sensitivity but confidence intervals of 48-100% (De Bruïne *et al.*, 2013). Fractional anisotropy at term equivalent age in the corpus callosum was found to predict motor and cognitive scores at 24 months (Duerden *et al.*, 2015) and to predict cognitive scores with a predictive value of 31%, 4% and 13% for FA, axial diffusivity (AD) and radial diffusivity (RD) (van Kooij *et al.*, 2012).

Internal Capsule

With regards to the internal capsule, lower mean diffusivity in the left anterior limb was related to impaired language score (Rogers *et al.*, 2016), while reduced FA in the posterior limb (van Kooij *et al.*, 2012; De Bruïne *et al.*, 2013) and increased mean diffusivity (Rose *et al.*, 2015) was associated with reduced cognitive and motor scores. The sensitivity of this measure to predict motor delay and cerebral palsy in the study by De Bruine et al was 100% with confidence intervals of 48-100% and 28-100% respectively.

Measure of white matter damage

In a study of extreme preterm infants, Parikh et al used an objective (automatic) quantification of diffuse excessive high signal intensity (DEHSI) at term equivalent age in 36 infants with extremely low birth weight (<1000g mean GA 25.6 weeks) (Parikh *et al.*, 2013). They found a correlation between those infants with abnormal cognitive and language scores and a significantly higher DEHSI volume with MD, AD and RD predicting between 30 and 34% of the variance in cognitive and language scores; this compared with no significant difference in Bayley scores when the MRI scans were diagnosed subjectively for DEHSI by neuroradiologists.

Other anatomical locations

Aeby et al studied a group of 242 infants with a gestational age of less than 32 weeks (range 26-34) of which 41 had complete and quality imaging (Aeby *et al.*, 2013). Of these 41 infants scanned at term equivalent age 41 had cognitive and 35 had motor assessment at 2 years using the Bayley 3. The only significant correlation with outcome was with the language composite score and reduced mean diffusivity around the left superior temporal gyrus. Another specific anatomical location defined using diffusion imaging is the left cingulum, where a higher FA was found in those with impaired socio-emotional competence (Rogers *et al.*, 2016) and higher FA was also found in this study in the right inferior temporal lobe related with impairment in motor scores, particularly fine motor scores.

Studies using MR spectroscopy

Spectroscopy investigating ratios of N-acetylaspartate (NAA) to choline (Cho) and N-acetylaspartate to myo-inositol (MI) in the hippocampal cortex and sub ventricular zones is used by Bapat et al in a cohort of 43 infants with a gestational age of less than 25 weeks (Bapat *et al.*, 2014). The rate of abnormalities on MRI at term in this extremely preterm cohort is 11 normal scans, 18 with mild injury and 2 with moderate or severe injury. In this study, the NAA to Choline in the sub ventricular zone and cerebral cortex and NAA to myo-inositol in the sub ventricular zone were significantly associated with Bayley III outcomes (Bapat *et al.*, 2014). Kendall et al analyse a cohort

who were born at less than 32 weeks and were still hospital inpatients when they were scanned at term equivalent age thereby potentially selecting an unrepresentative cohort requiring prolonged admissions to the neonatal intensive care unit (Kendall *et al.*, 2014). They found significant correlation between NAA and Cho and all Bayley III scores and between Cho/Cr ratio and gross and composite motor scores (correlation coefficients of -0.45 and 0.437). The mean Bayley III scores of the preterm infants in the cohorts studied by Bapat and Kendall were within the normal range. Hart et al studied a cohort of infants with a gestational age at birth of less than 35 weeks and found a significant relationship between reduced fine motor skills and a visible lactate doublet in the posterior white matter ($p = 0.034$ but no effect size given). In addition, the average cognitive composite score differs between the 12 infants with lactate doublets (who have an average of 89.6) and the 26 infants who did not and had an average score of 101.4 (Hart *et al.*, 2014). Other studies using measures of spectroscopy (Augustine *et al.*, 2008; Van Kooij *et al.*, 2012) did not find associations with outcome. All the studies looking at magnetic resonance spectroscopy used an unselected cohort.

Table3.1 relevant studies

Reference	Study Population	Methods	Results and Conclusions
Gui L, Loukas S et al. Longitudinal study of neonatal brain tissue volumes in preterm infants and their ability to predict neurodevelopmental outcome. Neuroimage 185 728-741 (2019).	74 preterm infants (26-36 weeks GA) who had undergone MRI after birth, at TEA and outcome. Exclusion criteria: presence of congenital or chromosomal abnormalities, major brain pathology (IVH grade 3 or higher) and/or parenchymal haemorrhagic infarction on early CrUSS. Major lesions on term scan also led to exclusion.	MRI (some at 1.5T, some 3T), T2 automatic tissue segmentation and tissue volumes scanned during natural sleep. General linear models and correlation analysis to study the relation between brain volume and growth and perinatal variables. Linear discriminant classifier to predict outcome at 18-24 months (and 5 years) based on Bayley II scores and outcome categorised into normal and abnormal.	Brain tissue volumes at TEA (and birth) contributed to the prediction of motor outcomes at 18-24 months (and to prediction of cognitive scores at 5 years). Cognitive outcomes best predicted by GA and SES. Motor outcomes best predicted with GA SES and volumetric data measured at birth and TEA (r^2 of 0.2576)
Tortora D, Martinetti C et al. The effects of mild germinal matrix-intraventricular haemorrhage on the developmental white matter microstructure of preterm neonates: a DTI study. Eur Radiol, March 28(3): 1157-1166 (2018).	48 preterm infants <32 weeks GA - 24 infants with mGMH-IVH grades 1 and II (from a cohort of 248 consecutive MRI scans of whom 135 had DTI sequences) and controls matched by gestational age at birth and sex. 10 < 29weeks GA, 14 >29 weeks GA	MRI 1.5T. Natural sleep. Tract-based spatial statistics performed on the diffusion data to compare parameters. The relationship between DTI abnormalities and outcome as assessed by Griffiths' Developmental Scale at 24 months using Spearman correlation analysis.	Neonates with GA greater than 29 weeks had milder white matter changes while those born before 29 weeks GA who had lower FA, higher RD and MD of the corpus callosum, limbic pathways and cerebellar tracts associated with poorer visuomotor and locomotor skills at 24 months. Adverse neurodevelopmental outcome was more frequently seen in infants with mGMH-IVH ($p < 0.048$). Correlations between DTI measures and different neurodevelopmental scales plotted for different brain regions (corpus callosum, cingulum, uncinate and inferior front-occipital fasciculus

			and superior cerebellar peduncle), but no r^2 included.
Edwards AD, Redshaw ME et al. Effect of MRI on preterm infants and their families: a randomised trial with nested diagnostic and economic evaluation. Arch Dis Child Fetal Neonatal Ed. 103(1): F15-F21, (2018).	511 infants born before 33 weeks' gestation from 14 London hospitals. Unselected cohort.	MRI at 3T using chloral hydrate sedation. MRI structural images from 484 infants scored as per Woodward et al 2006. Bayley III (motor, cognitive and language) and GMFCS (Palisano et al 1997) performed around 24 months corrected age. Parallel-group randomised trial comparing MRI at term equivalent age with ultrasound. Main outcome measure of study was maternal anxiety (EPRIME cohort).	Positive predictive value of Bayley III motor score less than 85 was 38.9%, cognitive 43.1%, language 48.6% while sensitivity was 38.9%, 27.9% and 19.9%. GMFCS had a sensitivity of 60.6% but a PPV of 27.8%. Confidence intervals are given in the text. The area under the receiver operating characteristics (AUROC) follow the same pattern with language tending toward 0.5: GMFCS 0.74, Bayley III <85 for motor 0.64, cognitive 0.58 and language 0.54.
Ball G, Aljabar P et al. Multimodal image analysis of clinical influences on preterm brain development. Ann Neurology; 82: 233-246, (2017).	449 infants born under 33 weeks. Exclusion for major congenital malformations.	MRI 3T at TEA. Sedation with Chloral hydrate. Jacobian maps derived from T1, diffusion data to derive maps of fractional anisotropy and mean diffusivity, linked ICA, clinical data, neurodevelopmental outcome for 425 infants. Bayley III at 24 months corrected age (EPRIME cohort).	Cognitive, motor and language outcomes were significantly associated with the group of imaging markers (increases in grey matter volume, white matter FA and decreased grey matter MD: also, with decreased WM and subcortical GM signal) which are associated with increasing birth weight and gestational age.
Tusor, N. Benders MJ et al. Punctate white matter lesions associated with altered brain development and adverse motor outcome in preterm infants. Scientific Reports (2017).	511 infants with gestational age at birth of <33 weeks of whom imaging and follow up was collected in 281 without cerebral lesions, 114 with punctate white matter lesions and no other cerebral lesions.	MRI 3T at TEA. Sedation with Chloral Hydrate. Structural analysis, diffusion imaging. Bayley III at median corrected 20.2 months (range 18.4 - 29.3) (EPRIME cohort).	Larger lesion load correlated with reduced motor scores ($p<0.001$), but not language ($p<0.07$) or cognitive scores ($p=0.25$). Correlation between lesion load and thalamic volume ($r^2=0.26$ $p<0.001$).
Moeskops, P. et al. Prediction of cognitive and motor outcome of preterm infants	66 infants born at less than 28 weeks GA.	Structural MRI 3T at 30 weeks PMA and 40 weeks PMA. Sedation with chloral hydrate 50-	Prediction approach that is able to identify preterm infants at risk of cognitive and motor impairment at 2-3 years chronological age.

based on automatic quantitative descriptors from neonatal MR brain images. Sci Rep 7, 2163 (2017).		60 mg/kg at term and 30 mg/kg at preterm at discretion of attending clinician. 8 tissue volumes (including basal ganglia and thalami (BGT), intracranial volume, 4 measures of cortical morphology and GA modelled. No clinical information included. Support vector machine classifier evaluating difference between scans at 30 weeks and those at 40 weeks. Identified infants with low cognitive and/or motor outcomes (<85) at 2-3 years.	Neurodevelopment outcome best predicted from neonatal MRI at 30 weeks PMA. Best descriptors are gyrification index, inner cortical surface area, CSF volume and brain volume. Not BGT. Achieved an area under the curve score (AUC) of 0.78 for cognitive outcome and 0.80 for motor outcome using 30-week scan.
George JM, Fiori S *et al.* Validation of an MRI Brain Injury and Growth Scoring System in Very Preterm Infants Scanned at 29- to 35-Week Postmenstrual Age. AJNR Am J Neuroradiol (2017).	83 preterm infants imaged between 29- and 35-weeks PMA. 77 had a scan at term also. Outcome assessed at 12 months corrected age. Prospective cohort study.	3T MRI Structural images during natural sleep. Scored with generated WM, cortical grey matter, deep grey matter, cerebellum. Outcome at 12 months with Bayley III and Neuro-Sensory-Motor developmental assessment (NSMD). Uni- and multivariate regression analysis at preterm and term.	Scanning at 30 weeks PMA enables identification of infants at risk of adverse outcomes before the current standard of term-equivalent age. Global WM and deep grey matter negatively associated with Bayley III motor ($p < 0.01$), NSMD $p = 0.02$, cerebellar scores negatively associated with NSMD $p = 0.04$ Results confirmed with term-equivalent MRI. Early and term MRI best predicted motor outcome using deep grey matter with a sensitivity of 40% (CI 16-68) and 36% (13-65). Cognitive score best predicted with global score (sensitivity 50% (12-88) at early scan and WM, cerebellum and global score at term, sensitivity 33 (4-78).
Brouwer, M. J. *et al.* Preterm brain injury on term-equivalent age MRI in relation to perinatal factors and neurodevelopmental	239 extremely preterm infants (24-28 weeks GA) admitted between 2006-2012. Infants with congenital anomalies were excluded.	MRI 3T. Sedation with Chloral Hydrate 50-60mg/kg. Kidokoro scoring system used to score T1 and T2 TEA-MRI images. Multivariable regression analysis. Compare patterns of brain injury between this cohort and original St Louis/Christchurch NZ/Melbourne	Different pattern of brain abnormalities than St Louis cohort. Mechanical ventilation >7 days, parenteral nutrition > 21 days identified as independent perinatal risk factors. Cognition exclusively related to cerebellum scores ($p = 0.002$, $r^2 = 0.223$) while fine motor scores

outcome at two years. PLoS ONE 12, e0177128 (2017).		Australia Cohort. Outcome at either 24 or 30 months depending on inclusion in another study (using Bayley iii). Relationship between TEA MRI and develop evaluated using multivariable regression analysis.	were only associated with white matter scores ($p=0.004$ r^2 0.134). Gross motor outcome related to deep GM ($p = < 0.001$ r^2 0.206).
Kawahara, J. *et al.* BrainNetCNN: Convolutional neural networks for brain networks; towards predicting neurodevelopment. Neuroimage 146, 1038–1049 (2017).	DTI between 27- and 46-weeks GA. 168 preterm infant brain networks.	Cohort overlaps with Chau et al 2013 with an additional 18 infants. Imaging parameters are found in Booth BG et al 2016) MRI at 1.5T. DTI used to construct a dataset of structural brain connectivity networks. Used to predict Bayley III cognitive and motor scores, assessed at 18 months of age (corrected).	Correlation values for neurodevelopmental outcome scores were 0.310 for motor scores, compared with 0.866 for age (better at predicting postmenstrual age at the time of the scan). Connections from primary and premotor cortices were predictive of motor outcomes.
Kersbergen KJ, Leroy F et al. Relation between clinical risk factors, early cortical changes, and neurodevelopmental outcome in preterm infants. Neuroimage Nov 15; 142:301-310 (2016).	71 extremely preterm infants underwent structural evaluation at 30 weeks gestational age and term equivalent and subsequent neurodevelopmental assessment at 2 years	As for Moeskops above. Structural MRI 3T at 30 weeks PMA and 40 weeks PMA. Sedation with chloral hydrate 50-60 mg/kg at term and 30 mg/kg at preterm at discretion of attending clinician. 8 tissue volumes (including basal ganglia and thalami BGT), intracranial volume, 4 measures of cortical morphology and GA modelled. No clinical information included. Support vector machine classifier evaluating difference between scans at 30 weeks and those at 40 weeks. to Identified infants with low cognitive and/or motor outcomes (<85) at 2-3 years.	No significant correlations between gross, fine motor or cognitive outcome and brain size or sulcal folding were found.
Keunen, K. et al. Brain Volumes at Term-Equivalent Age in Preterm Infants: Imaging Biomarkers for Neurodevelopmental Outcome through Early	112 infants. mean GA 28.6 (+-1.7 weeks). Term imaging at <44 weeks PMA. Exclusions for congenital anomalies, genetic disorders,	3T MRI at term. Sedation with 50-60 mg/kg chloral hydrate. Segmentation of structural images. White matter scoring according to Woodward et al (2006), cerebellar injury according to Kidokoro et al (2013) and brain injury by neonatologists experienced in	Ventricular volume negatively related to all neurodevelopmental subscales at 24 months. After adjusting for severe brain lesions, association with cognitive composite score, fine motor scaled score (but not gross motor) at 2 years persisted. Unmyelinated white matter

School Age. J. Pediatr. 172, 88–95 (2016).	inborn errors of metabolism or congenital infections and motion).	neonatal imaging. Follow up at 24 months corrected age with Bayley iii and other assessments of neurodevelopment assessment (also at 3.5 years and 5.5 years).	measures were related to gross motor performance at 2 years after correcting for maternal education and severe brain lesions. P values included but no r^2 to judge effect size.
Rogers CE et al. Regional white matter development in very preterm infants: perinatal predictors and early developmental outcomes. Pediatric Research 79, 1 (2016).	50 infants born at less than 30 weeks (mean 26.6 weeks GA) underwent serial diffusion tensor imaging up to four times (at least 3 weeks apart) from 26-42 weeks post menstrual age. 65 infants had both serial scans and developmental follow up at 2 years.	MRI 3T at multiple time points. Natural sleep. Fractional anisotropy and mean diffusivity were calculated for regions of interest for the 50 children with more than 2 scans. Children were categorised as having WM injury based on presence of grade III/IV IVH and/or focal extensive or cystic WM lesions. Neurodevelopmental follow up at 2 years with Bayley III Scale of Infant development. Feed and wrap. Linear mixed models analysis (adjusted p values for multiple comparisons).	Perinatal factors including sepsis and antenatal steroids affected rate of change of FA between the two timepoints of the scans (FA slope). Lower MD in the left anterior limb internal capsule (ALIC) was related to impaired performance on language composite score. Higher FA in left inferior temporal lobe was related to higher motor composite scores and lower FA in right side was associated with higher motor composite scores. Specific regions vulnerable to injury. Correlation between hemispheric asymmetry and motor composite scores (r^2= 0.43) which was stronger for fine motor scores than gross motor. Term scans: significant relationship between both motor and cognitive scores with fractional anisotropy (FA) in the medial prefrontal cortex and inferior fronto-occipital fasciculus. Effect sizes were small (r^2 0.09, 0.04). No significance with language outcomes. Significant association between FA in superior portion of corona radiate, genu of corpus callosum but no effect size given. Small subset scanned at < 30 weeks - did not predict neurodevelopment outcome.
Duerden, E. G. *et al.* Tract-Based Spatial Statistics in Preterm-Born Neonates Predicts Cognitive and Motor Outcomes at 18 Months. AJNR Am J Neuroradiol 36, 1565–1571 (2015).	infants <32 weeks GA. 153 had DTI at 32 weeks PMA and 105 had DTI at 39.6 weeks PMA. Exclusions for congenital malformations or syndrome, antenatal infection or large PHI (parenchymal haemorrhagic infarction).	MRI 1.5T T1 structural and TBSS on infant scans. Un-sedated. Grouped into none, mild and moderate-severe WM injury. Bayley III Scale of Infant development and Peabody Developmental Motor Scales 2nd Ed. At 18 months corrected GA. Linear regression (Spearman correlations).	
Rose, J. *et al.* Neonatal brain microstructure correlates of	102 very low birthweight preterm infants (<1500g, <32 weeks GA).	MRI 3T at near term. Feed and wrap. "Sedation was not utilised as part of the	Cognitive composite: MD PLIC (left) r= -0.368

neurodevelopment and gait in preterm children 18-22 mo of age: an MRI and DTI study. Pediatr. Res. 78, 700–708 (2015).	66 had DTI and 38 did not – with lower incidence of NEC, sepsis and ROP and ventilated days (8.7 +- 14.4). of DTI infants, 60 underwent Bayley III and 52 completed gait evaluation. Prospective cohort.	research protocol and was typically not utilized for routine near-term MRI." Structural assessment and DTI (FA and MD) in 6 subcortical brain regions defined by DiffeoMap atlas. Bayley III and gait assessment using an instrumented mat.	Motor composite: MD PLIC (left) r= -0.354 Fine motor: FA ALIC (left) r= 0.304, FA PLIC (left) r= 0.257, MD ALIC (right) r=-0.264, MD PLIC (left) r= -0.368 Gross motor: not significant Gait velocity: FA Genu r= 0.315, MD Genu r=-0.311 Thalamus not significant. Multivariate analysis modelling was able to predict cognitive score (calculated r^2 0.247) where left PLIC MD and genu MD were the significant predictors and motor score (calculated r^2 0.131) where left PLIC MD was the significant predictor.
Hintz SR, Barnes PD et al Neuroimaging and neurodevelopmental outcome in extremely preterm infants. Pediatrics Jan;135(1):e32-42 (2015).	480 infants <28 weeks GA who survived to near term. Unselected cohort.	Cranial USS and un-sedated conventional MRI at 1.5T near term (37.9 weeks). Outcomes were death, Bayley III scores of cognitive composite score < 70, significant gross motor impairment, severe hearing or visual impairment. Multivariate models evaluated predictive value of neuroimaging.	Late CrUSS (not early) and MRI was associated with adverse outcomes, with white matter abnormalities and cerebellar lesions predicting outcome at 18 months corrected age.
Ball, G. *et al.* Thalamocortical Connectivity Predicts Cognition in Children Born Preterm. Cereb Cortex 25, 4310–4318 (2015).	57 infants. Diffusion MRI at term equivalent age in infants born < 35 weeks GA (range 25 +5 to 34 +4) with no evidence of focal abnormality on MRI	3.0 T MRI at term, probabilistic tractography from thalamus to cortex. Sedated with chloral hydrate 25-50 mg/kg. Cognitive assessment at 2 years (corrected GA) using Bayley III.	Cognitive scores at 2 years were correlated with connectivity between thalamus and extensive cortical regions, explaining 11% of the variance in cognitive scores. The model, which included GA at birth and parental socioeconomic group, explained 26% of the variance.
Kidokoro, H. *et al.* Brain injury and altered brain growth in preterm infants: predictors and prognosis.	VPT infants (less than 30 weeks). 325 infants from 3 different cohorts without congenital or chromosomal abnormality. 33%	1.5T and 3T MRI (depending on site of recruitment) at term-equivalent age without sedation. Brain growth assessed with biparietal width (BPW) and inter hemispheric distance,	(see Brouwer et al above). Severe brain injury and a characteristically impaired growth pattern were independently associated with

Pediatrics 134, e444-453 (2014).	had some grade of brain injury with 10% severe.	IVH grades 1-4 and cerebellar haemorrhage. Bayley II at 2 years in the Christchurch and Melbourne cohorts, Bayley III in the St Louis Cohort.	perinatal risk factors and delayed cognitive development. No effect sizes given.
Hart AR, Smith MR et al. Diffusion-weighted imaging and magnetic resonance proton spectroscopy following preterm birth. Clin Radiol Aug 69 (8):870-9 (2014).	Prospective cohort study of 67 infants <35 weeks GA. Those with congenital infections, developmental brain abnormalities and metabolic/genetic disorders were excluded.	1.5T MRI DWI and MRS between 37- and 44-weeks GA and developmental assessment at 18 months (CA). During sleep. Relationship between ADC values and MRS results. Feed and wrap. Outcome groups split into with and without severe developmental difficulties.	No relationship between ADC values and MRS results or outcome. NAA from posterior WM associated with severe and moderate to severe difficulties. Reduced fine motor scores associated with visible lactate doublet in the posterior WM ($p = 0.034$ but no effect size given. 12 infants with cog comp score average 89.6 had lactate doublets, 26 infants with cog comp score 101.4 did not).
Paul RA, Symser CD et al A allometric scaling relationship in the brain of preterm infants. Ann Clin Transl Neurol Nov; 1(11): 933-937 (2014).	58 infants < 30 weeks GA without severe brain injury. Grade III/IV IVH, moderate-severe cerebellar haemorrhage, or PVL were excluded leaving 49 infants of whom 27 had MRI and follow up.	T1 and T2 MRI 3.0T soon after birth (26-41 weeks). Feed and wrap. Measurements of total cerebral volume and cortical surface area using semi-automated cortical segmentation (ANTS software). Bayley III. Linear regressions.	No associations with Bayley III cognitive, language or motor scores and cortical surface area or total cerebral volume.
Shim, S.-Y. *et al.* Serial diffusion tensor images during infancy and their relationship to neuromotor outcomes in preterm infants. Neonatology 106, 348–354 (2014).	21 preterm infants < 35 weeks GA at birth. (mean 28 +1) without apparent brain abnormalities. 15 healthy term infants for control scans. A separate group controls were recruited for MRI and neurodevelopment assessment at 1 year.	MRI 3T. Feed and wrap. Structural and DTI scans at term for preterm infants and 14 term infants and at 1 year (CA). Preterm infants received neurodevelopment follow-up at 1 year. Bayley ii. Multiple linear regression analysis corrected for clinical variables	No correlation between FA values in CC at TEA and the MDI or PDI scores at 1 year of age.
Brouwer MJ, van Kooli BJ et al. Sequential cranial ultrasound and cerebellar diffusion weighted imaging contribute to the early	93 preterm infants, <31 weeks (range 25-30.9) weeks gestational age. Prospective cohort study.	MRI at 3T at term. Sedation with 50-60 mg/kg Chloral Hydrate. Preterm and term CrUSS. T1 and T2 weighted, scored according to Kidokoro scoring. Diffusion weighting imaging at term to calculate ADCs in 4 WM	Kidokoro scores did not correlate with cognitive or motor outcomes. Adding cerebellar ADC scores and enlargement of CSF spaces to the cranial ultrasound and clinical

prognosis of neurodevelopmental outcome in preterm infants. PLoS One Oct 20;9(10) (2014).		regions and both cerebellar hemispheres. Linear regression used to explore correlation between neuroimaging results (24 months CA using Bayley III) and outcome.	variables model improved the predictive value from r^2 of 0.339 to r^2 of 0.364
Bapat, R., Narayana, P. A., Zhou, Y. & Parikh, N. A. Magnetic resonance spectroscopy at term-equivalent age in extremely preterm infants: association with cognitive and language development. Pediatr. Neurol. 51, 53–59 (2014).	Methods say 43 extremely low birthweight infants (GA average 25 weeks) who survived to >34 weeks but didn't have high ventilatory requirements by that time. Exclusions for known congenital anomalies, chromosomal abnormalities. Data available for 11 term infants and 29 preterm infants of whom 3 were unable to complete the Bayley examination.	MRI 3T. Natural sleep. Spectroscopy. ratios of N-acetylaspartate to choline-containing compounds and N-acetylaspartate to myo-inositiol in the hippocampus, cortex and sub ventricular zone. Bayley mental, cognitive and language scores at 18-22 months' corrected age related to the metabolite ratios using linear regression.	NAA to Cho in the SVZ (p 0.04) associated with Bayley III. Wide confidence intervals, but not crossing zero. NAA to CHO ratios in the SVZ (p = 0.01) and the cortex (P= 0.04) and RAA to MI ratios in the SVZ p 0.03) were associated with language scores. No effects sizes are given.
Pogribna U, Burson K et al. Role of diffusion tensor imaging as an independent predictor of cognitive and language development in extremely low birth weight infants. AJNR Apr; 35(4) 790-796 (2014).	39 extremely low birth weight (<1000g) infants and 14 term infants. Exclusion criteria were congenital CNS abnormalities, or unstable and ventilated at time of enrolment.	3T MRI feed and wrap. DWI to measure FA and MD in 7 vulnerable cerebral regions (ROIs from Boardman 2010). Bayley III at 18-22 months (CA). Multiple linear regression modelling to identify DTI measures which predict Bayley scores over known predictors.	Model of birth weight, white matter injury on ultrasound and abnormal MRI at term; plus MD centrum semiovale for mental and language scores and FA subventricular zone for cognitive scores. Calculated $r^2$for model predicting mental score 0.34, for model predicting language score 0.37 and predicting cognitive score 0.30.
Kendall, G. S. *et al.* White matter NAA/Cho and Cho/Cr ratios at MR spectroscopy are predictive of motor outcome in preterm infants. *Radiology* **271,** 230–238 (2014).	43 infants born at <32-week GA (mean GA 26.9 weeks, range 22.9 - 31.9 weeks). Still an inpatient at UCL MRI scan between 37-42 weeks.	MRI 1.5T. Sedation with oral Chloral Hydrate 50 mg/kg. imaging (DTI and conventional) and single voxel point spectroscopy in posterior white matter. (N-acetylaspartate and Choline) at 40.4 weeks GA (37.9 - 44.0 weeks). Bayley III at 1-year corrected age. Scaled scores for fine motor (FM), gross motor (GM),	Elevated Cho/Cr ratio (p 0.004) and reduced NAA/Cho ratio (p 0.005) in babies associated with poorer gross motor outcome (correlation coefficients of -0.45 and 0.437).

		expressive and receptive communication. Composite scores for cognitive, language and motor.	
Park, H. W. *et al.* Brain MRI Measurements at a Term-Equivalent Age and Their Relationship to Neurodevelopmental Outcomes. American Journal of Neuroradiology 35, 599–603 (2014).	ELBW infants (<1000g) admitted between Jan 2001 and December 2010 AND <1500g with clinical indication for MR (seizures, hypoxic events, suspected PVL after USS). Severe congenital abnormalities (chromosomal or brain) were excluded. 53% had ROP (23.3% laser treatment), 24% has bronchopulmonary dysplasia	MRI 3T at term. Sedation with chloral hydrate (25-50 mg/kg) or morphine (0.05 mg/kg iv) to measure trans-cerebellar diameter (TCD) and anteroposterior length of corpus callosum. Bayley II at 2 years corrected age (16.1 months +- 6.4 months SD)	Short TCD associated with poor motor (p = 0.03 OR 0.780) and cognitive function (p= 0.04 OR 0.785). Short AP length of corpus callous associated with MDI <70 (p = 0.047 OR 0.876) and 'high-risk' or diagnosed cerebral palsy (p=0.049 OR 0.915). NB short CC associated with small head circumference at time of MR imaging and use of prenatal steroids and AED medication.
He L, Parikh NA. Atlas-guided quantification of white matter signal abnormalities on term-equivalent age MRI in very preterm infants: findings predict language and cognitive development at two years of age. Plos One. 8(12);e85475 (2013).	Cohort of 50 extremely low birthweight infants (mean 25.5 weeks GA. Without major congenital abnormalities. Postmenstrual age at scan ranged from 34.1 to 43.9 weeks. 38 with imaging and follow up. (47 returned for follow up of which 9 were excluded for behavioural problems (7), excessive motion (1) severe encephalomalacia (1)	3T MRI T2. Feeding and wrapping technique. Atlas segmentation via probabilistic atlas for very preterm infants based on a random selection of 19 infants from the cohort. Bayley III at two years of age using linear regression analysis. To investigate DEHSI (white matter signal abnormality WMSA) using quantitative methods.	White matter signal abnormality volume with language (r^2 = 0.2215, p = 0.003) and cognitive outcomes (r^2 = 0.1558, p= 0.014). WMSA within centrum semiovale better predictor with r^2 0.3912 p = <0.0001.
De Bruine FT, van Wezel-Meijer G. Tractography of white matter tracts in very preterm infants: a 2 year follow up study. Dev Med Child Neurol May 55(5) 427-33 (2013).	64 infants <32 weeks GA (mean 29.1 weeks). Scanned between 40- and 62-weeks GA. Infants with congenital brain abnormalities were excluded.	3.0 T MRI Sedation with Chloral hydrate (55mg/kg). DWI and qualitative WM injury Follow up at 2 years (range 23-44 months) with Bayley III and Child Behaviour checklist. Univariate and logistic regression analyses between DTI values and follow up parameters. Receiver operating characteristic curves.	Infants with psychomotor delay and CP had lower FA of the PLIC. Psychomotor delay associated with higher ADC values of corpus callosum (splenium) AUC 0.80 (sensitivity 100% (CI 48-100%). FA in PLIC predicted motor delay AUC 0.89 (sensitivity 100% CI 48-100) and CP AUC 0.79 (sensitivity 80% CI

			28-100). No correlation between DTI parameters and Child Behaviour checklist.
Parikh, N. A. *et al.* Automatically quantified diffuse excessive high signal intensity on MRI predicts cognitive development in preterm infants. Pediatr. Neurol. 49, 424–430 (2013).	36 infants with extremely low birth weight (<1000g). Mean 25.6 weeks. Mechanical ventilation median 26 days.	Term MRI 3T (range of 40-62 weeks). Sedation with chloral hydrate (55 mg/kg). Objectively quantified diffuse excessive high signal intensity (DEHSI). Bayley III at 18-22 months corrected age.	Study infants with abnormal cognitive and language scores exhibited significantly higher DEHSI volume, MD sum, AD sum and RD sum. All predicted between 30 and 34% of the variance.
Aeby, A. *et al.* Language development at 2 years is correlated to brain microstructure in the left superior temporal gyrus at term equivalent age: a diffusion tensor imaging study. Neuroimage 78, 145–151 (2013).	242 infants GA <32 weeks and or BW < 1500g prospectively enrolled between 2005 and 2009. GA birth (30.2 26-34). PMA at scan 38.3 (35.3 - 42.1) Exclusions: brain malformation, congenital infection, metabolic disease. 41 had cognitive, 40 language assessment and 35 motor assessment at 2 yrs.	MRI 1.5T, DTI at term equivalent age. Natural sleep. Bayley III at 2 years corrected. Used composite scores for cognitive, language and motor. Neurological examination to assess quality of movements, posture, reflexes and muscular tone led to categorisation as normal, mild, or cerebral palsy. Correlation analysis.	Cognitive and motor effects were not significant. Significant decrease in linear mean diffusivity (and longitudinal and transverse diffusivity), with increase in language scores was found around the left superior temporal gyrus. P values were between 0.0001 and 0.0003 with r^2 of 28% - 40%. FA not significant.
Chau V, Synnes A, et al. Abnormal brain maturation in preterm neonatates associated with adverse developmental outcomes. Neurology; 81(24):2082-2089 (2013).	Prospective cohort 157 infants between 24- and 32-weeks GA. Exclusions were congenital malformation/syndrome, large parenchymal venous haemorrhagic infarction (>2cm).	1.5T MRI after birth and then at TEA in natural sleep. Scoring WM injury severity, FA from 7 WM and 5 grey matter regions and NAA/Choline ratio in basal nuclei and white matter regions. Comparison of FA and NAA/Choline between the two scan timepoints and Linear regression with motor and cognitive scores of Bayley III at 18 months (CA).	Severe WMI on both scans was associated with motor outcome (p = 0.005 but based on 8 infants in the severe WMI category (IVH and cerebellar haemorrhage were not significantly associated with outcome). 18 newborns without WMI on first scan (1 on second) were found to have decreased motor scores. Basal ganglia injury seen in 4 – 2 died, survivors had abnormal motor outcome (spastic quadriparesis and low normal motor score). Change in NAA/choline slower with increasing adverse gross motor, cognitive and language outcomes.

Skiöld B, Vollmer B et al. Neonatal magnetic resonance imaging and outcome at age 30 months in extremely preterm infants. Journal of Pediatrics, Apr:160(4):559-566 (2012).	85 preterm infants (GA <27 weeks). 85 Term-born controls followed up at 30 months. Exclusions for malformations, abnormal chromosomes and congenital infections.	Conventional MRI at 1.5T and Bayley III at 30 months. Chloral Hydrate 30 mg/kg sedation early in the study, natural sleep during the last year of the study. Subgroup analysis according to gestation at birth, presence of no-mild v. moderate-severe WMI. Correlation analysis focusing on WM injury (scored using Woodward et al) and gestational age at birth	Diffuse excessive high signal intensities (DEHSI) was not associated with cerebral palsy or neurodevelopmental outcome. Moderate-severe WM abnormalities associated with CP. Moderate/severe WM – cognitive Mod/severe and GA – language. Neither mode/severe or GA affected motor outcome.
Van Kooji BJ, Benders MJ et al. Cerebellar volume and proton magnetic resonance spectroscopy at term, and neurodevelopment at 2 years of age in preterm infants. Dev Med Child Neurol. 54(3):260-266 (2012a).	58 infants less than 31 weeks GA. Exclusions for dysmorphic features and CNS infection.	MRS of cerebellum at TEA using 3T MRI and cognitive scores at 2 years corrected age. Sedation with 50-60 mg/kg chloral hydrate orally. Correlation analysis.	No association between MRS at term and outcome at 2 years
Thompson DK, Inder TE et al Corpus callosum alterations in very preterm infants: perinatal correlates and 2-year neurodevelopmental outcome. Neuroimage Feb 15; 59(4): 3571-3581 (2012).	106 infants (<30 weeks GA or <1250g birth weight) (as per Tich et al above). Prospective observational cohort study enrolling 348 VPT infants. Exclusions for congenital anomalies.	MRI 1.5T. T1 and DWI during natural sleep. Subjects scanned with different DTI protocols). Corpus callosum was traced and divided into 6 sub-regions. FA, mean, axial and radial diffusivity sampled. Bayley III at two years. Linear regression	No association between CC size and neurodevelopmental function at 2 years. Reduced posterior skew associated with impaired cognitive development described as a trend (71.4 (CI 25.0, 118) p=0.003. but with wide confidence intervals.
van Kooij, B. J. M. *et al.* Neonatal tract-based spatial statistics findings and outcome in preterm infants. AJNR Am J Neuroradiol 33, 188–194 (2012b).	63 preterm infants <31 weeks GA (mean 28.7 weeks GA) at term equivalent age. Exclusion for dysmorphic features and CNS infection.	3T MRI imaging and DTI at TEA. Sedation with Chloral hydrate (50-60 mg/kg). Voxel-wise analysis using TBSS (FA) in multiple WM regions at term equivalent age. Bayley III at 2 years (CA) to assess cognitive, fine-motor	Relationship between FA, AD and RD in the corpus callosum and cognitive scores (r^2= 0.3, r^2= 0.04, r^2= 0.13).

		and gross motor scores (mean 24.1 +/- 0.3 months).	Relationship between FA, AD and RD in posterior limb of internal capsule and fine motor scores (r^2 0.26, r^2 = 0.04, r^2 = 0.28). Relationship between FA, AD and RD in left PLIC and gross motor function (r^2 = 0.26, r^2 = 0.02, r^2 0.22)
Hart A, Whitby E et al. Neuro-developmental outcome at 18 months in premature infants with diffuse excessive high signal intensity on MR imaging of the brain. Pediatr Radiol Oct;41(10):1284-92 (2011).	Prospective observational study of 67 preterm infants to determine whether preterm children with DEHSI at TEA have abnormal neuro-developmental outcome.	MRI at TEA combining structural scoring with diffusion values (ADC). Images reported as normal, abnormal or DEHSI (defined scoring ADCs and visual appearance at 6 ROIs). Bayley III at 18 months (CA). Analysis done between groups.	No significant difference between those with and without DEHSI regardless of whether a structural or diffusion definition was used.
Tich SN, Anderson PJ. Neurodevelopmental and perinatal correlates of simple brain metrics in very preterm infants. Arch Pediatr Adolsc Med Mar;15(3);216-22 (2011).	Prospective cohort study. GA less than 30 weeks or weight less than 1250g. 348 eligible infants of whom 236 were recruited. 187 MRI studies completed.	MRI – 1.5T. Natural sleep. Qualitative white matter assessment, grey matter abnormalities (signal abnormalities, gyral maturation, size of subarachnoid space. Biparietal (BPD), bifrontal and transverse cerebellar diameter. Bayley II at 24 months (CA). Between group (white matter abnormality) testing and multivariate regression model including brain metrics and sex.	BPD most predictive of cognitive and motor abilities. Expressed as mean differences in MDI or PDI for each unit change in brain diameters. Mean differences are small.
Lind A, Parkkola R et al Associations between regional brain volumes at term-equivalent age and development at 2 years of age in preterm children. Pediatr Radiol Aug;41(8);953-61 (2011).	164 very low birthweight infants divided into children without neurodevelopmental impairments at two years (148) and those with (16).	Comparison of brain volumes in those with and without neurodevelopmental impairment (cerebral palsy, hearing loss, blindness and significantly delayed cognitive skills). Analysis done between groups.	Total brain volume, cerebrum, frontal lobes, basal ganglia, thalami and cerebellum were significantly smaller in those with impairments. Cerebellar volume was correlated with poorer neurological outcome in those without severe impairments.

Boardman JP, Craven C et al. A common neonatal image phenotype predicts adverse neurodevelopmental outcome in children born preterm. Neuroimage, Aug 15;52(2): 409-14 (2010).	80 preterm infants <34 weeks GA (mean 29 +6 GA) and 20 term-born infants at TEA. Exclusions for congenital malformation or congenital CNS infection, cystic PVL, HPI or post-haemorrhagic ventricular dilation.	MRI 1.5T Diffusion MRI to determine diffuse white matter injury (abnormal ADC in one or more WM regions of interest). Structural MRI using deformation-based morphometry. Sedated with chloral hydrate. Griffiths Mental Development Scales administered for neurodevelopmental follow up (27.5 months for preterm infants and 31.1 months term controls). Preterm imaging phenotype identified.	Neonatal imaging phenotype associated with a reduced developmental quotient at 2 years ($p < 0.001$) using non parametric Kruskal-Wallis test. Consisted of diffuse WM injury, tissue volume reduction in DM nucleus of thalamus, globus pallidus, periventricular WM, corona radiate and centrum semiovale (central region). Linear relationship between DQ and GA at birth ($r^2 = 0.246$).
Kaukola T, Perhomaa M et al Apparent diffusion coefficient on magnetic resonance imaging in pons and in corona radiate and relation with the neurophysiologic measurements and the outcome in very preterm infants. Neonatology 97(1) 15-21 (2010).	30 infants <32 weeks GA and BW < 1000g. Exclusions: Infants with major destructive brain lesions.	MRI DWI. ADC in ROIs known to contain motor fibres. Brain stem auditory evoked potential (BAEP) at term age. Griffith Scales at 2 years (CA). Correlation analysis	Poor gross motor outcome associated with higher ADC in corona radiata (mean = 1.343 vs 1.197 $p < 0.004$).
Counsell SJ, Edwards AD et al. Specific relations between neurodevelopmental abilities and white matter microstructure in children born preterm. Brain Dec;131(Pt 12);3201-8 (2008).	33 children born at <32 weeks GA (average of 28+5 weeks GA range 24+4 – 32+1). Infants with structural abnormalities on MRI (overt focal lesions, post-haemorrhagic hydrocephalus, congenital abnormalities or metabolic disease) were excluded.	MRI 3T DTI imaging at TEA. Sedation with Chloral hydrate (100 mg/kg up to max 1g). Griffiths Mental Development Scale at 2 years corrected age (24-27 months). Correlation analysis	DQ was linearly related to FA values in parts of corpus callosum. Eye-hand co-ordination with FA in the cingulum, fornix, anterior commissure, corpus callosum and right uncinate fasciculus. Slope values given: range from 0.003 to 0.006).
Augustine EM, Spielman DM et al Can magnetic resonance spectroscopy	36 infants (<32 weeks GA, birth weight <1510g).	MRI at 1.5T 35-43 weeks GA. Spectroscopy and metabolite ratios calculated in thalamus and basal ganglia. Bayley Scale of Infant	No correlation with outcome

predict neurodevelopmental outcome in very low birth weight preterm infants? J Perinatol 28(9): 611-618 (2008).		Development between 18 and 24 months (CA). Unpaired t-tests between those classed as 'normal' and 'abnormal' and metabolite ratios.	
Beauchamp, M.H. et al Preterm infant hippocampal volumes correlate with later working memory deficits. Brain 131, 2986-2994, (2008).	227 very preterm infants (<30 weeks' gestation) or <1250g. Mean GA was 27.4 weeks (range 22-32).	MRI 1.5T scan at term equivalent age (38-42 weeks GA). Structural scans parcellated into 8 areas. Assessment of memory (delayed alternation) at 2 years corrected age. ANOVA for continuous variables and Peason's chi-square statistic for categorical variables.	Dorsolateral prefrontal cortex and parietal-occipital volumes at TEA were not associated with performance. Significant (but small) difference in hippocampal volume between children who failed to learn or persist with the working memory task and those who did not. Manually segmented hippocampal volumes on the right and left were 1.16, 1.14 for fail group, 1.10, 1.08 for those who did not persist and 1.18, 1.16 in the intact working memory group.
Krishnan ML, Dyet LE et al. Relationship between white matter apparent diffusion coefficients in preterm infants at term-equivalent age and developmental outcome at 2 years. Pediatrics 120(3) 604-609 (2007).	38 infants born at less than 34 weeks GA and without severe cerebral pathology on MRI	Terms DWI at the level of centrum semiovale. Griffith Mental Development Scale at 2 years (CA). Correlation analysis.	None of the children had significant neurological problems. Higher ADC in white matter at TEA is associated with lower DQ at 2 years.
Drobyshevsky A, Bregman J et al. Serial diffusion tensor imaging detects white matter changes that correlate with motor outcome in premature infants. Dev Neurosci. 29(4-5): 289-301 (2007).	140 met enrolment criteria of <32 weeks GA without major congenital anomalies, cranial ultrasound scan within first week of life and stable at approximately 30 weeks' gestation. 24 infants were enrolled. They were compared with a stratified control group of 24 of whom 11 were	MRI strength not stated. Serial DTI at 30- and 36-weeks GA. FA and ADC calculated. Bayley Scales of Infant Development II used to stratify into controls, mild injury and severe injury (CP). Correlation analysis. Feed and wrap.	ADC higher in severe injury group at 36 weeks GA in central and occipital white matter and corona radiate. Only FA in PLIC at 30 weeks (r^2 0.55) was significantly correlated with psychomotor outcome scores, not significant by MRI at 36 weeks. Change in FA per week (occipital white matter and internal capsule) between scans was also significantly associated with psychomotor index (r^2 0.63).

	normal, 6 had grades 1-2 IVH and 6 had grades 3-4 IVH. 12 followed up with neurodevelopmental testing		The 12 infants who had neurodevelopmental outcome tests at 2 years old were Caucasian with health insurance. No data on socioeconomic status of parents was collected.
Woodward LJ, Edgin JO, Thompson D, Inder TE. Object working memory deficits predicted by early brain injury and development in the preterm infant. Brain 128, 11, 2578-2587 (2005).	Prospective cohort of 119 infants <32 weeks GA and <1500g without congenital abnormalities of whom 100 (mean GA of 27.9 weeks) underwent MRI at 40 weeks. 76 successful datasets acquired. Comparison group of term infants (average GA 39.6 weeks) selected from delivery register (gender matched). Infants with congenital abnormalities excluded	1.5T MRI at term equivalent age using feed and wrap technique. 24 months (CA) underwent Bayley II neurodevelopment testing and object working memory test. T2 image segmented into 5 tissue classes and reported as tissue volumes. Qualitative assessment of WM abnormality. Correlation analysis for continuous variables and Chi squared test of independent for dichotomous variable.	Infants with moderate-severe WM abnormalities had the lowest rate of task completion on working memory test. Reductions in volumes of tissues in specific regions within left and right dorsal prefrontal cortex and posterior motor regions were related to performance but with low r^2 (0.01-0.09). Significant linear relationship between CSF volume at term and decreased task performance at 2 years: not found with other tissue volumes. White matter severity was predictive of outcome.

Aims and objectives

The work in this thesis aims to provide imaging biomarkers at term equivalent age to enable trials of targeted interventions both during the preterm period and after discharge from the neonatal unit. This would also give invaluable information to parents and health professionals about difficulties in specific domains which the child might face. A poor prognosis, especially with regards to gross motor outcome, can currently be made for some infants using MRI or ultrasound by the time of normal birth. The work presented in this thesis focuses on the outcome of those infants born preterm, who are known to be at risk of adverse outcomes, but whose outcome we cannot predict from clinical examination or MRI by the time of normal birth.

In order to achieve this, I have developed and extended methodology of resting state functional connectivity from that used in adults by Zhang et al 2008 to map cortico-subcortical connectivity in infants at the time of normal birth by parcellating the thalamus and the striatum according to their connections with the neocortex and subsequently analysing this connectivity according to gestational age at birth in preterm and term infants. I have used neurodevelopmental follow up, collected by others in conjunction with the EPRIME project, to investigate the connection between outcome in motor, cognitive and language domains and functional connectivity at the time of normal birth as measured using correlations of blood oxygen level dependent signal between cortical and subcortical regions at the time of normal birth.

Part Two

Materials and Methods

Chapter Four

General methods

Basic physics of magnetic resonance imaging

As Isidor Rabi, credited for the discovery of nuclear magnetic resonance (NMR), wrote in 1938

"If a small oscillating magnetic field is applied at right angles to a much larger constant field, a re-orientation of the nuclear spin and magnetic moment with respect to the constant field will occur when the frequency of the oscillating field is close to the Larmor frequency of precession of the particular angular momentum vector in question." Rabi II, Zacharias JR, Milman S, Kusch P. A new method of measuring nuclear magnetic moment (letter). Physics Review 1938: 53:318. (Rabi *et al.*, 1938).

Nuclear Magnetic resonance (NMR) is a non-ionising imaging technique, first discovered in the late 1940s (Bloch, 1946; Purcell *et al.*, 1946) with the first image produced using this technique showing a beaker containing two water-filled test-tubes (Lauterbur, 1973). Imaging of the structure of tumours ex-vivo (Damadian, 1971), in-vivo in mouse (Damadian *et al.*, 1976) and in vivo in human followed in 1977 showing the basic structures of the chest (Damadian *et al.*, 1977). It now has widespread use as a clinical imaging technique allowing the visualisation of internal structures and as it is non-ionising, has wide-ranging uses in research as well. Its use in the neonatal population allows in vivo study of brain structure, investigation into microstructural alterations, connectivity analyses and the ability to assess functional alterations in those born preterm. In addition to the in-text references, this appendix has been informed by the following widely-used reference books: (Jezzard *et al.*, 2001; Huettel *et al.*, 2014; Bijsterbosch *et al.*, 2017; Jenkinson and Chappell, 2018; Westbrook and Talbot, 2019).

Magnetic properties

Molecules, such as the abundant water in the human body, have nuclear magnetic resonance property (NMR) due to two characteristics of their hydrogen atoms: generation of magnetic moments and angular momentum. Angular momentum results from the spinning motion of the nucleus of the hydrogen atom as a result of the odd number of protons (single proton): in a nucleus with equal numbers of protons and neutrons, the spinning motion would cancel out. The nucleus itself is charged as a result of the internal composition of the proton, consisting of three spinning quarks, two which spin upwards and one which spins down, generating a total charge of +1 (Westbrook and Talbot, 2019). The single proton of the hydrogen atom will therefore spin around its axis and because the nucleus has a net positive charge, this spin will generate an electrical current on the surface. This charged moving particle creates a magnetic field (as stated by Faraday's law of electromagnetic induction) with a north and a south pole of equal strength and is referred to as a magnetic moment.

In the absence of a strong static magnetic field, the axes around which the protons spin will be oriented randomly, and effects of magnetic moments will cancel each other out and be undetectable (no net magnetisation).

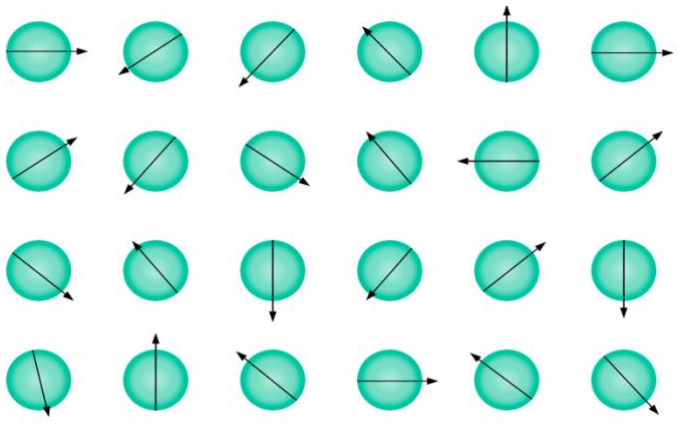

Figure 4.1. Random alignment of hydrogen nuclei

A strong static magnetic field, known as B_0 and measured in units of Tesla, is required for the hydrogen nuclei to change from a random alignment (fig. 4.1 above) where there is no net magnetisation, to becoming aligned parallel to this magnetic field.

According to quantum theory, hydrogen nuclei exist in high and low energy states, with the low energy protons aligning parallel to the magnetic field (known as spin up) and those with high energy protons anti-parallel (spin down) (Jezzard *et al.*, 2001). Although the magnetic moments of the hydrogen spins are moving between the high and low energy states, at any one moment there is a greater proportion of nuclei with their magnetic moments aligned in the same direction as the B_0 field than there are antiparallel. This state of balance between parallel and anti-parallel protons in a static magnetic field is described as the net magnetisation vector (NMV). The NMV is greater at higher B_0 field strengths as fewer protons have the energy to be anti-parallel and this results in a greater proportion of lower-energy parallel-aligned protons. This is defined by the Boltzmann equation.

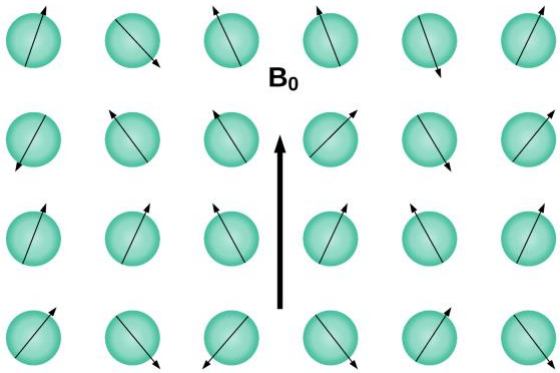

Figure 4.2. Application of an external magnetic field along the direction of B_0 (the static magnetic field of the MRI scanner) causes alignment of the magnetic moments of the hydrogen nuclei either parallel or antiparallel to the magnetic field.

The proportion of spin up versus spin down nuclei is predicted by the Boltzmann equation which relates the number of spins in the high or low energy populations (N+/N-) with the temperature of the tissue in Kelvin. Where delta E is the energy difference between high and low energy populations in joules (j), k is Boltzmann's constant (1.381×10^{-23} joules /°K) and T is the temperature of the tissue in Kelvin (K). Thermal equilibrium is assumed in MRI and so the right side of the equation is dictated by the strength of the external magnetic field (B_0).

$$N+/N- = e^{\frac{-\Delta E}{kT}}$$

equation 4.1

Precession

In addition to the parallel and antiparallel states, a further property of the net magnetisation in a strong static magnetic field is its precession around the B_0 axis, with the frequency of the rotation being proportional to the B_0 field and any other fields it experiences. In the case of a hydrogen atom, the frequency is 42.58 MHz times the main B_0 field giving a frequency of approximately 64 MHz at 1.5 T and 128 MHz at 3T (Jezzard *et al.*, 2001). The relationship between precession frequency and field strength is governed by the Larmor equation and the frequency of the precession is known as the Larmor frequency or resonant frequency. The gyro-magnetic ratio is different for different MR-active molecules, the ratio for hydrogen being 42.58 MHz/T. The equation (4.2) is given below where the precessional frequency (Lamour frequency) is equal to the gyro-magnetic ratio in MHz/Tesla multiplied by the static magnetic field strength (B_0 field) in units of Tesla.

Larmor equation

$$\omega_0 = \gamma B_0$$ Equation 4.2

Figure 4.3: The fixed angle (thick arrow) of the net magnetisation vector precessing around the B_0 field (longitudinal axis)

Resonance and excitation

Due to the earth's magnetic field, Hydrogen nuclei always demonstrate precession. They undergo nuclear magnetic resonance (NMR), however, when exposed to an oscillating perturbation with a frequency the same as their resonance frequency (Larmor frequency). The Larmor frequency of the hydrogen nucleus is in the radio frequency band of the electromagnetic spectrum allowing the required frequency to be transmitted using a radio frequency pulse emitted from an RF coil. It is applied at 90 degrees to the B0 field resulting in the angle of the NMV being tipped into the transverse plane and the magnetic moments of the hydrogen nuclei precessing in phase with each other. The magnetic fields induced by RF coils are only produced for short periods of time and are called RF pulses.

In accordance with Faraday's law of induction, the change of the NMV from the B0 field to the transverse plane results in the generation of an electric current. This current induces a voltage in a receiver coil placed in the moving magnetic field with the magnitude of the signal being determined by the amount of in-phase magnetisation present in the transverse plane and the frequency of the signal being determined by the frequency of the rotation of the magnetic field. This is the magnetic resonance signal. As the coils are orthogonal to the B_0 axis, changes in the net magnetisation are only detected in this transverse plane.

Image formation

The data acquired according the principles set out so far, contain the summed properties of the spins of the hydrogen nuclei within the tissues, but are unable to convey spatial information. Further carefully controlled spatially varying superimposed magnetic fields (gradient fields), where the field changes linearly, are imposed in order to relate frequency to location. As seen above in the Larmor equation, a different magnetic field strength will result in a different and predictable precessional frequency. At least three of these gradient fields are needed in order to acquire signal and assign a spatial location and these are provided by three different gradient coils.

Slice selection is the restriction of the MR signal to a two-dimensional slice at a time. The precession frequency of the spins within the desired slice are matched to the radio frequency excitation pulse, thereby inducing the protons in that slice to absorb energy and change from low to high energy states. When the excitation pulse stops, the MR signal will be emitted from spins in this particular slice. This process involves the generation of one gradient across space and one single RF excitation pulse and therefore can be completed very rapidly.

Frequency encoding and phase encoding are required to cause spins at different locations to precess at different rates and therefore be assigned to a spatial location. Firstly, a gradient is applied to the slice (frequency encoding) allowing spatial reconciliation of spins precessing at any one of the frequencies in the gradient. The second gradient is applied sequentially (termed phase encoding) so that the spins along the first gradient would already be precessing at different rates depending on spatial locations by the time the second gradient is introduced: their current angle of precession, or phase, would be different along the gradient first applied. Data from each signal position are stored as data points in K-space which places frequency along the horizontal axis and phase along the vertical axis. This information is then decomposed using the Fourier transform into a matrix of pixels (same dimension as K-space) with each pixel being allocated a point on the grey-scale which corresponds to the amplitude of the frequencies of that spatial location.

Contrast

The magnitude of the signal measured depends on the density of hydrogen nuclei at a particular location and a simple image can be created where image intensity is related to this (proton density weighted image or PD weighted image). There is only a relatively small difference in the water content between different tissues, so PD imaging provides only modest contrast between different brain tissues such as fluid-filled spaces, grey or white matter.

Relaxation

In order to provide a greater contrast between tissue types than is provided by proton density imaging, the relaxation properties of the hydrogen nuclei are commonly used. There are two constants (T1 and T2) which describe the way in which nuclei revert to the original NMV after the RF pulse. T1 describes the realignment of the NMV with the longitudinal axis (B0) as some of the high energy nuclei revert to low energy states in accordance with the principles of thermodynamics. In addition, there is de-phasing of the precession of the nuclei and decrease in transverse magnetisation, described as T2. This decay in transverse magnetisation is due to the different environments experienced by the hydrogen nuclei: for example, proximity to heterogenous populations of molecules causing inhomogeneous magnetic fields and therefore altered rates of precession of the spins with consequent de-phasing. The effect of local B0 field inhomogeneities are a second reason for dephasing and the T2* relaxation time describes the combination of both the T2 effects.

These relaxation times (PD, T1 and T2) are constants but by manipulating the sequence parameters such as the echo time and repetition time, different types of structural image can be obtained in order to gain the greatest contrast between tissue types and thereby maximise contrast to noise ratio (CNR).

Maximising contrast from relaxation

At the time point of the 90-degree RF excitation pulse, there is no magnetisation in the longitudinal component (B0) and the transverse component is at a maximum. After the RF excitation pulse has ended, the longitudinal component now increases (T1) and

the transverse component reduces according to T2 dephasing. Sequences can favour the acquisition of T1 contrast, maximising the difference between white matter, grey matter and CSF through careful choosing of the repetition time (TR). The decision as to how long to wait after excitation before encoding the signal (the echo time or TE) determines the T2 contrast between tissues (TE). In the transverse plane, there is high signal from the tissues immediately after excitation, when the NMV is at 90 degrees, but all tissues will have approximately the same magnetisation giving a high signal but no tissue contrast. As different tissues dephase at different rates (have a different T2 decay time), there is a subsequent time point where this difference between signal and tissue contrast is optimised. T2 dephasing is a very rapid process in comparison to T1 recovery time.

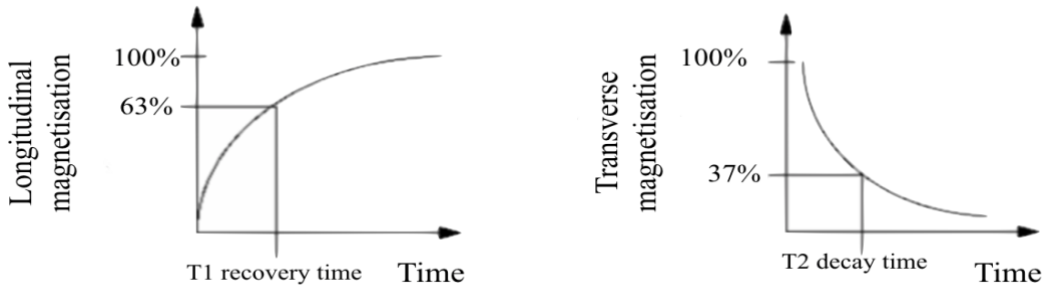

Figure 4.4. T1 recovery time (left) is a constant for a given tissue and is defined as a gain of 63% of the longitudinal net magnetisation vector. T2 decay (right) is a constant for a given tissue and defined as a loss of 63% of magnetisation in the transverse plane so that the % of magnetisation remaining is 37% of the maximum transverse magnetisation achieved.

Echo Planar Imaging

Echo Planar imaging was developed to fill the entire k-space with a single acquisition in order to investigate rapidly changing processes such as the diffusion of water molecules in diffusion MRI and blood oxygenation in functional MRI. Although the contrast is poorer, geometric distortions are introduced and the resolution significantly lower than for structural imaging, the trade-off in terms of the ability to capture in vivo dynamic processes has led to its wide-spread use as a research and clinical tool. Both diffusion and BOLD imaging utilise EPI sequences, but with regards to BOLD imaging, the sequence parameters are optimised so that the echo time (TE) is similar to that of the T2* of grey matter optimising the detection of the BOLD effect. The

sensitisation to T2* to capture the desired inhomogeneity from BOLD contrast results in sensitisation to all B_0 inhomogeneities such as signal loss near air interfaces resulting in an additional disadvantage in comparison with diffusion imaging.

Diffusion MRI

Metrics obtained using diffusion MRI are used as surrogate markers of the microstructural properties and anatomical connectivity of the brain. Metrics reflecting these properties (of axon size, density and myelination) can be obtained in individual subjects and then statistical tests used to look for correlations with variables, or group differences. Secondly, tractography can be used to estimate the connectivity of one area of the brain with another providing a method of looking at structural connectivity in vivo (Jenkinson and Chappell, 2018). Diffusion MRI is based on the movement of water molecules. Water molecules are in constant motion at temperatures above absolute zero (thermally-driven) and the pattern of motion is random. This feature of water was first described by Robert Brown and is referred to as Brownian motion (Robert Brown 1773-1858). In 1905, Albert Einstein applied this to particles in a homogenous space without barriers, where the mean squared displacement ($<r^2>$) is directly proportional to the observation time (t) and D represents the diffusion coefficient of the medium, which at body temperature of 37 °C will be equal to 10^{-3} mm^2/s (Le Bihan *et al.*, 1991).

$$<r^2> = 2Dt \qquad \text{Equation 4.3}$$

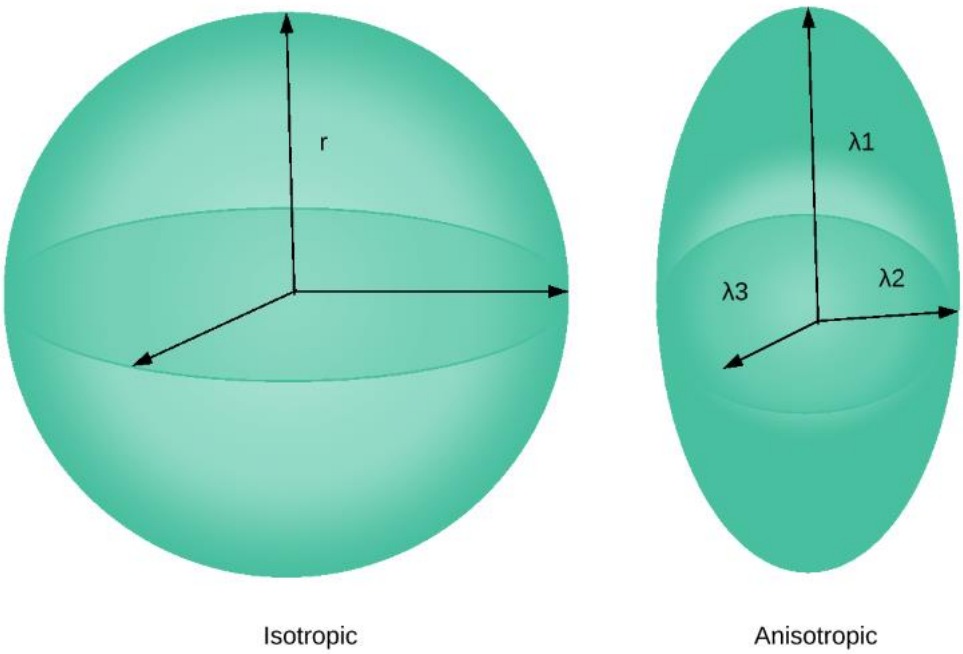

Figure 4.5. Isotropic and anisotropic diffusion

In free diffusion, the displacement distribution ($<r^2>$) is a Gaussian function and can be represented by a sphere as the probability of a molecule reaching any point by a certain time point, is equal in all directions (Fig. 5). There is no preferred direction for water diffusion, and this is described as isotropic. However, movement of water molecules within the white matter of the brain are restricted by membranes and tissue boundaries rendering diffusion anisotropic in white matter (Beaulieu, 2002). This preference can be exploited to probe the movement along the axon as compared with movement in other directions, thereby defining the direction of the axon. Diffusion tensor imaging describes a single direction of movement of water within a voxel and is described in terms of the mean diffusivity (MD) and fractional anisotropy (FA). Fractional anisotropy is described as low when water is able to move equally in all directions and high when there is a preference of diffusion direction. In addition, this can be classed as diffusion along the axis of highest diffusivity (axial diffusivity, AD), contrasted with diffusion perpendicular to this direction which is called radial diffusivity (RD) (Jenkinson et al 2018). These are indirect measures of the underlying biological properties of the tissue. The application of tractography algorithms produces a map of the principle diffusion direction from voxel to voxel.

Spectroscopy (MRS)

In addition to hydrogen atoms, other atoms, such as Choline (CHO), N-acetylasparate (NAA) and Creatinine have nuclear magnetic resonance properties (NMR). As each of these molecules has a different cloud of electrons which shield the nucleus from the magnetic field in a different way, the frequency of the signal emitted by these molecules as a result of the application of a magnetic field, is different from each other. This is called chemical shift and the different contributions of different molecules can be determined by carefully measuring the frequency components of the signal (Brown *et al.*, 1982). Given the small concentration of these molecules, the signal to noise ratio must be optimised by using a single, but very large voxel thereby sacrificing spatial resolution.

Functional Imaging

Foundations of BOLD response

The ability to image blood flow in the brain over time is possible due to the different effects of oxygenated and deoxygenated blood on a magnetic field. As a result of unpaired electrons, deoxygenated blood has a magnetic moment and is paramagnetic with a magnetic susceptibility of 20% more than fully oxygenated blood (Pauling and Coryell, 1936). Deoxygenated blood therefore interacts with the magnetic field differently from the surrounding oxygenated tissue (Ogawa *et al.*, 1990a). The field surrounding deoxygenated blood is distorted (due to increased B0 inhomogeneity) causing local protons to experience different field strengths and a more rapid decay of transverse magnetisation (Ogawa *et al.*, 1990b) but with no effect on the T1 relaxation time. However, arterioles are sensitive to a small increase in local oxygen consumption and increases in neuronal activity lead to an increase in cerebral blood flow which over-compensates for the neuronal activity (Fox and Raichle, 1986; Fox *et al.*, 1988). The net result is a relative increase in oxygenated blood and increased signal at the location of the neuronal activity when compared with the baseline state of that tissue. This is the basis of the blood oxygenation level dependent (BOLD) effect and is quantified by the T2* relaxation time where the increase in MR signal from the increase in oxygenated haemoglobin provides contrast with the surrounding tissues.

To quantify this increase in signal as a result of the BOLD effect, a hand squeezing task, known as a reliable and robust way to stimulate BOLD response, increases the signal at voxels in the primary motor cortex by about 5% in adults (Huettel *et al.*, 2014).

Neuronal correlates of the BOLD response

Neuronal membrane potentials, and therefore neuronal activity, require energy for their maintenance and restoration. These membrane potentials are maintained and restored with the use of pumps which move ions across the membrane against their concentration gradient and this requires a source of energy. In the case of the ubiquitous sodium-potassium pump, which restores the asymmetric distribution of sodium and potassium across the membrane after a depolarisation, one exchange done by the pump requires the energy of one molecule of adenosine triphosphate (ATP) to be converted to adenosine diphosphate (ADP). Energy is also required for a hyper polarisation (Inhibitory postsynaptic potential, IPSP) or depolarisation (Excitatory postsynaptic potential, EPSP) of the post-synaptic membrane. Glucose is the major source of energy in the brain, most efficiently converted to ATP in the presence of oxygen. Although this is stored in the rest of the body as glycogen, there is very little glycogen storage in the brain and therefore energy in the brain requires a constant source of glucose and oxygen via the vascular system. Glucose is transported from capillaries into the cell cytoplasm where it costs two ATP to break it down, but in the presence of oxygen (aerobic respiration) the overall process releases 36 molecules of ATP from each molecule of glucose. Although 'housekeeping' processes such as synthesis of protein, maintenance of membranes and production of neurotransmitters require energy, the majority of energy is used in the process of restoring the asymmetric distribution across membranes following action potentials, EPSP and IPSPs. It is known that regional increases in glucose consumption in the brain are accompanied by increases in blood flow to the same region (Sokoloff *et al.*, 1977). Indeed, this has been modelled with the injection of penicillin to the motor cortex of rats to induce seizure in discrete parts of the cortico-striato-thalamo-cortical loop involved, resulting in increased glucose utilisation in contralateral motor cortex, ipsilateral and contralateral putamen and globus pallidus, ipsilateral and contralateral

thalamic nuclei and substantia nigra (Kennedy *et al.*, 1975). In addition to the evidence linking the BOLD response with energy requirements, there is evidence from simultaneous fMRI with electroencephalogram (EEG) reviewed by Logothetis (Logothetis, 2003). Variation in the alpha rhythm of the EEG is correlated with the time series of the fMRI (Goldman *et al.*, 2002), further suggesting a neuronal cause for resting state networks (Beckmann *et al.*, 2005). The relationship between neuronal activity and the BOLD response is still not completely understood and the differences in the time and spatial extent of the haemodynamic response to stimulation will be mentioned briefly.

Spatial specificity of BOLD response

In response to a sensory stimulation, Ngai et al, demonstrated that the vascular diameter of arterioles in the brain increased rapidly at the beginning of the stimulation and reached a peak 5.5 seconds later (Ngai *et al.*, 1988). The diameter of the artery increased about 33% during this time and subsequently contracted to a plateau which was 10% above the baseline until the stimulation was removed. Iadecola et al recorded increases of up to 26% in arterioles supplying activated neurons, while larger arterioles, millimetres away, where no field potentials were recorded, also dilated by 8% (Iadecola, 1998). Neuronal activity, therefore, produces a haemodynamic response over an area greater than that of the increased neuronal activity and this has important consequences for the interpretation of results.

Temporal implications of BOLD response

As outlined above, the BOLD response to an increase in neuronal activity is a much slower response that that of the neuronal changes themselves, taking around 6 seconds to reach a peak after the onset of a stimulus and around 20 seconds to return to the baseline. The imaging sequences required for functional imaging are different from structural imaging as the whole brain needs to be imaged as simultaneously as possible and between 200 and 300 images are necessary for statistical analysis of the BOLD response. Echo planar imaging (EPI), in which a single excitation, followed by rapid gradient switching, is used to fill up the entire k-space provides a suitable technique (Mansfield, 1977; Mansfield and Maudsley, 1977). This is in contrast to the traditional

method of filling up k-space line-by-line with multiple excitations. Very strong gradients are required as well as a pattern of collection of data in which alternating lines are filled in opposite directions. This increased speed of image collection also uses a bigger voxel size (reduced spatial resolution), has limited tissue contrast (focuses on T2* effects) and involves greater geometric distortion and susceptibility to artefacts. It, however, enables us to capture a changing dynamic process of oxygen consumption and to identify the spatial location of that oxygen consumption in our study at a resolution of 2.5mm x 2.5mm with a slice thickness of 3.25mm (voxel size).

Resting state networks

Resting state networks describe distributed areas of the brain which statistically covary over the course of a functional scan, traditionally describing neocortical areas which covary. Belliveau et al are credited as the first to publish results using the idea of increased blood flow as an indicator of increased neuronal activity, showing, with the use of gadolinium as contrast agent, blood volume changes in the visual cortex as the result of visual stimulation (Belliveau *et al.*, 1991). In 1991 (and published in 1992) three separate papers used blood oxygen level dependent contrast to show brain activation without any exogenous contrast (Bandettini *et al.*, 1992; Kwong *et al.*, 1992; Ogawa *et al.*, 1992). These original papers use BOLD imaging in task-based experiments, statistically contrasting the signal intensity during periods of stimulus with periods where no stimulus is offered. Biswal et al first demonstrated the use of fMRI in the absence of a task, modelling the most active part of the brain during a finger tapping task and finding that this part of the primary motor cortex was also statistically covarying in the absence of the task paradigm (Biswal *et al.*, 1995). The identification of the visual system (DeYoe *et al.*, 1994), auditory system, including receptive and expressive language (Yetkin *et al.*, 1995; Cordes *et al.*, 2000) and more complex spatially-distributed network present at rest, followed.

Importantly for study of resting state networks, they are consistent across healthy subjects (Damoiseaux *et al.*, 2006) and found to be altered in some diseases (Lowe *et al.*, 2002; Greicius *et al.*, 2004; Woodward *et al.*, 2012). The congruence between

functional networks at rest and during task-based paradigms first demonstrated by Biswal et al in 1995 has been established with meta-analysis of task-based activation maps and those found in the adult resting brain (Smith *et al.*, 2009). This conclusion that the adult brain 'rehearses' a complete repertoire of networks in the absence of task-based paradigms is of special interest in the study of the neonatal brain where task-based paradigms are limited. Resting state networks reflect large-scale neuronal functional systems and can be identified in the absence of well-defined models (Smith *et al.*, 2012) and show similarities with structural connections of the brain (Honey *et al.*, 2009). There are known interactions between networks, such as default mode and task positive networks (Fox *et al.*, 2005).

Resting state networks in infants

During the last trimester of pregnancy, functional magnetic resonance imaging (fMRI) detects the emergence of coordinated, spontaneous fluctuations in the Blood Oxygen Level Dependent (BOLD) signals, which are closely linked with the development of electroencephalographic activity (Vanhatalo and Kaila, 2006; Omidvarnia *et al.*, 2013) and develop into a near-facsimile of the mature adult resting state network architecture by the normal age of birth at 38-42 weeks gestational age (Doria *et al.*, 2010). The exception to this is the default mode network which appears only in its component parts in infants, rather than as a covarying spatially-distributed network as in adults (Fransson *et al.*, 2007; Doria *et al.*, 2010). The finding of a fragmented default mode network at birth led to the hypothesis that resting state architecture developed during childhood as the accompanying cognitive processes developed. However, a study of 7-9 years olds found that it was still fragmented in spite of the ability of children of this age to perform tasks such as mentalising and processes using episodic memory and theory of mind (Fair et al 2008) and concluded that the changes observed with greater age must reflect other changes in the network, not captured in the current models of resting state networks. These ideas of efficiency (Fair *et al.*, 2008), stationarity (Chang and Glover, 2010) and complex network measures (Rubinov and Sporns, 2010; Vértes *et al.*, 2012) provide the basis of future directions for further interrogating resting state networks in neonates.

Having established that resting state networks are consistent across healthy adult subjects (Damoiseaux *et al.*, 2006) it has also been found that they are robust to the effects of prematurity as assessed at the time of normal birth (Fransson *et al.*, 2007; Damaraju *et al.*, 2010; Doria *et al.*, 2010; Lee *et al.*, 2013) and still at 18 months (Damaraju *et al.*, 2010). By 36 months however, there is some evidence that the strength of connectivity within certain networks (not difference in the spatial distribution) is increased in children born at term although the numbers in this study are small (9) and there are no other published investigations at 36 months with which to compare (Damaraju *et al.*, 2010). A more recent study finds the same increased magnitude of connectivity, but no different in topography, between cortico-cerebellar connectivity in term-born infants when compared with those born preterm (Herzmann *et al.*, 2018).

Judged by anatomical distribution, rather than by magnitude, phase or other measures, analysis of resting state networks (which have mainly focused on cortical areas only) seem robust to the effects of prematurity. They therefore provide an ideal way of defining cortical areas of function as an alternative to the anatomical and whole-lobe cortical parcellations used in adult studies. Resting state networks are used in this study to define cortical areas with which to study the covariance of the BOLD time course between cortex and thalamus or striatum.

Functional connectivity

Introduction

Functional connectivity is defined as "temporal correlations between remote neurophysiological events" and is in contrast to the idea of effective connectivity which models the influence of one system over another (Friston, 1994). With regards to resting state fMRI, functional connectivity identifies the relationship between BOLD signal in two discrete parts of the brain with the underlying assumption that if two separate areas of the brain engage in coherent oscillations of BOLD contrast over

time, then they are functionally connected. There is no information on causality or directionality as to which region is driving the signal, indeed correlations between two areas do not necessarily reflect direct connectivity as statistical dependency between two areas may be mediated by a third (non-estimated) area. This is important when considering and striatocortical connectivity in this work. The choice of description (corticothalamic, or thalamocortical for example) when applied to functional connectivity, is arbitrary and does not implying direction of information flow (Smith *et al.*, 2011).

Statistical Modelling

Individual subject

Independent Component Analysis (ICA)

ICA is central to the methodology of many of the resting state functional connectivity studies reviewed above and so will be described here. It was used in this thesis in order to define areas of the cortex which were functionally coherent in the group of infants from which to perform subsequent seed-based correlation analysis between voxels of the thalamus or basal ganglia and cortical regions of interest. As already stated, T2* weighted imaging to maximise the BOLD response is subject to poor signal to noise ratio which further obscures an already small change from the baseline. The other sources of variability include machine artefacts, respiratory and cardiac pulsations, head motion as well as haemodynamic changes from neuronal 'housekeeping' and other sources. The result is a mixture of underlying signals, from which ICA attempts to expose statistically independent source signals based on the central limit theorem of statistics which states that any mixture of distributions tends to be more Gaussian than each of the contributing signals (Bijsterbosch *et al.*, 2017). McKeown and colleagues proposed that ICA as applied to the BOLD fluctuations in the brain could be used to identify these different spatial patterns of neuronal activations (signal of interest) (McKeown *et al.*, 1998). By contrasting features of timecourses uncovered by ICA, such as spatial location and frequency, noise could also be identified. ICA was pioneered for use in analysis of resting state functional connectivity data by Christian Beckmann and implemented as part of Oxford University FSL by Christian Beckmann et al (Beckmann *et al.*, 2005). An accessible and historical perspective of the development of ICA can be found (Beckmann, 2012).

The process is as follows. All voxels for each time-point are rearranged into a row, thereby having one row for each 3D image. From this, two new matrices are derived: the first one having a time-series from each column (each individual voxel over time) and the second containing a spatial component's map in each row. Each component can therefore be described as a spatial map reflecting where in the brain the component is detected, and a time series to show how that signal varied over the time.

Independent component analysis assumes the following model

$$Y = AM + \varepsilon$$

Equation 4.4

In this linear model, Y is the matrix of fMRI time series (made up of T time samples x V voxels). M is the matrix of the spatial components of the independent components, A is the matrix of the corresponding time courses and ε is the matrix of the residuals of the ICA model which is assumed to comprise the unstructured noise prior to the decomposition into independent components (Beckmann and Smith, 2004). In this way a set of components with accompanying time courses are generated.

The number of components into which the signal can be decomposed (dimensionality) is specified by the investigator. An analogy I have found useful is that of listening to an *a capella* choir of 10 singers: an un-mixing of the signal into two might separate the high voices from the low voices, whilst a separation into 4 might identify soprano, alto, tenor and bass lines. A separation into 10 might identify all the different individual singers. Dimensionality is arbitrary and analysis with a higher dimensionality will result in a component obtained in a lower dimensionality analysis being split/fragmented into two spatially distinct components (Bijsterbosch *et al.*, 2017). This might be desirable, but as the example of the choir of 10 shows, imposing a dimensionality of 20 might not be desirable as dimensionality needs to be in proportion to the amount of data analysed and the question asked.

ICA to identify noise

In addition to the identification of resting state networks, independent component analysis has been found to be a powerful tool in identifying noise in datasets. In the model of ICA above (equation 4), this is expressed in the term ε (the residuals of the ICA model) and in A and M, either in the form of artefactual time courses or spatial maps (Salimi-Khorshidi *et al.,* 2014). As resting state networks display different spatial and temporal characteristic from noise, this allows components to be categorised, and those of interest to be selected for use in further analysis. Examples of components not related to neuronal processes, include movement-related artefacts where the increased frequency occurs at locations on the edges of the brain and vasculature where the high frequency component corresponds to the anatomical location of the sagittal sinus. Separating components into those of interest and those not of interest, can be done by someone experienced in looking at ICA but this is time-consuming, expertise-driven and potentially a source of bias if carried out by two different people on subject data forming a group analysis. As time series of interest are expected to be normally-distributed, and the frequencies of the power spectra in artefacts (such as those caused by the scanner) can be bimodal 'noise' can be modelled automatically (Salimi-Khorshidi *et al.,* 2014).

Group level analysis

ICA and dual regression

In the case of group ICA, the BOLD data from multiple subjects are first registered to a common spatial template and are then then concatenated into a single 4D dataset. This is then decomposed using ICA to identify patterns of functional connectivity in the dataset. Dual Regression is the method used in this thesis to obtain and therefore compare individual subject spatial component maps. In detail, the first regression consists of using the spatial maps from the group ICA as the independent variables in a multiple regression using each individual subject's BOLD data as the dependent variables. This provides a time course representing each of the group spatial maps for each subject. Secondly, this time course is then regressed against the subject's data in order to obtain the subject-specific spatial representation (maps) of each component (Filippini *et al.,* 2009). If networks are to be compared, it is this output per subject

which can be compared with the spatial representation of that network in another subject.

Seed-based Correlation Analysis

Functional connectivity can be assessed by calculating partial correlations between two areas In this thesis, it was carried out between the timeseries in individual voxels of the subcortical structure and the eigen timeseries of a cortical region in order to measure the strength of the linear relationship between the subcortical voxel and the cortical regions while controlling for the effect of the time series in the other cortical regions. Such methods were developed for parcellation of the cerebellum in adults according to connectivity with the neocortex by O'Reilly et al (O'Reilly *et al.*, 2010).

Linear regression finds the straight line which best fits a series of data pairs according to the equation

$$Y = a + bX$$

Equation 4.5

Where X is the explanatory variable and Y the dependent variable, b is the slope of the line and a is the y intercept. To measure how closely aligned the data pairs are to the line, the correlation coefficient is calculated (R) and is between -1 and 1 indicating the strength of the association between the two variables. This valued squared (r^2), defines the percent of the variation in the y variable which is due to variation in the x data. For example, if a correlation is 0.8, the r^2 of 0.64 means that 64% of the variation in the y data is due to variation in the x data. It does not imply causation, but correlation.

Appropriate statistical testing

As it is not known whether the seed-based correlations have a Gaussian distribution, permutation testing can be used in order to establish the null distribution from the sample. If there is no observed difference between the groups within the sample, a random sample of subjects from the whole sample could be analysed to create a distribution which would be expected under the null hypothesis. The p value of this nonparametric permutation is the proportion of the permuted statistic values that are the same or greater than the value actually observed in the sample (Nichols and Hayasaka, 2003). As the total number of possible permutations even in a small dataset

is prohibitively large, an amount of permutations (determined by the researcher and often 5,000 or 10,000 in resting state studies) are selected at random in order to determine the null distribution. Given the large number of statistical tests carried out, a p value of $p<0.05$ would allow an unacceptable number of false positive (1 in 20 tests). There is no consensus on how to control for multiple comparisons (Nichols and Hayasaka, 2003). A correction is needed, but as the result in one voxel is not independent of the neighbouring voxels (the statistical map has a degree of spatial smoothness as a result of the spatial extent of the BOLD response, amongst other factors) a true Bonferroni correction (p value divided by the number of tests) is not appropriate. A few approaches to this problem have been developed such as voxel-based and cluster-based thresholding, but a third approach, threshold-free cluster enhancement (TFCE) has advantages and was used in this study. It takes advantage of the strengths of both voxel and cluster based methods: voxel-based thresholding which applies thresholds according to the maximum test statistics in a voxel and cluster-based thresholding which gives weight to the spatial extent of an activation but involves the user to input an arbitrary size of a cluster to be significant. TFCE effectively up-weights high voxels involved in clusters and down-weights high voxels which are not (Smith and Nichols, 2009).

Chapter Five

Study-specific materials and methods

The EPRIME Study

Over a period of three years (2010-2013) study participants were recruited at birth as part of the Evaluation of Preterm Imaging Study (e-Prime) (NCT01049594) from hospitals in the North and Southwest London Perinatal Network. The purpose of this cohort was to compare the effect of receiving prognostic information based on MRI with that based on cranial ultrasound as well as looking at the effect on parental anxiety, health costs and quality of life (Edwards *et al.*, 2018). Eligibility included birth before 33 weeks gestational age to a mother who was aged over 16 years and able to speak English. Infants were excluded if they were subject to child protection proceedings, had a major congenital malformation, had metallic in-plants or had prior experience of MRI or treatments in a centre which carried out routine MRI. MRI and ultrasound were carried out at a single neonatal imaging centre when the infant was a gestational age of 38-44 weeks after which time, infants were randomised for their caregivers to receive the results from only one modality: MRI or cranial ultrasound. Parents had the choice for their infant to receive chloral hydrate sedation (25-50 mg kg) for the MRI scan. Results from this cohort with regards to the correlation of MRI at the time of birth and outcome using is included in Literature/Neuroimaging at birth and outcome around two years in the studies by Edwards 2018, Ball 2018 and Tusor 2017. The neurodevelopmental outcomes of these 511 infants are typical of populations presented in other studies of preterm infants, such as EPIPAGE (Larroque *et al.*, 2008).

Image Acquisition

All images were acquired on a 3 Tesla Philips Achieva MRI scanner (Best, Netherlands) and supervised by an experienced paediatrician. Pulse oximetry,

temperature and electrocardiography data were monitored throughout. Ear protection was provided with silicone-based putty placed in the external ear (President Putty, Coltene, Whaledent, Mahwah, NJ) and Minimuffs (Natus Medical Inc, San Carlos, CA). Whole-brain functional imaging was performed using a T2* gradient echo planar image acquisition (sequence parameters: TR = 1.5 s; TE = 45 ms; flip angle = 90º, 256 volumes, slice thickness 3.25mm, in plane resolution 2.5mm2 22 slices, scan duration = 6.4 minutes) with an 8 channel phased array head coil. T2-weighted fast-spin echo MRI was acquired using: TR: 14,730 ms; TE: 160 ms; flip angle 90°; slice thickness 2 mm; field of view: 220 mm; matrix: 256 × 256 (voxel size: 0.86 × 0.86 × 1 mm). T1 high resolution scans using magnetisation-prepared rapid acquisition of gradient echo (MPRAGE) were acquired for diagnostic purposes with parameters: TR: 17ms; TE :4.6ms; flip angle: 13 degrees; slice thickness: 0.8mm; field of view: 210mm; and matrix: 256 x 256 (voxel size, 0.82 x 0.82 x 0.8mm) resulting in 240 slices.
High resolution anatomical scans (T1 and T2 weighted MRI scans) were reviewed by an expert in perinatal MRI: none had major focal destructive parenchymal lesions.

Subjects

Introduction

From the cohort recruited for the EPRIME project, detailed above, subjects were selected for investigation. In order to fulfil the aims and objectives of this study, firstly to firstly investigate and striatocortical connectivity at the time of birth and the effect of prematurity, and secondly, to investigate the connection between outcome at 20 months and connectivity at birth on those born preterm, two separate cohorts needed. The first, would be answered by a group of both preterm and term infants with MRI data all acquired at the same gestational age, and the second by data collected from preterm infants at the time of normal birth and neurodevelopment follow-up at the age of two years gestational age (corrected). The investigation of cortical-subcortical connectivity was done first and by the time the cohort was selected, the data from around 150 infants from the EPRIME cohort was available. The inclusion criteria are

below. At the time, the availability of normal term scans was much more limited than it is today, and consisted of term infants who had been recruited at another hospital as part of a study of the effect of fish oil on brain connectivity, with the addition of a few infants born to staff members. The quality criteria stated below were applied to these term-born scans until a cohort of 19 was achieved (the preterm cohort of 49 was already in place). Sedation was administered in all but one term-born infant. At the time, I understood that all 19 term-born infants had received sedation, but I rechecked this prior to publication (late 2014) and discovered that one infant in the term cohort had not received sedation.

Cohort One: study of cortical-subcortical connectivity

Inclusion criteria

Acknowledging the sensitivity of functional data to motion (Van Dijk *et al.*, 2012; Murphy *et al.*, 2013) and with the aim of investigating a small structure such as the thalamus, only datasets with very low motion were eligible for inclusion. Within the premature cohort, 150 datasets were examined, of which 47 met the criteria for inclusion in this study. After head motion correction with FSL MCFLIRT (Jenkinson *et al.*, 2002) and exclusion of the first six volumes in every subject, only scans with 200 contiguous volumes with motion of ≤0.08 mm relative mean displacement were included. ICA was then performed on individual datasets using FSL MELODIC (Beckmann *et al.*, 2005), because an ICA-based identification of artefacts, including head motion, has been shown to be a very sensitive approach (Griffanti *et al.*, 2014; Salimi-Khorshidi *et al.*, 2014). In addition to 47 included subjects, 5 additional subjects who met the motion criteria of ≤0.08 mm relative mean displacement were excluded at this point, because it was found in these subjects that there was still significant motion as defined by either component with spectra in the high-frequency range and/or spatial representations around the edge of the brain (Beckmann, 2012). Nineteen term subjects were selected using the same motion criteria, providing a dataset with minimal observed head motion. There was no difference in motion between the infants born preterm and those born at the normal time. Motion parameters based on the relative mean displacement were 47 infants born preterm

mean = 0.052 mm (range = 0.03–0.08 mm) and 19 infants born at the normal time of birth mean = 0.050 mm (range = 0.03–0.08 mm).

Table 5.1. Demographic information - gestational age at birth, scan and gender

	Preterm group	Term group	66 infants
Mean gestational age at birth (range)	29.86 (24.71 – 32.86)	39.91 (36.29 – 41.86)	32.76 (24.71 – 41.86)
Mean gestational age at scan (range)	42.38 (40 – 44.56)		42.71 (40 – 48.28)
Gender % female	57%	88%	60%

Cohort two: study of connectivity at birth and outcome at twenty months

Inclusion criteria

The cohort assembled to answer the question of imaging at birth and correlation with outcome differed from cohort one (above) for a number of reasons. Firstly, the EPRIME dataset of 511 infants was complete. Secondly, as the term-born infants included in the study of cortical-subcortical connectivity had not received the same follow-up was the EPRIME cohort, and because the outcome study would have resulted in a numerically unbalanced cohort with many more preterm infants than term-born infants, the outcome study cohort consists exclusively of preterm infants. Because of the time involved in the single subject ICA noise classifying process detailed above, and because a more principled automatic process had become available (FSL FIX Salimi-Khorshidi *et al.*, 2014; Griffanti *et al.*, 2017), the inclusion criteria with regards to motion was changed and is detailed below. Lessons in assembling a cohort were learned and with the increased number of subjects available, inclusion criteria for cohort two included an upper age at scan of 44 weeks gestational age.

Subjects

The study was reviewed and approved by the National Research Ethics Service and all infants were studied with written consent of their parents. All 102 infants were scanned once at the estimated time of completed gestation with neurodevelopmental follow-up performed around 20 months of age, corrected for gestational age at birth.

A cohort of 102 preterm infants was established as follows. 511 infants recruited into the EPRIME study were born at less than 33 weeks completed gestation (GA) and were scanned once at term equivalent age (defined as 38-42 weeks from the last menstrual period). Of the 277 infants with complete follow-up and full functional MRI data, 11 were excluded for inadequate fMRI coverage. Acknowledging the sensitivity of functional data to motion (Van Dijk *et al.*, 2012; Murphy *et al.*, 2013) and with the aim of investigating small subcortical structures in infants, only datasets with very low motion were eligible for inclusion, in this case, relative mean displacement of ≤ to 0.08mm and absolute motion of < 2mm (same initial motion criteria as cohort one). This resulted in the exclusion of 122 of the remaining 266 subjects. 15 were then excluded as they had been scanned at > 44 weeks postmenstrual age. Of the remaining 107 infants, 5 had structural brain abnormalities leaving 102 infants who met the inclusion criteria. Chloral hydrate sedation (25-50mg/kg) was administered in all these infants (Finnemore *et al.*, 2014).

Table 5.2 Demographic information for cohort of 102 preterm infants. Table of demographics from the full EPRIME cohort can be found in Edwards AD et al 2018.

Mean gestational age in weeks at birth (range)	30 (24.43 - 32.86)
Mean birth weight in grams (range)	1360.3 (600 – 2510)
Mean numbers of days ventilated (range)	1.74 (0 – 16)
Mean gestational age (in weeks) at scan (range)	41.9 (38.29 - 44)
Mean score for prognosis on term MRI scan (range) (Woodward *et al.*, 2006). no abnormality = 9 mild abnormality = 79 moderate abnormality = 14.	8 (5 – 12)
Mean gestational age in months at neurodevelopmental follow up	19.91 (19-23)
Sex (% female)	44 (45 female, 57 male)
Gross Motor composite score (range)	96.10 (range 61 - 118)
Cognitive composite score (range)	94.22 (range 65 - 130)
Language score (range)	16.67 (4 – 31)

Subjects were then followed up with assessments of neuropsychological and behavioural functioning at an average age of 19.1 months (range 19 to 23 months) including the Bayley Scales of Infant Development III (‘Bayley Scales of Infant and Toddler Development®, Third Edition’, 2017) of which the gross motor scaled score, the cognitive scaled score and the language sum scaled score were used in this study. Mean and range for the composite scores are shown in the table above as these are comparable across populations with a population mean of 100 and standard deviation of 15.

Analysis tools used

In the first year of my fellowship, I attended the year-long graduate course at FMRIB, a multi-disciplinary neuroimaging research facility within the Nuffield Department of Clinical Neurosciences at Oxford University, studying MRI physics, statistical analysis and presenting an image analysis project using adult data. The comprehensive suite of analysis tools devised by this group is known as FSL and is one of a handful of analysis suites used for analysis of MRI in adults world-wide. The open source software can be downloaded at https://fsl.fmrib.ox.ac.uk/fsl/fslwiki/FslInstallation. A glossary of tools used for analysis of data in this thesis, with their references, are detailed below in the order in which they are used in the analysis pipeline.

FSL 5.0	released in September 2012 and used for analysis of data in this thesis. Superseded by FSL 6.0 in October 2018
BET	Brain extraction tool for structural MRI images. A brain only mask is required as an input for the first level of image alignment of non-linear registration (Smith, 2002).
FAST	Tissue segmentation tool with pre-set contrasts for grey matter, white matter and CSF from adult structural brain data (Zhang *et al.*, 2001).
FLIRT	Linear registration tool used for registering an EPI image with a structural image from the same subject. Rigid body (6 degrees of freedom, which are rotations and translations along the x, y and z axes) chosen for within-subject spatial transformation of data. This preserves all points lying on a single line with their ratio of distances between each other (Jenkinson and Smith, 2001).
BBR	Boundary-based registration which improves echo planar to structural registration during the linear stage of image registration (Greve and Fischl, 2009). Parameters need to be altered for neonatal brain contrast.

For example, in an adult T1, the cortical ribbon appears darker (grey matter) compared with the white matter adjacent: a neonatal T1 has a paler cortical ribbon than the tissue adjacent. The sign of the boundary slope needs to be inverted for neonatal registration and the tissue segmentation done manually. This is carried out using command line linear registration (with FLIRT) and specifying the -bbrslope and a bespoke neonatal segmentation (using FAST) in order to specify the white matter segmentation using -wmseg. This adaptation of adult methodology was developed for this thesis by the author. Further details are provided in Appendix A.

FNIRT — FNIRT requires the input of the transformation performed by FLIRT (rotations, translations) and performs additional affine transformations (scalings and shears) and subsequent local warps. It is required to obtain good quality registrations between different subjects, allowing points along a single line to be represented with different distances between each other (Woolrich *et al.*, 2009; Jenkinson *et al.*, 2012).

MELODIC — Multivariate Exploratory Linear Optimized Decomposition into Independent Components is the analysis tool in FSL which carries out independent component analysis (Beckmann *et al.*, 2005) and is a good way to analyse motion artefact (Griffanti *et al.*, 2014). The generation of resting state networks, or components was used in this thesis in the group of 66 preterm and term infants to analyse motion. It was also used throughout to model the cortical contribution to resting state networks, the eigen timeseries of which was then used in seed-based connectivity analysis.

Dual Regression is the method used in this thesis to obtain, and therefore compare, individual subject spatial component maps from those derived in the group as a whole. It is carried out as part of the FSL MELODIC analysis tool (Filippini *et al.*, 2009).

FIX — FIX attempts to analyse components identified by MELODIC and classify them into signals of interest and those which are not (ie noise) (Salimi-Khorshidi *et al.*, 2014; Griffanti *et al.*, 2017). The 'noise' can then be regressed from the dataset prior to analysis. FIX is available as a plugin for FSL and is used in the processing pipeline of the human connectome project. It avoids the need for the expertise and time required for manual classification and achieves over 99% classification accuracy on high quality data from the human connectome project.

REGFILT — This analyses the first stage output of the dual regression (set of time courses, one for each group map) and filters the component as to their frequency (using the -F option). The identification of a component as high frequency at the subject level, indicates that this is probably not a blood oxygen level dependent timeseries that has been identified. If a cortical component was identified as high frequency in more than 10% of subjects (an arbitrary cut-off), the cortical component was not included in the group analysis going forwards.

CC — FSL CC was used to perform cross correlation on the spatial maps of derived from GICA of neonates with that of adult maps using GICA from a published set of adult networks (Smith *et al.*, 2012).

SBCA — In this thesis, seed-based correlation analysis (SBCA) was performed between cortical regions of interest and each voxel of thalamus or striatum in order to measure the strength of the linear relationship between the time series in subcortical structure and that in each cortical region while controlling for the effect of the time series in the other cortical regions.

Study-specific methods

Cohort One: Cortical-subcortical connectivity at birth

Data Analysis.

Pre-processing.

After removal of non-brain structures from the T2-weighted structural image using a neonatal tissue segmentation algorithm (Makropoulos *et al.*, 2014), fMRI pre-processing was carried out using tools from the Oxford Centre for Functional Magnetic Resonance Imaging of the Brain Software Library, FSL (Jenkinson *et al.*, 2012). Pre-statistical processing consisted manual inspection of raw data for detection of scanner artefacts, correction for head motion using the middle volume as reference image (Jenkinson *et al.*, 2002), removal of first six functional volumes to allow for magnetisation to reach steady state, spatial smoothing by using a Gaussian kernel of FWHM of 5 mm (2x voxel width), and high-pass temporal filtering (200 seconds). Functional volumes were registered to the subject's T2-weighted structural image (Jenkinson *et al.*, 2002), with boundary-based registration (Greve and Fischl, 2009) optimised for neonatal tissue contrasts. Brain mask for use in registration steps was created by segmenting the T2 structural image and then using relevant cortical structures to create a binarised brain mask (using FSL). The initial step of creating the tissue segmentations in individual subjects was kindly carried out by Antonios Makropoulos according to his published work (Makropoulos *et al.*, 2014) (Makropoulos *et al.*, 2014).

It is not possible to reliably identify single voxels of cerebrospinal fluid from the echo planar image of an infant at the time of normal birth, a step used in adult analysis in order to model noise and regress this identified signal from the time course, because neonatal ventricles are too small and there would be partial volume effects. Therefore, cerebrospinal fluid was identified on the subject's T2 structural image, and data from voxels corresponding to these areas were discarded. The remaining data were then transformed to a population-based neonatal template (Kuklisova-Murgasova *et al.*, 2011) using nonlinear registration (Jenkinson *et al.*, 2012).

Defining a region of interest

To allow for plasticity and the error that inaccurate structural regions of interest can introduce (Smith *et al.*, 2011) and acknowledging that cortical areas cannot be defined from task-based paradigms at this age, cortical regions of interest were defined by ICA. Pre-processed functional data containing 200 time points per subject were temporally concatenated across subjects to produce a single 4D dataset, and resting-state components common to the group were defined using MELODIC (Beckmann *et al.*, 2005) with a fixed dimensionality of 25, which achieved a good balance between interpretability and robustness, similar to that used in adults (Smith *et al.*, 2012). ICA maps were thresholded using an alternative hypothesis test based on fitting a Gaussian/γ-mixture model to the distribution of voxel intensities within spatial maps (to reflect the Gaussian and non-gaussian properties of signal of interest and noise, and controlling the local false discovery rate at $p < 0.05$ (Beckmann *et al.*, 2005). The resulting maps and full ICA decomposition are shown in Figure 6.1. Nonoverlapping cortical component masks were created by assigning each cortical voxel to a specific resting-state component depending on which network had the highest z score at that voxel.

Defining a region of interest for study of thalamocortical connectivity

For analysis of connectivity of the thalamus, we selected nine bilateral cortical areas based on prior anatomical knowledge and previous work in adults (Smith *et al.*, 2012), term infants (Doria *et al.*, 2 010), and animals (Table 5.3). From 25 ICA components, we discarded subcortical components (thalamus, cerebellum, brainstem, and basal ganglia), components where the power spectra (in the frequency domain) in individuals was in the high-frequency range in more than 10% of subjects (an arbitrary cut-off threshold), and unilateral components. The exception was the primary visual component: the anatomical position of the primary visual cortex leaves it vulnerable to noise caused by dense vasculature and motion, and this component was included, despite being characterised by high-frequency power spectra in 7 of 66 subjects (10.6%) as the spatial cross-correlation with the visual cortex in adults was 0.56 (Smith *et al.*, 2012). Of the remaining components, spatial correlation with adult networks reported in the work by Smith et al. (Smith *et al.*, 2012) was tested using cross-correlation (Table 5.3). Visual and auditory components were represented more

than one time: in this case, we selected the network best corresponding with the anatomical position of primary visual and auditory cortex.

Table 5.3 Cross correlation with adult cortical networks (cohort one)

Infant RSN	Adult RSN	Correlation
Primary sensory-motor	5	0.43
Primary auditory	6	0.38
Sensory motor association	9	0.34 (and RSN5 at 0.3)
Primary visual	1	0.56
Temporal	12	0.12
Pre-frontal	15	0.30 (and RSN18 0.25)
Lateral parietal	12	0.28 (RSN 8 0.23 RSN 11 0.22)
Fronto-parietal-insular	7	0.45
Anterior cingulate	9	0.15

Defining a region of interest for striatocortical connectivity

For analysis of corticostriatal connectivity we selected eight bilateral cortical areas based on prior anatomical knowledge, and previous work in adults (Smith *et al.*, 2012), term infants (Doria *et al.*, 2010). From the 25 ICA components, we discarded subcortical components (thalamus, cerebellum, brainstem and striatum), components where the power spectra (in the frequency domain) in individuals was in the high frequency range in more than 10% of subjects, and unilateral components. Of the remaining components, spatial correlation with adult networks reported in Smith et al (Smith *et al.*, 2012) was tested using cross correlation (see Table 5.3). Voxels in masks adjacent to the striatal seed mask were removed to ensure that no cortical components overlapped or were directly adjacent to the striatum. In order investigate the organisation of striato-frontal connectivity, all eligible frontal components were included (addition of the orbitofrontal component compared with thalamus analysis above). Without a strong hypothesis as to where visual cortex might be represented in

the neonatal striatum (unlike the investigation of the thalamus and connectivity with the lateral geniculate nucleus), the visual cortex was not included as it exceeded the threshold of 10% of subjects having high frequency power spectra in this component.

Dual Regression

Within a group-defined cortical functional area, there is likely to be some heterogeneity at the subject level. For each individual subject, each component identified at the group level was mapped back to each subject's dataset through a spatial regression of the group ICA maps on the individual fMRI dataset followed by a regression of the resulting time series on the same dataset (Filippini *et al.*, 2009): this two-step process is known as dual regression. To ensure that the first Eigen time series at the subject-specific level best represented the function determined by the group analysis rather than another functional area within the same group-defined cortical region, for each subject, the components were thresholded at $Z = 1.96$, and the remaining voxels inside the group-defined mask were used as the cortical target from which the first Eigen time series was taken. The resulting component maps in individual subjects derived using this dual regression approach were used as regions of interest.

Subcortical seed masks

Masks of the subcortical structures were created using a neonatal-specific template (Makropoulos *et al.*, 2014). The thalamus mask includes right and left thalamus. The basal ganglia mask includes caudate, putamen and globus pallidus. Voxels in cortical components adjacent to either subcortical seed mask were removed to ensure that no cortical components overlapped was directly adjacent to the seed masks.

Seed-based correlation analysis

Partial correlation analysis was performed between individual subject's cortical components and subcortical (thalamic or striatal) masks in each subject (O'Reilly *et al.*, 2010).

Group analysis of connectivity

Group analysis of thalamocortical connectivity

Correlation scores for each component were combined using fixed effects analysis, and the results were used to parcellate the thalamus (Figure 6.3) assigning thalamic voxel membership according to the cortical component with which it had the highest average correlation score in the group (Zhang *et al.*, 2008). In addition to the fixed effects model to show dominant connectivity, significance ($p < 0.05$ corrected for multiple comparisons after threshold-free cluster enhancement (TFCE)) was assessed using nonparametric permutation testing (Smith and Nichols, 2009) and results are shown in Figure 6.4. To illustrate which regions of the thalamus are significantly connected with more than one cortical area, the resulting nine significant thalamic maps (Figure 6.4) were binarised and summed (Figure 6.5). Finally, using a general linear model of gestational age at birth, the correlation maps shown in figure 6.4 were tested voxel-wise for statistically significant associations with gestational age at birth using nonparametric permutation testing (Nichols and Holmes, 2002). The results were spatial maps characterising the effect of prematurity on connectivity Figure 6.6A, upper) and scatterplots showing the correlations coefficients in each infant according to gestational age at birth (Figure 6.6, lower).

Group analysis of striatocortical connectivity

Correlation scores for each component were combined using fixed-effects analysis, the results were used to parcellate the striatum (Figure 7.2) assigning striatal voxel membership according to the cortical component with which it had the highest average correlation score in the group (Zhang *et al.*, 2008). In addition to the fixed effects model to show dominant connectivity, significance ($p < 0.05$ corrected for multiple comparisons after threshold-free cluster enhancement) was assessed using non-parametric permutation testing (Nichols and Holmes, 2002) and results shown in Figure 7.1. Finally, using a general linear model of gestational age at birth, the corticostriatal correlation maps shown in Figure 7.1 were tested voxel-wise for statistically significant associations with gestational age at birth using nonparametric permutation testing (Nichols and Holmes, 2002). This resulted in spatial maps characterising the effect of prematurity on corticostriatal connectivity shown in Figure

7.3A and scatterplots showing the correlations coefficients in each infant according to gestational age at birth are shown in Figure 7.3B.

Cohort Two

Study-specific methods for cortico-subcortical connectivity at birth and its relationship with outcome at 2 years

Image acquisition parameters were the same as for cohort one above. The main differences in the following steps are the implementation of different parameters for cortical component selection, the implementation of FIX for motion correction and the correlation with outcome at 20 months. Summary of correlations between components in cohort two and those in cohort one can be seen in table 5.4.

Data analysis

Pre-processing

The first 6 volumes of each subject were removed to allow for equilibration of the T1 component, and motion correction using MCFLIRT was applied (Jenkinson *et al.*, 2012). Using FSL FIX (Salimi-Khorshidi *et al.*, 2014) to perform denoising, single subject ICA was performed on each dataset with automatic dimensionality using MELODIC (Beckmann and Smith, 2004), high pass temporal filtering of 0.008Hz with a 125 second cut-off, without slice-timing correction or spatial smoothing to preserve the high-frequency spatial and temporal signal. Dimensionality was estimated automatically. In adults, de-noising using FIX would then involve registration to the adult Montreal Neurological Institute MNI152 atlas, whereas in the neonatal population, this step was modified to use a population-specific neonatal template with tissue priors rather than registration (Serag *et al.*, 2012). MELODIC provides components which undergo automatic component classification by FIX, which allows the unique variance of each noise component to be regressed out of the data alongside the full variance of the motion parameters and derivatives (Satterthwaite *et al.*, 2012; Griffanti *et al.*, 2014). This has been shown to be an effective method in infants (Ball *et al.*, 2016). The training dataset required prior to

using FIX was performed for a separate study (Ball *et al.*, 2016) and FIX de-noising was performed on the data of 102 infants by Jonathan O'Muircheartaigh.

Defining a region of interest

To generate functionally-defined regions of interest in each subject to use for seed-based correlation analysis the following process was followed. This is similar, but not identical to the process used in cohort one. Functional volumes were registered to the subject's T2-weighted structural image (Jenkinson *et al.*, 2002) with boundary-based registration (Greve and Fischl, 2009) as implemented by FMRIB's boundary-based registration (FSL- BBR) optimised for neonatal tissue contrasts. These images were then transformed to a population-based neonatal template (Kuklisova-Murgasova *et al.*, 2011) using nonlinear registration (Jenkinson *et al.*, 2012). It is not possible to reliably identify single voxels of cerebrospinal fluid from the echo planar image of an infant at the time of normal birth as is done in adult studies to model time course regressors, as ventricles are too small to avoid partial volume effects. Therefore, a mask of cerebrospinal fluid was applied to individual datasets at this point and data from voxels corresponding to these areas were discarded. In order to allow for plasticity and to acknowledge that cortical areas cannot be defined from task-based paradigms at this age, cortical regions of interest were defined using components from independent component analysis. Pre-processed functional data containing 250 time points per subject were temporally concatenated across subjects to produce a single 4D data set and resting state and resting state components common to the group were defined using MELODIC (Beckmann *et al.*, 2005) with a fixed dimensionality of 25 which achieves a good balance between interpretability and robustness similar to that reported in adults (Smith *et al.*, 2012). ICA maps were thresholded using an alternative hypothesis test based on fitting a Gaussian/Gamma mixture model to the distribution of voxel intensities within spatial maps and controlling the local false discovery rate at $p < 0.05$ (Beckmann *et al.*, 2005). The resulting maps and full ICA decomposition are shown in figure 8.1. Cross correlations with adult networks (Smith *et al.*, 2012) and with the group of 66 term and preterm infants are shown in Table 5.4.

Non-overlapping cortical component masks were created by assigning each cortical voxel to a specific resting state component depending on which network had the

highest z-score at that voxel. For analysis of connections between thalamus and cortex and basal ganglia and cortex, power spectra analysis in the frequency domain was performed and components with high frequency in more than 10% of subjects were excluded (using FSL REGFILT analysis). The spatial correlation with adult networks was also tested using cross correlations after registration of infant data to an adult template (adult components made available in Smith et al 2012). Remaining bilateral components were selected for analysis: 11 in total. Of note, therefore, are the omission of the unilateral components, all of which had counterparts in the contralateral hemisphere: numbered 14 and 16 (medial visual), 18 and 21 (auditory) and 22 and 23 (sensory-motor lateral portion).

Table 5.4 Cross correlation of components in cohort two with adult cortical networks (Smith *et al.*, 2012) and with components in cohort one

	Infant resting state network in cohort two (numbers as per Table 8.1)	Corresponding adult resting state network (Smith 2012)	Correlation with Smith 2012	Correlations with infant resting state networks in cohort one
1	Posterior cingulate	16	0.44 (also 17 0.40)	0.6, 0.52
2	Lateral parietal	12	0.35	0.8
3	Fronto-parietal-insula	7	0.65	0.62
4	Primary sensory motor (medial)	5	0.56	0.46
5	Motor association	9	0.39	0.69
6	Superior frontal	15	0.43	0.68
7	Orbito-frontal	18	0.32	0.69
8	Visual	2	0.63	0.34
9	Pre-frontal	18	0.54	0.61
10	Lateral pre-frontal	20	0.49	0.38
11	Anterior cingulate	16	0.28	0.5

Dual Regression

Within a group-defined cortical functional area, there is likely to be some heterogeneity as the subject level. For each individual subject, each component identified at the group level was mapped back to each subject's data set through a

spatial regression of the group ICA maps on the individual fMRI dataset, followed by a regression of the resulting time series on the same dataset (Filippini *et al.*, 2009). To ensure that the first eigen timeseries at the subject specific level best represented the function determined by the group analysis rather than to another functional area within the same group defined cortical region, for each subject, the components were thresholded at Z=1.96 and the remaining voxels inside the group-defined mask were used as the cortical target from which the first eigen timeseries was taken. The resulting component maps in individual subjects derived using this dual regression approach were used as regions of interest and partial correlation scores were calculated with the time series of each thalamic or striatal voxel (O'Reilly *et al.*, 2010).

Subcortical seed masks

Masks of the subcortical structures were created using a neonatal-specific template (Makropoulos *et al.*, 2014). The thalamus mask includes right and left thalamus. The basal ganglia mask includes caudate, putamen and globus pallidus. Voxels in cortical components adjacent to either subcortical seed mask were removed to ensure that no cortical components overlapped was directly adjacent to the seed masks.

Seed-based correlation analysis

Partial correlation analysis was performed between individual subject's cortical components and subcortical (thalamic or striatal) masks in each subject (O'Reilly *et al.*, 2010). Significant correlations between cortical areas and thalamus or striatum are shown in Figure 8.2 which can be compared with Figures 6.4 and Figure 7.1 ($p < 0.05$, corrected for multiple comparisons after threshold-free cluster enhancement).

Correlation with outcome at two years

Neurological and developmental testing was performed at 20 months of age, corrected for gestational age at birth, using the Bayley Scales of Infant and Toddler Development, Third Edition (Bayley-III) ('Bayley Scales of Infant and Toddler Development®, Third Edition', 2017) by researchers experienced in neurodevelopmental testing. Using a general linear model, with gestational age at birth, gender and postmenstrual age at scan included as explanatory variables, the corticothalamic and corticostriatal correlations were tested voxel-wise for statistically

significant associations with tests administered at 20 months of age (corrected) using nonparametric permutation testing (Nichols and Holmes, 2002) tested at a significance $p < 0.05$ (corrected for multiple comparisons after threshold-free cluster enhancement). Figures showing the correlation between neurodevelopmental outcome and cortico-subcortical connectivity at birth are shown in Figure 8.4 (thalamocortical connectivity at birth and outcome at 2 years) and Figure 8.3 (striatocortical connectivity at birth and outcome at two years).

Part Three

Results and Discussions

Chapter Six

Specialisation and integration of functional connectivity in the human infant

Results

The spatial distribution of the whole brain BOLD signal in the group, assessed in all subjects at the time of normal birth (gestational age 38-42 weeks) using Independent Component Analysis (ICA) was similar to that described previously (Fransson *et al.*, 2011; Smyser *et al.*, 2011), including a combined sensory-motor component, auditory, visual, subcortical components and a fragmented default mode network, and did not differ according to gestational age of the infant at birth. This finding is in accord with previous data (Damaraju *et al.*, 2010; Doria *et al.*, 2010; Fransson *et al.*, 2011).

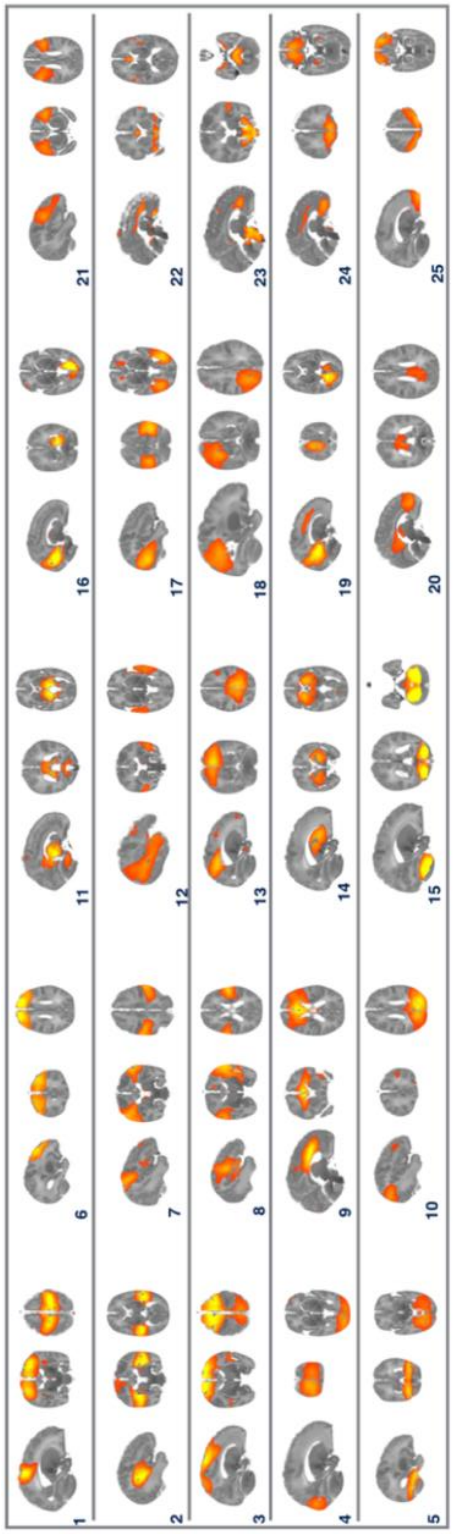

Figure 6.1. Temporal concatenation ICA-estimated resting pattern in the group of 66 subjects. Sagittal, coronal and axial views of the spatial map for each component. Images are z-statistics overlaid on the template 41-week brain. Red to yellow indicates z values ranging from 2 to 12. The right hemisphere of the brain corresponds to the left sides of the coronal and axial images. Components 1-9 correspond to functional cortical components described in Table 6.1.

Table 6.1. Nine functional cortical components defined using independent component analysis with anatomical areas. Full list of 25 components from ICA in Figure 6.1.

Functional cortical component	Description	Number in S1
Primary sensory-motor	Pre and post central gyrus (pale blue)	1
Primary auditory	Superior temporal gyrus (red)	2
Sensory-motor association	Superior parietal, superior frontal gyrus (yellow)	3
Primary visual	Peri-calcarine (lilac)	4
Temporal	Fusiform gyrus (posterior part), medial and inferior temporal gyrus (dark blue)	5
Pre-frontal	Dorsal pre-frontal cortex (orange)	6
Lateral parietal	Post central gyrus (lateral portion), pale pink (not represented in figure 1)	7
Fronto-parietal-insula	Insula cortex (left) and bilateral lateral fronto-parietal junction (dark pink)	8
Anterior cingulate	Anterior cingulate cortex (green)	9

Functional parcellation of the thalamic dominant functional connectivity at the time of normal birth

Hard-thresholding the functional connectivity estimates of nine functionally-defined cortical areas selected from the group ICA on neuroanatomical grounds (Table 6.1) revealed a predominantly symmetrical topographical representation of these cortical regions in the thalamus. Chapter 6, figure 3 shows this topographical organisation of the thalamus defined by the cortical component with which each voxel is most highly correlated.

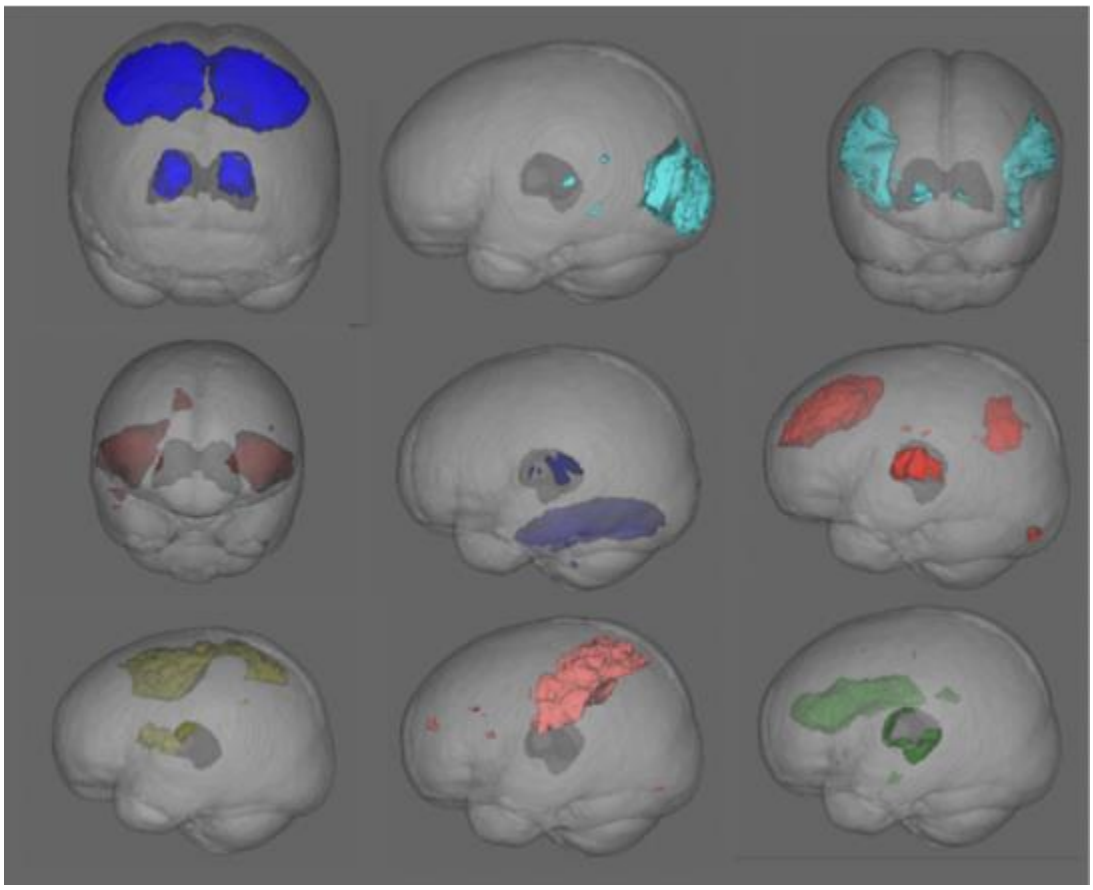

Figure 6.2. Movies of cortical areas and their dominant thalamic territories (individually clickable rotating brains) can be seen online as part of Toulmin PNAS 2015. Column 1: networks 1,2,3. Column 2: networks 4,5,6. Column 3: networks 7,8,9.

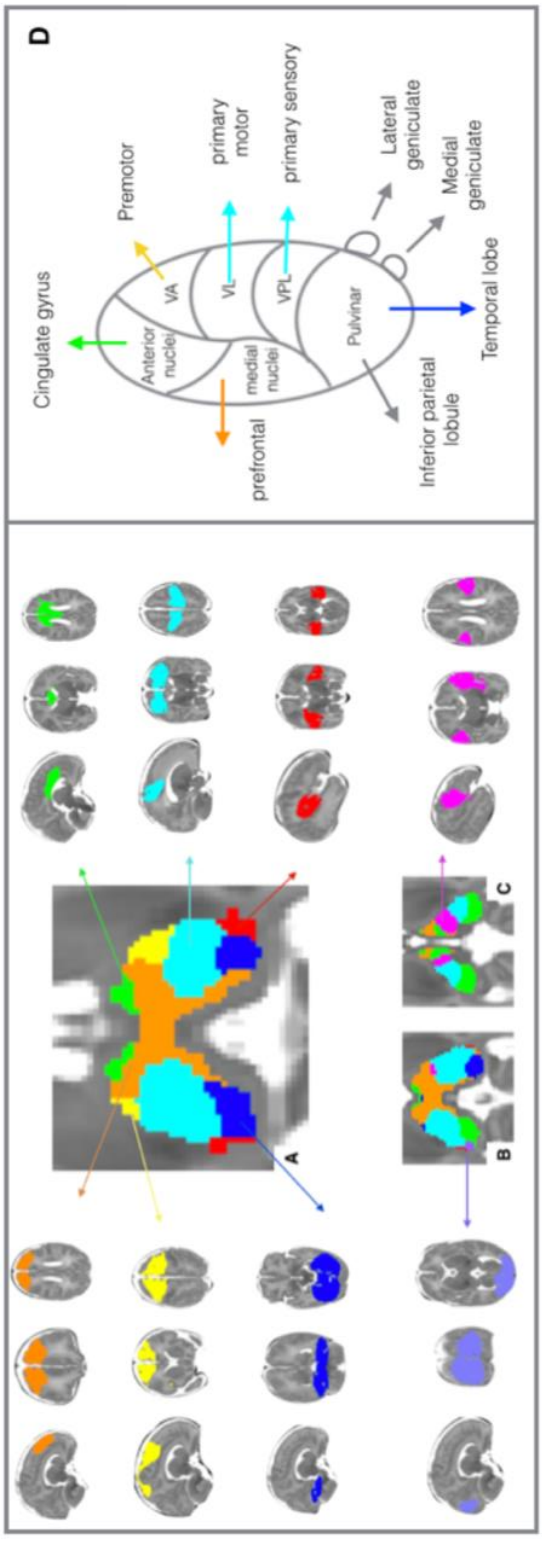

Figure 6.3. Dominant correlations from 9 functionally-defined cortical regions using maximum partial correlation coefficient. (A) Mid-thalamic view, (B) Posterior view, (C) Inferior view. Lateral parietal component does not have any dominant territory. Table 6.1 for anatomical descriptions and colours. (D) After Sherman and Guillery (2013) showing cortical targets from specific thalamic nuclei. Images are displayed as per radiological convention.

The primary sensory-motor component had the largest territory of thalamic dominance and provided the dominant cortical connectivity for the lateral portion of the thalamus with some posterior extension (the territory of the ventral lateral nucleus (VL) and ventral posterolateral (VPL) nuclei) and an extension towards the medial thalamus in the territory of the centromedian (CM) nucleus. The anterior lateral portion of the thalamus was most highly correlated with sensory-motor association areas encompassing the premotor, supplementary motor and posterior parietal areas and the frontal operculum. This is in the territory of the ventral anterior nuclei. The anterior medial thalamus was most strongly connected with the anterior cingulate. The inferior thalamus at this location was dominantly connected with the prefrontal component. Inferiorly, the central portion of the thalamus was dominantly correlated with the fronto-parietal-insular cortex. The medial thalami were dominated by connections to prefrontal cortex. The posterior medial extent of the thalamus was most correlated with the temporal cortical component, composed of the fusiform gyrus (posterior part) and the medial and inferior temporal gyri. The infero-posterior aspect of the thalamus was most strongly correlated with the anterior cingulate component. The postero-lateral thalamus most strongly correlated with primary auditory cortex in the superior temporal gyrus bilaterally and the primary visual component of the striate cortex on the right side inferiorly. The lateral parietal component, including the post-central gyrus, was not found to have an area of dominant connectivity with the thalamus.

The neonatal thalamus does not have sufficient contrast to identify thalamic nuclei from high resolution structural MR images and changes shape somewhat during development making direct registration of infant results onto an adult map difficult. There is no neonatal thalamic atlas and therefore it necessary to suggest anatomical locations with reference to the adult thalamic atlas (Krauth *et al.*, 2010) with these caveats in mind. Considering the thalamus from anterior to posterior and beginning medially, the territory of the anterior group nuclei is most strongly correlated with the BOLD signal from the anterior cingulate. Moving laterally, the territory of the ventral anterior nucleus is most highly correlated with sensory motor association network reflecting the efferent fibres from the VA (VA pars compacta) which pass into the premotor cortex for imitation and planning of movement (McFarland and Haber, 2002). Primary motor cortex and somatosensory cortex (figure 6.3, network 1, pale

blue) are the cortical area most correlated with thalamus of the territory of the ventral lateral (VL) and ventral posterolateral (VPL) nuclei; there is some posterior extension into the posterior nuclear group and medial extension into part of the medial nuclear group. Cortical network one's dominance also extends medially to the territory of the centromedian nucleus (CM) which has been shown to be connected anatomically with the motor cortex (Catsman-Berrevoets and Kuypers, 1978).

The medial nuclear group of the thalamus, which includes the mediodorsal nucleus (MD) is dominated by connectivity with the prefrontal cortex (figure 6.3, orange) consistent with the literature where there are reciprocal connections between these two areas. The MD is also known to be connected with other areas including cortical areas modelled in my study: cingulate, insula, premotor and parietal cortices. All of these cortical areas showed significant correlations with the medial area of the thalamus.

At the posterior medial extent of the thalamus, in the territory of the medial nuclear group of the pulvinar, the dominant connectivity is with the temporal component (figure 6.3, dark blue) which comprises the Fusiform gyrus (posterior part) and the medial and inferior temporal gyrus. This part of the pulvinar is known to be connected with the superior temporal gyrus, but also with the prefrontal cortex, cingulate and posterior parietal cortices. In figure 6.4, showing areas of significant correlation between cortex and thalamus, it can be seen that these cortical areas are significantly correlated with the posterior medial portion of the thalamus. In addition, it is one of the only places with which the sensory motor component (figure 6.3, pale blue) is not significantly correlated.

Inferior to this in the territory of the inferior pulvinar group of nuclei, the dominant connectivity is with the anterior cingulate gyrus (figure 6.3, green) which is an unexpected result as this area is concerned with visual processing. The primary visual cortex (figure 6.3, lilac) modelled in this study had a higher incidence of noise than other components selected, and it is possible that the eigen timeseries modelled from this cortical area was more heterogenous, leading to lower correlations in the group and therefore no dominance in this area. The visual cortex was significantly correlated with a small area of the inferior pulvinar on the right side only. Lateral to this in the

Lateral pulvinar group of nuclei, the connectivity is strongest with the auditory cortex (figure 6.3, red) bilaterally, and with the primary visual cortex figure 6.3, lilac) on the right side only and this approximates the areas of the median and lateral geniculate nuclei.

Inferiorly, the area of the thalamus in the territory of the parafascicular nucleus, and intralaminar nuclei (see figure 6.3c), is most strongly correlated with fronto-parietal-insula (figure 6.3, dark pink). The parafascicular nucleus has been shown to be critical for behavioural flexibility in rodents (Brown *et al.*, 2010) as well as the area thought to support pain processing (Vogt *et al.*, 2008). It is also dominantly correlated with the inferior part of the ventrolateral nucleus (VL). In addition to its reciprocal connections with the basal ganglia, the posterior part of the ventral lateral nucleus is known to be connected with the anterior parietal cortex which is included in the fronto-parietal-insula area. There remains no area of the thalamus to which lateral sensory cortex (figure 6.2, pink) is most strongly correlated.

Specialised and integrated connectivity at the time of normal birth

Using maps of dominant connectivity to characterise thalamic organisation underestimates the complexity of connectivity by discarding information about shared or integrated thalamic targets. Consideration of the full distribution of pair-wise correlations reveals that by the time of normal birth, the large-scale neuronal dynamics of the cortex share substantial parts of the anatomical infrastructure of the thalamus. Figure 6.4 shows each cortical component and its territory of significant thalamic correlations thresholded at a significance of $p < 0.05$.

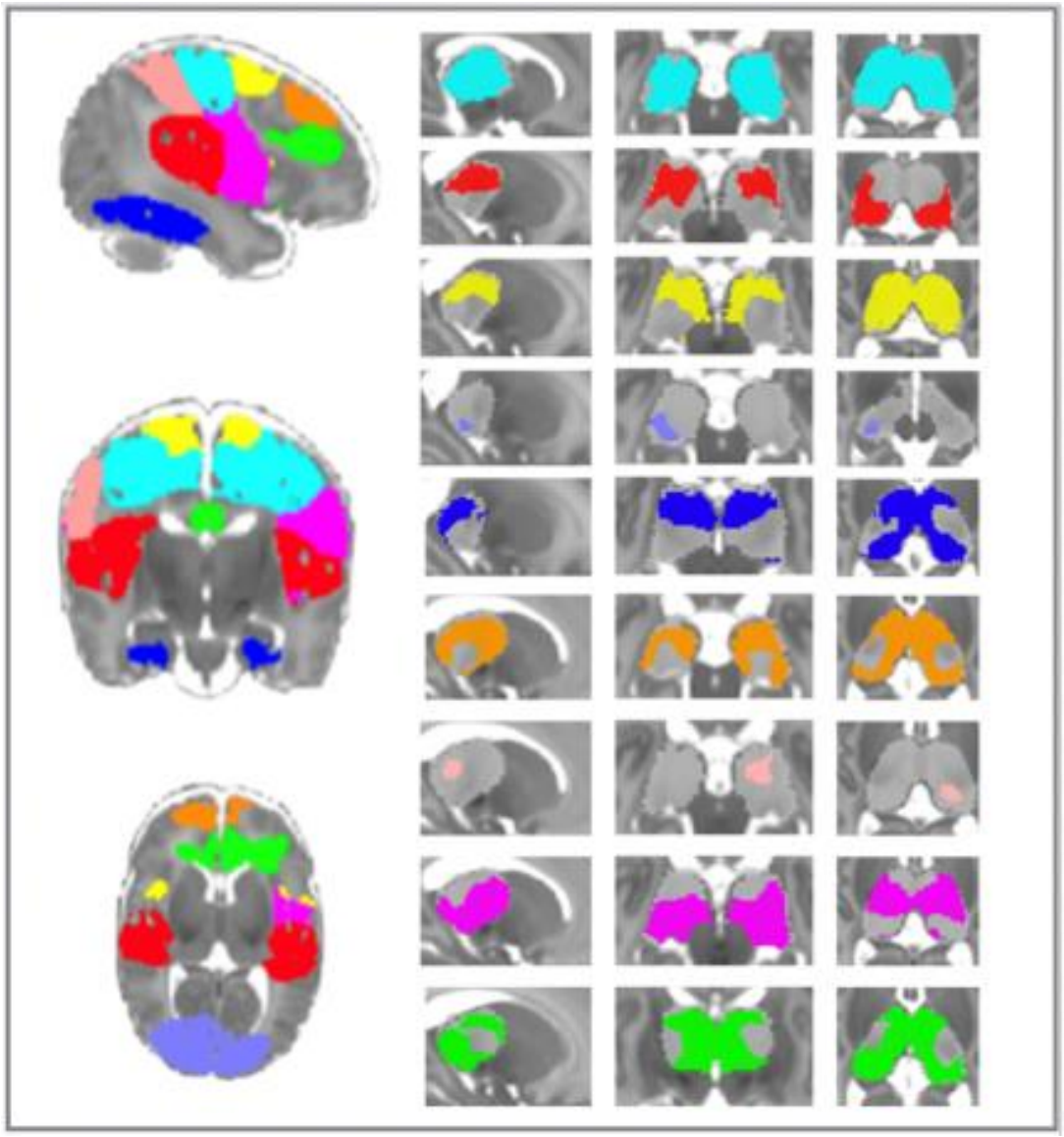

Figure 6.4. Areas of thalamus significantly correlated with cortical areas. Partial correlations are thresholded at a significance of $p < 0.05$ FWE corrected except for primary visual network (lilac) shown at $p < 0.06$ FWE corrected (see text). Primary sensory motor (pale blue), primary auditory (red), sensory-motor association (yellow), primary visual (lilac), temporal (dark blue), pre-frontal (orange), lateral parietal (pink), fronto-parietal-insula (dark pink) and anterior cingulate (green). Images are displayed as per radiological convention.

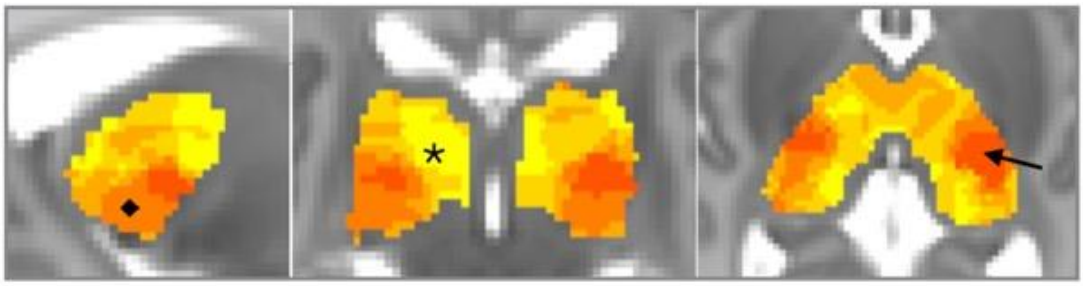

Figure 6.5. Number of components significantly correlated with activity in thalamic voxels at the time of normal birth. Red (arrowhead) shows significant connectivity with 2 cortical areas (primary sensory-motor and fronto-parietal-insula). Orange (diamond) connected with 3 cortical components (primary sensory-motor, fronto-parietal-insula and anterior cingulate). Yellow medial thalamus (*) shows territory with connectivity to 6 cortical components.

Visual inspection of these maps shows that connectivity naturally divides into components with widespread connectivity throughout the thalamus (primary sensory-motor, temporal, medial prefrontal cortex, anterior cingulate and fronto-parietal-insular cortex) and components whose connectivity was mainly limited to their areas of dominance (primary auditory, primary visual and lateral parietal) (Figure 6.4). Thalamic connectivity with the visual cortex is included in this figure but only reaches a significance of $p < 0.06$ possibly due to its location on the edge of the thalamus. Figure 6.5 is a summary of Figure 6.4 and shows, for every thalamic voxel, the number of components with significantly correlated BOLD activation. The central portion of the thalamus has significant connectivity with only 2 cortical components (sensory-motor and fronto-parietal-insula) joined by a third (anterior cingulate component) in the postero-inferior portion. The medial territories of both thalami are significantly connected with 6 out of the 9 studied cortical components, with no significant correlation with primary visual, primary auditory or lateral parietal components.

Thalamocortical connectivity is affected by premature birth

Of nine cortical areas examined, four showed a difference in correlation with the thalamus according to the degree of prematurity experienced by the subject. A decrease in magnitude of connectivity ($p < 0.05$) was found in premature infants in 3 of the 9 components investigated (Figure 6.6i, ii, iii). This decreased connectivity was found between the fronto-parietal-insula component and a widespread area of the thalamus; reduced connectivity with prematurity was also found between thalamus and the anterior cingulate and prefrontal components ($p < 0.05$). The difference in connectivity between the anterior cingulate component and the thalamus was observed within the area of its dominant thalamic connectivity; whereas the difference between medial prefrontal component and thalamus was detected on the right side only, and outside its dominant territory. connectivity involving the fronto-parietal-insular cortex, however, was affected by prematurity both in the territory of its dominant connectivity and also outside it, in areas dominantly connected with sensory-motor and anterior cingulate components. The only cortical area where connectivity increased with prematurity was the lateral parietal component. This small area of the thalamus with increased connectivity is identified from the segmentation in Figure 6.3 as being most connected with the sensory motor cortex. The r^2 shown in Figure 6.6 Bi is 0.3788, Bii 0.2129, Biii 0.1723 and Biv 0.1543.

There was no relationship between gestational age at birth and motion ($r=0.055$, $df=65$ $p>0.5$) or age at scan and motion ($r=0.064$, $df=65$, $p>0.5$).

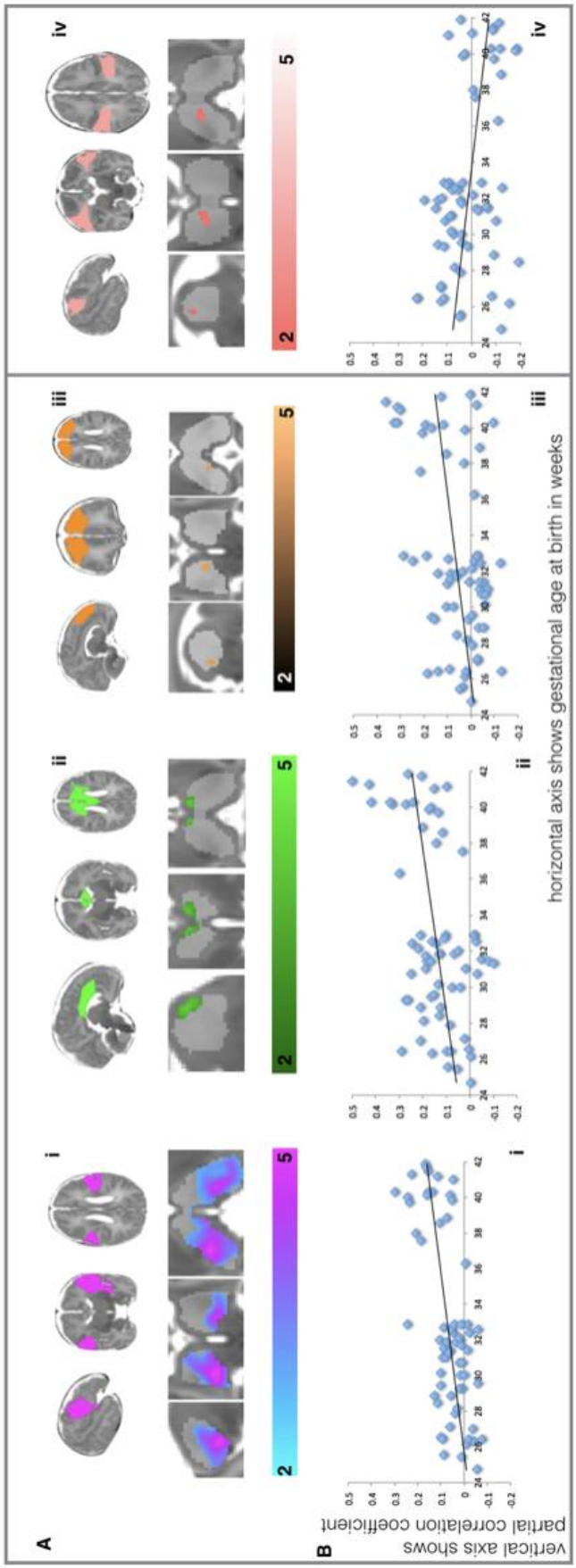

Figure 6.6 Thalamocortical connections altered by preterm birth (contd).

Figure 6.6 Thalamocortical connections altered by preterm birth. Reduced gestational age at birth was associated with reduced connectivity between thalamus and fronto-parietal-insula (i), anterior cingulate (ii) and prefrontal cortex (iii) and increased connectivity with lateral parietal cortex (iv). Significance testing using randomization shown at $p<0.05$ FWE-corrected, using a general linear model to determine the relationship between gestational age at birth and the partial correlation scores between each cortical component and the thalamus by the time of normal birth. Panel A shows cortical components above and corresponding areas of different connectivity with the thalamus below. Panel B shows scatterplots showing the association between connectivity (vertical axis) for each component and gestational age at birth in week (horizontal axis). The images are displayed as per radiological convention.

Discussion

The results presented confirms that at the time of normal birth, the infant brain has robust, predominantly symmetrical network architecture. They also show that by the time of normal birth, the topographical organisation of functional connectivity defined by strongest connectivity is consistent with information on the mature non-primate brain using tracer methods (Goldman-Rakic and Porrino, 1985; Morel *et al.*, 1997; Rouiller *et al.*, 1999; López-Bendito and Molnár, 2003) diffusion studies in adults and young children (Behrens *et al.*, 2003; Counsell *et al.*, 2007) and functional imaging in adult subjects (Zhang *et al.*, 2008). This adds to the growing evidence of the maturity of the human brain by the time of normal birth (Doria *et al.*, 2010; Ball *et al.*, 2014; van den Heuvel *et al.*, 2014) and these results were published in Proceedings of the National Academies of Science in 2015 (Toulmin *et al.*, 2015).

Parcellation

Although the topography demonstrated in figure 6.3 is commensurate with adult thalamic topography derived using other imaging modalities, there are subtle differences with the adult functional parcellations produced by Zhang et al and the tractography by Behrens et al, possibly because the initial parcellations in this study are defined functionally rather than with cortical lobes and combinations of lobes. Studies of longitudinal development of connectivity have used adult-defined cortical regions of interest and analysed thalamic correlations to these areas in neonates and children rather than using areas of cortical activity that are coherent at the time of normal birth as in this study. The methodological difference, perhaps, accounts for the

difference in results found (Alcauter *et al.*, 2014). With reference to the anterior cingulate, Zhang et al 2008 and Behrens et al 2003 both include this in the prefrontal cortex/pre-frontal-temporal regions of interest, while in our case the anterior cingulate is part of a separate component. Neither of the studies in adult subjects, model connectivity with the insular cortex.

Dominance of primary sensory motor component

The almost universal coverage of significant correlation between primary sensory-motor cortical component (See Chapter 6 figure 4, pale blue) and thalamus may be interpreted in light of the anatomical connections between both structures and basal ganglia, which are not represented in this analysis. The centromedian nucleus of the thalamus plays a particular role having reciprocal connections with all the sensorimotor territory of the striatum (Sadikot and Rymar, 2009) as well as input from the sensory motor cortex, which also sends efferents to the putamen and projections to the motor and premotor cortices (Catsman-Berrevoets and Kuypers, 1978).

Overlapping connectivity profiles

A more detailed analysis of thalamic connectivity reveals overlapping connectivity profiles that share links with multiple cortical territories. The thalamus is differentiated between regions with connectivity to multiple cortical components and regions with connectivity to only two areas. The thalamic areas connected to multiple cortical regions are not connected to primary visual, primary auditory or lateral parietal components. These different connectivity profiles seem to reflect the functional role of the respective units. With the exception of primary sensory motor connectivity, units involving primary cortex seemed more restricted than those with connections to heteromodal cortex. Given the age of the subjects, this result may represent a developmental stage, or may be a feature of mature connections. It is notable, however, that analysis of adult data shows that human association cortices participate in multiple networks and provide functionally specialised and flexible regions, whilst somatomotor and visual cortices participate in single networks (Yeo *et al.*, 2011, 2014).

Location of difference according to gestational age at birth

More immature areas?

Cortical regions with reduced thalamic connections in preterm infants are areas receiving higher-order thalamic input: circuits receiving cortical input rather than subcortical input. Whatever nomenclature or categorisation of the thalamus is adopted (see Chapter 1), neurons from thalamus destined for primary cortex reach the subplate, and subsequently their cortical destinations, earlier than those from 'higher order' (or association) nuclei. For example, the first projections arrive at the subplate of the somatosensory cortex between 14-17 weeks gestational age while those from the pulvinar reach the subplate of the peristriate cortex between 17-20 week, not reaching the peristriate cortex itself until 26 weeks gestational age (Kostovic and Rakic, 1990; Purves *et al.*, 2011). This might make these connections with association cortex more vulnerable to preterm birth. The microstructure of these 'higher' cortical regions, as assessed with diffusion imaging, is less mature than primary cortical regions but develops rapidly during the preterm period (Ball *et al.*, 2013). There is evidence also at the molecular level, with Growth-Association Protein (GAP-43), found in growing axons but lost when stable connections are made, being absent from axonal connections to first order relays (Feig, 2005) such as primary cortex, but persisting in regions of heteromodal cortex where it may mediate experience-dependent plasticity (Benowitz and Routtenberg, 1997). The comparative vulnerability of association over primary cortex is starting to be understood with results from the auditory cortex showing primary cortex unperturbed by preterm birth, whereas non-primary auditory cortex shows delayed maturation associated with poorer language development in childhood (Monson *et al.*, 2018).

Due to increased sensory input?

We also found increased connectivity with prematurity between the thalamus and a single cortical component, the lateral parietal component, which in adults is involved in processing signals from face, lips, jaw, tongue and throat (Purves *et al.*, 2011). This raises the hypothesis that premature exposure to activities such as breast and bottle-feeding may serve to increase functional connectivity to regions of cortex with more mature microstructure. Increased functional connectivity is not to be regarded as a positive or an advantage. In an experiment using valproic acid to disrupt subplate

development, an area of altered connectivity was followed by a general hyper-connectivity shortly after ear opening (Nagode *et al.*, 2017). In the human, there is the possibility that an initial disruption could be further exacerbated by the increased sensory experience of the preterm infant (sensory, auditory and visual) which further disrupts the experience-dependent development. Increased early sensory experiences have been shown to have an anatomical consequence with volume loss in the somatosensory regions of the thalamus found in extremely preterm infants who had undergone many (necessary) painful invasive procedures as part of their neonatal care (Duerden *et al.*, 2018b, a). These authors find reduced thalamic growth to be related to the motor and cognitive outcomes of the infants.

Metabolic demands?

The medial dorsal and anterior nuclei have an increased density of interneurons which are known to have increased metabolic needs compared with other cell types and constitute up to 50% of cells of the anterior nuclei (Mai and Paxinos, 2012). The structures with which they are connected (medial, lateral parietal and prefrontal cortices) show elevated levels of aerobic glycolysis in the adult brain (Vaishnavi *et al.*, 2010) in bilateral areas of prefrontal cortex, lateral parietal cortex, posterior cingulate/precuneus, lateral temporal gyrus and caudate nuclei. These areas correspond to two known adult brain networks, the default mode network and the executive control network. It is possible that hypoxia-ischaemia, or nutritional insufficiency, preferentially affect these highly metabolic areas (Volpe, 2009).

Unique properties of the fronto-parietal-insula connections?

The most striking results are from the fronto-parietal-insular cortical network with bilateral differences in correlations according to prematurity leading to the possibility that there is something uniquely vulnerable in this coupling when exposed to preterm birth. The fronto-parietal brain network is composed of flexible hubs which in adults have been shown to be able to 'flexibly and rapidly shift their brain-wide functional connectivity patterns to implement cognitive control across a variety of tasks.' (Cole *et al.*, 2010). In adult studies, this 'task-positive' system (Fox *et al.*, 2005), cognitive control network (Cole and Schneider, 2007) or multiple-demand system (Duncan,

2010) has come to be defined as a core set of brain regions including portion of lateral prefrontal cortex, anterior insular cortex, medial prefrontal cortex and posterior parietal cortex of which the first two are included in this study.

The anterior insula is considered by some as the hub of the salience network whose main role is in information flow across other brain networks involved in cognition and attention (Menon and Uddin, 2010). Studies have suggested a widespread role for the insula in higher-order mental processes guiding behaviour, as well as in social and affective processes which Menon and Uddin suggest are unified by the detection of novel salient stimuli across visual, tactile and auditory modalities (Menon and Uddin, 2010). The ventroposterior lateral (VPL) nucleus of the thalamus receives input from the spinothalamic tract (information about touch, pressure, pain and temperature) which projects onwards to both to the post-central gyrus (primary somatosensory cortex) and onwards to the insular cortex. Given the increased sensory input received by the preterm infant, this may be another potential example of mildly-perturbed early circuitry which is then subject to subsequent abnormal experiences.

In the adult brain, the fronto-insular cortices and anterior cingulate, share similar cytoarchitecture with agranular cortices and also have large bipolar projection neurons located in layer 5b described by Santiago Ramon Y Cajal as giant fusiform cells and subsequently named von Economo neurons (VENs) with a unique neurochemical signature (Dijkstra *et al.*, 2018). The region they occur in has been shown to host autonomic and socio-emotional functions (Damasio, 1999; Craig, 2002; Seeley *et al.*, 2007; Allman *et al.*, 2011). They appear very late compared with other neurons, firstly in small numbers around the 36th week post conception (38 weeks gestational age) and increase in numbers during the first 8 months postnatally, but it is not known what triggers their arrival (personal communication with JM Allman). It is suggested that, due to their large size and simple structure, they send basic information over long distances (Allman *et al.*, 2011) and ‘represent a specialist type of heteromodal cortex involved in networks with social-emotional and autonomic functions’ (Seeley *et al.*, 2007; Anderson *et al.*, 2009; Bud Craig, 2011).

Comparison with other published studies

In 2017, Hwang et al published a comprehensive study titled 'The human thalamus is an integrative hub for functional brain network' in Journal of Neuroscience (Hwang *et al.*, 2017). In this work, parcellation of the thalamus is investigated in adult subjects using resting state functional connectivity data from 303 subjects with 6.2 minutes of fMRI data each with a repetition time of 3000 ms. The voxel size was comparable to our own, but there were more axial slices in their study due to adult brain size, leading to a greater quantity of data per slice. They replicated their study with data from 62 adults with a longer acquisition time and shorter repetition time of 1400 ms, and performed extensive nuisance regression, but no spatial smoothing. Correlations were obtained using cortical parcellations derived from the group cortical functional networks (modelling 9 networks), the DTI Oxford-FSL atlas and the Morel Atlas. The results obtained in this adult dataset are similar to those presented above in infants at the time of normal birth, in spite of the difference in pre-processing methods, analysis methods and size of cohort studied. To investigate the hub properties of thalamic nuclei, Hwang et al used graph theory metrics, finding that thalamic nuclei whether defined as first order or higher order, display a higher degree of within-module degree values than most of the cortical regions of interest, showing increased within-network connections of thalamic nuclei. This was a metric not explored in this thesis. However, the participation coefficient analysis, defining hubs which act as connecting hubs showed a similarity with the map of overlapping connectivity presented above figure 6.5): the area of thalamus connected with somatomotor cortex is relatively unconnected (at 30%) when compared with the connectivity of other cortical regions of interest, which is what is found in this cohort of preterm infants also.

The study most closely reflecting the age group studied in this thesis is that by Alcauter et al (Alcauter *et al.*, 2014). Published at around the same time as the results above (Toulmin *et al.*, 2015), it looks at a different developmental window, that of birth to two years old, compared with the study presented in this thesis which examines the period of and corticostriatal development prior to the time of normal birth. There are methodological differences between the work presented in this thesis and the paper by Alcauter et al that allow our results, although consistent with those of Alcauter et al, to be more detailed. Importantly, Alcauter et al examine connectivity relative to adult

networks (defined by Smith et al 2009). I took a different approach, which enabled me to avoid the problem of comparing data between brains of such different sizes and proportions as that of an adult and a newborn. I defined the cortical function regions of interest without any assumption of a relation to more mature networks, obtaining each subjects' own individual representation of connectivity and avoiding the a priori assumption that networks and their spatial distribution are the same in neonates as they are in adults. This approach avoids averaging a time-series over a part of cortex not involved in a particular network and also circumvents the problem of averaging multiple parts of cortex present in a network in adulthood (such as the salience network or default network) which have been shown to be functioning differently at the time of normal birth than in adulthood. One example of the benefit of this approach can be seen from my data which show that the anterior medial thalamus is significantly correlated with the anterior cingulate cortex by the time of normal birth, whereas Alcauter et al did not find thalamus-salience network connectivity until the cohort of 1-year olds. I introduced a number of further technical refinements in both the data acquisition and processing. I used 200 contiguous volumes for each subject compared with Alcauter et al where a minimum (but varying number) of 90 volumes per subject were used. My choice of 200 contiguous volumes per subject and the avoidance of scrubbing or spike regression avoided the introduction of temporal autocorrelations in the data and heteroscedasticity. I also used a specific neonatal template and boundary-based registration specially adapted to the neonatal population: these methods improved registration accuracy. Finally, the voxel size used in my study was smaller (2.4 x 2.5 x 3.25mm) compared with 4mm isotropic in the Alcauter study. This enabled a more detailed parcellation of small structures.

Three studies in infants directly investigating thalamocortical connectivity in preterm infants have been published after, and refer to, the results detailed in Study One (Connectivity at the time of normal birth) (Cai *et al.*, 2017; Duerden *et al.*, 2018b; Ferradal *et al.*, 2018). The first closely mirrors the techniques used in this thesis, including the use of independent component analysis to select cortical areas for investigation and an inclusion criterion of continuous volumes after removal of motion (greater than 150 continuous volumes with a frame-wise displacement threshold of 0.5mm in this study, compared with 200 volumes with a mean displacement of

0.08mm in this thesis). Rather than treating gestational age as a continuous variable, Cai et al partition their subjects into three separate groups: normal preterm infants (NP 22 infants, 4 of whom were GA 28-32 weeks, 18 33-<37 weeks), those with posterior white matter lesions (PWML 22 infants, 6 of whom were GA 28-32 weeks and 16 33-<37 weeks) and full-term infants (FT 31 infants >37 weeks gestational age). The NPs were scanned at between 34 and 39.86 weeks, the PWMLs between 32.86 and 38.43 weeks and the FTs between 38.43- and 42.12-weeks' gestation. In terms of study design, the timing of scans with different gestational ages in different cohorts is problematic and results are best viewed as a longitudinal study looking at the development of connectivity during the late third trimester rather than for the effects of prematurity by term equivalent age. However, the thalamic parcellation achieved is somewhat similar to that shown in figure 6.3. Compared with the infants with posterior white matter lesions, the sensorimotor cortex correlated with the thalamus in the normal preterm group (NP) was much more discrete and unilateral on the left side only (Cai *et al.*, 2017). The differences found between normal preterms and those with posterior white matter lesions with regards to the salience network, did not survive correction for the difference in the postmenstrual ages of the infants in the groups. Cai et al identify that the differences between their results and those in this thesis might be to do with their use of a dimensionality of 15 compared with 25 in this work which results in a finer parcellation in Toulmin et al. They also identify that most of the infants in their study were scanned before term equivalent age leading to a more immature cohort.

Also published after the results detailed above, the study by Ferradal et al was designed to compare structural and functional methods of defining connectivity. They conclude that regions involving primary sensory cortices show more agreement between structural and functional modalities than those involving association cortices (Ferradal *et al.*, 2018). Using 7 adult-derived anatomical regions of interest (prefrontal, premotor, primary motor, somatosensory, posterior parietal, occipital and temporal), partial correlations were mapped between the time series of each individual thalamic voxel and the mean time series of the cortical regions of interest. They find

that their results are broadly comparable to those in Toulmin et al, for similar anatomical regions

of interest. As in the results presented above, they find that medial areas of the thalamus are significantly connected with more cortical regions than more lateral areas and that the middle portion of the thalamus is most correlated with the somatosensory cortex.

Chapter Seven

Specialisation and integration of functional striatocortical connectivity in the human infant

Results

Cortical networks defined using independent component analysis

As seen in the resting state network decomposition in Chapter Six (Figure 6.1) the spatial distribution of the whole brain BOLD signal in the group, assessed in all subjects at the time of normal birth (gestational age 38-42 weeks) using Independent Component Analysis (ICA) was similar to that described previously (Fransson *et al.*, 2011; Smyser *et al.*, 2011), including a combined sensory-motor component, auditory, visual, subcortical components and a fragmented default mode network and did not differ according to gestational age of the infant at birth. This is in accord with previous data (Damaraju *et al.*, 2010; Doria *et al.*, 2010; Smyser *et al.*, 2010; Fransson *et al.*, 2011; Lee *et al.*, 2013).

Functional cortical component	Description	Number in S1
Primary sensory-motor	Pre and post central gyrus (pale blue)	1
Sensory-Motor Association	Superior parietal, superior frontal gyrus (yellow)	3
Temporal	Fusiform gyrus (posterior part), medial and inferior temporal gyrus (dark Blue)	5
Pre-frontal	Dorsal pre-frontal cortex (orange)	6
Lateral Parietal	Post central gyrus (lateral portion), pale pink (not represented in figure 1)	7
Fronto-parietal-insula	Insula cortex (left) and bilateral lateral fronto-parietal junction (dark pink)	8
Anterior Cingulate	Anterior cingulate cortex (green)	9
Orbito frontal	Lateral orbito-frontal cortex (white)	25

Table 7.1. Eight functional cortical components defined using independent component analysis with anatomical areas (all 25 components in Figure 6.1).

Significant correlations in the group

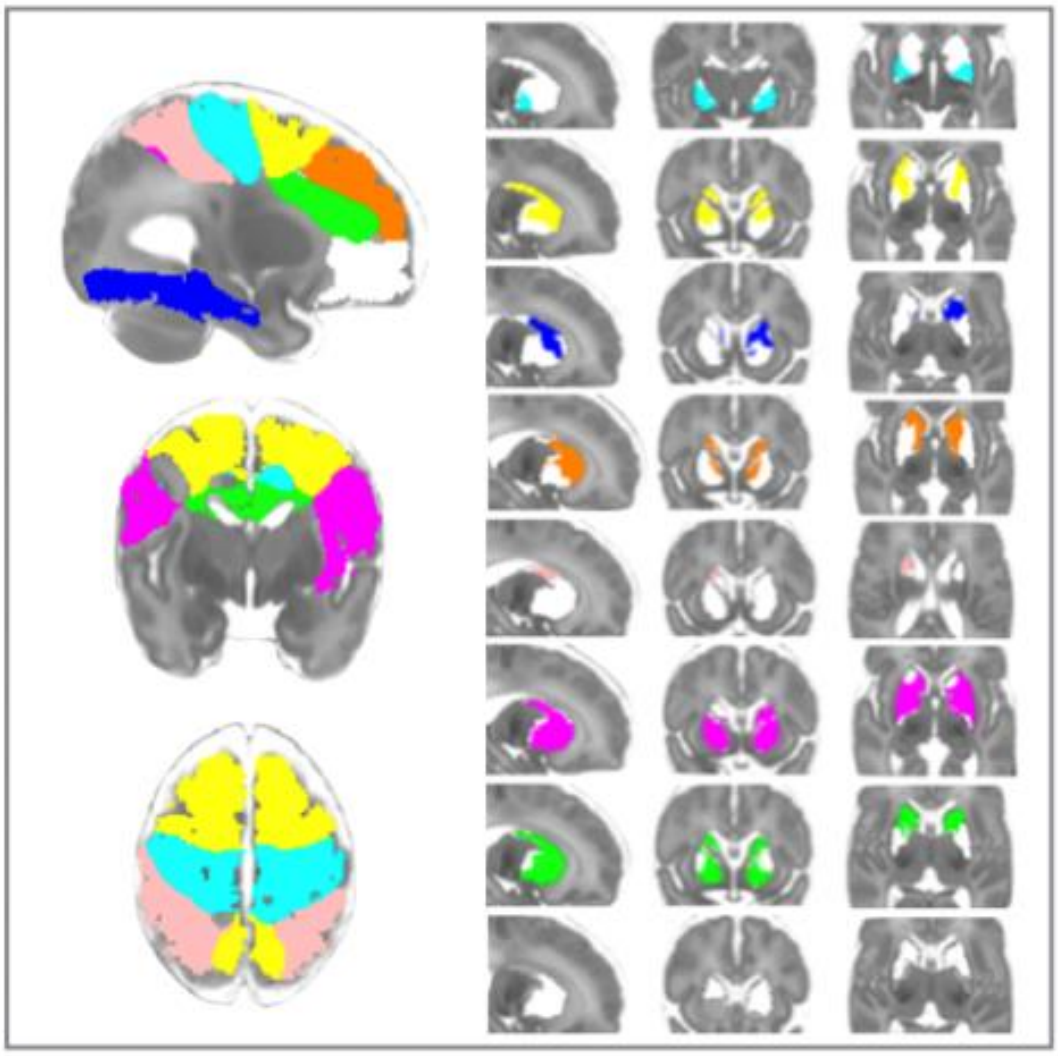

Figure 7.1 shows the area of the striatum significantly correlated with each cortical area in the group of infants at the time of normal birth (thresholded at $p < 0.05$ corrected for family-wise error).

Striatum and cortex are functionally connected by the time of normal birth

Significant striatocortical correlations at the time of normal birth are shown in Figure 7.1. The orbitofrontal component (Figure 7.1, white) is correlated with the caudate head in the superior portion and throughout the body and into the area of the tail, as well as parts of both the globes pallidus and putamen. The prefrontal component (Figure 7.1, orange) is correlated with: the head and much of the body of the caudate bilaterally; the anterior putamen; and anterior part of the lentiform. The anterior cingulate component (Figure 7.1, green) has widespread correlations, covering the caudate head, body and tail and extending into the lentiform nuclei. The sensory-motor

association component contains both the premotor area and a portion of medial primary sensory cortex (Figure 7.1, yellow). This cortical area is correlated with the lateral part of the head of the caudate, the body of the caudate and anterior parts of both putamen and globus pallidus. The fronto-parietal-insula component is correlated with; the caudate head and tail bilaterally, the body of the caudate on the left only and the lentiform nucleus. The cortical component encompassing the pre and post central gyrus (primary sensory-motor, pale blue) is significantly correlated with a discrete posterolateral portion of the lentiform nucleus, encompassing the territory of both the lateral posterior globus pallidus and lateral posterior putamen. The lateral parietal component (Figure 7.1, pale pink) is correlated with part of the caudate body/tail on the right side only. The temporal component (Figure 7.1, dark blue) is correlated with the striatum predominantly on the left side. On the left side it is correlated with the caudate head and body with a small extension to the lateral anterior lentiform in the location of the putamen.

Assigning voxels to a single cortical area

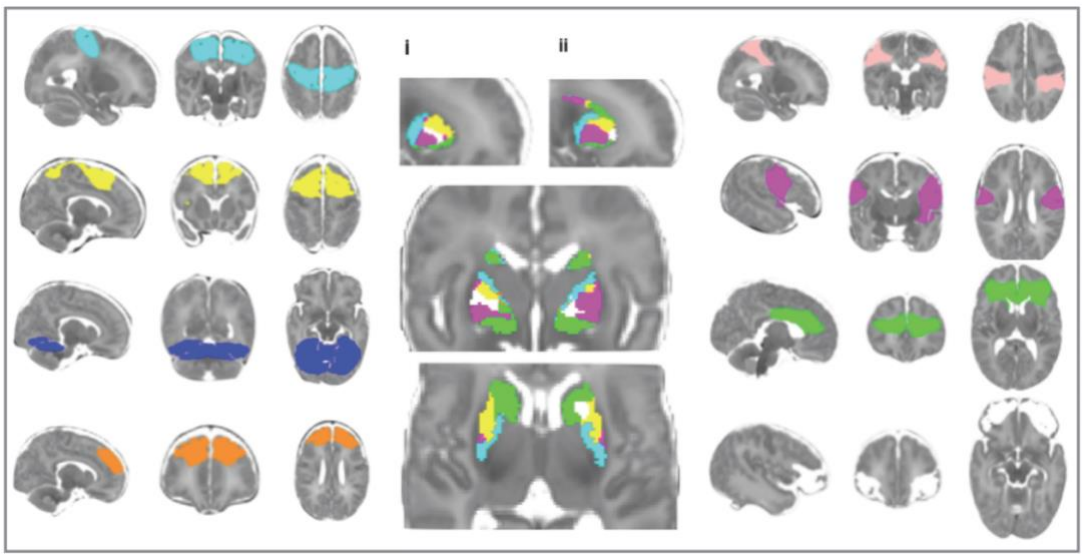

Figure 7.2. Dominant connections between 8 functionally derived cortical regions and basal ganglia using maximum partial correlation coefficient. Left (i) and right (ii) parasagittal sections are shown with corresponding coronal and axial sections.

Figure 7.2 shows the topographical organisation of the basal ganglia defined by the cortical component with which each voxel is most highly correlated. Components represented in the striatum using this technique are exclusively those which include frontal lobe territories with a predominantly symmetrical topographical representation dominated by frontal association cortices (Figure 7.2). There is no representation of the temporal lobe component (dark blue) or parietal lobe component (pale pink). Connectivity with the sensory-motor component is restricted to a bilateral area of the lentiform in the territory of the putamen, adjacent to the internal capsule and posterior to the territory of the sensory-motor association component. Sensory-motor association correlations are dominant in the superior part of the putamen, with a greater territory of dominance on the right side than the left. Dorsolateral prefrontal cortex is dominant only in the left striatum where it 'wins' a small area mainly in the caudate head. The fronto-parietal-insula component is also important, making up the central portion of the lentiform correlations with a small contribution to the body of the caudate on the left side only (Figure 7.2 ii). Anterior cingulate correlations with the body of the caudate define a region wrapped around the anterior portion of the striatum. On the right side, the orbitofrontal component is medial and non the right takes a lateral position in the putamen; it is ref repented in the caudate head on the right side only. In the posterior part of the lentiform, the bilateral pattern from superior to inferior is primary sensory-motor, fronto-parietal-insula, anterior cingulate (pale blue, dark pink, green). The anterior lentiform connectivity from anterior to posterior is sensory-motor-association, orbito-frontal, fronto-parietal-insula, anterior cingulate (yellow, white, dark pink, green) bilaterally.

Analysis of overlapping connectivity

There is no clear symmetry of territories which have multiple or single connections with the exception of the posterior parts of the lentiform which are correlated with only two cortical components, sensory-motor and fronto-parietal-insula. As can be seen from Figure 7.1, the majority of the lentiform is variously composed of different combinations of fronto-parietal-insula, orbitofrontal, sensory-motor association, anterior cingulate components with contribution from the sensory-motor component.

Corticostriatal connectivity is affected by preterm birth

Striatocortical correlations with sensory-motor association component (Figure 7.3, yellow) and fronto-parietal-insula component (Figure 7.3, dark pink) are affected by degree of prematurity ($p<0.01$ for the front-parietal insula component and $p < 0.03$ for the sensory-motor association component). The spatial location of these differences is at the junction of caudate and putamen (Figure 7.3). In the case of the fronto-parietal-insula component, a decrease in magnitude of corticostriatal connectivity according to gestational age at birth was found. This was mainly confined to the caudate nuclei (bilaterally) but extending into the lentiform superiorly from anterior to posterior in the location of the anterior-most portion of the anterior limb of the internal capsule. The medial-most part of this area of decreased connectivity on the right, adjacent to the lateral ventricle is the same location as the area of increased connectivity with prematurity with the sensory-motor association cortical component. In contrast, connectivity between sensory-motor association component (Figure 7.3, yellow) and striatum was increased according to degree of prematurity in the area of the anterior limb of the internal capsule especially at the genuflects of the internal capsule on the right side.

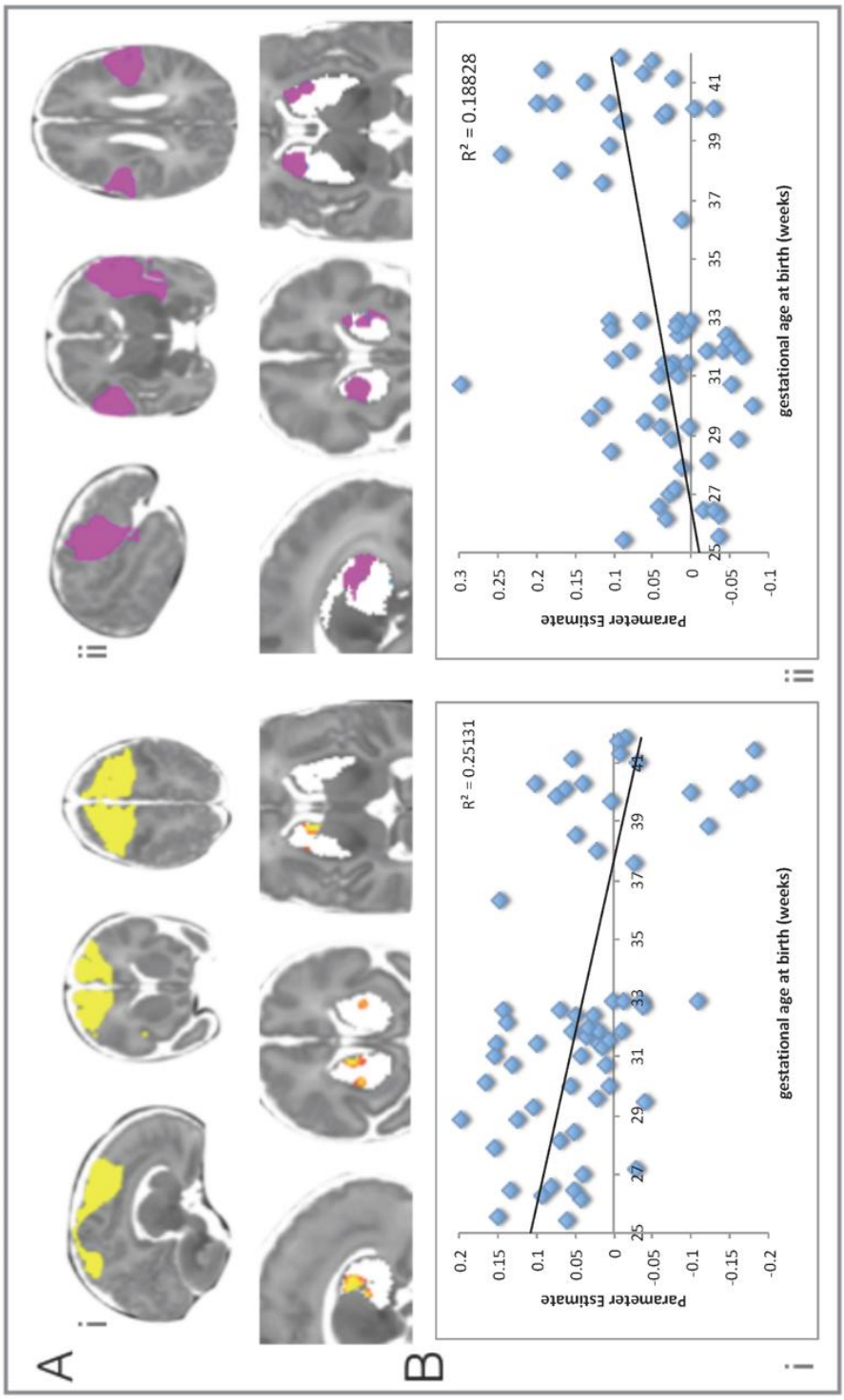

Figure 7.3. Correlations between striatum and cortex are significantly altered by preterm birth. Correlations between sensory-motor association areas and striatum (Ai) and between fronto-parietal-insular cortex and striatum (Aii) are decreased in premature infants compared with those born at the normal time. Significance testing using randomisation is shown at $p<0.05$ (family-wise error corrected) using a general linear model to determine the relationship between gestational age at birth and the partial correlation scores between each cortical component and the basal ganglia. (B) Scatterplots showing the association between corticostriatal connectivity (vertical axis) for each component and gestation age at birth in weeks (horizontal axis). Images are displayed as per radiological convention.

There was no relationship between gestational age at birth and motion ($r=0.055$, $df=65$ $p>0.5$) or age at scan and motion ($r=0.064$, $df=65$, $p>0.5$).

Discussion

At the time of normal birth, connectivity between cortex and basal striatum is detectable between frontal areas of cortex and the basal ganglia with the majority of basal ganglia territory significantly correlated with different combinations of overlapping association cortex. These findings are novel and, in contrast with the connectivity of the human thalamus with cortex at the time of normal birth, do not resemble an adult-like pattern of connectivity. Striatocortical connections affected are to sensory-motor cortex and fronto-parietal-insular cortex.

Striatum and cortex are functionally connected by the time of normal birth

Projections from the primary motor cortex in primates terminate almost exclusively in the putamen (Künzle, 1975, 1978; McFarland and Haber, 2000). In our cohort of 66 term and preterm infants (figure 7.1, sensory-motor component, pale blue), the area of significant connectivity is restricted to the posterolateral lentiform. There is no significant correlation with the caudate. The area of significant correlation is restricted when compared with the areas of significant correlation with other frontal cortical areas which is congruent with the restricted spatial location found in imaging studies in adults (Lehéricy *et al.*, 2004; Draganski *et al.*, 2008; Choi *et al.*, 2012; Verstynen *et al.*, 2012; Pauli *et al.*, 2016) and children (Greene *et al.*, 2014). The distinct motor territory of the lateral putamen is thus detectable by the time of normal birth.

The cortical area which makes up the Sensory-Motor Association component (figure 7.1, yellow) contains both superior parietal cortex and premotor areas. In non-human primates, premotor areas terminate in caudate and putamen with their projections adjacent to those of the primary motor area (Mai and Paxinos, 2012). This same topographical relationship is found with connections of the two cortical areas in the putamen. This is also in agreement with the spatial location of basal ganglia known to be associated with sensorimotor processes in a study of 5,809 human task-based

imaging studies concerning the striatum (Pauli *et al.*, 2016). This study found that the posterior putamen coactivated with sensorimotor cortices including secondary somatosensory cortices and insula and we also find significant correlation with the fronto-parietal-insula component in this location (figure 7.1, dark pink).

The Prefrontal component (figure 7.1, orange) is significantly correlated with the caudate head and body in our cohort with the addition of a modest extension into the putamen closely resembling findings from anatomical tracing studies (Goldman and Nauta, 1977; Yeterian and Van Hoesen, 1978). With regards to the anterior cingulate (figure 7.1, green), tracer studies show that, unlike other prefrontal areas, projections from the anterior cingulate cortex overlap with focal projections from other prefrontal areas extending further afield to areas of the caudate and putamen which do not receive input from other prefrontal areas (Haber *et al.*, 2006). We found the anterior cingulate to have significant correlations with almost all of the basal ganglia and this is in common with the findings of Pauli et al who find it strongly associated with all striatal zones in their study. A reason for its wide area of correlation may be the involvement of the anterior cingulate with a wide range of psychological tasks (Dosenbach *et al.*, 2007) as well as extensive connections with motor cortex, premotor cortex and supplementary motor area and spinal cord (Paus, 2001). With regards to the anterior cingulate and orbitofrontal components, we found their distribution to be broadly similar, reflecting tracing results in non-human primates (Haber *et al.*, 2006). The most anterior portion of the caudate head was significantly correlated with both the anterior cingulate (green) and the dorsolateral prefrontal cortex (orange) a pattern also found in adults (Hedden and Gabrieli, 2010).

The corpus striatum is dominantly connected with association cortices of the frontal lobe

Only the association cortices of the frontal lobe are represented in the dominant connectivity parcellation (figure 7.2). The front-parietal-insula component had significant connectivity with almost all of the striatum tested (figure 7.1). In the developing brain assessed with fMRI-EEG, the insula assumes a critical hub function as a major source of spontaneous neuronal bursts (Arichi *et al.*, 2017) which are correlated with brain growth (Benders *et al.*, 2015) and disappear between 38-42

weeks post menstrual age (Arichi *et al.*, 2017). It is possible that after this period, the dominance of the insula on the correlated BOLD signal decreases. We observed that the sensory-motor component had a restricted territory consistent with the finding of few projections from sensorimotor cortex compared with other frontal areas found in diffusion imaging (Verstynen *et al.*, 2012). The conclusion that the majority of the striatum is concerned with association cortex is also found in adult studies using MRI (Choi *et al.*, 2012).

Integration in the striatum

Results in this thesis show overlapping connectivity profiles of cortical areas in thalamus, with more densely connected areas being those between heteromodal cortex and thalamus, while those areas of thalamus with connections to only two cortical areas relating to primary sensory and motor areas. In thalamus, different cortical areas are most strongly connected with discrete segregated areas similar to those seen in anatomical studies in animals and post-mortem adult human subjects (Jones, 2007; Sherman and Guillery, 2013), diffusion tensor imaging (Behrens *et al.*, 2003; Counsell *et al.*, 2007; O'Muircheartaigh *et al.*, 2011) and corticotopic organisation using functional connectivity MRI (Zhang *et al.*, 2008). This has also now been demonstrated using resting-state functional connectivity metrics in healthy adult subjects (O'Muircheartaigh *et al.*, 2015; Kumar *et al.*, 2017; van Oort *et al.*, 2017), human full-term infants (Ferradal *et al.*, 2018) and preterm infants (Cai *et al.*, 2017).

In contrast to the thalamus, the perinatal striatum does not have an established hierarchy of correlations resulting in an adult-like parcellation by the time of normal birth. This may be due to differential developmental profiles of thalamus and striatum. The immunohistochemical matrix and striosome structure of the striatum, as analysed with dopamine and acetylcholinesterase (AChE), only begins to resemble that seen in adults by the fourth postnatal month (Graybiel and Ragsdale, 1980; Graybiel, 1984) when AChE assumes its classical role of inactivating the neurotransmitter acetylcholine. As different cortical areas in adults preferentially target matrix (thalamostriatal, motor and sensory cortex) or striosomes (cortical limbic areas) from different layers of cortex in human, non-human primate and rodents (Reiner *et al.*,

2003; Crittenden and Graybiel, 2011; Friedman *et al.*, 2015) the process of establishing this complex circuitry may not be established by the time of normal birth. Another explanation may be that the small size of the basal ganglia at term and the known organisation of the striatum with overlapping areas of connectivity and multiply-connected areas some with reciprocal connections and some without (Haber and Knutson, 2010) may require a higher signal to noise in order to define the underlying structure. Finally, the results may be influenced by an underlying asymmetry in the way in which the unilateral cortical components modelled connect with the basal ganglia.

Correlations between cortex and striatum are altered by preterm birth

Sensory-motor association component and putamen

Prematurity appears to have a dose-dependent effect on correlations between basal ganglia and two cortical areas; Sensory-motor association and fronto-parietal-insula (Figure 7.3) with an overlapping spatial representation and the most widespread alterations in the connections between caudate and the fronto-parietal-insula component. Correlations are increased according to prematurity with the sensory-motor association areas in a bilateral area plus an area of the right basal ganglia only. The bilateral location is in the anterior putamen at the lateral boundary with the head of the caudate, adjacent to the internal capsule. This area of the anterior putamen has also been found to be differently correlated during a task-based segmentation of the striatum in individuals with Autism Spectrum Disorders and typically developing individuals (Balsters *et al.*, 2017). It is in the area of significant correlation of the sensory-motor association cortex with the basal ganglia. In a study of the striatum using task-based fMRI data which divided the striatum according to psychological processes in adults (Pauli *et al.*, 2016), this area of increased connectivity according to prematurity is located in an area associated with future social and language functions. Infants born preterm have experienced a longer period of social interaction by the time of normal birth than the term-born cohort and it is possible that this leads to the increase in connectivity reflecting disordered circuit formation. There is also a unilateral increase in correlation according to degree of prematurity between the

sensory-motor association area and the medial caudate head in the location of the caudothalamic notch, which extends into the right medial putamen.

Fronto-parietal-insula component and caudate head

The fronto-parietal-insula component has the most widespread area of difference in connectivity with the striatum, as it also did with the thalamus. The spatial location of the increase in correlation between striatum and sensory-motor association component in the caudate described above, is the same location as the decrease in correlation between fronto-parietal-insular cortex and striatum. This is predominantly confined to the caudate and more dominant on the right side than the left, although it does have bilateral spatial representation in both caudate heads. The difference with prematurity in this case, does not exclusively occupy areas of significant correlations between fronto-parietal-insula and striatum even though this cortical area has widespread areas of significant correlation, but instead occupies the portion of the anterior head of caudate which is bilaterally excluded from significant correlations in the group (figure 7.1, dark pink) this anterior head of the caudate being significantly correlated with the anterior cingulate (green) and dorsolateral prefrontal cortex (orange). It is possible, that this reduced connectivity according to prematurity, is the reason that this portion of the anterior caudate is not significantly correlated with the fronto-parietal-insula component in the group.

It is possible, that germinal matrix haemorrhage, such as types one and two which resolve by the time of a term equivalent age MRI scan, might account for these results. The blood supply to the frontal part of the caudate head is from the recurrent artery of Heubner which also supplies part of the germinal matrix in fetal life. In adults post-mortem, there is variation in its origin, such that it arises from the junction of the first two segments of the anterior cerebral artery in 76.3% following a superior course in 62.1% and anterior course in 30.2% (Matsuda *et al.*, 2018). It is possible that the variation in anatomy might lead to greater or lesser vulnerability for the territory supplied by this artery from downstream effects of venous congestions resulting from germinal matrix haemorrhage (Ghazi-Birry *et al.*, 1997). It is likely that, as a vascular end zone, the area supplied by the recurrent artery of Heubner is vulnerable to ischaemic injury (Volpe, 2018).

A more global hypoxic ischaemic experienced by preterm infants might preferentially affect areas of the striatum. There is evidence that caudate medium spiny neurons, the main projection neurons of the basal ganglia, are specifically vulnerable to the type of transient cerebral hypoxia-ischaemia experienced by preterm infants. In the preterm period, cortical projection neurons have been shown to respond to hypoxia-ischaemia not with neuronal cell death, but with a reduction in dendritic arbor complexity (Dean *et al.*, 2013) and this is the mechanism in the basal ganglia also. MRI measurements showing a reduction in the size of the caudate nucleus in particular (Abernethy *et al.*, 2004) results from diffuse reductions in the maturation of medium spiny neurons of the caudate, specifically the basal dendritic arbor: the other neurons and interneurons of the caudate nucleus remaining unaffected (McClendon *et al.*, 2014). The result is a significant alteration of the contribution of glutamate receptors and a resulting change to the magnitude and kinetics of synaptic currents. As the balance of activity between inhibitory pathways regulates the excitatory innervation of the basal ganglia (in mouse) during development (Kozorovitskiy *et al.*, 2012), such a selective impact of prematurity could alter corticostriatal dynamics and therefore also the correlations between a specific cortical area and its area of striatal input. This can be seen in a mouse model of autism where early hyperactivity of the circuitry involving the basal ganglia leads to increased excitatory synapses and corticostriatal hyper-connectivity (Peixoto *et al.*, 2016).

Comparison with other published studies

There is difficulty comparing these results with other imaging studies especially with regards to the hard parcellation of the striatum. Investigations such as that by Draganski et al using diffusion weighted imaging employ separate analyses for caudate and putamen, excluding globus pallidus, whereas the basal ganglia is considered together in our study (Draganski *et al.*, 2008). No other studies model the insula and the contribution of this cortical area to our results is discussed above. The results of Lehericy et al show a similar area of distribution for the primary motor cortex, as well as that of the premotor cortex (included in the sensory-motor association component in our study). The other two cortical areas modelled by Lehericy et al are a very large prefrontal cortex and small orbitofrontal cortex which

do not correspond well to cortical areas examined here (Lehéricy *et al.*, 2004). The results from Verstynen et al using diffusion imaging in adults are more comparable (Verstynen *et al.*, 2012). The limbic area (a much more widespread cortical area than the cingulate component in our study) was connected to the caudate head, with overlapping contribution from other prefrontal areas as was also found in infants in this thesis.

In one of only two studies of corticostriatal connectivity in children (subjects were 7-12 years old) using resting state functional connectivity, the primary sensory-motor component is also restricted to the posterior putamen (Greene *et al.*, 2014). Here, the cortical regions of interest are defined by independent component analysis in adults and by the age of 7-12 years, cortical areas have a much more restricted representation in the striatum than found in our infant cohort. The restricted appearance of the sensory-motor component by the time of normal birth could reflect a more mature developmental stage of this system when compared with other cortical areas examined. Finally, considering the connectivity of the insula and anterior cingulate, Di Martino et al find that the typically-developing children in their study display connectivity between these paralimbic areas and both ventral striatum and dorsal caudate: the typically-developing adults in this study do not have significant functional connectivity between these areas (Di Martino *et al.*, 2011). This adds to the evidence that the functional connectivity of the insula with the basal ganglia found in this thesis may be a feature of infancy which reduces with development.

Chapter Eight

Cortical-subcortical connectivity at term and outcome at two years after preterm birth using fMRI

Results

Table 8.1. Eleven Bilateral regions of interest: functional cortical components defined using independent component analysis with anatomical areas (full list of 25 components from Figure 8.1 below).

Functional cortical component	Description	Number in S1
Posterior Cingulate	Posterior cingulate and parietal lobe (orange)	1
Lateral Parietal	Primary sensory and superior parietal (red)	2
Fronto-parietal-insula	Insula cortex and bilateral lateral fronto-parietal junction (pale blue)	3
Primary sensory-motor	Medial primary motor cortex, medial primary sensory cortex, extending into premotor cortex (burgundy)	4
Motor Association	Superior frontal including premotor cortex (royal blue)	5
Superior frontal	Frontal lobe including anterior cingulate	6
Orbito frontal	Frontal orbital cortex (salmon pink)	7
Visual cortex	Occipital lobe	8
Pre-frontal	Frontal medial cortex, paracingulate gyrus (bright pink)	9
Lateral pre-frontal	Inferior frontal gyrus including Broca's area (pale orange)	10
Anterior Cingulate	Anterior and middle part of cingulate gyrus	11

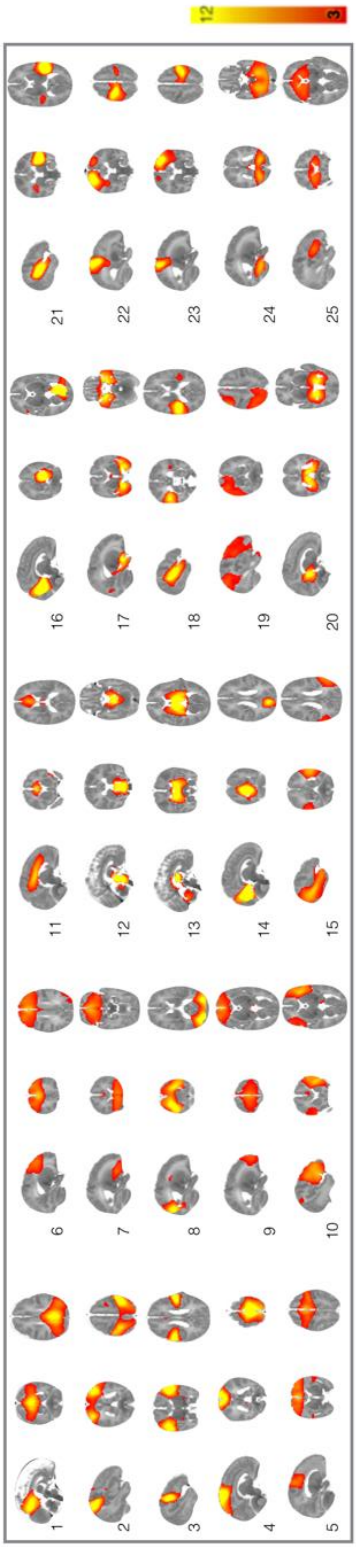

Figure 8.1. Temporal concatenation ICA-estimated resting pattern in the group of 102 subjects. Sagittal, coronal and axial views of the spatial map for each component. Images are z-statistics overlaid on the template 41-week brain. Red to yellow indicates z values ranging from 3 to 12. The right hemisphere of the brain corresponds to the left sides of the coronal and axial images. Components 1-11 correspond to functional cortical components described in table 8.1.

Connectivity between large group of preterm infants and earlier study of preterm and term infants

First considering the connectivity and the areas of agreement with results in Chapters 6 and 7. This study is not designed to be compared with the earlier study, which looks at the spatial correlations between cortical and subcortical structures at the time of normal birth in a group of preterm and term-born infants. Visual inspection between the two studies however, reveal that resting state networks correlated with basal ganglia in both studies are broadly similar, for example, the primary sensory-motor component (burgundy) is highly correlated with the whole thalamus, while restricted to postero-lateral territory of the lentiform, with no representation in the caudate as it was also represented in the cohort of 66 term and preterm infants. The motor association (royal blue) is significantly correlated with wide areas of both thalamus and striatum suggesting as it was in the previous cohort (figure 7.1 component in yellow includes the premotor cortex). Thalamic networks differ in so far as the introduction of analysis of a posterior cingulate network redistributes the spatial domain of the anterior cingulate network to that of the posterior cingulate. Primary sensory-motor, fronto-parietal-insula and sensory-motor association correlations continue to be significantly correlated with large areas of the thalamus.

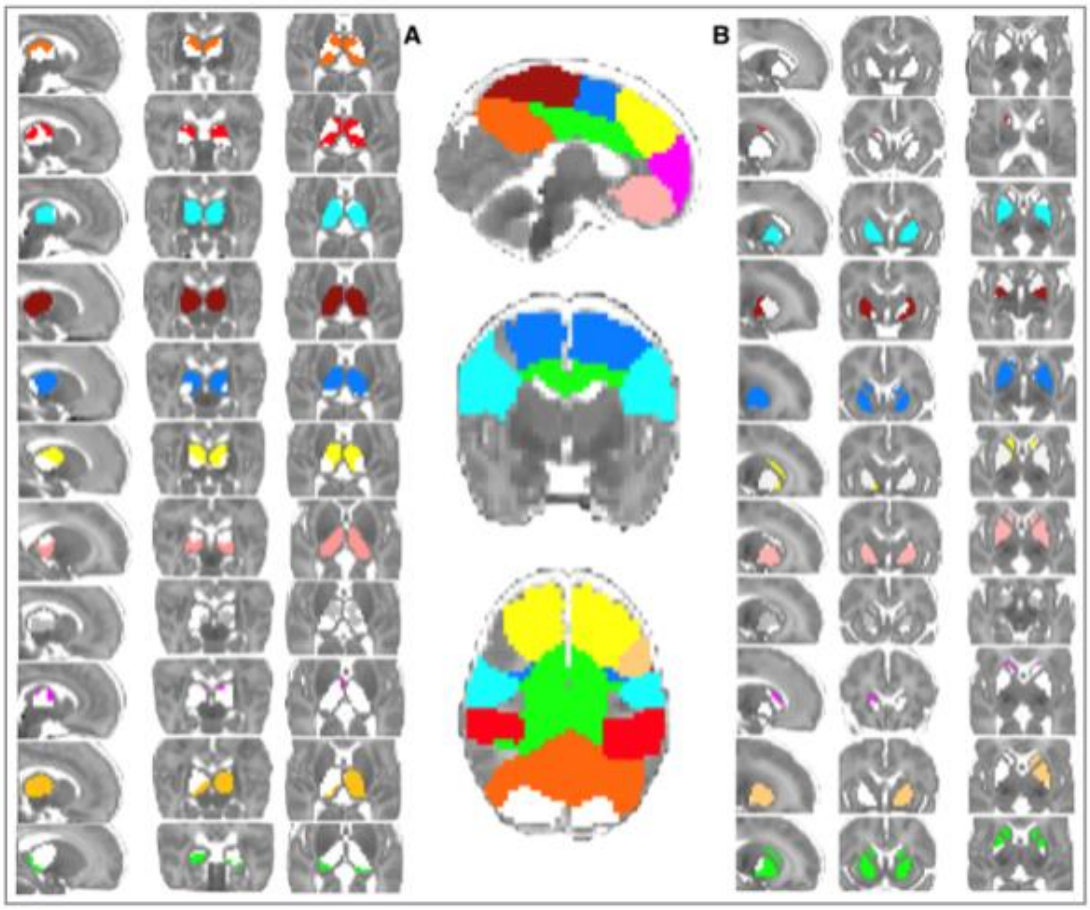

Figure 8.2. Significant correlations between 11 cortical regions of interest and thalamus (A) and basal ganglia (B) in 102 preterm infants at the time of normal birth. Partial correlations (group mean) are thresholded at a significance of $P < 0.05$ (family-wise error corrected). The cortical network shown in orange (B - top) has no significant area of correlation with the basal ganglia in these prematurely-born infants. The middle panel shows the anatomical area of the cortical regions of interest examined.

Connectivity at the time of normal birth and motor and cognitive outcome at two years

Connections between cortical components tested and striatum at the time of normal birth were significantly correlated with outcome at two years between striatum and two cortical components: the sensory-motor component and premotor components. Correlations between striatum and other cortical areas were not significantly associated with development (Figure 8.3). The central inferior portion of Figure 8.3 Ai (motor outcome) remains significant at a level of $p<0.01$. This area of the lentiform is not significantly correlated with this cortical area in the group as a whole but is

significantly correlated with the premotor component in the group. Figure 8.3 Aiii shows the area of the left anterior lentiform in the location of the putamen where lower correlations with the premotor region of interest at the time of normal birth predict higher language scores at 2 years old. This is also a unilateral result.

With regards to thalamocortical connections, only cognitive and motor scores at two years old were correlated with connectivity at birth (figure 8.4). The connectivity of the premotor component with the thalamus is correlated with motor outcome at 2 years old (Figure 8.4, royal blue). The area showing difference with motor outcome is a large bilateral area of the frontal and medial thalamus in the area of the ventral anterior and ventral lateral nucleus of the thalamus on the left side, extending into the medial and anterior nuclei. A unilateral area of left medial thalamus stretching the whole anterior-posterior length of the thalamus is significant at a level of $p<0.01$.

The connectivity of the primary sensory-motor component with the thalamus at the time of normal birth is correlated with cognitive outcome at two years old in the right anterior thalamus only (Figure 8.4 Aii). The area is discrete, but adjacent to the motor correlations statistic (blue). These results in the thalamus are confined to the anterior half of the thalamus, in the area of the ventral nuclear groups, medial nuclei and anterior nuclei.

Striatum in detail

Connections between cortical areas and basal ganglia at the time of normal birth are significantly correlated with outcome at two years in all three domains tested, but only between two cortical components: sensory-motor component and premotor cortex. Correlations between other cortical areas are not significantly associated with development at 2 years old. Significant results are in the medial portion of the lentiform nuclei. Figure 8.3 Ai shows the area of the right lentiform where the correlation coefficients with sensory-motor region of interest at the time of normal birth are significantly correlated with gross motor outcome at 2 years old. The central

inferior portion remains significant at a level of $p<0.01$. This area of the lentiform is not significantly correlated with this cortical area in the group as a whole (see Figure 8.2). This is a unilateral result with the left basal ganglia not reaching a level of $p<0.5$ indicating that this is not an artefact of statistical thresholding. Figure 8.3 Aii shows the areas of the left medial lentiform where the correlation coefficients with the premotor cortex at the time of normal birth are significantly correlated with cognitive scores at 2 years old. This result is in the same location but in the left lentiform as the result shown in Ai (Figure 8.3 Ai). On close inspection, however, this result probably reflects a bilateral change to lentiform as the same area of the corresponding right lentiform reaches significance of $p<0.07$). This is in an area which is significantly correlated with the premotor component in the group (see Figure 8.2). Figure 8.3 Aiii shows the area of the left anterior lentiform in the location of the putamen where the correlation coefficient with the premotor region of interest at the time of normal birth are negatively correlated with language scores at 2 years old. This last result with language scores does not a strict survive thresholding for multiple testing of the three neurodevelopmental outcome scores, but likely reflects a unilateral change with right lentiform failing to reach a statistical level of $p < 0.5$.

Figure 8.3 (below, next page). Corticostriatal connectivity. Significant correlations with outcome at 2 years: (Ai) shows the area of the right lentiform where the correlation coefficients with the primary sensory motor region of interest at the time of normal birth is significantly correlated with motor outcome at 2 years old. (Aii) shows the area of the left medial lentiform where the correlation coefficients with the premotor region at the time of normal birth are significantly correlated with cognitive scores at 2 years old. (Aiii) shows the location of the left anterior lentiform where the correlation coefficients with the premotor region of interest at the time of normal birth are negatively correlated with language scores at 2 years. (B) Scatterplots showing the association between the connectivity between cortical area and basal ganglia (vertical axis) and outcome score for that subject (horizontal axis). Significance testing using randomisation is shown at $P<0.05$ (family-wise error corrected) using a general linear model to determine the relationship between correlation coefficients at the time of normal birth and outcome at 2 years old. Language correlation is shown with threshold-free cluster enhancement (tfce) $p<0.05$ but the area of significance does not survive fdr for multiple comparisons. Images are shown in radiological convention. Cortical region of interest and basal ganglia statistical image are shown in the same colours as per table 8.1.

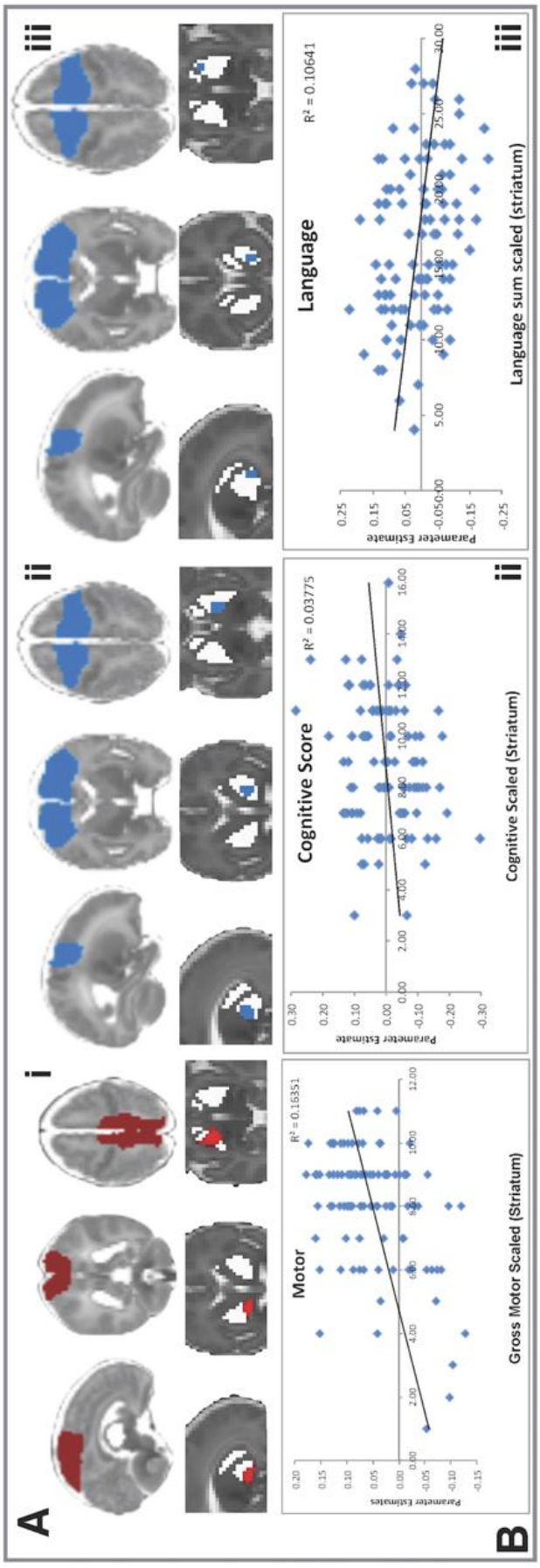

Figure 8.3. Corticostriatal connectivity.

Thalamus in detail

Only cognitive score and motor scores at two years old were correlated with connectivity at birth (Figure 8.4). The premotor component's connectivity with the thalamus is correlated with motor outcome at 2 years old (figure 8.4, royal blue). The area showing difference with motor outcome, is a large bilateral area of the frontal and medial thalamus in the area of the ventral anterior and ventral lateral nucleus of the thalamus on the left side, extending into the medial and anterior nuclei. On the right side, the area of correlation with outcome excludes the medial-fronto-lateral portion of the thalamus in the area of the ventral anterior nucleus. A unilateral area of left medial thalamus stretching the whole anterior-posterior length of the thalamus is significant at a level of $p<0.01$.

The primary sensory-motor component's connectivity with the thalamus at the time of normal birth is correlated with cognitive outcome at two years old in the right anterior thalamus only (figure 8.4 Ai). The area is discrete, but adjacent to the motor correlations statistic (blue). Figure 8.2 shows that the anatomical location on the contralateral thalamus is occupied by significant correlations with motor scores (blue) on the left anterior thalamus. The contralateral thalamus does not reach significance, but there is an area of the left thalamus which lies posterior to this position, which approaches significance ($p<0.06$). These results in the thalamus are confined to the anterior portion of the thalamus, in the area of the ventral nuclear groups, medial nuclei and anterior nuclei.

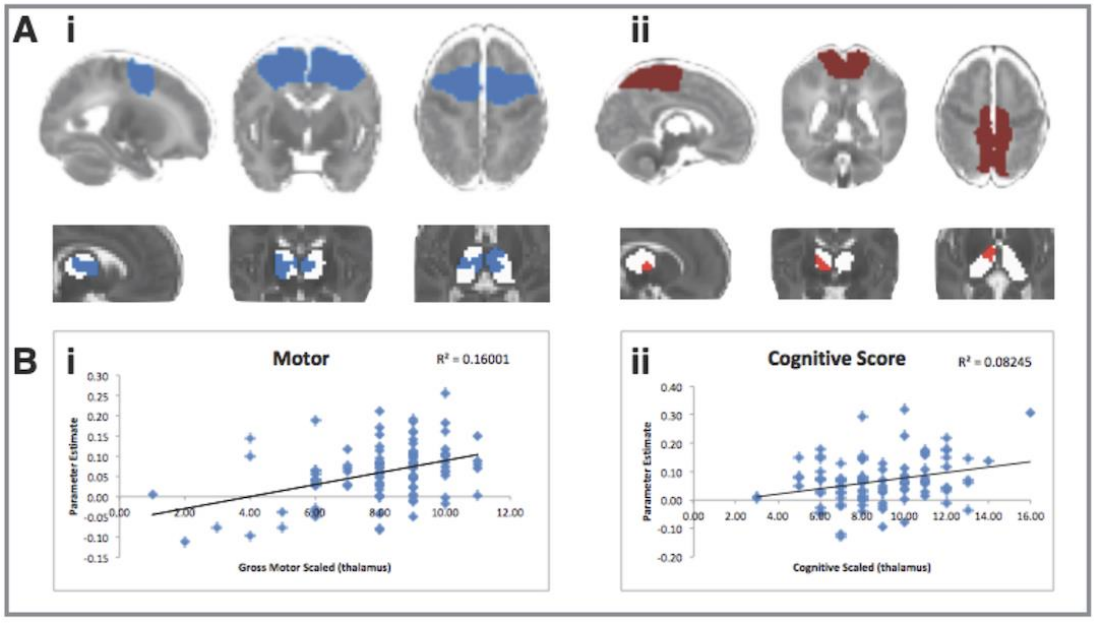

Figure 8.4. Significant correlations with outcome at 2 years. (Ai) shows the bilateral locations in the thalamus where the correlation coefficients with the premotor region of interest at the time of normal birth are significantly correlated with motor outcome at 2 years old. (Aii) Area of the right thalamus where the correlation coefficients with the sensory-motor region of interest at the time of normal birth is correlated with cognitive scores at 2 years old. (B) Scatterplots showing the association between correlations scores between thalamus and cortical area (vertical axis) and outcome score for that subject (horizontal axis). Images are shown in radiological convention. Significance testing using randomisation is shown at $p < 0.05$ (family-wise error corrected) using a general linear model to determine the relationship between correlation coefficients at the time of normal birth and outcome at 2 years old. Cortical region of interest and thalamus statistical image are shown in the same colours at per table 8.1.

There was no relationship between gestational age at birth and motion ($r = 0.03$, $df = 101$ $p > 0.5$) or the three variables of motor, cognitive or language outcome tests. Motor score and motion ($r = 0.01$, $df=101$, $p > 0.5$), cognitive score and motion ($r=0.088$, $df=101$, $p>0.5$) or language score ($r = 0.134$, $df = 101$, $p = 0.179$).

Discussion

Motor Circuits

Thalamic and striatal functional connectivity to primary sensory-motor and motor association cortex as measured using resting state functional connectivity, predicts neurodevelopmental performance at 20 months. Altered connectivity between the sensory motor component (trunk and legs), supplementary motor component (premotor cortex and supplementary motor area) and subcortical components predicted reduced scores in motor and cognitive outcome tests. The component comprising primary sensory-motor cortex concerning tongue and face was not included in the analysis as this network split between two separate components in this group of subjects. The location of these differences in the lentiform nuclei, including globus pallidus internal segment, and anterior half of thalamus in the territory of the ventral lateral, ventral anterior and midline (including centromedian) nuclei, suggests involvement of the motor circuit described and reviewed by Alexander, De Long and Strick 1986 (Alexander *et al.*, 1986). In brief, in this circuit, the putamen receives input from both the motor cortex (Künzle, 1975) and somatosensory cortex (Künzle, 1977) as well as from the premotor area and supplementary motor area (Künzle, 1978; Goldman-Rakic and Porrino, 1985). From here, the putamen connects with the globus pallidus and projects in turn to the ventrolateral nucleus of the thalamus which in turn projects to the supplementary motor area and onwards to influence programming and control of movement. The effects of this circuit are mediated through projections from supplementary motor area to motor and premotor cortex, (Muakkassa and Strick, 1979; Schell and Strick, 1984) and directly to the spinal cord (Biber *et al.*, 1978; Murray and Coulter, 1981; Palmer *et al.*, 1981; Macpherson *et al.*, 1982).

The findings in this study affecting the motor system at 2 years may be enduring: a study of very preterm and term children aged 12 finds that in term children, motor subset scores in aiming and catching and manual dexterity are associated with thalamus-motor connectivity while balance is associated with the basal-ganglia to motor network. In the preterm-born children, motor scores are not associated with these expected connectivity pairing, but rather show increased cerebellum network connectivity associated with improved performance (Wheelock *et al.*, 2018). This raises the possibility that the very preterm children may have adapted to alternative

(and less efficient) networks in order to perform motor tasks. Further evidence of enduring problems involving motor processing in preterm children without cerebral palsy have been described, such as increased difficulty with visuomotor tests in 8-year olds (Goyen *et al.*, 2011) and poorer motor skills than controls at 10 years (Grunewaldt *et al.*, 2014).

Widespread contribution of 'motor circuits' to other cognitive and social domains

Is it possible that only motor and premotor cortices which show significant correlation with functional connectivity in this study due to the underlying need for motor skills in order to acquire skills for success in all neurodevelopmental tests at 2 years: the example of the role of motor skills in behavioural and psychiatric disorders is presented in the next paragraph. Another explanation, as seen in Chapter 2, is that successful integration of the motor system has widespread consequences for movement as well as for context and reward-dependent actions, such as via the hyper direct, indirect and direct pathways of the basal ganglia's motor and premotor cortical loops (Kimura, 1990; Nambu *et al.*, 1996; Kawagoe *et al.*, 1998) as well as saccades and attention via joint inputs to the putamen from multiple sensory cortices and motor cortex (Kunimatsu *et al.*, 2018).

Motor circuits are involved in disorders which have been more traditionally thought to be behavioural or psychiatric and the results presented here may be early markers of these. In addition to an increased risk of autism spectrum disorder and anxiety disorders (D'Onofrio *et al.*, 2013; Treyvaud *et al.*, 2013) preterm infants are at increased risk of behavioural difficulties such as attention deficit hyperactivity disorder (Delobel-Ayoub *et al.*, 2009; Spittle *et al.*, 2009; Jaekel *et al.*, 2013; Marret *et al.*, 2013; Treyvaud *et al.*, 2013; Månsson *et al.*, 2014) where disordered development of motor skills are also seen (Mostofsky *et al.*, 2006). With regard to autism, motor delays are often the first area of concern (mean age of 14.7 months) reported by parents of children with Autism Spectrum disorders (Chawarska *et al.*, 2007) and persistent head lag (Flanagan *et al.*, 2012) and lower gross motor function (Lloyd *et al.*, 2013; Estes *et al.*, 2015) are early risk markers. Others identify difficulty

with motor planning and impaired fine motor control as the most prevalent and earliest identifiable motor deficits in children with autism (Teitelbaum *et al.*, 1998; Green *et al.*, 2009; Fournier *et al.*, 2010) Indeed, sensorimotor difficulties, defined as 'an impairment in the pathway involving motor activity triggered by sensory stimuli and repetitive motor movements' are included in the diagnostic criteria for autism (American Psychiatric Association. and American Psychiatric Association. DSM-5 Task Force., 2013). It has also been hypothesised that difficulties with motor coordination and sensory difficulties may underlie the social and communication deficits, for example impairments in skilled motor gestures (Mostofsky *et al.*, 2009) and connection between children with motor coordination difficulties and reduced competency in recognising emotions in others (Cummins *et al.*, 2005). Impairments found in the thalamic and striatal motor circuits may underlie other neurodevelopmental sequelae of preterm birth.

The success of cortical subcortical connectivity to predict outcome at two years

With regards to motor outcome, the subcortical-cortical pairings identified, account for 16% of the variance in motor scores while those for cognitive and language perform less well, with the parameter estimates of connectivity between subcortical-cortical pairing accounting for between 4-8% of the variation in cognitive score and 10% of the variation in language score (premotor cortex and striatum). In context of the other studies reviewed in Chapter 3, the most comparable cohort with which a comparison can be made (inclusion of R or r^2 in the results), Ball et al find an r^2 of 11% with regards to cognitive scores (Ball *et al.*, 2015): when gestational age at birth (included in our model) and socio-economic status were added to their model, 26% of the variance in cognitive score was explained.

As with many other studies, greater success was achieved with regards to imaging and gestational age at birth (r^2 of 38% Figure 6.6 for thalamocortical connections and 25% for striatocortical connections (Figure 7.3) rather than with outcome where best r^2 was 16%). As seem in chapter two, the Bayley neurodevelopmental examination has been adopted by most studies attempting to predict outcome from imaging at the time of normal birth and is therefore the best standardised tool to use. However, it is important

to briefly mention the underlying strengths and weaknesses of the Bayley neurodevelopmental examination when assessing preterm infants. With regards to cognitive function, Bayley III has shown to have a poor predictive value for cognitive function at school age in a cohort of extremely low birth weight infants, with better performance in those with neurosensory impairments than those without (Hack *et al.*, 2005). The Bayley motor scale itself, when assessing preterm children without cerebral palsy, has a predictive value for motor functioning at early school age of r = 0.34 with an explained variance (r^2) of 12% (Luttikhuizen dos Santos *et al.*, 2013). Preterm infants regularly perform within the normal range of the Bayley III tests, but it is commented that their scores are significantly lower than their term counterparts (Skiöld *et al.*, 2012; Bapat *et al.*, 2014; Kendall *et al.*, 2014) indicating that there is something about the range of difficulties in multiple domains experienced by preterm infants as they grow up which is not captured in the scoring system of the Bayley III scale.

Lateralisation

Bilateral networks were chosen as it is not known what the effect of modelling both bilateral and unilateral cortical areas would be on subcortical structures. Two bilateral cortical networks appear to have significantly different connectivity with regards to outcome scores in unilateral subcortical structures, with nothing approaching significance in the contralateral subcortical structure. Firstly, the increased connectivity in infants with lower language scores is found unilaterally in the left anterior putamen. The normal trajectory of language lateralisation is suggested to be U-shaped with initial change from the weak inter-hemispheric connectivity seen in utero and preterm (Doria *et al.*, 2010) to a bilateral symmetrical representation by the time of normal birth (Perani *et al.*, 2011) and then to the left lateralised distribution seen at the age of 7 year and upwards (Zuo *et al.*, 2010; Nielsen *et al.*, 2013; Emerson *et al.*, 2016). It is possible therefore that the asymmetry we find at the time of normal birth represents a disorder of this process. Secondly, connectivity in children with reduced gross motor scores is only reduced between primary sensory motor component and right putamen (Figure 8.3). Atypical rightward lateralisation of motor circuit connectivity has been found in children with autism spectrum conditions (ASC)

associated with poor performance on all categories of motor skills as assessed using the Physical and Neurological Examination of Subtle Signs (PANESS) (Denckla, 1985; Floris *et al.*, 2016) suggesting that this unilateral result may also represent disordered development in our cohort who are at increased risk of autism (Pritchard *et al.*, 2016). Lateralised results involving medial dorsal nucleus of thalamus and left putamen are also found in a subset of adolescents with ADHD and deficits of executive functions (Stevens *et al.*, 2017).

Part Four

Closing Remarks

Chapter Nine

Methodological limitations

Introduction

I have developed the methods of resting state functional connectivity for use in the neonatal brain in order to investigate connectivity between thalamus and cortex and striatum and cortex at the time of birth and to relate this connectivity to outcome at two years in preterm infants: this has been an exciting opportunity to investigate the developing human brain in vivo. Understanding both the underlying biology and the effect on the data of making choices concerning statistical methods with which to investigate these underlying systems enabled me to make careful and principled choices concerning the pre-processing steps which are required to maximise the signal to noise of the underlying BOLD signal. The management of motion is of great concern in the field, with many and varied opinions and the choices I made were on the conservative side of those made in adult cohorts given the small size of the structures which I wished to investigate.

Motion

Concerns about the influence of head motion (Buckner, 2010) which has been demonstrated to affect functional coupling between specific networks in a young healthy adult population, but without effect on the majority of functional connectivity MRI variation (Van Dijk *et al.,* 2012), have been addressed in a few different ways in this thesis. Firstly, selection of datasets with low motion, secondly the use of functional regions of interest and thirdly, partial correlation analysis. The second and third points have been discussed in other places in this thesis. The motion thresholds chosen compare favourably with those of other published studies with infant

populations such as Alcauter et al (who used a motion parameter of 0.5mm frame wise displacement and a signal change of <0.5% as their threshold for scrubbing) and Greene et al modelling the basal ganglia in children (who used a motion parameter of 0.25mm frame wise displacement and a signal change of 2%) (Alcauter *et al.*, 2014; Greene *et al.*, 2014). There were no correlations between variables investigated and motion in the experiments in this thesis.

Sedation

As can be seen from table 3.1 (Table of relevant studies), sedation was a popular way to control head motion in many neonatal studies. The infants in the EPRIME cohort and all but one of the term controls investigated in this thesis were sedated with chloral hydrate (Finnemore *et al.*, 2014) which is a light enough sedative as to be ineffective if the infant is hungry (personal observation). Sedating well infants at term equivalent age is no longer current practice in neonatal scanning, and successful protocols for feeding and wrapping infants have been adopted for initiatives such as the developing Human Connectome project (dHCP) (Hughes *et al.*, 2017). There have been concerns in adult populations that changes in vigilance and arousal during the course of data collection may modulate neuronal activity (Massimini *et al.*, 2005; Saper *et al.*, 2005; Deco *et al.*, 2014) and therefore confound extraction of functional networks (Larson-Prior *et al.*, 2009; Chang *et al.*, 2013) although oculomotor, somatomotor, visual and default mode have shown to be coherent even under anaesthetic levels which induce a profound loss of consciousness (Vincent *et al.*, 2007). Particular concerns have been raised with regards to thalamocortical connectivity in different arousal states (Hale *et al.*, 2016) as a result of the known role of the reticular nucleus of the thalamus and its widespread influence on all cortical areas (Guillery *et al.*, 1998) but these concerns were focused on differences in stationarity and non-stationarity in adults in light sleep compared with being awake. Although not a completely satisfactory answer, it has been shown that periods of more rapid cycling between different networks (measured as non-stationarity) happen in both in the anaesthetised vigilance state in macaques and the awake state in humans (Hutchison *et al.*, 2013). There may, therefore, be advantages in neonatal MRI as the subject remains in the same (asleep) state for the duration of the scan, rather than risk changes in vigilance, such as awake versus asleep,

as is a potential confounder in adult populations. It is now possible in the adult population, to combine fMRI, electrophysiology and eyelid behaviour in order to track arousal (Chang *et al.*, 2016) but this has many challenges both to accomplish and to interpret in the neonatal population. Physiological metrics were not collected during the MRI scans in these infants in this study, metrics which could be used to model arousal states and which are commonly used in adult studies to model the respiratory cycle and heart rate in order to regress this from the data prior to analysis (Smith *et al.*, 2013).

Connectivity

Hard parcellations of the cortex to define regions of interest and subsequent 'winner-takes-all' analysis of connectivity has shown the neonatal thalamus to have similar connections with cortex as described in animal tracer studies but this methodology sacrifices rich information concerning multiple connections which have been seen in Chapters One and Two to be a better representation of the underlying neural substrate. In addition, there is no metric as to how 'dominant' the connectivity is, only that it is more dominant than that with other cortical areas: rich information about potential correlations with other areas is lost. Methodology in this thesis does not allow comparative differences in hierarchy of connectivity between pairs of regions to be measured and related to outcome: for example, two areas which vary together for short but frequent periods of time in one subject, may end up with similar connectivity scores as those subjects who have sustained covariance throughout the data acquisition. Attempts to study stationarity and non-stationarity (Chang and Glover, 2010) and complex network measures (Rubinov and Sporns, 2010; Vértes *et al.*, 2012), try to capture the temporal fluctuations in resting state connectivity. This is a current challenge for the field of neuroimaging (Liégeois *et al.*, 2017) but is a very exciting avenue of investigation with regards to the possible underlying disordered network balance in infants born preterm. Preliminary studies have sought to expose differences in cortical phase synchrony and network coherence using scalp electroencephalography with reference to different vigilance states and found that preterm birth affects phase synchrony in frontally-connected networks (Tokariev *et al.*, 2018). Partial correlation analysis and other chosen statistical methodologies,

however, address some of the important problems of motion and low signal to noise suffered by BOLD imaging and therefore the choice of losing some detail in favour of retaining high fidelity information was made.

Seeking to address this question of multiply-connected areas, the analysis of overlapping areas of significant connectivity presented in Chapter 6, (figure 6.5) has yielded rich new information, suggesting the thalamus is already multiply-connected by the time of normal birth and that some areas are multiply-connected and others more singly connected. This result has been replicated in adult studies which also find that association cortices often belong to more than more network, while primary motor and visual networks are more independent (Yeo *et al.*, 2014). However, when a primary area (the primary visual cortex) is examined in detail in mouse, it is found that neuronal projections target at least 18 cortical and subcortical regions with most individual neurons targeting multiple cortical areas (Han *et al.*, 2018) suggesting a degree of complexity impossible to model using the imaging resolution currently available in humans in vivo.

With regards to the organisation of striatum, the methodology of dominant connectivity appears to be a more significant problem: striatal tracing studies show different areas of striatum to have different levels of converging projections from widespread cortical regions, suggesting that there are many complex and subtle gradients of connectivity. In addition, cortex only projects to input areas of striatum, with internal connections and multiple feedbacks within basal ganglia and thalamus providing the remaining signal. To sample the BOLD signal in the cortex and represent the voxel in the striatum where that signal is most correlated is to vastly underestimate the complexity of the system. In addition, parts of the basal ganglia, such as the subthalamic nucleus and substantia nigra could not be included in this analysis due to their size and lack of resolution on MRI at the time of birth. It is a particular problem, given the finding of the association between motor and premotor cortex and outcome, that the cerebellum is omitted from analysis. As seen in chapters one and two, it is an integral part of the motor system and studies using MRI or extended cranial ultrasound, find that cerebellar scores at term equivalent age correlate with cognitive outcome (Lind *et al.*, 2011; Brouwer *et al.*, 2017) and cerebellar macrostructure (Rose

et al., 2015), with a short trans-cerebellar diameter related to both motor and cognitive outcome in a very preterm population (Park *et al.*, 2014). The acquisition of cerebellar resting state data is technically difficult as a result of drop-out and modelling the cerebellum would therefore have reduced the number of subjects eligible for inclusion in the study.

Neurovascular coupling

There is a substantial difference in the time taken to maximum response of the BOLD signal in adults compared with infants (Colonnese *et al.*, 2008) and preterm infants (Arichi *et al.*, 2012) as well as a lesser magnitude of response in infants. This haemodynamic response function is important to characterise when modelling tasks in task-based fMRI, but as this study does not involve a stimulus and the subsequent modelling of activations in parts of the brain, it cannot be included in the general linear model. It is, however, possible that differences in the haemodynamic response function are responsible for the statistical difference in BOLD coherence between preterm and term infants perhaps representing a marker of altered vessel formation as seen in adults born preterm (Mercuro *et al.*, 2013), variation in haematocrit (potentially confounded by the introduction of delayed cord clamping), variable size and density of vasculature, or perhaps in response to germinal matrix haemorrhage. The difference in functional connectivity estimates in an adult sample were found to be up to 50% in a resting state study comparing a model using HRF deconvolution with one where the HRF was not accounted for (Rangaprakash *et al.*, 2018). The majority of false connections found when HRF was not modelled, were found in networks with anatomically distinct components between different lobes (such as the adult default mode network); a problem which is perhaps not so acute in this thesis where cortical components consist of anatomically coherent regions only.

Control group

Prior to the developing human connectome project (dHCP) initiative, data from control infants was difficult to obtain, due to the ethical difficulty of sedating a well new-born baby with no clinical complications. The control subjects in this study,

therefore, came from two diverse groups: infants born to researchers in our department, who were not all followed up, and a study of hypertensive and diabetic mothers taking supplements of fish oil during pregnancy. These infants were controls for the purpose of prematurity but had risk factors for brain development from hypertension and diabetes not experienced by other infants: these infants were scanned at our institution, but the study was carried out elsewhere and we have been told that these infants all had neurodevelopmental outcomes within the normal range at 2 years. The children born to researchers in the department were also full-term controls, but in terms of subsequent neurodevelopment, they could not form a distributed group with which to draw conclusions about outcome, even though they had neurodevelopmental follow up at two years. Consequently, the study of outcome in this thesis in Chapter Eight was confined to infants all born between 24 and 32. With regards to connectivity at the time of normal birth (Chapters Six and Seven) there are no data points for the continuous variable of gestational age at birth between 34 and 37 weeks. It is likely that the data missing here is linear and so does not disturb our model: population studies suggest that for each additional week of gestation after 33 weeks, there is a linear decrease in adverse outcomes (Vohr, 2013).

Appendix A

Boundary Based Registration

As the contrast of an echo planar image is based on blood oxygen level-dependent contrast and the contrast in a structural T1 or T2 based on protons from water, traditional algorithms (correlation ratio or normalised mutual information etc) for spatial transformation from echo planar image to structural template are imperfect. A new method, novel for treating the two images very differently, emerged (Greve and Fischl, 2009). Boundary-based registration requires a tissue segmentation of the high-resolution image, performs a traditional registration of the low resolution (EPI) image which it then optimises by aligning the input image to the reference by maximising the intensity gradient across the tissue boundaries. This was implemented into FSL 5.0 in September 2011 and provided a much greater accuracy in adult studies. It did not initially work in neonatal images for two reasons. Firstly, the boundary slope parameter assumed adult tissue contrasts between cortex and white matter which are different in neonatal brains due to the immaturity of myelination (Appendix Figure 1). CSF has the same intensity in both age groups, but the contrast between cortex and white matter changes with myelination rendering the adult white matter dark in comparison to the cortex. In the neonate, the cortex is dark in comparison to the white matter. The second issue is related: the tissue segmentation performed (FSL FAST), does not expect neonatal tissue contrasts and therefore selects the wrong segmentation to estimate the white matter boundary. Having re-coded this part of the FSL script, I was able to perform boundary-based registration for neonatal subjects. By comparing the images, especially the position of ventricles and CSF, it was now possible to visually check that the thalamus was correctly aligned to the structural image.

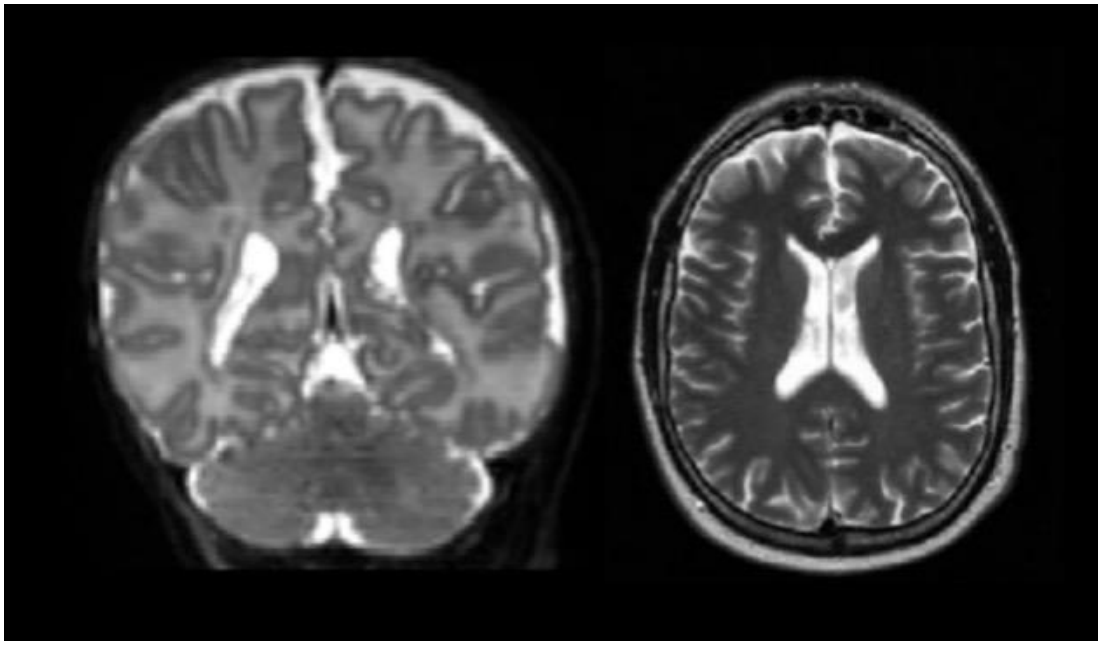

Figure 1. Different contrast of a T2-weighted image according to age of subject: neonatal brain (left) compared with adult (right).

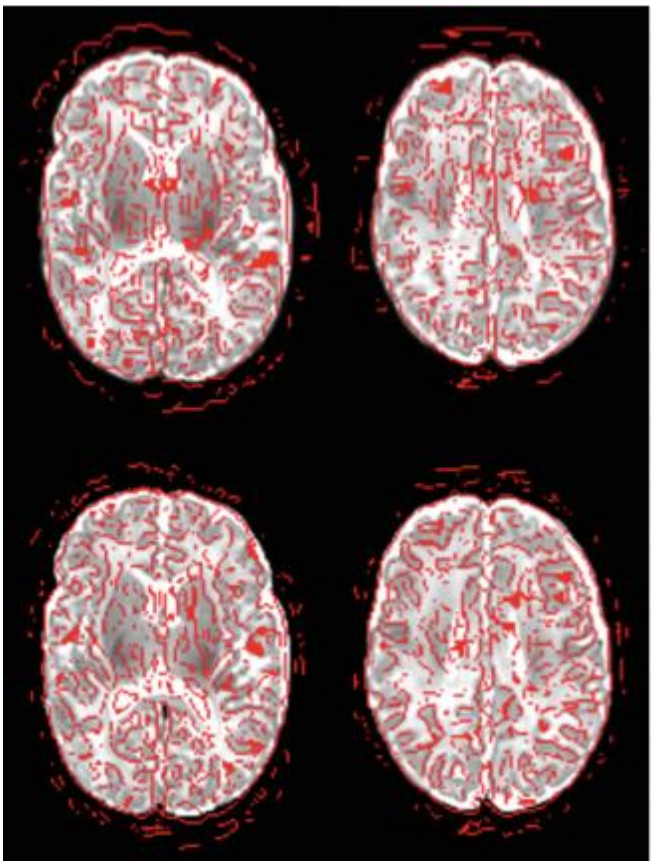

Figure 2. Comparison of traditional rigid registration with 6 degrees of freedom and correlation cost function (top row) with the addition of boundary-based registration (bottom row).

Appendix B

Can predictions be made prior to term equivalent age?

Structural measurements prior to term equivalent age

A few studies collected data close to pre-term birth and again at term equivalent age to explore the possibility of predicting outcome prior to term equivalent age. In an attempt to provide earlier biomarkers, George et al compared images collected at 30-week gestational age and those at term with outcome scores collected at 12 months corrected age (George *et al.*, 2017b). The images collected were scored using the Kidokoro scoring system and reconfirmed at term equivalent MR imaging. Outcome data using the Bayley III were collected at 12 months and global, white matter and deep grey matter scores were negatively associated with motor scores. Cerebellar scores were not significantly associated with Bayley III scores, but were negatively associated with a separate neurodevelopmental assessment; the Neuro-sensory motor developmental Assessment, which assesses quality of movements and has been shown to predict motor and cognitive outcome and cerebral palsy at the age of 4 (Spittle *et al.*, 2015). They conclude that the scoring system is suitable to use in infants born prior to 30 weeks and scanned between 29 and 35 weeks. Paul et al investigated the use of semi-automated cortical segmentation in a cohort of 58 infants scanned soon after birth (26-41 weeks gestational age). They did not find associations between cortical surface area or total cerebral volume with Bayley III cognitive, language or motor scores (Paul *et al.*, 2014). Other studies looking at early MRI using structural measures could not predict outcome (Young *et al.*, 2015; Kersbergen *et al.*, 2016).

Diffusion

Studies which attempted to predict outcome from early diffusion measurements have been less successful, with the exception of the early serial DTI study by Drobyshevsky et al (2007) which showed a correlation between the psychomotor index (average of motor and cognitive scores) and fractional anisotropy on the early scan at 30 weeks gestational age with an r^2 of 0.55 (Drobyshevsky *et al.*, 2007): similar measurement taken at 36 weeks were not significant. The change in FA per week in the occipital white matter and internal capsule explained 63% of the psychomotor score at 2 years. There were only 12 infants in this American study, all were Caucasian with health

insurance, leaving the generalisability of the results in question. Diffusion imaging used by Kawahara et al in 115 infants acquired in infants between 27- and 46-weeks gestational age was used to construct a structural brain connectivity network predict cognitive and motor scores of the Bayley III tests at 18 months of age. These neural network frameworks were better able to predict the age of the child at scan than they were to predict outcome measures (Kawahara *et al.*, 2017) with correlation scores of 0.866 to predict neurodevelopmental outcome from gestational age compared with 0.31 from motor scores. Similar methodology was also used by Duerden et al who scanned 153 infants of less than 32 weeks gestational age at 2 different time points to determine the value of early preterm scans compared with term equivalent age scans to predict neurodevelopmental outcome. The early scans had only limited positive associations, whereas the term equivalent scans showed significant relationships between both motor and cognitive scores and fractional anisotropy in the corpus callosum and corticospinal tracts (Duerden *et al.*, 2015).

Spectroscopy prior to term equivalent age

Chau et al show an association between severe white matter injury and motor outcome, which is unsurprising, but they also show that the change in NAA/choline ratio is slower in those with adverse outcomes (Chau *et al.*, 2013). While the change over time between two scanning points does not provide an earlier biomarker, this might capture features of injury leading to adverse outcome not otherwise available with other modalities which could form part of a multivariate model.

Cranial Ultrasound

In a relatively small cohort of 39 infants with a birth weight below 1000g, white matter injury on cranial ultrasound within the first 28 days of life was a significant predictor of score in motor, cognitive and language domains of the Bayley III assessments (Pogribna *et al.*, 2014). Their model used birth weight, white matter injury on ultrasound and abnormal scan at birth with the addition of the mean diffusivity of the centrum semiovale to predict mental scores (calculated r^2 0.34) and language score (calculated r^2 0.37) and the addition of fractional anisotropy of the sub ventricular

zone to predict cognitive scores (calculated r^2 0.30). A larger study of 480 infants did not find an early cranial ultrasound to be predictive of outcome, only that at term when combined with structural MRI (Hintz *et al.*, 2015).

Longitudinal MRI datasets

Although not able to generate earlier biomarkers as data from both time points are required for analysis, investigations into change over time and the connection with outcome could provide insight into the natural progression of injurious processes and how they might be affected by different clinical variables. This strategy has been adopted in three studies using structural measures (Kersbergen *et al.*, 2016; George *et al.*, 2017a; Moeskops *et al.*, 2017). Automatic quantitative descriptors of tissue volumes at two age points, 30 weeks post menstrual age and 40 weeks post menstrual age in 173 subjects, including the basal ganglia and thalamus, were used by Moeskops et to evaluate preterm infants at risk of cognitive and motor impairment and 2-3 years (Moeskops *et al.*, 2017). A support vector machine classifier was generated to evaluate the difference between the scans at 30 and 40 weeks and it was found that the scan at 30 weeks better predicts outcome at 2-3 years. This study used chronological age for the neurodevelopmental evaluation. The best descriptors from the 30-week scan were the gyrification index, inner cortical surface area, CSF volume and the total brain volume. The basal ganglia and thalamus were not found to be good descriptors. Comparing predictions from early and term scans, Moeskops et al found that low cognitive/motor outcome (scores of less than 85) were best predicted from the early scans (AUC of 0.78 and 0.80). A similar conclusion that features of an early scan at between 29- and 35-weeks postmenstrual age rather than term equivalent age better correlated with outcome, with greater sensitivity and narrower confidence intervals, was found in a study of 83 infants by George et al. In this study deep grey matter predicted motor outcome with a sensitivity of 40% (CI 16-68) on early scan and 36% (13-65) on scan at TEA, while cognitive score was best predicted with the global imaging score at early scan (sensitivity 50% CI 12-88). Term scans were best at predicting cognitive score using measurements for white matter, cerebellum and global score combined (sensitivity 33%, CI 4-78) (George *et al.*, 2017a). In a study of infants born at less than 32 weeks gestational age, Young et al compared structural

MRI in the first few weeks of life and then again at term equivalent age. With regards to the basal ganglia, they found that the growth of the caudate and globus pallidus between preterm and term-equivalent age predicted visual motor integration scores (Young *et al.*, 2015). They also found that caudate and putamen growth to be associated with IQ and language scores.

Appendix C Definitions of preterm birth

Term	Birth after the 37th completed week of gestation
Preterm	Birth before the 37th completed week of gestation
Late preterm	Birth at 34th - 36th completed week of gestation
Moderately preterm	Birth at 32nd - 33rd completed weeks of gestation
Very preterm	Birth at less than 33 weeks' gestation
Extremely preterm	Usually refers to births at less than 28 completed weeks of gestation, but also used for those born at less than 26 completed weeks of gestation

Bibliography

Aarnoudse-Moens CSH, Weisglas-Kuperus N, van Goudoever JB, Oosterlaan J. Meta-analysis of neurobehavioral outcomes in very preterm and/or very low birth weight children. Pediatrics 2009; 124: 717–28.

Abernethy LJ, Cooke RWI, Foulder-Hughes L. Caudate and hippocampal volumes, intelligence, and motor impairment in 7-year-old children who were born preterm. Pediatr. Res. 2004; 55: 884–93.

Aeby A, De Tiège X, Creuzil M, David P, Balériaux D, Van Overmeire B, et al. Language development at 2 years is correlated to brain microstructure in the left superior temporal gyrus at term equivalent age: a diffusion tensor imaging study. Neuroimage 2013; 78: 145–151.

Aggleton JP, Desimone R, Mishkin M. The origin, course, and termination of the hippocampothalamic projections in the macaque. J. Comp. Neurol. 1986; 243: 409–421.

Aggleton JP, O'Mara SM, Vann SD, Wright NF, Tsanov M, Erichsen JT. Hippocampal-anterior thalamic pathways for memory: uncovering a network of direct and indirect actions. Eur. J. Neurosci. 2010; 31: 2292–2307.

Alcauter S, Lin W, Smith JK, Short SJ, Goldman BD, Reznick JS, et al. Development of thalamocortical connectivity during infancy and its cognitive correlations. J. Neurosci. 2014; 34: 9067–9075.

Alexander GE, Crutcher MD, DeLong MR. Basal ganglia-thalamocortical circuits: parallel substrates for motor, oculomotor, "prefrontal" and "limbic" functions. Prog. Brain Res. 1990; 85: 119–46.

Alexander GE, DeLong MR, Strick PL. Parallel organization of functionally segregated circuits linking basal ganglia and cortex. Annu. Rev. Neurosci. 1986; 9: 357–381.

Allendoerfer KL, Shatz CJ. The subplate, a transient neocortical structure: Its role in the development of connections between thalamus and cortex. Annu. Rev. Neurosci. 1994; 17: 185–218.

Allman JM, Tetreault NA, Hakeem AY, Manaye KF, Semendeferi K, Erwin JM, et al. The von Economo neurons in the frontoinsular and anterior cingulate cortex. Ann. N. Y. Acad. Sci. 2011; 1225: 59–71.

American Psychiatric Association., American Psychiatric Association. DSM-5 Task Force. Diagnostic and statistical manual of mental disorders : DSM-5. American Psychiatric Association; 2013.

Amunts K, Zilles K. Architectonic mapping of the human brain beyond Brodmann. Neuron 2015; 88: 1086–1107.

Ancel P-Y, Livinec F, Larroque B, Marret S, Arnaud C, Pierrat V, et al. Cerebral palsy among very preterm children in relation to gestational age and neonatal ultrasound abnormalities: The EPIPAGE Cohort Study. Pediatrics 2006; 117: 828–835.

Anderson K, Bones B, Robinson B, Hass C, Lee H, Ford K, et al. The morphology of supragranular pyramidal neurons in the human insular cortex: a quantitative Golgi study. Cereb. Cortex 2009; 19: 2131–44.

Angevine JB, Sidman RL. Autoradiographic study of cell migration during histogenesis of cerebral cortex in the mouse. Nature 1961; 192: 766–8.

Arbuthnott GW, MacLeod NK, Maxwell DJ, Wright AK. Distribution and synaptic contacts of the cortical terminals arising from neurons in the rat ventromedial thalamic nucleus. Neuroscience 1990; 38: 47–60.

Arichi T, Fagiolo G, Varela M, Melendez-Calderon A, Allievi A, Merchant N, et al. Development of BOLD signal hemodynamic responses in the human brain. Neuroimage 2012; 63: 663–673.

Arichi T, Whitehead K, Barone G, Pressler R, Padormo F, Edwards AD, et al. Localization of spontaneous bursting neuronal activity in the preterm human brain with simultaneous EEG-fMRI. Elife 2017; 6.

Aron AR, Behrens TE, Smith S, Frank MJ, Poldrack RA. Triangulating a cognitive control network using diffusion-weighted magnetic resonance imaging (MRI) and functional MRI. J. Neurosci. 2007; 27: 3743–3752.

Asanuma C, Thach WR, Jones EG. Anatomical evidence for segregated focal groupings of efferent cells and their terminal ramifications in the cerebellothalamic pathway of the monkey. Brain Res. 1983a; 286: 267–97.

Asanuma C, Thach WT, Jones EG. Distribution of cerebellar terminations and their relation to other afferent terminations in the ventral lateral thalamic region of the monkey. Brain Res. 1983b; 286: 237–65.

Augustine EM, Spielman DM, Barnes PD, Sutcliffe TL, Dermon JD, Mirmiran M, et al. Can magnetic resonance spectroscopy predict neurodevelopmental outcome in very low birth weight preterm infants? J. Perinatol. 2008; 28: 611–8.

Averbeck BB, Lehman J, Jacobson M, Haber SN. estimates of projection overlap and zones of convergence within frontal-striatal circuits. J. Neurosci. 2014; 34: 9497–9505.

van Baar AL, Vermaas J, Knots E, de Kleine MJK, Soons P. Functioning at school age of moderately preterm children born at 32 to 36 weeks' gestational age. Pediatrics 2009; 124: 251–7.

Baleydier C, Mauguiere F. The duality of the cingulate gyrus in monkey. Neuroanatomical study and functional hypothesis. Brain 1980; 103: 525–54.

Ball G, Aljabar P, Arichi T, Tusor N, Cox D, Merchant N, et al. Machine-learning to characterise neonatal functional connectivity in the preterm brain. Neuroimage 2016; 124: 267–275.

Ball G, Aljabar P, Nongena P, Kennea N, Gonzalez-Cinca N, Falconer S, et al. Multimodal image analysis of clinical influences on preterm brain development. Ann. Neurol. 2017; 82: 233–246.

Ball G, Aljabar P, Zebari S, Tusor N, Arichi T, Merchant N, et al. Rich-club organization of the newborn human brain. Proc. Natl. Acad. Sci. U. S. A. 2014; 111: 7456–61.

Ball G, Boardman JP, Aljabar P, Pandit A, Arichi T, Merchant N, et al. The influence of preterm birth on the developing thalamocortical connectome. Cortex. 2013a; 49: 1711–1721.

Ball G, Boardman JP, Rueckert D, Aljabar P, Arichi T, Merchant N, et al. The effect of preterm birth on thalamic and cortical development. Cereb. Cortex 2011; 22: 1–9.

Ball G, Pazderova L, Chew A, Tusor N, Merchant N, Arichi T, et al. Thalamocortical connectivity predicts cognition in children born preterm. Cerebral Cortex 2015; 25: 4310–4318.

Ball G, Srinivasan L, Aljabar P, Counsell SJ, Durighel G, Hajnal J V, et al. Development of cortical microstructure in the preterm human brain. Proc Natl Acad Sci 2013; 110: 9541–6.

Ballabh P. Intraventricular hemorrhage in premature infants: mechanism of disease. Pediatr. Res. 2010; 67: 1–8.

Ballabh P, Braun A, Nedergaard M. Anatomic analysis of blood vessels in germinal matrix, cerebral cortex, and white matter in developing infants. Pediatr. Res. 2004; 56: 117–124.

Balsters JH, Mantini D, Wenderoth N, Henk J, Neural B. Connectivity-based parcellation reveals distinct cortico-striatal connectivity fingerprints in Autism Spectrum Disorder. Neuroimage 2017; 170: 1–12.

Bandettini PA, Wong EC, Hinks RS, Tikofsky RS, Hyde JS. Time course EPI of human brain function during task activation. Magn. Reson. Med. 1992; 25: 390–397.

Bapat R, Narayana PA, Zhou Y, Parikh NA. Magnetic resonance spectroscopy at term-equivalent age in extremely preterm infants: association with cognitive and language development. Pediatr. Neurol. 2014; 51: 53–59.

Barbas H, Henion THH, Dermon CR. Diverse thalamic projections to the prefrontal cortex in the rhesus monkey. J. Comp. Neurol. 1991; 313: 65–94.

Barnett ML, Tusor N, Ball G, Chew A, Falconer S, Aljabar P, et al. Exploring the multiple-hit hypothesis of preterm white matter damage using diffusion MRI. NeuroImage Clin. 2018; 17: 596–606.

Baxter LR. Neuroimaging studies of obsessive compulsive disorder. Psychiatr. Clin. North Am. 1992; 15: 871–84.

Beauchamp MH, Thompson DK, Howard K, Doyle LW, Egan GF, Inder TE, et al. Preterm infant hippocampal volumes correlate with later working memory deficits. Brain 2008; 131: 2986–2994.

Beaulieu C. The basis of anisotropic water diffusion in the nervous system - a technical review. NMR Biomed. 2002; 15: 435–455.

Beckmann CF. Modelling with independent components. Neuroimage 2012; 62: 891–901.

Beckmann CF, DeLuca M, Devlin JT, Smith SM. Investigations into resting-state connectivity using independent component analysis. Philos. Trans. R. Soc. London - Ser. B Biol. Sci. 2005; 360: 1001–1013.

Beckmann CF, Smith SM. Probabalistic independent component analysis for functional magnetic resonance imaging. IEEE Trans Med Imaging; 2004; 23: 137–152.

Behrens TEJ, Johansen-Berg H, Woolrich MW, Smith SM, Wheeler-Kingshott CAM, Boulby PA, et al. Non-invasive mapping of connections between human thalamus and cortex using diffusion imaging. Nat. Neurosci. 2003; 6: 750–7.

Belliveau J, Kennedy D, McKinstry R, Buchbinder B, Weisskoff R, Cohen M, et al. Functional mapping of the human visual cortex by magnetic resonance imaging. Science (80-.). 1991; 254: 621–768.

Benders MJ, Palmu K, Menache C, Borradori-Tolsa C, Lazeyras F, Sizonenko S, et al. Early brain activity relates to subsequent brain growth in premature infants. Cereb. Cortex 2015; 25: 3014–24.

Benevento LA, Miller J. Visual responses of single neurons in the caudal lateral pulvinar of the macaque monkey. J. Neurosci. 1981; 1: 1268–78.

Benowitz LI, Routtenberg A. GAP-43: an intrinsic determinant of neuronal development and plasticity. Trends Neurosci. 1997; 20: 84–91.

Bhutta A, Casey P, Cradock M, Anand K, Cleves MA. Cognitive and behavioral outcomes. Jama 2002; 288: 728–737.

Biber MP, Kneisley LW, LaVail JH. Cortical neurons projecting to the cervical and lumbar enlargements of the spinal cord in young and adult rhesus monkeys. Exp. Neurol. 1978; 59: 492–508.

Del Bigio MR, Bigio D, R M, Del Bigio MR. Cell proliferation in human ganglionic eminence and suppression after prematurity-associated haemorrhage. Brain 2011; 134: 1344–61.

Bijsterbosch J, Smith S, Beckmann C. An introduction to resting state fMRI functional connectivity. Oxford University Press; 2017.

Birnholz JC, Benacerraf BR. The development of human fetal hearing. Science 1983; 222: 516–8.

Biswal B, Zerrin Yetkin F, Haughton VM, Hyde JS. Functional connectivity in the motor cortex of resting human brain using echo-planar mri. Magn. Reson. Med. 1995; 34: 537–541.

Blakemore S-J, Wolpert DM, Frith CD. Central cancellation of self-produced tickle sensation. Nat. Neurosci. 1998; 1: 635–640.

Blencowe H, Cousens S, Oestergaard MZ, Chou D, Moller A-B, Narwal R, et al. National, regional, and worldwide estimates of preterm birth rates in the year 2010 with time trends since 1990 for selected countries: a systematic analysis and implications. Lancet 2012; 379: 2162–2172.

Bloch F. Nuclear Induction. Phys. Rev. 1946; 70: 460–474.

Boardman JP, Craven C, Valappil S, Counsell SJ, Dyet LE, Rueckert D, et al. A common neonatal image phenotype predicts adverse neurodevelopmental outcome in children born preterm. Neuroimage 2010; 52: 409–414.

Brazel CY, Romanko MJ, Rothstein RP, Levison SW. Roles of the mammalian subventricular zone in brain development. Prog. Neurobiol. 2003; 69: 49–69.

Brouwer MJ, Kersbergen KJ, van Kooij BJM, Benders MJNL, van Haastert IC, Koopman-Esseboom C, et al. Preterm brain injury on term-equivalent age MRI in relation to perinatal factors and neurodevelopmental outcome at two years. PLoS One 2017; 12: e0177128.

Brown HD, Baker PM, Ragozzino ME. The parafascicular thalamic nucleus concomitantly influences behavioral flexibility and dorsomedial striatal acetylcholine output in rats. J. Neurosci. 2010; 30: 14390–8.

Brown T, Kincaid B, Ugurbil K. NMR chemical shift imaging in three dimensions. Proc Natl Acad Sci 1982; 79: 3523–3526.

De Bruïne FT, Van Wezel-Meijler G, Leijser LM, Steggerda SJ, Van Den Berg-Huysmans AA, Rijken M, et al. Tractography of white-matter tracts in very preterm infants: a 2-year follow-up study. Dev. Med. Child Neurol. 2013; 55: 427–433.

Brumbaugh JE, Hansen NI, Bell EF, Sridhar A, Carlo WA, Hintz SR, et al. Outcomes of Extremely Preterm Infants With Birth Weight Less Than 400 g. JAMA Pediatr. 2019; 173(5):434-455.

Buckner RL. Human functional connectivity: New tools, unresolved questions. Proc. Natl. Acad. Sci. 2010; 107: 10769–10770.

Bud Craig AD. Significance of the insula for the evolution of human awareness of feelings from the body. Ann. N. Y. Acad. Sci. 2011; 1225: 72–82.

Bystron I, Blakemore C, Rakic P. Development of the human cerebral cortex: Boulder Committee revisited. Nat. Rev. Neurosci. 2008; 9: 110–122.

Cai Y, Wu X, Su Z, Shi Y, Gao J-HH. Functional thalamocortical connectivity development and alterations in preterm infants during the neonatal period. Neuroscience 2017; 356: 22–34.

Catsman-Berrevoets C, Kuypers H. Differential laminar distribution of corticothalamic neurons projecting to the VL and the center median. An HRP study in the cynomolgus monkey. Brain Res 1978; 154: 359–65.

Chang C, Glover GH. Time-frequency dynamics of resting-state brain connectivity measured with fMRI. Neuroimage 2010; 50: 81–98.

Chang C, Leopold DA, Schölvinck ML, Mandelkow H, Picchioni D, Liu X, et al. Tracking brain arousal fluctuations with fMRI. Proc. Natl. Acad. Sci. 2016; 113: 4518–4523.

Chang C, Liu Z, Chen MC, Liu X, Duyn JH. EEG correlates of time-varying BOLD functional connectivity. Neuroimage 2013; 72: 227–236.

Chau V, Synnes A, Grunau RE, Poskitt KJ, Brant R, Miller SP. Abnormal brain maturation in preterm neonates associated with adverse developmental outcomes. Neurology 2013; 81: 2082–2089.

Chawarska K, Paul R, Klin A, Hannigen S, Dichtel LE, Volkmar F. Parental recognition of developmental problems in toddlers with autism spectrum disorders. J. Autism Dev. Disord. 2007; 37: 62–72.

Cheong JL, Doyle LW. Increasing rates of prematurity and epidemiology of late preterm birth. J. Paediatr. Child Health 2012; 48: 784–788.

Cheong JL, Doyle LW, Burnett AC, Lee KJ, Walsh JM, Potter CR, et al. Association between moderate and late preterm birth and neurodevelopment and social-emotional development at age 2 years. JAMA Pediatr. 2017; 171(4).

Cheong JLY, Thompson DK, Spittle AJ, Potter CR, Walsh JM, Burnett AC, et al. Brain volumes at term-equivalent age are associated with 2-year neurodevelopment in moderate and late preterm children. J. Pediatr. 2016; 174: 91-97.

Chikama M, McFarland NR, Amaral DG, Haber SN. Insular cortical projections to functional regions of the striatum correlate with cortical cytoarchitectonic organization in the primate. J. Neurosci. 1997; 17: 9686–705.

Choi EY, Yeo BTT, Buckner RL. The organization of the human striatum estimated by intrinsic functional connectivity. J. Neurophysiol. 2012; 108: 2242–2263.

Cole MW, Pathak S, Schneider W. Identifying the brain's most globally connected regions. Neuroimage 2010; 49: 3132–3148.

Cole MW, Schneider W. The cognitive control network: Integrated cortical regions with dissociable functions. Neuroimage 2007; 37: 343–60.

Colonnese MT, Phillips MA, Constantine-Paton M, Kaila K, Jasanoff A. Development of hemodynamic responses and functional connectivity in rat somatosensory cortex. Nat. Neurosci. 2008; 11: 72–79.

Constantinople CM, Bruno RM. Deep cortical layers are activated directly by thalamus. Science 2013; 340: 1591–4.

Conturo TE, Lori NF, Cull TS, Akbudak E, Snyder AZ, Shimony JS, et al. Tracking neuronal fiber pathways in the living human brain. Proc. Natl. Acad. Sci. 1999; 96: 10422–7.

Cordes D, Haughton VM, Arfanakis K, Wendt GJ, Turski PA, Moritz CH, et al. Mapping functionally related regions of brain with functional connectivity MR imaging. AJNR. Am. J. Neuroradiol. 2000; 21: 1636–44.

Costeloe KL, Hennessy EM, Haider S, Stacey F, Marlow N, Draper ES. Short term outcomes after extreme preterm birth in England: comparison of two birth cohorts in 1995 and 2006 (the EPICure studies). BMJ 2012; 345: e7976.

Counsell SJ, Dyet LE, Larkman DJ, Nunes RG, Boardman JP, Allsop JM, et al. Thalamo-cortical connectivity in children born preterm mapped using probabilistic magnetic resonance tractography. Neuroimage 2007; 34: 896–904.

Craig AD. How do you feel? Interoception: the sense of the physiological condition of the body. Nat. Rev. Neurosci. 2002; 3: 655–666.

Creutzfeldt O, Lee B, Elepfandt A. A quantitative study of chromatic organisation and receptive fields of cells in the lateral geniculate body of the rhesus monkey. Exp Brain Res 1979; 2: 527–45.

Crick F, Jones E. Backwardness of human neuroanatomy. Nature 1993; 361: 109–10.

Crittenden JR, Graybiel AM. Basal ganglia disorders associated with imbalances in the striatal striosome and matrix compartments. Front. Neuroanat. 2011; 5: 59.

Cserjesi R, Van Braeckel KNJA, Butcher PR, Kerstjens JM, Reijneveld SA, Bouma A, et al. Functioning of 7-year-old children born at 32 to 35 weeks' gestational age. Pediatrics 2012; 130: e838–e846.

Cummins A, Piek JP, Dyck MJ. Motor coordination, empathy, and social behaviour in school-aged children. Dev. Med. Child Neurol. 2005; 47: 437–42.

D'Onofrio BM, Class QA, Rickert ME, Larsson H, Långström N, Lichtenstein P. Preterm birth and mortality and morbidity: a population-based quasi-experimental study. JAMA psychiatry 2013; 70: 1231–40.

Damadian R. Tumor detection by nuclear magnetic resonance. Science 1971; 171: 1151–3.

Damadian R, Goldsmith M, Minkoff L. NMR in cancer: XVI. FONAR image of the live human body. Physiol. Chem. Phys. 1977; 9: 97–100, 108.

Damadian R, Minkoff L, Goldsmith M, Stanford M, Koutcher J. Field focusing nuclear magnetic resonance (FONAR): visualization of a tumor in a live animal. Science 1976; 194: 1430–2.

Damaraju E, Phillips JR, Lowe JR, Ohls R, Calhoun VD, Caprihan A. Resting-state functional connectivity differences in premature children. Front. Syst. Neurosci. 2010; 84: 169-180.

Damasio AR. How the brain creates the mind. Sci. Am. 1999; 281: 112–7.

Damoiseaux JS, Rombouts SARB, Barkhof F, Scheltens P, Stam CJ, Smith SM, et al. Consistent resting-state networks across healthy subjects. Proc. Natl. Acad. Sci. 2006; 103: 13848–53.

Dean JM, McClendon E, Hansen K, Azimi-Zonooz A, Chen K, Riddle A, et al. Prenatal Cerebral Ischemia Disrupts MRI-Defined Cortical Microstructure Through Disturbances in Neuronal Arborization. Sci. Transl. Med. 2013; 5: 168ra7.

Deco G, Hagmann P, Hudetz AG, Tononi G. modeling resting-state functional networks when the cortex falls asleep: local and global changes. Cereb. Cortex 2014; 24: 3180–3194.

Delobel-Ayoub M, Arnaud C, White-Koning M, Casper C, Pierrat V, Garel M, et al. Behavioral problems and cognitive performance at 5 years of age after very preterm birth: The EPIPAGE Study. Pediatrics 2009; 123: 1485–1492.

DeLong MR, Crutcher MD, Georgopoulos AP. Primate globus pallidus and subthalamic nucleus: functional organization. J. Neurophysiol. 1985; 53: 530–43.

Denckla MB. Revised Neurological Examination for Subtle Signs (1985). Psychopharmacol. Bull. 1985; 21: 773–800.

DeYoe EA, Bandettini P, Neitz J, Miller D, Winans P. Functional magnetic resonance imaging (FMRI) of the human brain. J. Neurosci. Methods 1994; 54: 171–87.

Difiglia M, Pasik P, Pasik T. Early postnatal development of the monkey neostriatum: A Golgi and ultrastructural study. J. Comp. Neurol. 1980; 190: 303–331.

Van Dijk KRA, Sabuncu MR, Buckner RL. The influence of head motion on intrinsic functional connectivity MRI. Neuroimage 2012; 59: 431–8.

Dijkstra AA, Lin L-C, Nana AL, Gaus SE, Seeley WW. Von Economo Neurons and Fork Cells: A neurochemical signature linked to monoaminergic function. Cereb. Cortex 2018; 28: 131–144.

Dixon G, Harper CG. Quantitative analysis of glutamic acid decarboxylase-immunoreactive neurons in the anterior thalamus of the human brain. Brain Res. 2001; 923: 39–44.

Doria V, Beckmann CF, Arichi T, Merchant N, Groppo M, Turkheimer FE, et al. Emergence of resting state networks in the preterm human brain. Proc. Natl. Acad. Sci. 2010; 107: 20015–20020.

Dosenbach NUF, Fair DA, Miezin FM, Cohen AL, Wenger KK, Dosenbach RAT, et al. Distinct brain networks for adaptive and stable task control in humans. Proc. Natl. Acad. Sci. 2007; 104: 11073–8.

Doyle LW, Roberts G, Anderson PJ, Victorian Infant Collaborative Study Group. Changing long-term outcomes for infants 500-999 g birth weight in Victoria, 1979-2005. Arch. Dis. Child. - Fetal Neonatal Ed. 2011; 96: F443–F447.

Draganski B, Kherif F, Klöppel S, Cook PA, Alexander DC, Parker GJM, et al. Evidence for segregated and integrative connectivity patterns in the human Basal Ganglia. J. Neurosci. 2008; 28: 7143–52.

Duerden EG, Foong J, Chau V, Branson H, Poskitt KJ, Grunau RE, et al. Tract-based spatial statistics in preterm-born neonates predicts cognitive and motor outcomes at 18 months. AJNR. Am. J. Neuroradiol. 2015; 36: 1565–1571.

Duerden EG, Grunau RE, Guo T, Foong J, Pearson A, Au-Young S, et al. Early procedural pain is associated with regionally-specific alterations in thalamic development in preterm neonates. J. Neurosci. 2018; 38: 878–886.

Duerden EG, Halani S, Ng K, Guo T, Foong J, Glass TJA, et al. White matter injury predicts disrupted functional connectivity and microstructure in very preterm born neonates. NeuroImage Clin. 2019; 21:101596

Duncan J. The multiple-demand (MD) system of the primate brain: mental programs for intelligent behaviour. Trends Cogn. Sci. 2010; 14: 172–179.

Dyet LE, Kennea N, Counsell SJ, Maalouf EF, Ajayi-Obe M, Duggan PJ, et al. Natural history of brain lesions in extremely preterm infants studied with serial magnetic resonance imaging from birth and neurodevelopmental assessment. Pediatrics 2006; 118: 536–548.

Eblen F, Graybiel AM. Highly restricted origin of prefrontal cortical inputs to striosomes in the macaque monkey. J. Neurosci. 1995; 15: 5999–6013.

Edwards AD, Redshaw ME, Kennea N, Rivero-Arias O, Gonzales-Cinca N, Nongena P, et al. Effect of MRI on preterm infants and their families: a randomised trial with nested diagnostic and economic evaluation. Arch. Dis. Child. Fetal Neonatal Ed. 2018; 103: F15–F21.

Emerson RW, Gao W, Lin W. Longitudinal study of the emerging functional connectivity asymmetry of primary language regions during infancy. J. Neurosci. 2016; 36: 10883–10892.

Engle WA, American Academy of Pediatrics Committee on Fetus and Newborn. Surfactant-replacement therapy for respiratory distress in the preterm and term neonate. Pediatrics 2008; 121: 419–432.

Estes A, Zwaigenbaum L, Gu H, St. John T, Paterson S, Elison JT, et al. Behavioral, cognitive, and adaptive development in infants with autism spectrum disorder in the first 2 years of life. J. Neurodev. Disord. 2015; 7: 24.

Fair DA, Bathula D, Mills KL, Dias TGC, Blythe MS, Zhang D, et al. Maturing thalamocortical functional connectivity across development. Front. Syst. Neurosci. 2010; 4: 10.

Fair DA, Cohen AL, Dosenbach NUF, Church JA, Miezin FM, Barch DM, et al. The maturing architecture of the brain's default network. Proc. Natl. Acad. Sci. 2008; 105: 4028–4032.

Feekes JA, Cassell MD. The vascular supply of the functional compartments of the human striatum. Brain 2006; 129: 2189–2201.

Feig SL. The differential distribution of the growth-associated protein-43 in first and higher order thalamic nuclei of the adult rat. Neuroscience 2005; 136: 1147–57.

Ferradal SL, Gagoski B, Jaimes C, Yi F, Carruthers C, Vu C, et al. System-specific patterns of thalamocortical connectivity in early brain development as revealed by structural and functional MRI. Cereb. Cortex 2019; 29(3): 1218-1229.

Filippini N, MacIntosh BJ, Hough MG, Goodwin GM, Frisoni GB, Smith SM, et al. Distinct patterns of brain activity in young carriers of the APOE-epsilon4 allele. Proc. Natl. Acad. Sci. U. S. A. 2009; 106: 7209–7214.

Finnemore A, Toulmin H, Merchant N, Arichi T, Tusor N, Cox D, et al. Chloral hydrate sedation for magnetic resonance imaging in newborn infants. Paediatr. Anaesth. 2014; 24: 190–5.

Fischi-Gómez E, Vasung L, Meskaldji D-E, Lazeyras F, Borradori-Tolsa C, Hagmann P, et al. Structural brain connectivity in school-age preterm infants provides evidence for impaired networks relevant for higher order cognitive skills and social cognition. Cereb. Cortex 2015; 25: 2793–2805.

Fischl B, van der Kouwe A, Destrieux C, Halgren E, Ségonne F, Salat DH, et al. Automatically parcellating the human cerebral cortex. Cereb. Cortex 2004; 14: 11–22.

Flaherty AW, Graybiel AM. Two input systems for body representations in the primate striatal matrix: experimental evidence in the squirrel monkey. J. Neurosci. 1993; 13: 1120–37.

Flanagan JE, Landa R, Bhat A, Bauman M. Head lag in infants at risk for autism: A Preliminary Study. Am. J. Occup. Ther. 2012; 66: 577–585.

Floresco S, Grace A. Gating of hippocampal-evoked activity in prefrontal cortical neurons by inputs from the mediodorsal thalamus and ventral tegmental area. J. Neurosci 2003; 23: 3930–43.

Floris DL, Barber AD, Nebel MB, Martinelli M, Lai M-C, Crocetti D, et al. Atypical lateralization of motor circuit functional connectivity in children with autism is associated with motor deficits. Mol. Autism 2016; 7: 35.

Forutan F, Mai JK, Ashwell KW, Lensing-Höhn S, Nohr D, Voss T, et al. Organisation and maturation of the human thalamus as revealed by CD15. J. Comp. Neurol. 2001; 437: 476–95.

Fournier KA, Hass CJ, Naik SK, Lodha N, Cauraugh JH. Motor coordination in autism spectrum disorders: a synthesis and meta-analysis. J. Autism Dev. Disord. 2010; 40: 1227–1240.

Fox MD, Snyder AZ, Vincent JL, Corbetta M, Van Essen DC, Raichle ME. The human brain is intrinsically organized into dynamic, anticorrelated functional networks. Proc. Natl. Acad. Sci. 2005; 102: 9673–9678.

Fox P, Raichle M. Focal physiological uncoupling of cerebral blood flow and oxidative metabolism during somatosensory stimulation in human subjects. Proc Natl Acad Sci U S A 1986; 83: 1140–1144.

Fox P, Raichle M, Mintun M, Dence C. Nonoxidative glucose consumption during focal physiologic neural activity. Science. 1988; 241: 4462–464.

Fransson P, Aden U, Blennow M, Lagercrantz H. The functional architecture of the infant brain as revealed by resting-state fMRI. Cereb. Cortex 2011; 21: 145–154.

Fransson P, Skiöld B, Horsch S, Nordell A, Blennow M, Lagercrantz H, et al. Resting-state networks in the infant brain. Proc. Natl. Acad. Sci. 2007; 104: 15531–6.

Friauf E, Shatz CJ. Changing patterns of synaptic input to subplate and cortical plate during development of visual cortex. J. Neurophysiol. 1991; 66: 2059–71.

Friedman A, Homma D, Gibb LG, Amemori K, Rubin SJ, Hood AS, et al. A corticostriatal path targeting striosomes controls decision-making under conflict. Cell 2015; 161: 1320–1333.

Friston KJ. Functional and effective connectivity in neuroimaging: A synthesis. Hum. Brain Mapp. 1994; 2: 56–78.

George JM, Fiori S, Fripp J, Pannek K, Bursle J, Moldrich RX, et al. Validation of an MRI brain injury and growth scoring system in very preterm infants scanned at 29- to 35-week postmenstrual age. Am. J. Neuroradiol. 2017; 38: 1435–1442.

Gerraty RT, Davidow JY, Foerde K, Galvan A, Bassett DS, Shohamy D. Dynamic flexibility in striatal-cortical circuits supports reinforcement learning. J. Neurosci. 2018: 2084–17.

Ghazi-Birry HS, Brown WR, Moody DM, Challa VR, Block SM, Reboussin DM. Human germinal matrix: venous origin of hemorrhage and vascular characteristics. AJNR. Am. J. Neuroradiol. 1997; 18: 219–229.

Gilbert CD, Kelly JP. The projections of cells in different layers of the cat's visual cortex. J. Comp. Neurol. 1975; 163: 81–105.

Gloor P. The temporal lobe and limbic system. Oxford University Press; 1997.

Goldman-Rakic PS, Porrino LJ. The primate mediodorsal (MD) nucleus and its projection to the frontal lobe. J. Comp. Neurol. 1985; 242: 535–60.

Goldman PS, Nauta WJ. An intricately patterned prefronto-caudate projection in the rhesus monkey. J. Comp. Neurol. 1977; 72: 369–86.

Goldman RI, Stern JM, Engel J, Cohen MS. Simultaneous EEG and fMRI of the alpha rhythm. Neuroreport 2002; 13: 2487–2492.

Goyen T-A, Lui K, Hummell J. Sensorimotor skills associated with motor dysfunction in children born extremely preterm. Early Hum. Dev. 2011; 87: 489–93.

Graybiel AM. Correspondence between the Dopamine islands and striosomes of the mammalian striatum. Neuroscience 1984; 13: 1157–1187.

Graybiel AM, Ragsdale CW. Histochemically distinct compartments in the striatum of human, monkeys, and cat demonstrated by acetylthiocholinesterase staining. Proc. Natl. Acad. Sci. 1978; 75: 5723–6.

Graybiel AM, Ragsdale CW. Clumping of acetylcholinesterase activity in the developing striatum of the human fetus and young infant. Neurobiology 1980; 77: 1214–1218.

Green D, Charman T, Pickles A, Chandler S, Loucas T, Simonoff E, et al. Impairment in movement skills of children with autistic spectrum disorders. Dev. Med. Child Neurol. 2009; 51: 311–6.

Greene DJ, Laumann TO, Dubis JW, Ihnen SK, Neta M, Power JD, et al. Developmental changes in the organization of functional connections between the basal ganglia and cerebral cortex. J. Neurosci. 2014; 34: 5842–5854.

Greicius MD, Srivastava G, Reiss AL, Menon V. Default-mode network activity distinguishes Alzheimer's disease from healthy aging: Evidence from functional MRI. Proc. Natl. Acad. Sci. 2004; 101: 4637–4642.

Greve DN, Fischl B. Accurate and robust brain image alignment using boundary-based registration. Neuroimage 2009; 48: 63–72.

Griffanti L, Douaud G, Bijsterbosch J, Evangelisti S, Alfaro-Almagro F, Glasser MF, et al. Hand classification of fMRI ICA noise components. Neuroimage 2017; 154: 188–205.

Griffanti L, Salimi-Khorshidi G, Beckmann CF, Auerbach EJ, Douaud G, Sexton CE, et al. ICA-based artefact removal and accelerated fMRI acquisition for improved resting state network imaging. Neuroimage 2014; 95: 232–47.

le Gros Clark WE. The termination of ascending tracts in the thalamus of the macaque monkey. J. Anat. 1936; 71: 7–40.

Grunau RE, Whitfield MF, Petrie-Thomas J, Synnes AR, Cepeda IL, Keidar A, et al. Neonatal pain, parenting stress and interaction, in relation to cognitive and motor development at 8 and 18 months in preterm infants. Pain 2009; 143: 138–146.

Grunewaldt KH, Fjørtoft T, Bjuland KJ, Brubakk A-M, Eikenes L, Håberg AK, et al. Follow-up at age 10years in ELBW children — Functional outcome, brain morphology and results from motor assessments in infancy. Early Hum. Dev. 2014; 90: 571–578.

Gui L, Loukas S, Lazeyras F, Hüppi PS, Meskaldji DE, Borradori Tolsa C. Longitudinal study of neonatal brain tissue volumes in preterm infants and their ability to predict neurodevelopmental outcome. Neuroimage 2018; 185: 728–741.

Guillery RW. Patterns of fiber degeneration in the dorsal lateral geniculate nucleus of the cat following lesions in the visual cortex. J. Comp. Neurol. 1967; 130: 197–221.

Guillery RW. Is postnatal neocortical maturation hierarchical? Trends Neurosci. 2005; 28: 512–517.

Guillery RW, Feig SL, Lozsádi DA. Paying attention to the thalamic reticular nucleus. Trends Neurosci. 1998; 21: 28–32.

Haber SN. The primate basal ganglia: Parallel and integrative networks. In: Journal of Chemical Neuroanatomy. 2003. p. 317–330.

Haber SN. The place of dopamine in the cortico-basal ganglia circuit. Neuroscience 2014; 282: 248–257.

Haber SN, Kim K-S, Mailly P, Calzavara R. Reward-related cortical inputs define a large striatal region in primates that interface with associative cortical connections, providing a substrate for incentive-based learning. J. Neurosci. 2006; 26: 8368–8376.

Haber SN, Knutson B. The reward circuit: linking primate anatomy and human imaging. Neuropsychopharmacology 2010; 35: 4–26.

Hack M, Taylor HG, Drotar D, Schluchter M, Cartar L, Wilson-Costello D, et al. Poor predictive validity of the bayley scales of infant development for cognitive function of extremely low birth weight children at school age. Pediatrics 2005; 116: 333–341.

Hale JR, Mayhew SD, Mullinger KJ, Wilson RS, Arvanitis TN, Francis ST, et al. Comparison of functional thalamic segmentation from seed-based analysis and ICA. Neuroimage 2015; 114: 448–465.

Hale JR, White TP, Mayhew SD, Wilson RS, Rollings DT, Khalsa S, et al. Altered thalamocortical and intra-thalamic functional connectivity during light sleep compared with wake. Neuroimage 2016; 125: 657–667.

Halliday HL. History of Surfactant from 1980. Neonatology 2005; 87: 317–322.

Han Y, Kebschull JM, Campbell RAA, Cowan D, Imhof F, Zador AM, et al. The logic of single-cell projections from visual cortex. Nature 2018; 556: 51–56.

Hart A, Whitby E, Wilkinson S, Alladi S, Paley M, Smith M. Neuro-developmental outcome at 18 months in premature infants with diffuse excessive high signal intensity on MR imaging of the brain. Pediatr. Radiol. 2011; 41: 1284–1292.

Hart AR, Smith MF, Whitby EH, Alladi S, Wilkinson S, Paley MN, et al. Diffusion-weighted imaging and magnetic resonance proton spectroscopy following preterm birth. Clin. Radiol. 2014; 69: 870–879.

Hashimoto-Torii K, Motoyama J, Hui C-C, Kuroiwa A, Nakafuku M, Shimamura K. differential activities of sonic hedgehog mediated by gli transcription factors define distinct neuronal subtypes in the dorsal thalamus. Mech. Dev. 2003; 120: 1097–111.

He L, Parikh NA. Atlas-guided quantification of white matter signal abnormalities on term-equivalent age MRI in very preterm infants: findings predict language and cognitive development at two years of age. PLoS One 2013; 8: e85475.

Heckemann R, Hajnal J, Aljabar P. Automatic anatomical brain MRI segmentation combining label propagation and decision fusion. Neuroimage 2006; 33(1): 115-126.

Hedden T, Gabrieli JDE. Shared and selective neural correlates of inhibition, facilitation, and shifting processes during executive control. Neuroimage 2010; 51: 421–431.

Heimer L, Kalil R. Rapid transneuronal degeneration and death of cortical neurons following removal of the olfactory bulb in adult rats. J. Comp. Neurol. 1978; 178: 559–609.

Heimer L, Wilson R. The subcortical projections of the allocortex. Similarities in the neural associations of the hippocampus, the piriform cortex and the neocortex. In: Santini M, editor(s). Golgi Centennial Symposium : perspectives in neurobiology. New York: New York, Raven Press; 1975. p. 668.

Herzmann CS, Snyder AZ, Kenley JK, Rogers CE, Shimony JS, Smyser CD. Cerebellar Functional Connectivity in Term- and Very Preterm-Born Infants. Cereb. Cortex 2018; 29(3); 1174-1184.

van den Heuvel MP, Kersbergen KJ, de Reus MA, Keunen K, Kahn RS, Groenendaal F, et al. The neonatal connectome during preterm brain development. Cereb. Cortex 2014; 25: 1–14.

Hintz SR, Barnes PD, Bulas D, Slovis TL, Finer NN, Wrage LA, et al. Neuroimaging and neurodevelopmental outcome in extremely preterm infants. Pediatrics 2015; 135: e32–e42.

Hirai T, Jones EG. A new parcellation of the human thalamus on the basis of histochemical staining. Brain Res. Rev. 1989; 14: 1–34.

Honey CJ, Sporns O, Cammoun L, Gigandet X, Thiran JP, Meuli R, et al. Predicting human resting-state functional connectivity from structural connectivity. Proc. Natl. Acad. Sci. 2009; 106: 2035–2040.

Van Horn SC, Sherman SM. Differences in projection patterns between large and small corticothalamic terminals. J. Comp. Neurol. 2004; 475: 406–415.

Hubel DH, Wiesel TN. Receptive fields, binocular interaction and functional architecture in the cat's visual cortex. J. Physiol. 1962; 160: 106–54.

Hubel DH, Wiesel TN. Effects of varying stimulus size and color on single lateral geniculate cells in Rhesus monkeys. Proc. Natl. Acad. Sci. 1966; 55: 1345–6.

Huettel SA, Song AW, McCarthy G. Functional magnetic resonance imaging. 3rd Edition. Sinauer Associates; 2014.

Hughes EJ, Bond J, Svrckova P, Makropoulos A, Ball G, Sharp DJ, et al. Regional changes in thalamic shape and volume with increasing age. Neuroimage 2012; 63: 1134–1142.

Hughes EJ, Winchman T, Padormo F, Teixeira R, Wurie J, Sharma M, et al. A dedicated neonatal brain imaging system. Magn. Reson. Med. 2017; 78: 794–804.

Hutchinson EA, De Luca CR, Doyle LW, Roberts G, Anderson PJ, Victorian Infant Collaborative Study Group, et al. School-age outcomes of extremely preterm or extremely low birth weight children. Pediatrics 2013; 131: e1053-61.

Hutchison RM, Womelsdorf T, Gati JS, Everling S, Menon RS. Resting-state networks show dynamic functional connectivity in awake humans and anesthetized macaques. Hum. Brain Mapp. 2013; 34: 2154–77.

Hwang K, Bertolero MA, Liu WB, D'Esposito M. The human thalamus is an integrative hub for functional brain networks. J. Neurosci. 2017; 37: 5594–5607.

Iadecola C. Neurogenic control of the cerebral microcirculation: is dopamine minding the store? Nat. Neurosci. 1998; 1: 263–265.

Ilinsky IA, Jouandet ML, Goldman-Rakic PS. Organization of the nigrothalamocortical system in the rhesus monkey. J. Comp. Neurol. 1985; 236: 315–30.

Ilinsky IA, Kultas-Ilinsky K. Sagittal cytoarchitectonic maps of theMacaca mulatta thalamus with a revised nomenclature of the motor-related nuclei validated by observations on their connectivity. J. Comp. Neurol. 1987; 262: 331–364.

Inder TE, Warfield SK, Wang H, Hüppi PS, Volpe JJ. Abnormal cerebral structure is present at term in premature infants. Pediatrics 2005; 115: 286–94.

Insausti R, Amaral DG, Cowan WM. The entorhinal cortex of the monkey: III. Subcortical afferents. J. Comp. Neurol. 1987; 264: 396–408.

Irle E, Markowitsch HJ. Connections of the hippocampal formation, mamillary bodies, anterior thalamus and cingulate cortex. A retrograde study using horseradish peroxidase in the cat. Exp. brain Res. 1982; 47: 79–94.

Jaekel J, Wolke D, Bartmann P. Poor attention rather than hyperactivity/impulsivity predicts academic achievement in very preterm and full-term adolescents. Psychol. Med. 2013; 43: 183–96.

Janvier A, Farlow B, Baardsnes J, Pearce R, Barrington KJ. Measuring and communicating meaningful outcomes in neonatology: A family perspective. Semin. Perinatol. 2016; 40: 571–577.

Jenkinson M, Bannister P, Brady M, Smith S. Improved Optimization for the Robust and Accurate Linear Registration and Motion Correction of Brain Images. Neuroimage 2002; 17: 825–841.

Jenkinson M, Beckmann CF, Behrens TEJ, Woolrich MW, Smith SM. FSL. Neuroimage 2012; 62: 782–790.

Jenkinson M, Chappell M. Introduction to neuroimaging analysis. Oxford University Press; 2018.

Jenkinson M, Smith S. A global optimisation method for robust affine registration of brain images. Med. Image Anal. 2001; 5: 143–156.

Jezzard P, Matthews PM, Smith SM. Functional MRI : an introduction to methods. Oxford University Press; 2001.

Johansen-Berg H, Behrens TEJ, Sillery E, Ciccarelli O, Thompson AJ, Smith SM, et al. Functional–anatomical validation and individual variation of diffusion tractography-based segmentation of the human thalamus. Cereb. Cortex 2005; 15: 31–39.

Johnson MH. Autism as an adaptive common variant pathway for human brain development. Dev. Cogn. Neurosci. 2017; 25: 5–11.

Johnson S, Evans TA, Draper ES, Field DJ, Manktelow BN, Marlow N, et al. Neurodevelopmental outcomes following late and moderate prematurity: a population-based cohort study. Arch. Dis. Child. - Fetal Neonatal Ed. 2015; 100: F301–F308.

Johnson S, Marlow N. Early and long-term outcome of infants born extremely preterm. Arch. Dis. Child. 2017; 102: 97–102.

Jones EG. Thalamic organization and function after Cajal. Prog. Brain Res. 2002; 136: 333–57.

Jones EG. The Thalamus. 2nd Edition. Cambridge University Press; 2007.

Jones EG, Coulter JD, Burton H, Porter R. Cells of origin and terminal distrubution of corticostriatal fibers arising in the sensory-motor cortex of monkeys. J. Comp. Neurol. 1977; 173: 53–80.

Jones EG, Coulter JD, Hendry SHC. Intracortical connectivity of architectonic fields in the somatic sensory, motor and parietal cortex of monkeys. J. Comp. Neurol. 1978; 181: 291–347.

Jürgens U. Afferent fibers to the cingular vocalization region in the squirrel monkey. Exp. Neurol. 1983; 80: 395–409.

Kaas JH. The thalamus revisited: where do we go from here? Brain 2007; 130: 2470–2473.

Kaas JH, Lyon DC. Pulvinar contributions to the dorsal and ventral streams of visual processing in primates. Brain Res. Rev. 2007; 55: 285–296.

Kalpakidou AK, Allin MPG, Walshe M, Giampietro V, McGuire PK, Rifkin L, et al. Functional neuroanatomy of executive function after neonatal brain injury in adults who were born very preterm. PLoS One 2014; 9: e113975.

Kanold PO, Kara P, Reid RC, Shatz CJ. Role of subplate neurons in functional maturation of visual cortical columns. Science 2003; 301: 521–5.

Kanold PO, Shatz CJ. Subplate neurons regulate maturation of cortical inhibition and outcome of ocular dominance plasticity. Neuron 2006; 51: 627–638.

Karolis VR, Froudist-Walsh S, Kroll J, Brittain PJ, Tseng C-EJEJ, Nam K-WW, et al. Volumetric grey matter alterations in adolescents and adults born very preterm suggest accelerated brain maturation. Neuroimage 2017; 163: 379–389.

Kasdon DL, Jacobson S. The thalamic afferents to the inferior parietal lobule of the rhesus monkey. J. Comp. Neurol. 1978; 177: 685–706.

Kaukola T, Perhomaa M, et al. Apparent diffusion coefficient on magnetic resonance imaging in pons and in corona radiata and relation with the neurophysiologic measurement and the outcome in very preterm infants. Neonatology 2010; 97: 15–21.

Kawagoe R, Takikawa Y, Hikosaka O. Expectation of reward modulates cognitive signals in the basal ganglia. Nat. Neurosci. 1998; 1: 411–416.

Kendall GS, Melbourne A, Johnson S, Price D, Bainbridge A, Gunny R, et al. White matter NAA/Cho and Cho/Cr ratios at MR spectroscopy are predictive of motor outcome in preterm infants. Radiology 2014; 271: 230–238.

Kennedy C, Des Rosiers MH, Jehle JW, Reivich M, Sharpe F, Sokoloff L. Mapping of functional neural pathways by autoradiographic survey of local metabolic rate with (14C)deoxyglucose. Science 1975; 187: 850–3.

Kersbergen KJ, Leroy F, Išgum I, Groenendaal F, de Vries LS, Claessens NHP, et al. Relation between clinical risk factors, early cortical changes, and neurodevelopmental outcome in preterm infants. Neuroimage 2016; 142: 301–310.

Keunen K, Išgum I, van Kooij BJMM, Anbeek P, van Haastert IC, Koopman-Esseboom C, et al. Brain volumes at term-equivalent age in preterm infants: imaging biomarkers for neurodevelopmental outcome through early school age. J. Pediatr. 2016; 172: 88–95.

Kidokoro H, Anderson PJ, Doyle LW, Woodward LJ, Neil JJ, Inder TE. Brain injury and altered brain growth in preterm infants: predictors and prognosis. Pediatrics 2014; 134: e444-453.

Kidokoro H, Neil JJ, Inder TE. New MR imaging assessment tool to define brain abnormalities in very preterm infants at term. AJNR. Am. J. Neuroradiol. 2013; 34: 2208–14.

Kiecker C, Lumsden A. Hedgehog signaling from the ZLI regulates diencephalic regional identity. Nat. Neurosci. 2004; 7: 1242–1249.

Kievit J, Kuypers HG. Organization of the thalamo-cortical connexions to the frontal lobe in the rhesus monkey. Exp. brain Res. 1977; 29: 299–322.

Kim D-J, Park B, Park H-J. Functional connectivity-based identification of subdivisions of the basal ganglia and thalamus using multilevel independent component analysis of resting state fMRI. Hum. Brain Mapp. 2013; 34: 1371–1385.

Kimura M. Behaviorally contingent property of movement-related activity of the primate putamen. J. Neurophysiol. 1990; 63: 1277–1296.

Van Kooij BJM, Benders MJNL, Anbeek P, Van Haastert IC, De Vries LS, Groenendaal F. Cerebellar volume and proton magnetic resonance spectroscopy at term, and neurodevelopment at 2years of age in preterm infants. Dev. Med. Child Neurol. 2012; 54: 260–266.

van Kooij BJM, de Vries LS, Ball G, van Haastert IC, Benders MJNL, Groenendaal F, et al. Neonatal tract-based spatial statistics findings and outcome in preterm infants. AJNR. Am. J. Neuroradiol. 2012; 33: 188–194.

Kostovic I, Judaš M. Prolonged coexistence of transient and permanent circuitry elements in the developing cerebral cortex of fetuses and preterm infants. Dev. Med. Child Neurol. 2006; 48: 388.

Kostović I, Judaš M, Judas M. The development of the subplate and thalamocortical connections in the human foetal brain. Acta Paediatr. 2010; 99: 1119–1127.

Kostović I, Judaš M, Sedmak G. Developmental history of the subplate zone, subplate neurons and interstitial white matter neurons: relevance for schizophrenia. Int. J. Dev. Neurosci. 2011; 29: 193–205.

Kostovic I, Rakic P. Cytology and time of origin of interstitial neurons in the white matter in infant and adult human and monkey telencephalon. J. Neurocytol. 1980; 9: 219–42.

Kostovic I, Rakic P. Developmental history of the transient subplate zone in the visual and somatosensory cortex of the macaque monkey and human brain. J. Comp. Neurol. 1990; 297: 441–470.

Kozorovitskiy Y, Saunders A, Johnson CA, Lowell BB, Sabatini BL. Recurrent network activity drives striatal synaptogenesis. Nature 2012; 485: 646–650.

Krauth A, Blanc R, Poveda A, Jeanmonod D, Morel A, Székely G. A mean three-dimensional atlas of the human thalamus: generation from multiple histological data. Neuroimage 2010; 49: 2053–2062.

Krishnan ML, Dyet LE, Boardman JP, Kapellou O, Allsop JM, Cowan F, et al. Relationship between white matter apparent diffusion coefficients in preterm infants at term-equivalent age and developmental outcome at 2 years. Pediatrics 2007; 120: e604-9.

Kuklisova-Murgasova M, Aljabar P, Srinivasan L, Counsell SJ, Doria V, Serag A, et al. A dynamic 4D probabilistic atlas of the developing brain. Neuroimage 2011; 54: 2750–2763.

Kultas-Ilinsky K, Fallet C, Verney C. Development of the human motor-related thalamic nuclei during the first half of gestation, with special emphasis on GABAergic circuits. J. Comp. Neurol. 2004; 476: 267–289.

Kultas-Ilinsky K, Sivan-Loukianova E, Ilinsky IA. Reevaluation of the primary motor cortex connections with the thalamus in primates. J. Comp. Neurol. 2003; 457: 133–58.

Kumar VJ, Mang S, Grodd W. Direct diffusion-based parcellation of the human thalamus. Brain Structure and Function 2015; 220(3): 1619-35.

Kumar VJ, van Oort E, Scheffler K, Beckmann CF, Grodd W. Functional anatomy of the human thalamus at rest. Neuroimage 2017; 147: 678–691.

Kunimatsu J, Maeda K, Hikosaka O. The caudal part of putamen represents the historical object value information. J. Neurosci. 2018; 39: 2534–18.

Künzle H. Bilateral projections from precentral motor cortex to the putamen and other parts of the basal ganglia. An autoradiographic study inMacaca fascicularis. Brain Res. 1975; 88: 195–209.

Künzle H. Projections from the primary somatosensory cortex to basal ganglia and thalamus in the monkey. Exp. brain Res. 1977; 30: 481–92.

Künzle H. An Autoradiographic Analysis of the efferent connections from premotor and adjacent prefrontal regions (areas 6 and 9) in macaca fascicularis. Brain. Behav. Evol. 1978; 15: 185–209.

Künzle H, Akert K. Efferent connections of cortical, area 8 (frontal eye field) in Macaca fascicularis. A reinvestigation using the autoradiographic technique. J. Comp. Neurol. 1977; 173: 147–64.

Kuo J-S, Carpenter MB. Organization of pallidothalamic projections in the rhesus monkey. J. Comp. Neurol. 1973; 151: 201–235.

Kuramoto E, Furuta T, Nakamura KC, Unzai T, Hioki H, Kaneko T. Two types of thalamocortical projections from the motor thalamic nuclei of the rat: a single neuron-tracing study using viral vectors. Cereb. Cortex 2009; 19: 2065–2077.

Kwong K, Belliveau J, Chesler D, Goldberg I, Weisskoff R, Poncelet B, et al. Dynamic magnetic resonance imaging of human brain activity during primary sensory stimulation. Proc Natl Acad Sci 1992; 89: 5675–5679.

De La Mothe LA, Blumell S, Kajikawa Y, Hackett TA. Thalamic connections of the auditory cortex in marmoset monkeys: Core and medial belt regions. J. Comp. Neurol. 2006; 496: 72–96.

Larroque B, Ancel P-YY, Marret S, Marchand L, André M, Arnaud C, et al. Neurodevelopmental disabilities and special care of 5-year-old children born before 33 weeks of gestation (the EPIPAGE study): a longitudinal cohort study. Lancet 2008; 371: 813–820.

Larson-Prior LJ, Zempel JM, Nolan TS, Prior FW, Snyder AZ, Raichle ME. Cortical network functional connectivity in the descent to sleep. Proc. Natl. Acad. Sci. 2009; 106: 4489–4494.

Lauterbur P. Image formation by induced local interactions: examples employing nuclear magnetic resonance. Nature1973; 242:190-191.

Lax ID, Duerden EG, Lin SY, Mallar Chakravarty M, Donner EJ, Lerch JP, et al. Neuroanatomical consequences of very preterm birth in middle childhood. Brain Struct. Funct. 2013; 218: 575–85.

Lee W, Morgan BR, Shroff MM, Sled JG, Taylor MJ. The development of regional functional connectivity in preterm infants into early childhood. Neuroradiology 2013; 55 Suppl 2: 105–111.

Lehéricy S, Ducros M, Van De Moortele P-FF, Francois C, Thivard L, Poupon C, et al. Diffusion tensor fiber tracking shows distinct corticostriatal circuits in humans: DTI Corticostriatal Fibers. Ann. Neurol. 2004; 55: 522–529.

Leitner Y, Weinstein M, Myers V, Uliel S, Geva K, Berger I, et al. Diffuse excessive high signal intensity in low-risk preterm infants at term-equivalent age does not predict outcome at 1 year: a prospective study. Neuroradiology 2014; 56: 669–678.

Lemmon ME, Ubel PA, Janvier A. Opinion. Estimating neurologic prognosis in children. High stakes, poor data. JAMA Neurol. 2019: E1–E2.

Leonzino M, Busnelli M, Antonucci F, Verderio C, Mazzanti M, Chini B. The Timing of the excitatory-to-inhibitory gaba switch is regulated by the oxytocin receptor via kcc2. Cell Rep. 2016; 15: 96–103.

Letinić K, Kostović I. Transient fetal structure, the gangliothalamic body, connects telencephalic germinal zone with all thalamic regions in the developing human brain. J. Comp. Neurol. 1997; 384: 373–95.

Levine MS, Fisher RS, Hull CD, Buchwald NA. Postnatal development of identified medium-sized caudate spiny neurons in the cat. Brain Res. 1986; 389: 47–62.

Li H, Fertuzinhos S, Mohns E, Hnasko TS, Verhage M, Edwards R, et al. Laminar and columnar development of barrel cortex relies on thalamocortical neurotransmission. Neuron 2013; 79: 970–86.

Liégeois R, Laumann TO, Snyder AZ, Zhou J, Yeo BTT. Interpreting temporal fluctuations in resting-state functional connectivity MRI. Neuroimage 2017; 163: 437–455.

Lind A, Parkkola R, Lehtonen L, Munck P, Maunu J, Lapinleimu H, et al. Associations between regional brain volumes at term-equivalent age and development at 2 years of age in preterm children. Pediatr. Radiol. 2011; 41: 953–961.

Linsell L, Johnson S, Wolke D, O'Reilly H, Morris JK, Kurinczuk JJ, et al. Cognitive trajectories from infancy to early adulthood following birth before 26 weeks of gestation: a prospective, population-based cohort study. Arch. Dis. Child. 2018; 103: 363–370.

Liu L, Johnson HL, Cousens S, Perin J, Scott S, Lawn JE, et al. Global, regional, and national causes of child mortality: an updated systematic analysis for 2010 with time trends since 2000. Lancet 2012; 379: 2151–2161.

Llano DA, Sherman SM. Evidence for nonreciprocal organization of the mouse auditory thalamocortical-corticothalamic projection systems. J. Comp. Neurol. 2008; 507: 1209–1227.

Lloyd M, MacDonald M, Lord C. Motor skills of toddlers with autism spectrum disorders. Autism 2013; 17: 133–46.

Logothetis NK. The underpinnings of the BOLD functional magnetic resonance imaging signal. J. Neurosci. 2003; 23: 3963–3971.

Loh WY, Anderson PJ, Cheong JLY, Spittle AJ, Chen J, Lee KJ, et al. Neonatal basal ganglia and thalamic volumes: very preterm birth and 7-year neurodevelopmental outcomes. Pediatr. Res. 2017; 82: 970–978.

López-Bendito G, Molnár Z. Thalamocortical development: how are we going to get there? Nat. Rev. Neurosci. 2003; 4: 276–289.

Lowe MJ, Phillips MD, Lurito JT, Mattson D, Dzemidzic M, Mathews VP. Multiple sclerosis: low-frequency temporal blood oxygen level-dependent fluctuations indicate reduced functional connectivity initial results. Radiology 2002; 224: 184–92.

Luttikhuizen dos Santos ES, de Kieviet JF, Königs M, van Elburg RM, Oosterlaan J. Predictive value of the Bayley scales of infant development on development of very preterm/very low birth weight children: a meta-analysis. Early Hum. Dev. 2013; 89: 487–96.

Macpherson J, Wiesendanger M, Marangoz C, Miles TS. Corticospinal neurones of the supplementary motor area of monkeys. A single unit study. Exp. brain Res. 1982; 48: 81–8.

Mai JK, Krajewski S, Reifenberger G, Genderski B, Lensing-Höhn S, Ashwell KW. Spatiotemporal expression gradients of the carbohydrate antigen (CD15) (Lewis X) during development of the human basal ganglia. Neuroscience 1999; 88: 847–58.

Mai JK, Paxinos G. The human nervous system. Elsevier Academic Press; 2012.

Mai JK, Schönlau C. Age-related expression patterns of the CD15 epitope in the human lateral geniculate nucleus (LGN). Histochem. J. 1992; 24: 878–89.

Mai JK and Majtanki M. Toward a common terminology for the thalamus. Frontiers in Neuroanatomy 2019, January 11.

Makropoulos A, Gousias IS, Ledig C, Aljabar P, Serag A, Hajnal J V, et al. Automatic whole brain mri segmentation of the developing neonatal brain. IEEE Trans. Med. Imaging 2014; 33: 1818–1831.

Malik S, Vinukonda G, Vose LR, Diamond D, Bhimavarapu BBR, Hu F, et al. Neurogenesis continues in the third trimester of pregnancy and is suppressed by premature birth. J. Neurosci. 2013; 33: 411–423.

Manent J-B, Represa A. neurotransmitters and brain maturation: early paracrine actions of gaba and glutamate modulate neuronal migration. Neurosci. 2007; 13: 268–279.

Mansfield P. Multi-planar image formation using NMR spin echoes. J. Phys. C Solid State Phys. 1977; 10: L55–L58.

Mansfield P, Maudsley AA. Medical imaging by NMR. Br. J. Radiol. 1977; 50: 188–194.

Månsson J, Stjernqvist K, Bäckström M. Behavioral outcomes at corrected age 2.5 years in children born extremely preterm. J. Dev. Behav. Pediatr. 2014; 35: 435–42.

Marlow N. Neurocognitive outcome after very preterm birth. Arch. Dis. Child. Fetal Neonatal Ed. 2004; 89: F224-8.

Marret S, Marchand-Martin L, Picaud J-C, Hascoët J-M, Arnaud C, Rozé J-C, et al. Brain injury in very preterm children and neurosensory and cognitive disabilities during childhood: the EPIPAGE cohort study. PLoS One 2013; 8: e62683.

Martin JA, Kung H-C, Mathews TJ, Hoyert DL, Strobino DM, Guyer B, et al. Annual Summary of Vital Statistics: 2006. Pediatrics 2008; 121: 788–801.

Di Martino A, Kelly C, Grzadzinski R, Zuo X-NN, Mennes M, Mairena MA, et al. Aberrant striatal functional connectivity in children with autism. Biol. Psychiatry 2011; 69: 847–56.

Di Martino A, Scheres A, Margulies DS, Kelly AMC, Uddin LQ, Shehzad Z, et al. Functional connectivity of human striatum: a resting state FMRI study. Cereb. Cortex 2008; 18: 2735–2747.

Massimini M, Ferrarelli F, Huber R, Esser SK, Singh H, Tononi G. Breakdown of cortical effective connectivity during sleep. Science 2005; 309: 2228–32.

Mathiasen R, Hansen BM, Andersen A-MNN, Forman JL, Greisen G. Gestational age and basic school achievements: A National Follow-up Study in Denmark. Pediatrics 2010; 126: e1553–e1561.

Matsuda W, Sonomura T, Honma S, Ohno S, Goto T, Hirai S, et al. Anatomical variations of the recurrent artery of Heubner: number, origin, and course. Anat. Sci. Int. 2018; 93(3) 317-322.

Mavridis I, Anagnostopoulou S. Comment on the brain areas whose blood supply is provided by the recurrent artery of Heubner. Surg. Radiol. Anat. 2010; 32: 91–91.

McClendon E, Chen K, Gong X, Sharifnia E, Hagen M, Cai V, et al. Prenatal cerebral ischemia triggers dysmaturation of caudate projection neurons. Ann. Neurol. 2014; 75: 508–24.

McFarland NR, Haber SN. convergent inputs from thalamic motor nuclei and frontal cortical areas to the dorsal striatum in the primate. J. Neurosci. 2000; 20: 3798–3813.

McFarland NR, Haber SN. Organization of thalamostriatal terminals from the ventral motor nuclei in the macaque. J. Comp. Neurol. 2001; 429: 321–36.

McFarland NR, Haber SN. Thalamic relay nuclei of the basal ganglia form both reciprocal and nonreciprocal cortical connections, linking multiple frontal cortical areas. J. Neurosci. 2002; 22: 8117–8132.

McKeown MJ, Makeig S, Brown GG, Jung TP, Kindermann SS, Bell AJ, et al. Analysis of fMRI data by blind separation into independent spatial components. Hum. Brain Mapp. 1998; 6: 160–88.

Menon V, Uddin LQ. Saliency, switching, attention and control: a network model of insula function. Brain Struct. Funct. 2010; 214: 655–667.

Mercuro G, Bassareo PP, Flore G, Fanos V, Dentamaro I, Scicchitano P, et al. Prematurity and low weight at birth as new conditions predisposing to an increased cardiovascular risk. Eur. J. Prev. Cardiol. 2013; 20: 357–367.

Merzenich MM, Reid MD. Representation of the cochlea within the inferior colliculus of the cat. Brain Res. 1974; 77: 397–415.

Middleton FA, Strick PL. Basal-ganglia ‘projections’ to the prefrontal cortex of the primate. Cereb. Cortex 2002; 12: 926–935.

Mikol J, Menini M, Brion S, Guicharnaud L. Connections of the laterodorsal nucleus of the thalamus in the monkey. Study of efferents. Rev Neurol 1984; 140: 615–24.

Miyachi S, Lu X, Imanishi M, Sawada K, Nambu A, Takada M. Somatotopically arranged inputs from putamen and subthalamic nucleus to primary motor cortex. Neurosci. Res. 2006; 56: 300–308.

Moeskops P, Išgum I, Keunen K, Claessens NHP, van Haastert IC, Groenendaal F, et al. Prediction of cognitive and motor outcome of preterm infants based on automatic quantitative descriptors from neonatal MR brain images. Sci. Rep. 2017; 7: 2163.

Monson BB, Eaton-Rosen Z, Kapur K, Liebenthal E, Brownell A, Smyser CD, et al. Differential rates of perinatal maturation of human primary and nonprimary auditory cortex. Eneuro 2018; 5(1).

Moore T, Hennessy EM, Myles J, Johnson SJ, Draper ES, Costeloe KL, et al. Neurological and developmental outcome in extremely preterm children born in England in 1995 and 2006: the EPICure studies. BMJ 2012; 345: e7961.

Morel A, Liu J, Wannier T, Jeanmonod D, Rouiller EM. Divergence and convergence of thalamocortical projections to premotor and supplementary motor cortex: a multiple tracing study in the macaque monkey. Eur. J. Neurosci. 2005; 21: 1007–1029.

Morel A, Magnin M, Jeanmonod D. Multiarchitectonic and stereotactic atlas of the human thalamus. J. Comp. Neurol. 1997; 387: 588–630.

Moreno-Juan V, Filipchuk A, Antón-Bolaños N, Mezzera C, Gezelius H, Andrés B, et al. Prenatal thalamic waves regulate cortical area size prior to sensory processing. Nat. Commun. 2017; 8: 14172.

Morley C, Robertson B, Lachmann B, Nilsson R, Bangham A, Grossmann G, et al. Artificial surfactant and natural surfactant. Comparative study of the effects on premature rabbit lungs. Arch. Dis. Child. 1980; 55: 758–65.

Mostofsky SH, Powell SK, Simmonds DJ, Goldberg MC, Caffo B, Pekar JJ. Decreased connectivity and cerebellar activity in autism during motor task performance. Brain 2009; 132: 2413–25.

Mostofsky SH, Rimrodt SL, Schafer JGB, Boyce A, Goldberg MC, Pekar JJ, et al. atypical motor and sensory cortex activation in attention-deficit/hyperactivity disorder: a functional magnetic resonance imaging study of simple sequential finger tapping. Biol. Psychiatry 2006; 59: 48–56.

Muakkassa KF, Strick PL. Frontal lobe inputs to primate motor cortex: evidence for four somatotopically organized 'premotor' areas. Brain Res. 1979; 177: 176–82.

Mufson EJ, Mesulam MM. Thalamic connections of the insula in the rhesus monkey and comments on the paralimbic connectivity of the medial pulvinar nucleus. J. Comp. Neurol. 1984; 227: 109–120.

Murphy K, Birn RM, Bandettini PA. Resting-state fMRI confounds and cleanup. Neuroimage 2013; 80: 349–59.

Murray EA, Coulter JD. Organization of corticospinal neurons in the monkey. J. Comp. Neurol. 1981; 195: 339–65.

Mwaniki MK, Atieno M, Lawn JE, Newton CRJC. Long-term neurodevelopmental outcomes after intrauterine and neonatal insults: a systematic review. Lancet 2012; 379: 445–452.

Nagode DA, Meng X, Winkowski DE, Smith E, Khan-Tareen H, Kareddy V, et al. Abnormal development of the earliest cortical circuits in a mouse model of autism spectrum disorder. Cell Rep. 2017; 18: 1100–1108.

Nagy Z, Lagercrantz H, Hutton C. Effects of preterm birth on cortical thickness measured in adolescence. Cereb. Cortex 2011; 21: 300–306.

Nambu A, Takada M, Inase M, Tokuno H. Dual somatotopical representations in the primate subthalamic nucleus: evidence for ordered but reversed body-map transformations from the primary motor cortex and the supplementary motor area. J. Neurosci. 1996; 16: 2671–83.

Nambu A, Tokuno H, Takada M. Functional significance of the cortico–subthalamo–pallidal 'hyperdirect' pathway. Neurosci. Res. 2002; 43: 111–117.

Nauta HJW, Cole M. Efferent projections of the subthalamic nucleus: An autoradiographic study in monkey and cat. J. Comp. Neurol. 1978; 180: 1–16.

Nauta W, Mehler W. Projections of the lentiform nucleus in the monkey. Brain Res 1966; 1: 3–42.

Ngai AC, Ko KR, Morii S, Winn HR. Effect of sciatic nerve stimulation on pial arterioles in rats. Am. J. Physiol. 1988; 254: 133-9.

Nichols T, Hayasaka S. Controlling the familywise error rate in functional neuroimaging: a comparative review. Stat. Methods Med. Res. 2003; 12: 419–46.

Nichols TE, Holmes A. Nonparametric permutation tests for functional neuroimaging: a primer with examples. Hum. Brain Mapp. 2002: 15 1-25.

Nielsen JA, Zielinski BA, Ferguson MA, Lainhart JE, Anderson JS. An evaluation of the left-brain vs. right-brain hypothesis with resting state functional connectivity magnetic resonance imaging. PLoS One 2013; 8: e71275.

Niemann K, Mennicken VR, Jeanmonod D, Morel A. The Morel stereotactic atlas of the human thalamus: atlas-to-MR registration of internally consistent canonical model. Neuroimage 2000; 12: 601–616.

Nieuwenhuys R. The insular cortex. In: Progress in brain research. 2012. p. 123–163.

Nieuwenhuys R. The myeloarchitectonic studies on the human cerebral cortex of the Vogt-Vogt school, and their significance for the interpretation of functional neuroimaging data. Brain Struct. Funct. 2013; 218: 303–52.

Nissl F. Die kerne des thalamus beim kaninchen. Neurol. Zentralbl 1889

Nosarti C, Nam KW, Walshe M, Murray RM, Cuddy M, Rifkin L, et al. Preterm birth and structural brain alterations in early adulthood. NeuroImage Clin. 2014; 6: 180–191.

Nunes D, Ianus A, Shemesh N. Layer-specific connectivity revealed by diffusion-weighted functional MRI in the rat thalamocortical pathway. Neuroimage 2019; 184: 646–657.

O'Muircheartaigh J, Keller SS, Barker GJ, Richardson MP. White matter connectivity of the thalamus delineates the functional architecture of competing thalamocortical systems. Cereb. Cortex 2015; 25: 4477–4489.

O'Muircheartaigh J, Vollmar C, Traynor C, Barker GJ, Kumari V, Symms MR, et al. Clustering probabilistic tractograms using independent component analysis applied to the thalamus. Neuroimage 2011; 54: 2020–2032.

O'Reilly JX, Beckmann CF, Tomassini V, Ramnani N, Johansen-Berg H. Distinct and overlapping functional zones in the cerebellum defined by resting state functional connectivity. Cereb. Cortex 2010; 20: 953–65.

Ogawa S, Lee TM, Kay AR, Tank DW. Brain magnetic resonance imaging with contrast dependent on blood oxygenation. Proc. Natl. Acad. Sci. 1990a; 87: 9868–9872.

Ogawa S, Lee TM, Nayak AS, Glynn P. Oxygenation-sensitive contrast in magnetic resonance image of rodent brain at high magnetic fields. Magn. Reson. Med. 1990b; 14: 68–78.

Ogawa S, Tank D, Menon R, Ellermann J, Kim S-G, Merkle H, et al. Intrinsic signal changes accompanying sensory stimulation: functional brain mapping with magnetic resonance imaging. Proc Natl Acad Sci 1992; 89: 5951–5955.

Oldehinkel M, Beckmann CF, Franke B, Hartman CA, Hoekstra PJ, Oosterlaan J, et al. Functional connectivity in cortico-subcortical brain networks underlying reward processing in attention-deficit/hyperactivity disorder. NeuroImage Clin. 2016; 12: 796–805.

Olszewski J. In: The Thalamus of the Macaca Mulatta. S. Karger AG; 1952. p. 33–93.

Omidvarnia A, Fransson P, Metsäranta M, Vanhatalo S. functional bimodality in the brain networks of preterm and term human newborns. Cereb. Cortex 2014: 24(10) 2657-68.

Ongür D, Price JL. The organization of networks within the orbital and medial prefrontal cortex of rats, monkeys and humans. Cereb. Cortex 2000; 10: 206–19.

van Oort ESBB, Mennes M, Navarro Schröder T, Kumar VJ, Zaragoza Jimenez NI, Grodd W, et al. Functional parcellation using time courses of instantaneous connectivity. Neuroimage 2017: 1–10.

Padberg J, Krubitzer L. Thalamocortical connections of anterior and posterior parietal cortical areas in New World titi monkeys. J. Comp. Neurol. 2006; 497: 416–435.

Palisano R, Rosenbaum P, Walter S, Russell D, Wood E, Galuppi B. Development and reliability of a system to classify gross motor function in children with cerebral palsy. Dev. Med. Child Neurol. 1997; 39: 214–23.

Palmer C, Schmidt EM, McIntosh JS. Corticospinal and corticorubral projections from the supplementary motor area in the monkey. Brain Res. 1981; 209: 305–14.

Pandya DN, Yeterian EH. Architecture and connections of cortical association areas. In: Peters A, Jones EG, editor(s). Association and auditory cortices. Springer US; 1985. p. 3–61.

Papile LA, Burstein J, Burstein R, Koffler H. Incidence and evolution of subependymal and intraventricular hemorrhage: a study of infants with birth weights less than 1,500 gm. J. Pediatr. 1978; 92: 529–34.

Papini C, White TP, Montagna A, Brittain PJ, Froudist-Walsh S, Kroll J, et al. Altered resting-state functional connectivity in emotion-processing brain regions in adults who were born very preterm. Psychol. Med. 2016; 46: 3025–3039.

Parent A. Extrinsic connections of the basal ganglia. Trends Neurosci. 1990; 13: 254–8.

Parent A, Bouchard C, Smith Y. The striatopallidal and striatonigral projections: two distinct fiber systems in primate. Brain Res. 1984; 303: 385–90.

Parent A, Hazrati L-N. Functional anatomy of the basal ganglia. Brain Res. Rev. 1995; 20: 91–127.

Parent A, Mackey A, De Bellefeuille L. The subcortical afferents to caudate nucleus and putamen in primate: a fluorescence retrograde double labeling study. Neuroscience 1983; 10: 1137–50.

Parent M, Lévesque M, Parent A. Two types of projection neurons in the internal pallidum of primates: single-axon tracing and three-dimensional reconstruction. J. Comp. Neurol. 2001; 439: 162–75.

Parent M, Parent A. Single-axon tracing and three-dimensional reconstruction of centre médian-parafascicular thalamic neurons in primates. J. Comp.Neurol. 2005; 481(1) 127-144.

Parikh NA, He L, Bonfante-Mejia E, Hochhauser L, Wilder PE, Burson K, et al. Automatically quantified diffuse excessive high signal intensity on MRI predicts cognitive development in preterm infants. Pediatr. Neurol. 2013; 49: 424–430.

Park HW, Yoon H-KK, Han SB, Lee BS, Sung IY, Kim KS, et al. Brain MRI measurements at a term-equivalent age and their relationship to neurodevelopmental outcomes. Am. J. Neuroradiol. 2014; 35: 599–603.

Parvizi J, Van Hoesen GW, Buckwalter J, Damasio A. Neural connections of the posteromedial cortex in the macaque. Proc. Natl. Acad. Sci. 2006; 103: 1563–1568.

Pasupathy A, Miller EK. Different time courses of learning-related activity in the prefrontal cortex and striatum. Nature 2005; 433: 873–876.

Paul RA, Smyser CD, Rogers CE, English I, Wallendorf M, Alexopoulos D, et al. An allometric scaling relationship in the brain of preterm infants. Ann. Clin. Transl. Neurol. 2014; 1: 933–7.

Pauli WM, O'Reilly RC, Yarkoni T, Wager TD, O'Reilly RC, Yarkoni T, et al. Regional specialization within the human striatum for diverse psychological functions. Proc. Natl. Acad. Sci. 2016; 113: 1907–1912.

Pauling L, Coryell CD. The magnetic properties and structure of hemoglobin, oxyhemoglobin and carbonmonoxyhemoglobin. Proc. Natl. Acad. Sci. 1936; 22: 210–6.

Paus T. Primate anterior cingulate cortex: Where motor control, drive and cognition interface. Nat. Rev. Neurosci. 2001; 2: 417–424.

Peixoto RT, Wang W, Croney DM, Kozorovitskiy Y, Sabatini BL. Early hyperactivity and precocious maturation of corticostriatal circuits in Shank3B-/- mice. Nat. Neurosci. 2016; 19: 716–724.

Pennartz CMA, Berke JD, Graybiel AM, Ito R, Lansink CS, van der Meer M, et al. Corticostriatal interactions during learning, memory processing and decision making J. Neurosci. 2009; 29(41) 12831-12838.

Perani D, Saccuman MC, Scifo P, Anwander A, Spada D, Baldoli C, et al. Neural language networks at birth. Proc. Natl. Acad. Sci. 2011; 108: 16056–16061.

Percheron G, François C, Talbi B, Meder JF, Fenelon G, Yelnik J. The primate motor thalamus analysed with reference to subcortical afferent territories. Stereotact. Funct. Neurosurg. 1993; 60: 32–41.

Percheron G, François C, Talbi B, Yelnik J, Fénelon G. The primate motor thalamus. Brain Res. Brain Res. Rev. 1996; 22: 93–181.

Petersen SE, Robinson DL, Morris JD. Contributions of the pulvinar to visual spatial attention. Neuropsychologia 1987; 25: 97–105.

Peterson BS, Vohr B, Staib LH, Cannistraci CJ, Dolberg A, Schneider KC, et al. Regional brain volume abnormalities and long-term cognitive outcome in preterm infants. JAMA 2000; 284: 1939–47.

Pierson CR, Folkerth RD, Billiards SS, Trachtenberg FL, Drinkwater ME, Volpe JJ, et al. Gray matter injury associated with periventricular leukomalacia in the premature infant. Acta Neuropathol. 2007; 114: 619–31.

Pogribna U, Burson K, Lasky RE, Narayana PA, Evans PW, Parikh NA. Role of diffusion tensor imaging as an independent predictor of cognitive and language development in extremely low-birth-weight infants. Am. J. Neuroradiol. 2014; 35: 790–796.

Postuma RB, Dagher A. Basal ganglia functional connectivity based on a meta-analysis of 126 positron emission tomography and functional magnetic resonance imaging publications. Cereb. Cortex 2006; 16: 1508–1521.

Power JD, Cohen AL, Nelson SM, Wig GS, Barnes KA, Church JA, et al. Functional network organization of the human brain. Neuron 2011; 72: 665–78.

Power JD, Mitra A, Laumann TO, Snyder AZ, Schlaggar BL, Petersen SE. Methods to detect, characterize, and remove motion artifact in resting state fMRI. Neuroimage 2014; 84: 320–41.

Pribram K, Chow K, Semmes J. Limit and organization of the cortical projection from the medial thalamic nucleus in monkey. J Comp Neurol 1953; 98: 433–48.

Pritchard MA, de Dassel T, Beller E, Bogossian F, Johnston L, Paynter J, et al. Autism in toddlers born very preterm. Pediatrics 2016; 137: e20151949.

Purcell EM, Torrey HC, Pound R V. resonance absorption by nuclear magnetic moments in a solid. Phys. Rev. 1946; 69: 37–38.

Rabi II, Zacharias JR, Millman S, Kusch P. A new method of measuring nuclear magnetic moment. Phys. Rev. 1938; 53: 318–318.

Rakić P, Sidman RL. Telencephalic origin of pulvinar neurons in the fetal human brain. Z. Anat. Entwicklungsgesch. 1969; 129: 53–82.

Rangaprakash D, Wu G-R, Marinazzo D, Hu X, Deshpande G. Hemodynamic response function (HRF) variability confounds resting-state fMRI functional connectivity. Magn. Reson. Med. 2018: 1–17.

Ray JP, Price JL. The organization of the thalamocortical connections of the mediodorsal thalamic nucleus in the rat, related to the ventral forebrain-prefrontal cortex topography. J. Comp. Neurol. 1992; 323: 167–197.

Reiner A, Jiao Y, Del Mar N, Laverghetta AV, Lei WL. Differential morphology of pyramidal tract-type and intratelencephalically projecting-type corticostriatal neurons and their intrastriatal terminals in rats. J. Comp. Neurol. 2003; 457: 420–440.

Robertson RT. Efferents of the pretectal complex: separate populations of neurons project to lateral thalamus and to inferior olive. Brain Res. 1983; 258: 91–5.

Rogers CE, Smyser T, Smyser CD, Shimony J, Inder TE, Neil JJ. Regional white matter development in very preterm infants: perinatal predictors and early developmental outcomes. Pediatr. Res. 2016; 79: 87–95.

Romanski LM, Giguere M, Bates JF, Goldman-Rakic PS. Topographic organization of medial pulvinar connections with the prefrontal cortex in the rhesus monkey. J. Comp. Neurol. 1997; 379: 313–32.

Rose J, Cahill-Rowley K, Vassar R, Yeom KW, Stecher X, Stevenson DK, et al. Neonatal brain microstructure correlates of neurodevelopment and gait in preterm children 18–22 mo of age: an MRI and DTI study. Pediatr. Res. 2015; 78: 700–708.

Rose JE. The ontogenetic development of the rabbit's diencephalon. J. Comp. Neurol. 1942; 77: 61–129.

Rose JE, Mountcastle VB. The thalamic tactile region in rabbit and cat. J. Comp. Neurol. 1952; 97: 441–89.

Ross G, Lipper E, Auld PAM. Consistency and change in the development of premature infants weighing less than 1,501 grams at birth. Pediatrics 1985; 76(6).

Rouiller EM, Tanne J, Moret V, Boussaoud D. Origin of thalamic inputs to the primary, premotor, and supplementary motor cortical areas and to area 46 in macaque monkeys: a multiple retrograde tracing study. J. Comp. Neurol. 1999; 409: 131–52.

Rowitch DH, Kriegstein AR. Developmental genetics of vertebrate glial–cell specification. Nature 2010; 468: 214–222.

Rubinov M, Sporns O. Complex network measures of brain connectivity: uses and interpretations. Neuroimage 2010; 52: 1059–1069.

Russchen FT, Amaral DG, Price JL. The afferent input to the magnocellular division of the mediodorsal thalamic nucleus in the monkey,Macaca fascicularis. J. Comp. Neurol. 1987; 256: 175–210.

Sachs E. On the structure and functional relations of the optic thalamus. Brain 1909; 32: 95–186.

Sadikot AF, Parent A, Smith Y, Bolam JP. Efferent connections of the centromedian and parafascicular thalamic nuclei in the squirrel monkey: A light and electron microscopic study of the thalamostriatal projection in relation to striatal heterogeneity. J. Comp. Neurol. 1992; 320: 228–242.

Sadikot AF, Rymar V V. The primate centromedian–parafascicular complex: Anatomical organization with a note on neuromodulation. Brain Res. Bull. 2009; 78: 122–130.

Saigal S, Doyle LW. An overview of mortality and sequelae of preterm birth from infancy to adulthood. Lance 2008; 371: 261–269.

Salgado S, Kaplitt MG. The Nucleus Accumbens: A Comprehensive Review. Stereotact. Funct. Neurosurg. 2015; 93: 75–93.

Salimi-Khorshidi G, Douaud G, Beckmann CF, Glasser MF, Griffanti L, Smith SM. Automatic denoising of functional MRI data: combining independent component analysis and hierarchical fusion of classifiers. Neuroimage 2014; 90: 449–468.

Salvan P, Tournier JD, Batalle D, Falconer S, Chew A, Kennea N, et al. Language ability in preterm children is associated with arcuate fasciculi microstructure at term. Hum. Brain Mapp. 2017; 38: 3836–3847.

Samejima K, Ueda Y, Doya K, Kimura M. Representation of action-specific reward values in the striatum. Science 2005; 310: 1337–40.

Sanefuji M, Craig M, Parlatini V, Mehta MA, Murphy DG, Catani M, et al. Double-dissociation between the mechanism leading to impulsivity and inattention in Attention Deficit Hyperactivity Disorder: A resting-state functional connectivity study. Cortex 2017; 86: 290–302.

Saper CB, Scammell TE, Lu J. Hypothalamic regulation of sleep and circadian rhythms. Nature 2005; 437: 1257–1263.

Satterthwaite TD, Wolf DH, Loughead J, Ruparel K, Elliott MA, Hakonarson H, et al. Impact of in-scanner head motion on multiple measures of functional connectivity: Relevance for studies of neurodevelopment in youth. Neuroimage 2012; 60: 623–632.

Sauer FC. Mitosis in the neural tube. J. Comp. Neurol. 1935; 62: 377–405.

Scannell JW. Determining cortical landscapes. Nature 1997; 386: 452.

Scannell JW. The connectional organization of the cortico-thalamic system of the cat. Cereb. Cortex 1999; 9: 277–299.

Scannell JW, Blakemore C, Young MP. Analysis of connectivity in the cat cerebral cortex. J. Neurosci. 1995; 15: 1463–83.

Scannell JW, Burns G a. PC, Hilgetag CC, O'Neil MA, Young MP. The connectional organization of the cortico-thalamic system of the cat. Cereb. Cortex 1999; 9: 277–299.

Scheibel ME, Scheibel AB. Structural organization of nonspecific thalamic nuclei and their projection toward cortex. Brain Res. 1967; 6: 60–94.

Schell GR, Strick PL. The origin of thalamic inputs to the arcuate premotor and supplementary motor areas. J. Neurosci. 1984; 4: 539–60.

Seeley WW, Menon V, Schatzberg AF, Keller J, Glover GH, Kenna H, et al. Dissociable intrinsic connectivity networks for salience processing and executive control. J. Neurosci. 2007; 27: 2349–2356.

Selemon LD, Goldman-Rakic PS. Longitudinal topography and interdigitation of corticostriatal projections in the rhesus monkey. J. Neurosci. 1985; 5: 776–94.

Serag A, Aljabar P, Ball G, Counsell SJ, Boardman JP, Rutherford MA, et al. Construction of a consistent high-definition spatio-temporal atlas of the developing brain using adaptive kernel regression. Neuroimage 2012; 59: 2255–65.

Sherman SM, Guillery R. Functional connections of cortical areas: a new view from the thalamus. MIT Press; 2013.

Sherman SM, Guillery RW. The role of the thalamus in the flow of information to the cortex. Philos. Trans. R. Soc. Lond. B. Biol. Sci. 2002; 357: 1695–708.

Shibata H, Naito J. Organization of anterior cingulate and frontal cortical projections to the anterior and laterodorsal thalamic nuclei in the rat. Brain Res. 2005; 1059: 93–103.

Shigematsu N, Ueta Y, Mohamed AA, Hatada S, Fukuda T, Kubota Y, et al. Selective thalamic innervation of rat frontal cortical neurons. Cereb. Cortex 2016; 26: 2689–2704.

Sidman RL, Rakic P. Neuronal migration, with special reference to developing human brain: a review. Brain Res. 1973; 62: 1–35.

Siwek DF, Pandya DN. Prefrontal projections to the mediodorsal nucleus of the thalamus in the rhesus monkey. J. Comp. Neurol. 1991; 312: 509–24.

Skiöld B, Vollmer B, Böhm B, Hallberg B, Horsch S, Mosskin M, et al. Neonatal magnetic resonance imaging and outcome at age 30 months in extremely preterm infants. J. Pediatr. 2012; 160: 559-566.

Slater L, Asmerom Y, Boskovic DS, Bahjri K, Plank MS, Angeles KR, et al. Procedural pain and oxidative stress in premature neonates. J. Pain 2012; 13: 590–597.

Smith SM. Fast robust automated brain extraction. Hum. Brain Mapp. 2002; 17: 143–55.

Smith SM, Beckmann CF, Andersson J, Auerbach EJ, Bijsterbosch J, Douaud G, et al. Resting-state fMRI in the Human Connectome Project. Neuroimage 2013; 80: 144–168.

Smith SM, Fox PTM, Miller KL, Glahn DC, Fox PTM, Mackay CE, et al. Correspondence of the brain's functional architecture during activation and rest. Proc. Natl. Acad. Sci. 2009; 106: 13040–13045.

Smith SM, Miller KL, Moeller S, Xu J, Auerbach EJ, Woolrich MW, et al. Temporally-independent functional modes of spontaneous brain activity. Proc. Natl. Acad. Sci. 2012; 109: 3131–3136.

Smith SM, Miller KL, Salimi-Khorshidi G, Webster M, Beckmann CF, Nichols TE, et al. Network modelling methods for FMRI. Neuroimage 2011; 54: 875–891.

Smith SM, Nichols TE. Threshold-free cluster enhancement: addressing problems of smoothing, threshold dependence and localisation in cluster inference. Neuroimage 2009; 44: 83–98.

Smyser CD, Inder TE, Shimony JS, Hill JE, Degnan AJ, Snyder AZ, et al. Longitudinal analysis of neural network development in preterm infants. Cereb. Cortex 2010; 20: 2852–2862.

Smyser CD, Snyder AZ, Neil JJ. Functional connectivity MRI in infants: exploration of the functional organization of the developing brain. Neuroimage 2011; 56: 1437–1452.

Sokoloff L, Reivich M, Kennedy C, Des Rosiers MH, Patlak CS, Pettigrew KD, et al. The [14C]deoxyglucose method for the measurement of local cerebral glucose utilization: theory, procedure, and normal values in the conscious and anesthetized albino rat. J. Neurochem. 1977; 28: 897–916.

Spittle AJ, Cheong J, Doyle LW, Roberts G, Lee KJ, Lim J, et al. Neonatal white matter abnormality predicts childhood motor impairment in very preterm children. Dev. Med. Child Neurol. 2011; 53: 1000–6.

Spittle AJ, Lee KJ, Spencer-Smith M, Lorefice LE, Anderson PJ, Doyle LW. Accuracy of two motor assessments during the first year of life in preterm infants for predicting motor outcome at preschool age. PLoS One 2015; 10: e0125854.

Spittle AJ, Treyvaud K, Doyle LW, Roberts G, Lee KJ, Inder TE, et al. Early emergence of behavior and social-emotional problems in very preterm infants. J. Am. Acad. Child Adolesc. Psychiatry 2009; 48: 909–918.

Stevens MC, Pearlson GD, Calhoun VD, Bessette KL. Functional neuroimaging evidence for distinct neurobiological pathways in attention-deficit/hyperactivity disorder. Biol. Psychiatry Cogn. Neurosci. Neuroimaging 2018; 3(8) 675-685.

Strick PL. Anatomical analysis of ventrolateral thalamic input to primate motor cortex. J. Neurophysiol. 1976; 39: 1020–1031.

Swanson LW. Brain Maps: Structure of the Rat Brain. Elsevier, Amsterdam; 1992.
Szabo N-E, Zhao T, Zhou X, Alvarez-Bolado G. The role of sonic hedgehog of neural origin in thalamic differentiation in the mouse. J. Neurosci. 2009; 29: 2453–2466.

Takada M, Tokuno H, Nambu A, Inase M. Corticostriatal input zones from the supplementary motor area overlap those from the contra- rather than ipsilateral primary motor cortex. 1998; 791 (1-2) 335-340.

Tanaka YH, Tanaka YR, Kondo M, Terada S-I, Kawaguchi Y, Matsuzaki M. Thalamocortical axonal activity in motor cortex exhibits layer-specific dynamics during motor learning. Neuron 2018; 100: 244-258.e12.

Teitelbaum P, Teitelbaum O, Nye J, Fryman J, Maurer RG. Movement analysis in infancy may be useful for early diagnosis of autism. Proc. Natl. Acad. Sci. 1998; 95: 13982–7.

Tepper J, Sharpe N, Koós T, Neuroscience FT-D, 1998 U. Postnatal development of the rat neostriatum: electrophysiological, light-and electron-microscopic studies. karger.com 1998; 20: 125–145.

Thompson DK, Inder TE, Faggian N, Warfield SK, Anderson PJ, Doyle LW, et al. Corpus callosum alterations in very preterm infants: perinatal correlates and 2 year neurodevelopmental outcomes. Neuroimage 2012; 59: 3571–81.

Tich SNT, Anderson PJ, Hunt RW, Lee KJ, Doyle LW, Inder TE. Neurodevelopmental and perinatal correlates of simple brain metrics in very preterm infants. Arch. Pediatr. Adolesc. Med. 2011; 165: 216–22.

Tokariev A, Stjerna S, Palva JM, Vanhatalo S. Preterm birth changes networks of newborn cortical activity. Cereb. Cortex 2019;2 814-826.

Tortora D, Martinetti C, Severino M, Uccella S, Malova M, Parodi A, et al. The effects of mild germinal matrix-intraventricular haemorrhage on the developmental white matter microstructure of preterm neonates: a DTI study. Eur. Radiol. 2018; 28: 1157–1166.

Toulmin H, Beckmann CF, O'Muircheartaigh J, Ball G, Nongena P, Makropoulos A, et al. Specialization and integration of functional thalamocortical connectivity in the human infant. Proc. Natl. Acad. Sci. 2015; 112(20) 6485-6490.

Traynor C, Heckemann RA, Hammers A, O'Muircheartaigh J, Crum WR, Barker GJ, et al. Reproducibility of thalamic segmentation based on probabilistic tractography. Neuroimage 2010; 52: 69–85.

Treyvaud K, Ure A, Doyle LW, Lee KJ, Rogers CE, Kidokoro H, et al. Psychiatric outcomes at age seven for very preterm children: rates and predictors. J. Child Psychol. Psychiatry. 2013; 54: 772–9.

Tusor N, Benders MJ, Counsell SJ, Nongena P, Ederies MA, Falconer S, et al. Punctate White Matter Lesions Associated With Altered Brain Development And Adverse Motor Outcome In Preterm Infants. Sci. Rep. 2017; 7: 13250.

Tyzio R, Cossart R, Khalilov I, Minlebaev M, Hübner CA, Represa A, et al. Maternal oxytocin triggers a transient inhibitory switch in GABA signaling in the fetal brain during delivery. Science 2006; 314: 1788–92.

Tziortzi AC, Haber SN, Searle GE, Tsoumpas C, Long CJ, Shotbolt P, et al. Connectivity-based functional analysis of dopamine release in the striatum using diffusion-weighted mri and positron emission tomography. Cereb. Cortex 2014; 24: 1165–1177.

Ullman H, Spencer-Smith M, Thompson DK, Doyle LW, Inder TE, Anderson PJ, et al. Neonatal MRI is associated with future cognition and academic achievement in preterm children. Brain A J. Neurol. 2015; 138: 3251–3262.

Vaishnavi SN, Vlassenko AG, Rundle MM, Snyder AZ, Mintun MA, Raichle ME. Regional aerobic glycolysis in the human brain. Proc. Natl. Acad. Sci. 2010; 107: 17757–17762.

Valeeva G, Valiullina F, Khazipov R. Excitatory actions of GABA in the intact neonatal rodent hippocampus in vitro. Front. Cell. Neurosci. 2013; 7: 20.

Vanhatalo S, Kaila K. Development of neonatal EEG activity: from phenomenology to physiology. Semin. fetal neonatal Med. 2006; 11: 471–478.

Verstynen T, Jarbo K, Pathak S, Schneider W. In vivo mapping of microstructural somatotopies in the human corticospinal pathways. J. Neurophysiol. 2011; 105: 336–346.

Verstynen TD, Badre D, Jarbo K, Schneider W. Microstructural organizational patterns in the human corticostriatal system. J. Neurophysiol. 2012; 107: 2984–95.

Vértes PE, Alexander-Bloch AF, Gogtay N, Giedd JN, Rapoport JL, Bullmore ET. Simple models of human brain functional networks. Proc. Natl. Acad. Sci. 2012; 109: 5868–73.

Vieira C, Garda A-L, Shimamura K, Martinez S. Thalamic development induced by Shh in the chick embryo. Dev. Biol. 2005; 284: 351–363.

Vinall J, Miller SP, Synnes AR, Grunau RE. Parent behaviors moderate the relationship between neonatal pain and internalizing behaviors at 18 months corrected age in children born very prematurely. Pain 2013; 154: 1831–1839.

Vincent JL, Patel GH, Fox MD, Snyder AZ, Baker JT, Van Essen DC, et al. Intrinsic functional architecture in the anaesthetized monkey brain. Nature 2007; 447: 83–86.

Vogt C. The myeloarchitecture of the thalamus of the cercopithecus. J. fur Psychol. 1909.

Vogt BA, Hof PR, Friedman DP, Sikes RW, Vogt LJ. Norepinephrinergic afferents and cytology of the macaque monkey midline, mediodorsal, and intralaminar thalamic nuclei. Brain Struct. Funct. 2008; 212: 465–479.

Vogt BA, Pandya DN, Rosene DL. Cingulate cortex of the rhesus monkey: I. Cytoarchitecture and thalamic afferents. J. Comp. Neurol. 1987; 262: 256–270.

Vogt BA, Rosene DL, Pandya DN. Thalamic and cortical afferents differentiate anterior from posterior cingulate cortex in the monkey. Science 1979; 204: 205–7.

Vohr B. Long-term outcomes of moderately preterm, late preterm, and early term infants. Clin. Perinatol. 2013; 40: 739–751.

Volpe JJ. Brain injury in premature infants: a complex amalgam of destructive and developmental disturbances. Lancet Neurol. 2009; 8: 110–124.

Volpe JJ. Volpe's neurology of the newborn. 6th Edition. 2018.

de Vries LS, van Haastert IC, Benders MJNL, Groenendaal F. Myth: Cerebral palsy cannot be predicted by neonatal brain imaging. Semin. Fetal Neonatal Med. 2011; 16: 279–287.

de Vries LS, Van Haastert ILC, Rademaker KJ, Koopman C, Groenendaal F. Ultrasound abnormalities preceding cerebral palsy in high-risk preterm infants. J. Pediatr. 2004; 144: 815–820.

Walker AE. The medial thalamic nucleus. A comparative anatomical, physiological and clinical study of the nucleus medialis dorsalis thalami. J. Comp. Neurol. 1940; 73: 87–115.

Wang JX, Kurth-Nelson Z, Kumaran D, Tirumala D, Soyer H, Leibo JZ, et al. Prefrontal cortex as a meta-reinforcement learning system. Nat. Neurosci. 2018: 21; 860-868.

Van der Werf YD, Witter MP, Groenewegen HJ. The intralaminar and midline nuclei of the thalamus. Anatomical and functional evidence for participation in processes of arousal and awareness. Brain Res. Brain Res. Rev. 2002; 39: 107–40.

Wess JM, Isaiah A, Watkins P V., Kanold PO. Subplate neurons are the first cortical neurons to respond to sensory stimuli. Proc. Natl. Acad. Sci. 2017; 114: 12602–12607.

Westbrook C, Talbot J. MRI in practice. 5th Edition. Wiley and Sons; 2019.

Wheelock MD, Austin NC, Bora S, Eggebrecht AT, Melzer TR, Woodward LJ, et al. Altered functional network connectivity relates to motor development in children born very preterm. Neuroimage 2018; 183: 574–583.

Wiegell MR, Tuch DS, Larsson HBW, Wedeen VJ. Automatic segmentation of thalamic nuclei from diffusion tensor magnetic resonance imaging. Neuroimage 2003; 19: 391–401.

Wigglesworth JS. Artificial surfactant therapy for hyaline membrane disease. Arch. Dis. Child. 1980; 55: 753–4.

Williams J, Lee KJ, Anderson PJ. Prevalence of motor-skill impairment in preterm children who do not develop cerebral palsy: a systematic review. Dev. Med. Child Neurol. 2010; 52: 232–237.

Wilson-Costello D, Friedman H, Minich N, Fanaroff AA, Hack M. Improved survival rates with increased neurodevelopmental disability for extremely low birth weight infants in the 1990s. Pediatrics 2005; 115: 997–1003.

Wilson SA. Five Cases Exhibiting Involuntary Movements. Proc. R. Soc. Med. 1925; 18: 34.

Wolpert DM, Ghahramani Z. Computational principles of movement neuroscience. Nat. Neurosci. 2000; 3 Suppl: 1212–7.

Wolpert DM, Miall RC. Forward models for physiological motor control. Neural Netw. 1996; 9: 1265–1279.

Wonders CP, Anderson SA. The origin and specification of cortical interneurons. Nat. Rev. Neurosci. 2006; 7: 687–696.

Wood NS, Costeloe K, Gibson AT, Hennessy EM, Marlow N, Wilkinson AR, et al. The EPICure study: associations and antecedents of neurological and developmental disability at 30 months of age following extremely preterm birth. Arch. Dis. Child. - Fetal Neonatal Ed. 2005; 90: F134–F140.

Woodward LJ, Anderson PJ, Austin NC, Howard K, Inder TE. Neonatal mri to predict neurodevelopmental outcomes in preterm infants. New England Journal of Medicine 2006; 355: 685-694.

Woodward LJ, Edgin JO, Thompson D, Inder TE. Object working memory deficits predicted by early brain injury and development in the preterm infant. Brain 2005; 128: 2578–2587.

Woodward ND, Karbasforoushan H, Heckers S. Thalamocortical dysconnectivity in schizophrenia. Am. J. Psychiatry 2012; 169: 1092–1099.

Woolrich MW, Jbabdi S, Patenaude B, Chappell M, Makni S, Behrens T, et al. Bayesian analysis of neuroimaging data in FSL. Neuroimage 2009; 45: S173–S186.

Wright CI, Groenewegen HJ. Patterns of overlap and segregation between insular cortical, intermediodorsal thalamic and basal amygdaloid afferents in the nucleus accumbens of the rat. Neuroscience 1996; 73: 359–73.

Wylie KP, Kronberg E, Maharajh K, Smucny J, Cornier M-A, Tregellas JR. Between-network connectivity occurs in brain regions lacking layer IV input. Neuroimage 2015; 116: 50–58.

Xu G, Broadbelt KG, Haynes RL, Folkerth RD, Borenstein NS, Belliveau RA, et al. Late development of the GABAergic system in the human cerebral cortex and white matter. J. Neuropathol. Exp. Neurol. 2011; 70: 841–58.

Yamada J, Okabe A, Toyoda H, Kilb W, Luhmann HJ, Fukuda A. Cl ⁻ uptake promoting depolarizing GABA actions in immature rat neocortical neurones is mediated by NKCC1. J. Physiol. 2004; 557: 829–841.

Yeo BTT, Krienen FM, Chee MWL, Buckner RL. Estimates of segregation and overlap of functional connectivity networks in the human cerebral cortex. Neuroimage 2014; 88: 212–227.

Yeo BTT, Krienen FM, Sepulcre J, Sabuncu MR, Lashkari D, Hollinshead M, et al. The organization of the human cerebral cortex estimated by intrinsic functional connectivity. J. Neurophysiol. 2011; 106: 1125–65.

Yeterian EH, Van Hoesen GW. Cortico-striate projections in the rhesus monkey: the organization of certain cortico-caudate connections. Brain Res. 1978; 139: 43–63.

Yeterian EH, Pandya DN. Corticothalamic connections of the superior temporal sulcus in rhesus monkeys. Exp. brain Res. 1991; 83: 268–84.

Yetkin FZ, Hammeke TA, Swanson SJ, Morris GL, Mueller WM, McAuliffe TL, et al. A comparison of functional MR activation patterns during silent and audible language tasks. AJNR. Am. J. Neuroradiol. 1995; 16: 1087–92.

Young JM, Powell TL, Morgan BR, Card D, Lee W, Smith M Lou, et al. Deep grey matter growth predicts neurodevelopmental outcomes in very preterm children. Neuroimage 2015; 111: 360–368.

Ystad M, Hodneland E, Adolfsdottir S, Haász J, Lundervold AJ, Eichele T, et al. Cortico-striatal connectivity and cognition in normal aging: a combined DTI and resting state fMRI study. Neuroimage 2011; 55: 24–31.

Yuan R, Di X, Taylor PA, Gohel S, Tsai Y-H, Biswal BB. Functional topography of the thalamocortical system in human. Brain Struct. Funct. 2016; 221: 1971–84.

Zhang D, Snyder AZ, Fox MD, Sansbury MW, Shimony JS, Raichle ME. Intrinsic functional relations between human cerebral cortex and thalamus. J. Neurophysiol. 2008; 100: 1740–1748.

Zhang S, Li C-SR. Functional Connectivity Parcellation of the Human Thalamus by Independent Component Analysis. Brain Connect. 2017; 7: 602–616.

Zhang Y, Brady M, Smith S. Segmentation of brain MR images through a hidden Markov random field model and the expectation-maximization algorithm. IEEE Trans. Med. Imaging 2001; 20: 45–57.

Zuo X-N, Kelly C, Di Martino A, Mennes M, Margulies DS, Bangaru S, et al. Growing together and growing apart: regional and sex differences in the lifespan developmental trajectories of functional homotopy. J. Neurosci. 2010; 30: 15034–15043.

Nieuwenhuys R, Voogd J, Huijzen C, editors. The Human Central Nervous System. Berlin, Heidelberg: Springer Berlin Heidelberg; 2008. Auditory system p. 733–750.

Purves D, Augustine G, Fitzpatrick D et al (editors). Neuroscience, Fifth Edition. Fifth Edit. Sinauer Associates; 2011.

Bayley Scales of Infant and Toddler Development®, Third Edition. 2017.